



Universidade do Porto
Faculdade de Engenharia

FEUP



Maria Olga de Amorim e Sá Ferreira

Modelling of Association Effects by Group-Contribution: Application to Natural Products

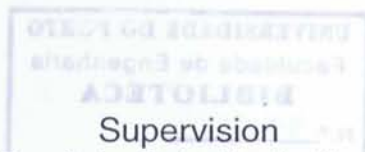


FEUP

**Modelling of association effects by group-
contribution: application to natural
products**

PhD Dissertation in Chemical Engineering

Maria Olga de Amorim e Sá Ferreira



Supervision

Prof. Maria Eugénia Rebello de Almeida Macedo

Prof. Esteban Alberto Brignole



Departamento de Engenharia Química
Faculdade de Engenharia Universidade do Porto

July 2003



Modeling of association effects by group-
contribution: application to natural
products

Author: [Name]

Advisor: [Name]

| | |
|------------------------------|--------------------|
| UNIVERSIDADE DO PORTO | |
| Faculdade de Engenharia | |
| BIBLIOTECA M | |
| N.º | <u>79600</u> |
| CDU | <u>54(043)</u> |
| Data | <u>13, 2, 2004</u> |



Department of Food Engineering
Faculty of Engineering, University of Porto

ACKNOWLEDGEMENTS

First of all, I would like to thank my mother and father for their love, support and encouragement. I would also like to thank my friends and family for their love and support.

To my mother, for her love and support, and for her prayers.

To my father, for his love and support, and for his prayers.

To my friends, for their love and support, and for their prayers.

To my teachers, for their love and support, and for their prayers.

To my friends, for their love and support, and for their prayers.

To my friends, for their love and support, and for their prayers.

To my friends, for their love and support, and for their prayers.

To my friends, for their love and support, and for their prayers.

To my parents

To my sisters

Acknowledgments

First of all, I would like to express my gratitude to my supervisors, Prof. Eugénia Macedo and Prof. Esteban Brignole for the opportunity of integrating this project and for their constant encouragement, guidance and friendship.

To Prof. Susana Bottini for her support, friendship and enlightenment discussions.

To Prof. Gloria Foco for her friendship and total collaboration at the experimental stage.

To the friends from *Laboratorio 50* and Bahia Blanca for their warm welcome and unlimited support during my stay.

To my colleagues and friends from FEUP for their companionship.

Special thanks to my friends Ania, Joaquim, Mónica, Nuno, Roxane, Selva, Tiago and to my brother in law, Paulo André.

To the *Laboratory of Separation and Reaction Engineering (LSRE)*, from DEQ, *Faculdade de Engenharia da Universidade do Porto*, headed by Prof. Alírio Rodrigues and *Planta Piloto de Ingeniería Química (PLAPIQUI)*, *Universidad Nacional del Sur*, CONICET, Bahia Blanca, Argentina for providing me all the necessary support and facilities to develop this work.

I would like to thank Prof. Madalena Dias for the help in the thesis edition.

To *Fundação para a Ciência e Tecnologia, Lisboa, Portugal*, for the PhD scholarship (reference SFRH/BD/879/2000) and for the financial support to participate in international scientific conferences.

Abstract

The design of extraction, fractionation and purification processes of natural products requires the existence of thermodynamic models that are able to accurately represent the phase equilibria behaviour of the highly complex mixtures involved in these unit operations. The complexity of these multi-component mixtures results from several reasons, *e.g.*, the significant differences in size between the recovered natural products and the corresponding solvents and the existence of specific interactions, like hydrogen-bonding.

The main purpose of this work is the development of thermodynamic models that take into account explicitly the self-association and/or solvation effects between molecules and its subsequent application to natural products mixtures. A compilation on the association theories, its analogies and limitations is presented. The application to multi-component mixtures, for which the available experimental information is scarce, suggests the use of group-contribution methods. Therefore, in this study, an association contribution based on the first order perturbation theory was developed following a group-contribution approach.

The phase equilibria predictions for these multi-components systems usually are made using an equation of state or an activity coefficient model. Two new models were developed, one for the calculation of activity coefficients (A-UNIFAC) and one equation of state for the calculation of fugacity coefficients (GCA-EoS).

The A-UNIFAC model results from the addition of one association term to the combinatorial and residual contributions from the original UNIFAC model. First, the interaction parameters of the model were obtained by correlating vapour-liquid equilibria (VLE), liquid-liquid equilibria (LLE) and infinite dilution activity coefficients of binary mixtures containing water, alcohols, acids, esters, aromatic compounds, alkyl chlorides and/or alkanes. Significant improvements were obtained relatively to the original UNIFAC model for the prediction of VLE and, specially, for the prediction of infinite dilution activity coefficients of associating components in inerts. After this, the model was used to predict the solid-liquid equilibria (SLE) and VLE of mono and disaccharides in polar solvents (water and alcohols). For that, new UNIFAC groups were defined to represent sugar molecules. The interaction parameters for these new groups were obtained using VLE and SLE of sugar-solvent binary mixtures. Finally, the model was applied to multi-component mixtures of industrial interest, for example, for the prediction of the water activity (in honey or fruit juices) or for the prediction of SLE of sugars in mixed solvents. This model is quite satisfactory in describing the non-idealities in the liquid phase in a wide range of compositions.

The equation for the fugacity coefficients calculation (the group-contribution with association equation of state, GCA-EoS) combines three terms: a repulsive term based on the hard-spheres theory, a NRTL group version for the attractive term and, finally, the group-contribution association term based on the first order perturbation theory. The association term has been revised to allow the extension of the model to several associating components, namely, carboxylic acids, esters, ketones in mixtures with water, alcohols and any number of inerts. The results obtained with the GCA-EoS are very satisfactory. These results compare favourably with the predictions of another group-contribution model that does not take into account explicitly association effects (MHV2 model), specially for mixtures of associating components with inerts.

The fugacity coefficients calculation for the liquid and vapour phases using an equation of state allows its application up to the critical region. The GCA-EoS was used to describe phase equilibria of mixtures containing fatty oils (triglycerides) and their derivatives (fatty acids, fatty acids esters, mono and diglycerides) with supercritical fluids (propane or carbon dioxide). The critical parameters of high molecular weight components are derived from infinite dilution activity coefficient data. New interaction parameters were calculated between the acid and the triglyceride group. As a complement to the available experimental information, infinite dilution activity coefficients for several solutes in mixtures of a triglyceride and a fatty acid were measured by inverse gas chromatography.

The GCA equation of state has shown a great flexibility to represent this type of mixtures containing polar mixtures with asymmetric components which supports its application in the design and optimization of separation processes of fatty oils mixtures with supercritical fluids.

Resumo

O projecto de processos de extracção, fraccionamento e purificação de produtos naturais requer a existência de modelos termodinâmicos capazes de representarem, com rigor adequado, o equilíbrio de fases das misturas altamente complexas, envolvidas nestas operações unitárias. A complexidade destas misturas multi-componentes encontra-se agravada por diversas razões, de que se podem destacar: as diferenças significativas de tamanho entre os produtos naturais recuperados e os respectivos solventes utilizados, e a existência de interacções específicas, tipo pontes de hidrogénio.

O objectivo principal deste trabalho consiste no desenvolvimento de modelos termodinâmicos que tenham em conta, de forma explícita, os efeitos de auto-associação e/ou solvatação entre moléculas e a sua posterior aplicação a misturas de produtos naturais. Neste trabalho apresenta-se uma compilação exaustiva sobre as teorias modernas de associação, as suas analogias e limitações. A sua aplicação a misturas multi-componentes, para as quais a informação experimental é escassa, sugere a utilização de métodos de contribuição de grupos. Assim, neste estudo, desenvolveu-se um termo associativo a contribuição grupal, baseada na teoria da perturbação de primeira ordem.

Para a previsão do equilíbrio de fases destes sistemas multi-componentes utilizam-se, em geral, equações de estado e/ou modelos para coeficientes de actividade.

Foram desenvolvidos dois novos modelos, um para o cálculo de coeficientes de actividade (A-UNIFAC) e uma equação de estado para o cálculo de coeficientes de fugacidade (GCA-EoS).

O modelo A-UNIFAC resulta da adição de um termo associativo às contribuições combinatorial e residual do modelo UNIFAC original. Numa primeira fase, os parâmetros de interacção do modelo foram obtidos correlacionando dados de equilíbrio líquido – vapor (ELV), equilíbrio líquido – líquido (ELL) e coeficientes de actividade a diluição infinita de misturas binárias contendo água, álcoois, ácidos, ésteres, compostos aromáticos, cloretos de alquila e/ou alcanos. Obtiveram-se melhorias significativas relativamente ao modelo UNIFAC original na previsão de ELV e, principalmente, na previsão de coeficientes de actividade a diluição infinita de compostos associativos em inertes. Numa fase posterior, este modelo foi aplicado à previsão do equilíbrio sólido-líquido (ESL) e ELV de mono e dissacáridos em solventes polares (água e álcoois). Para isso, foram definidos novos grupos UNIFAC para representarem esses açúcares. Os parâmetros de interacção para estes novos grupos foram obtidos utilizando dados ELV e ESL de misturas binárias de açúcar-solvente. Por fim, o modelo foi aplicado a misturas multi-componentes de interesse industrial como, por exemplo, na previsão da actividade da água (no mel ou em sumos de fruta) ou na previsão de ESL de açúcares em solventes mistos. Este modelo é bastante satisfatório para a descrição das não-idealidades em fase líquida numa ampla gama de composições.

A equação para o cálculo de coeficientes de fugacidade (*the group-contribution with association equation of state*, GCA-EoS) combina três termos: o termo repulsivo baseado na teoria de esferas rígidas, uma versão grupal do modelo NRTL para o termo atractivo e, finalmente, o termo associativo grupal baseado na teoria da perturbação de primeira ordem. O termo associativo foi revisto o que permitiu a sua extensão a vários componentes associativos, nomeadamente, ácidos carboxílicos, ésteres, cetonas, em misturas com água, álcoois e inertes. Os resultados alcançados com a GCA-EoS são muito satisfatórios. Os resultados do modelo foram ainda comparados com as previsões de um modelo baseado em contribuição de grupos que não tem em conta os efeitos associativos de forma explícita (equação MHV2) obtendo-se melhorias muito significativas especialmente para misturas de componentes inertes com componentes associativos.

O cálculo de coeficientes de fugacidade usando esta equação de estado para as fases líquida e de vapor possibilita a aplicação deste modelo até à região crítica. Esta equação foi usada na descrição do equilíbrio de fases de misturas de azeites (triglicéridos) e seus derivados (ácidos gordos, ésteres de ácidos gordos, mono e di-glicéridos) com fluidos supercríticos (propano ou dióxido de carbono). Os parâmetros críticos de compostos de elevado peso molecular são obtidos a partir de dados de coeficientes de actividade a diluição infinita. Determinaram-se novos parâmetros de interacção entre o grupo triglicérido e o grupo ácido. Como complemento à informação experimental disponível, mediram-se coeficientes de actividade a diluição infinita de vários solutos em misturas de um triglicérido com um ácido gordo, por cromatografia gasosa inversa.

A equação de estado GCA-EoS demonstrou uma grande flexibilidade na representação deste tipo de misturas polares com componentes assimétricos o que sugere a sua utilização na optimização e projecto de processos de separação de misturas de azeites com fluidos supercríticos.

Résumé

La conception de procédés d'extraction, de distillation et de purification de produits naturels nécessite l'existence de modèles thermodynamiques capables de représenter avec précision les équilibres de phases des mélanges hautement complexes rencontrés dans ces opérations unitaires. La complexité de ces mélanges multi constituants provient de plusieurs facteurs comme par exemple l'existence d'interactions spécifiques telles que des liaisons hydrogène ou une importante différence de taille entre les produits naturels à traiter et les solvants utilisés.

Le but principal de ce travail est d'une part le développement de modèles thermodynamiques qui prennent en compte explicitement l'auto association et/ou les effets de solvation entre les molécules et d'autre part l'application de ces modèles à des mélanges de produits naturels. L'application à des mélanges multi constituants pour lesquels peu de données expérimentales existent suggère l'utilisation de méthodes de contributions de groupes. C'est la raison pour laquelle, dans cette étude, un modèle d'association basé sur la théorie de la perturbation du premier ordre a été développé en suivant une approche par contributions de groupes. La prédiction des équilibres de phases pour ces systèmes multi constituants est généralement effectuée au moyen d'une équation d'état ou d'un modèle de coefficient d'activité. Deux nouveaux modèles ont été développés: il s'agit d'une part de A-UNIFAC pour le calcul des coefficients d'activité et d'autre part de GCA-EoS qui est une équation d'état pour le calcul des coefficients de fugacité.

Le modèle A-UNIFAC résulte de l'addition d'un terme d'association aux parties combinatoire et résiduelle du modèle UNIFAC original. Les paramètres d'interaction de ce nouveau modèle ont été obtenus par ajustement sur des données d'équilibre liquide-vapeur (ELV), d'équilibre liquide-liquide (ELL) ainsi que sur des données de coefficients d'activité à dilution infinie de systèmes binaires contenant de l'eau, des alcools, des acides, des esters, des composés aromatiques, des chlorures d'alkyle et/ou des alcanes. De nettes améliorations ont été obtenues par comparaison au modèle UNIFAC original pour la prédiction des ELV et plus spécialement pour la prédiction des coefficients d'activité à dilution infinie de composés associés dilués dans des solvants apolaires (inertes). Le modèle a ensuite été appliqué à la prédiction des équilibres liquide-solide (ELS) et liquide vapeur de mono et disaccharides dans des solvants polaires (eau et alcools). Pour cela de nouveaux groupes UNIFAC ont été définis afin de représenter les molécules de sucres. Les paramètres d'interaction pour ces nouveaux groupes ont été obtenus par régression de données d'ELV et d'ELS de systèmes binaires sucre-solvant. Finalement, le modèle a été appliqué à des mélanges multi constituants d'intérêt industriel comme par exemple pour la prédiction de l'activité de l'eau (dans du miel ou dans des jus de fruits) ou pour la prédiction d'ELS de sucres dans des solvants mixtes. Le modèle décrit de façon relativement satisfaisante la non idéalité de la phase liquide dans un large domaine de composition.

L'équation d'état GCA (group-contribution with association) pour le calcul des coefficients de fugacité combine trois termes: un terme répulsif basé sur la théorie des sphères dures, une version par contributions de groupes du modèle NRTL pour la partie attractive et finalement le terme d'association par contributions de groupes basé sur la théorie de la perturbation du premier ordre. Le terme d'association a été mis à jour pour permettre l'extension du modèle à divers composés associés à savoir les acides carboxyliques, les esters et les cétones en mélange dans l'eau et dans des alcools en présence d'un nombre quelconque d'inertes. Les résultats obtenus avec l'équation d'état GCA sont très satisfaisants. Ils sont meilleurs que ceux obtenus avec le modèle MHV2 qui est une autre méthode de contributions de groupes qui ne prend pas en compte explicitement les effets d'association. L'amélioration est particulièrement visible pour des mélanges renfermant des composés associés et des composés apolaires (inertes).

Le calcul des coefficients de fugacité pour les composés liquide et vapeur au moyen d'une équation d'état peut être appliqué jusque dans la région critique. L'équation d'état GCA a été utilisée pour décrire les équilibres de phases de mélanges contenant des triglycérides, des acides gras, des esters d'acides gras, des mono et diglycérides avec des fluides supercritiques (propane ou dioxyde de carbone). Les paramètres critiques des composés de haut poids moléculaire ont été déterminés à partir de données expérimentales de coefficients d'activité à dilution infinie. De nouveaux paramètres d'interaction ont été déterminés entre le groupe acide et le groupe triglycéride. Afin de compléter des données expérimentales existantes, les coefficients d'activité à dilution infinie de certains solutés dans des mélanges renfermant un triglycéride et un acide gras ont été mesurés par chromatographie inverse en phase gazeuse. L'équation GCA a montré une grande flexibilité pour représenter des mélanges renfermant des composés polaires et des composés de taille différente ce qui soutient son application dans la conception et l'optimisation de procédés de séparation d'huiles riches en composés gras au moyen de fluides supercritiques.

Resumen

Para el diseño de procesos de extracción, fraccionamiento y purificación de productos naturales se requiere disponer de modelos termodinámicos que representen con precisión el equilibrio entre fases de las complejas mezclas procesadas en estas operación de separación. La complejidad de estas mezclas multicomponentes es el resultado de varios factores, p.ej., existen significativas diferencias en el tamaño molecular de los productos naturales y solventes y tienen lugar interacción específicas del tipo de puente hidrógeno.

El principal propósito de este trabajo es el desarrollo de modelos termodinámicos que tengan en cuenta en forma explícita los efectos de autoasociación y/o solvatación entre compuestos y su consiguiente aplicación a mezclas de origen natural. En el trabajo se presenta una reseña exhaustiva sobre las teorías modernas de asociación, sus analogías y limitaciones. El tratamiento de mezclas multicomponentes, para las cuales la información experimental disponible es escasa, justifica el uso de métodos a contribución grupal. En consecuencia, en este trabajo, una componente de asociación basada en una teoría de perturbación de primer orden fué desarrollada siguiendo un enfoque a contribución grupal.

El cálculo del equilibrio entre fases para mezclas multicomponentes es llevado a cabo habitualmente utilizando modelos basados en ecuaciones de estado o en coeficientes de actividad. En este trabajo dos nuevos modelos fueron desarrollados: A-UNIFAC para el cálculo de coeficientes de actividad y GCA-EoS para el cálculo de coeficientes de fugacidad.

El modelo A-UNIFAC es el resultado del agregado de un término de asociación a las contribuciones residuales y combinatorias originales. Primeramente, los parámetros de interacción del modelo fueron obtenidos mediante la correlación de datos de equilibrio vapor líquido (EVL), equilibrio líquido-líquido (ELL) y coeficientes de actividad a dilución infinita en mezclas binarias, conteniendo agua, alcoholes, ácidos, esterés, compuestos aromáticos, hidrocarburos clorados y alcanos. Mejoras significativas fueron obtenidas relativas al modelo de UNIFAC original para la predicción de ELV y, especialmente, para la predicción de coeficientes de actividad de componentes que asocian en mezclas con componentes inertes. Posteriormente, el modelo fué usado para predecir el equilibrio sólido-líquido (ESL) y EVL de mono y disacaridos en solventes polares (agua y alcoholes). Con tal fin, nuevos grupos de UNIFAC fueron definidos para representar las moléculas de azúcar. Los parámetros de interacción para estos nuevos grupos fueron obtenidos a partir de EVL y ESL de mezclas binarias de azúcares con solventes. Finalmente, el modelo fué aplicado a sistemas multicomponentes de interés industrial, por ejemplo, para la predicción de la actividad del agua (en miel o jugos de frutas) o para la predicción de ESL en mezclas de solventes. El modelo se comporta muy satisfactoriamente en la descripción de las no idealidades en la fase líquida en un amplio rango de composiciones.

La ecuación para el cálculo de coeficientes de fugacidad (la ecuación de estado a contribución grupal GCA-EoS) combina tres términos: un término repulsivo basado en la teoría de esferas rígidas, una versión tipo NRTL (dependiente de la densidad) para el término atractivo y finalmente un término a contribución grupal basado en una aproximación de primer orden de una teoría de perturbación. El término de asociación se ha revisado para permitir la extensión del modelo a varios tipos de componentes asociativos, a saber: ácidos carboxílicos, esterés, cetonas en mezclas con agua, alcoholes y componentes inertes.

Los resultados obtenidos con la GCA-EoS son satisfactorios. Los mismos se comparan muy favorablemente con las predicciones de otra ecuación de estado a contribución grupal, (MHV2) que no toma en forma explícita los efectos de asociación, especialmente en el caso de mezclas de componentes asociativos con inertes.

La GCA-EoS fué utilizada para describir el equilibrio entre fases de mezclas que contienen aceites vegetales (triglicéridos) y sus derivados (ácidos grasos, esterés de ácidos grasos, mono y diglicéridos) con fluidos supercríticos (propano o dióxido de carbono). Los parámetros críticos de los componentes de alto peso molecular son deducidos a partir de coeficientes de actividad a dilución infinita. Nuevos parámetros de interacción han sido calculados entre el grupo ácido y el grupo triglicérido. Como un complemento a la información disponible, coeficientes de actividad de varios solutos en mezclas con triglicéridos y ácidos grasos fueron obtenidos a partir de experimentos de cromatografía gaseosa inversa.

La ecuación GCA-EoS ha mostrado una gran flexibilidad para representar mezclas con componentes polares con no polares y asimétricas en tamaño molecular, lo que justifica su aplicación en el diseño y optimización de procesos de separación de aceites grasos con fluidos supercríticos.

Contents

| | |
|--|-----------|
| LIST OF FIGURES | V |
| LIST OF TABLES | X |
| NOMENCLATURE..... | XII |
| 1. INTRODUCTION..... | 1 |
| 1.1 Importance and Motivation | 1 |
| 1.2 Objectives | 2 |
| 2. ASSOCIATION THEORIES | 4 |
| 2.1 Introduction | 4 |
| 2.2 Chemical theory | 4 |
| 2.2.1 Self-association | 5 |
| 2.2.2 Cross-association..... | 6 |
| 2.3 Quasi-chemical theory..... | 7 |
| 2.4 Physical theory..... | 7 |
| 2.4.1 Self-association..... | 11 |
| 2.4.2 Cross-association..... | 12 |
| 2.4.2.1 <i>Cross-association parameters</i> | 13 |
| 2.5 Equivalence between chemical and physical theories..... | 14 |
| 2.5.1 Ideal gas example | 14 |
| 2.5.2 Real gas example..... | 15 |
| 2.6 Chemical and physical cross-association solutions..... | 16 |
| 2.7 Conclusions..... | 19 |
| 3. PHASE EQUILIBRIA DESCRIBED BY G^E MODELS | 20 |
| 3.1 Introduction | 20 |
| 3.1.1 The original UNIFAC model | 20 |
| 3.1.2 Modified UNIFAC models..... | 22 |
| 3.1.3 G^E models that include the physical theory | 23 |
| 3.2 A-UNIFAC Model..... | 24 |
| 3.2.1 Description of the A-UNIFAC model..... | 24 |
| 3.2.2 Self-association | 27 |
| 3.2.2.1 <i>Association at infinite dilution</i> | 27 |
| 3.2.2.2 <i>Composition dependence of the association term</i> | 30 |
| 3.2.2.3 <i>Temperature dependence of the association term at infinite dilution</i> | 30 |
| 3.2.3 The vapour phase | 31 |
| 3.3 Rigorous model | 31 |
| 3.3.1 Model development..... | 31 |
| 3.3.2 Parameterization | 35 |
| 3.3.2.1 <i>Database</i> | 35 |
| 3.3.3 Results | 39 |
| 3.3.3.1 <i>Vapour-liquid equilibria</i> | 39 |
| 3.3.3.2 <i>Mutual solubilities for aqueous systems</i> | 40 |
| 3.3.3.3 <i>Infinite dilution activity coefficients</i> | 41 |

| | | |
|-----------|---|-----------|
| 3.4 | Approximated model | 45 |
| 3.4.1 | One- and two-site association models equivalence..... | 46 |
| 3.4.2 | Association at infinite dilution | 47 |
| 3.4.3 | Parameterization | 48 |
| 3.4.3.1 | Association parameters..... | 48 |
| 3.4.3.2 | Residual parameters | 50 |
| 3.4.4 | Results | 50 |
| 3.4.4.1 | Vapour-liquid equilibria | 50 |
| 3.4.4.2 | Ternary liquid-liquid equilibria prediction | 51 |
| 3.5 | Software developed in FORTRAN and VISUAL BASIC languages..... | 52 |
| 3.6 | Conclusions..... | 53 |
| 4. | PHASE EQUILIBRIA IN SUGAR SOLUTIONS WITH THE A-UNIFAC MODEL | 54 |
| 4.1 | Introduction | 54 |
| 4.2 | Chemical Structure..... | 56 |
| 4.2.1 | Monosaccharides | 56 |
| 4.2.2 | Disaccharides..... | 58 |
| 4.2.3 | Mutarotation equilibria..... | 59 |
| 4.2.3.1 | Influence of solvent | 59 |
| 4.2.3.2 | Influence of temperature | 60 |
| 4.3 | Revision of available models..... | 61 |
| 4.4 | The A-UNIFAC model for sugar mixtures..... | 65 |
| 4.4.1 | Calculation of thermodynamic properties | 65 |
| 4.4.1.1 | Vapour-Liquid equilibria..... | 65 |
| 4.4.1.2 | Solid-Liquid equilibria | 67 |
| 4.4.2 | Model parameters | 69 |
| 4.4.2.1 | Sugars Physical Properties | 69 |
| 4.4.2.2 | Residual Parameters..... | 71 |
| 4.4.2.3 | Association Parameters | 73 |
| 4.4.3 | New parameters for sugar/solvents..... | 74 |
| 4.4.3.1 | Database and optimization strategy | 74 |
| 4.4.4 | Results and Discussion | 77 |
| 4.4.4.1 | Correlation Results..... | 77 |
| 4.4.4.2 | Predictions..... | 81 |
| 4.4.4.3 | Predictions for sugar industrial systems..... | 85 |
| 4.5 | Conclusions..... | 88 |
| 5. | EQUATIONS OF STATE FOR POLAR AND ASSOCIATING MIXTURES – A GENERAL OVERVIEW | 90 |
| 5.1 | Introduction | 90 |
| 5.2 | Mixing rules from activity coefficient models | 92 |
| 5.2.1 | Huron and Vidal methodology | 92 |
| 5.2.2 | Density dependent mixing rules - The group-contribution equation of state..... | 96 |
| 5.3 | Equations of state that include association | 98 |
| 5.3.1 | Equations of state that include the chemical theory | 98 |
| 5.3.2 | Equations of state that include a physical theory | 102 |
| 5.3.2.1 | The Statistical Associating Fluid Theory – SAFT equation..... | 102 |

| | | |
|-----------|--|------------|
| 5.3.2.2 | <i>Semi empirical cubic equations of state</i> | 104 |
| 5.3.3 | Equations of state that include a quasi-chemical theory..... | 105 |
| 5.4 | Conclusions..... | 105 |
| 6. | MODELLING OF PHASE EQUILIBRIA FOR ASSOCIATING MIXTURES USING AN EQUATION OF STATE | 106 |
| 6.1 | The group-contribution with association equation of state..... | 106 |
| 6.2 | Extension of the model..... | 107 |
| 6.2.1 | Revision | 107 |
| 6.2.2 | Model development | 108 |
| 6.3 | Parameterization | 111 |
| 6.3.1 | Computer programme | 111 |
| 6.3.2 | Experimental Database | 112 |
| 6.3.3 | Attractive parameters | 113 |
| 6.3.4 | Association parameters..... | 114 |
| 6.3.5 | Repulsive parameters | 116 |
| 6.3.6 | Results and discussion..... | 116 |
| 6.3.6.1 | <i>Self-associating mixtures of acids and alkanes</i> | 116 |
| 6.3.6.2 | <i>Cross-associating mixtures with groups OH and COOH</i> | 120 |
| 6.3.6.3 | <i>Cross-associating mixtures with groups COOH and COOR</i> | 122 |
| 6.3.6.4 | <i>Cross-associating mixtures with groups OH and COOR</i> | 124 |
| 6.3.6.5 | <i>Cross-associating mixtures with groups OH and RCOR</i> | 125 |
| 6.3.6.6 | <i>Interaction between groups COOH and CO₂</i> | 127 |
| 6.4 | Approximated approach | 127 |
| 6.4.1 | Parameterization | 128 |
| 6.5 | Conclusions..... | 129 |
| 7. | APPLICATION OF THE GCA-EOS MODEL TO THE SUPERCRITICAL PROCESSING OF FATTY OIL DERIVATIVES | 130 |
| 7.1 | Introduction | 130 |
| 7.1.1 | Chemical composition | 132 |
| 7.1.2 | Phase behaviour | 133 |
| 7.2 | Previous work with the GC-EoS | 136 |
| 7.3 | Predictions using the GCA-EoS | 137 |
| 7.3.1 | Binary systems of CO ₂ and fatty acids | 137 |
| 7.3.2 | Binary systems of propane and fatty acids..... | 139 |
| 7.3.3 | Infinite dilution activity coefficients..... | 139 |
| 7.3.4 | Ternary systems of propane + oleic acid + cottonseed oil..... | 140 |
| 7.3.5 | Ternary system of CO ₂ + oleic acid + methyl oleate | 141 |
| 7.3.6 | Ternary system of CO ₂ +triolein+oleic acid | 142 |
| 7.4 | Conclusions..... | 143 |
| 8. | INFINITE DILUTION ACTIVITY COEFFICIENTS OF SOLVENTS IN FATTY OIL DERIVATIVES | 144 |
| 8.1 | Introduction | 144 |
| 8.2 | Experimental technique..... | 145 |
| 8.2.1 | Equipment | 145 |
| 8.2.2 | Stationary and Mobile Phases..... | 146 |

| | | |
|-----------|--|------------|
| 8.2.3 | Chemicals | 146 |
| 8.3 | Experimental data | 146 |
| 8.4 | Parameterization | 149 |
| 8.5 | Conclusions..... | 150 |
| 9. | CONCLUSIONS AND FUTURE WORK | 151 |
| 9.1 | Conclusions..... | 151 |
| 9.2 | Future work | 153 |
| | REFERENCES..... | 154 |
| A. | A-UNIFAC SOFTWARE DEVELOPED IN THIS WORK | 168 |
| A.1 | Introduction | 168 |
| A.2 | Input data files..... | 168 |
| A.2.1 | Create a new input file..... | 168 |
| A.2.1.1 | <i>Selection of components</i> | 168 |
| A.2.1.2 | <i>Parameters initial values</i> | 169 |
| A.2.1.3 | <i>Thermodynamic data</i> | 170 |
| A.2.1.4 | <i>Run</i> | 171 |
| A.2.1.5 | <i>Output results</i> | 172 |
| A.2.2 | Open an input file | 173 |
| A.2.2.1 | <i>Output results</i> | 173 |
| A.3 | Databases | 173 |
| A.3.1 | Pure component properties | 173 |
| A.3.1.1 | <i>Add a new component to the database</i> | 174 |
| A.3.1.2 | <i>Delete record</i> | 174 |
| A.3.1.3 | <i>Add or update properties</i> | 174 |
| A.3.2 | Residual groups parameters | 176 |
| A.3.2.1 | <i>New interaction residual parameters</i> | 177 |
| A.3.2.2 | <i>Add new residual groups</i> | 177 |
| A.3.2.3 | <i>Delete residual groups</i> | 178 |
| A.3.3 | Association group parameters..... | 178 |
| A.3.3.1 | <i>Update data</i> | 179 |
| A.3.3.2 | <i>Delete association group</i> | 179 |
| A.3.3.3 | <i>Add new associating group</i> | 179 |
| A.3.4 | Solvation parameters | 179 |
| A.4 | View equilibria data | 180 |
| A.5 | Options..... | 181 |
| B. | STRUCTURES OF SOME SUGARS..... | 182 |
| B.1 | D-aldoses | 182 |
| B.2 | D-ketoses | 183 |
| B.3 | Disaccharides..... | 184 |
| C. | INFINITE DILUTION ACTIVITY COEFFICIENTS DATA..... | 185 |
| C.1 | Experimental data | 185 |

List of Figures

| | |
|---|----|
| Figure 2.1 Schematic representation of the hysterical effects not allowed by TPT1..... | 8 |
| Figure 2.2 Schematic representation of the model of the square well potential. | 9 |
| Figure 3.1 Infinite dilution activity coefficients of an alcohol (ethanol or methanol) in a series of n-alkane solvents at 298.15K. Experimental values (Dohnal and Vrbka, 1997): ○ - methanol, △ - ethanol; Residual and association contributions (calculated by subtracting the original UNIFAC combinatorial term): ● - methanol, ▲ - ethanol. | 28 |
| Figure 3.2 Infinite dilution activity coefficients of n-alkanes in methanol at 298.15K. Experimental values (Dohnal and Vrbka, 1997): ○-1-propanol, △- 1-butanol; Residual and association contributions (calculated by subtracting the original UNIFAC combinatorial term): ●- 1-propanol, ▲- 1-butanol. | 29 |
| Figure 3.3 Partial derivative of the association activity coefficient of ethanol, with respect to ethanol mole fraction..... | 30 |
| Figure 3.4 Partial derivative of the association activity coefficient of hexane, with respect to ethanol mole fraction..... | 30 |
| Figure 3.5 Monomer fractions: (a) liquid water; (b) liquid ethanol. Calculated: --- SAFT at saturated liquid densities; — SAFT at constant saturated liquid density at 298.15K; — A-UNIFAC model. | 36 |
| Figure 3.6 VLE of binary mixtures: (a) heptane + acetic acid at 313 K; (b) 1-butanol + acetic acid at 323 K. Exp. Data (Gmehling <i>et al.</i> , 1977); — A-UNIFAC; --- Original UNIFAC. | 39 |
| Figure 3.7 VLE of binary mixtures: (a) water + acetic acid at 353 K; (b) toluene + 1-butanol at 373 K. Exp. Data (Gmehling <i>et al.</i> , 1977); — A-UNIFAC; --- Original UNIFAC. | 40 |
| Figure 3.8 Water – hydrocarbon mutual solubilities at 298K. Experimental data (Sørensen and Arlt, 1979): ● water sol.; □ hydrocarbons sol.; — A-UNIFAC; --- VLE -UNIFAC (Gmehling <i>et al.</i> , 1982); - - LLE -UNIFAC (Magnussen <i>et al.</i> , 1981). | 41 |
| Figure 3.9 Water – alcohols mutual solubilities at 298K. Experimental data (Sørensen and Arlt, 1979): ● water sol.; □ alcohols sol.; — A-UNIFAC correlation; --- UNIFAC correlation..... | 41 |
| Figure 3.10 Water – acids mutual solubilities at 298K. Experimental data (Sørensen and Arlt, 1979): ● water sol.; □ acids sol.; — A-UNIFAC prediction; --- UNIFAC prediction..... | 41 |
| Figure 3.11 Water – benzene mutual solubilities <i>versus</i> temperature. Experimental data (Sørensen and Arlt, 1979): ○ water sol.; ● benzene sol.; — A-UNIFAC correlation; --- UNIFAC correlation. | 41 |
| Figure 3.12 Infinite dilution activity coefficients of n-alkanes in ethanol <i>versus</i> temperature: ● Δ × experimental data (Tiegs <i>et al.</i> , 1986); — A-UNIFAC; --- UNIFAC- γ^∞ | 42 |
| Figure 3.13 Infinite dilution activity coefficients of ethanol in n-alkanes, <i>versus</i> temperature: ●○ experimental data (Tiegs <i>et al.</i> , 1986) — A-UNIFAC correlation; --- UNIFAC- γ^∞ correlation..... | 42 |
| Figure 3.14 Infinite dilution activity coefficients of in binary mixtures of: (a) benzene and ethanol; (b) acetic acid and ethyl acetate; (c) ethyl acetate in water; (d) water and acetic acid. Exp. Data (Tiegs <i>et al.</i> , 1986); — A-UNIFAC; --- Original UNIFAC. | 43 |
| Figure 3.15 Infinite dilution activity coefficients of several solutes in water at 298K <i>versus</i> carbon number of the solute. Exp. Data (Kojima <i>et al.</i> , 1997; Sørensen and Arlt, 1979; Hwang <i>et al.</i> , 1992; Pierotti <i>et al.</i> , 1959; Bergmann and Eckert, 1991; Li <i>et al.</i> , 1993; see Zhang <i>et al.</i> , 1998); — A-UNIFAC; --- Original UNIFAC; - * - Modified UNIFAC (Dortmund). | 44 |
| Figure 3.16 Infinite dilution activity coefficients at 298K <i>versus</i> carbon number of alkanes. Exp. Data (Sørensen and Arlt, 1979): ●n-alkanes in water; ○ water in n-alkanes. Models: — A-UNIFAC; - - Original UNIFAC; - * - Modified UNIFAC (Dortmund)..... | 44 |
| Figure 3.17 Schematic representation of the three types of associating groups. | 45 |
| Figure 3.18 Monomer fractions predicted by SAFT equation for liquid ethanol (---) and acetic acid (—). (a) at saturated liquid densities; (b) liquid densities at 298.15K. | 49 |
| Figure 3.19 Ethanol distribution coefficients between hexane and water at 298K: ◇ experimental data (Roddy and Coleman, 1981); — A-UNIFAC; --- UNIFAC. | 51 |

| | |
|---|----|
| Figure 3.20 Distribution coefficients of acetic acid between hexane and water at 298K: O experimental data (Sørensen and Arlt, 1979); — A-UNIFAC; -- UNIFAC. | 51 |
| Figure 3.21 Distribution coefficients of butyric acid between 1-hexanol and water at 303K: ■ experimental data (Sørensen and Arlt, 1979); — A-UNIFAC; -- UNIFAC. | 52 |
| Figure 3.22 The A-UNIFAC program. | 53 |
| Figure 4.1 Enantiomeric forms of glyceraldehyde. | 56 |
| Figure 4.2 Ring formation: (a) furanose and (b) pyranose. | 57 |
| Figure 4.3 Diastereomers of D-glucopyranose. | 58 |
| Figure 4.4 Tautomers equilibrium composition (mole %) of a sugar in water <i>versus</i> temperature: (a) D-glucose (Maple and Allerhand, 1987); (b) D-fructose (Lichtenthaler and Rønninger, 1990). Exp. data: — ◆— α -pyranose; —□— β -pyranose; —▲— α -furanose; —×— β -furanose. | 61 |
| Figure 4.5 UNIFAC groups defined by Gabas and Laguérie (1990) and Abed <i>et al.</i> (1992) to represent sugar molecules. | 62 |
| Figure 4.6 UNIFAC groups proposed by Catté <i>et al.</i> (1995) to represent sugar molecules. | 62 |
| Figure 4.7 D-glucose and D-fructose groups proposed in the Bio-UNIFAC model. | 63 |
| Figure 4.8 Thermodynamic cycle for the fugacity ratio calculation. | 67 |
| Figure 4.9 Monosaccharides solubility in binary aqueous mixtures <i>versus</i> temperature. Experimental data: ▲ □ (Jónsdóttir <i>et al.</i> , 2002); O (Vasátko and Smelik, 1967; Abed <i>et al.</i> , 1992; Young <i>et al.</i> , 1952); + (Stephen and Stephen, 1963; Young, 1957); Sugars Ideal solubility: —▲—; —□—; —O—; —+—. | 71 |
| Figure 4.10 Disaccharides solubility in binary aqueous mixtures <i>versus</i> temperature. Experimental data: ■+ (Jónsdóttir <i>et al.</i> , 2002); △(Mullin, 1972); ●(Mullin, 1972; Young and Jones, 1949); ◇ (Mullin, 1972; Jónsdóttir <i>et al.</i> , 2002; Stephen and Stephen, 1963); Sugars ideal solubility: —■—; —+—; —△—; —●—; —◇—. | 71 |
| Figure 4.11 Sugar solubility in binary aqueous mixtures <i>versus</i> temperature. Experimental data: O △ (Jónsdóttir <i>et al.</i> , 2002); ◆ (Stephen and Stephen, 1963; Young, 1957, Abed <i>et al.</i> , 1992); — A-UNIFAC model correlation (D-glucose) and prediction (D-galactose and D-xylose). | 73 |
| Figure 4.12 Osmotic coefficients prediction for binary aqueous sugar mixtures at 298 K. Experimental data: ◆ O × (Miyajima <i>et al.</i> , 1983a); △ (Uedaira and Uedaira, 1969); — A-UNIFAC model predictions. | 74 |
| Figure 4.13 Osmotic coefficients data in binary aqueous sugar solutions at 298.15K. Experimental data: ◆ O × (Miyajima <i>et al.</i> , 1983a); — A-UNIFAC correlation. | 78 |
| Figure 4.14 Osmotic coefficients data in binary aqueous sugar solutions at 298.15K. Experimental data: ◆ O × (Miyajima <i>et al.</i> , 1983a); P&M UNIFAC model: — D-glucose(correlation); — D-galactose and D-mannose (prediction). | 78 |
| Figure 4.15 Osmotic coefficients data in binary aqueous sugar solutions at 298.15K. Experimental data: △ (Scatchard <i>et al.</i> 1938); ◆ Uedaira and Uedaira (1969), Miyajima <i>et al.</i> (1983b). Models: — A-UNIFAC correlation; —P&M UNIFAC prediction. | 79 |
| Figure 4.16 D-fructose solubility in alcohols <i>versus</i> temperature. Experimental data: ◆△ (Peres, 1998); × (Coulon <i>et al.</i> , 1997); — A-UNIFAC model correlation; — P&M UNIFAC prediction. | 79 |
| Figure 4.17 Sucrose solubility in alcohols <i>versus</i> temperature. Experimental data: ◆△ (Peres, 1998); ×□ (Moye, 1972); — A-UNIFAC model correlation. | 80 |
| Figure 4.18 Sucrose solubility in 1-propanol and 1-butanol <i>versus</i> temperature. Experimental data: ×△ (Moye, 1972); P&M UNIFAC prediction: — 1-propanol; —1-butanol. | 80 |
| Figure 4.19 Sugar solubility in water/methanol mixtures. Experimental data: ◆△ (Peres, 1998); — A-UNIFAC correlation; — P&M UNIFAC prediction. | 81 |
| Figure 4.20 Solubility in water <i>versus</i> temperature. Experimental data: ● △ (Jónsdóttir <i>et al.</i> , 2002); Model predictions: — P&M UNIFAC; — A-UNIFAC. | 82 |
| Figure 4.21 Disaccharides solubility in water <i>versus</i> temperature. Experimental data: △ (Jónsdóttir <i>et al.</i> , 2002); ◇ (Mullin, 1972); ●(Mullin, 1972; Young and Jones, 1949); ■ (Mullin, 1972; Jónsdóttir <i>et al.</i> , 2002; Stephen and Stephen, 1963);—A-UNIFAC model. | 83 |
| Figure 4.22 Cellobiose solubility in water <i>versus</i> temperature. Experimental data: ◆ (Jónsdóttir <i>et al.</i> , 2002); — A-UNIFAC model prediction; — A-UNIFAC model correlation. | 83 |

| | |
|--|-----|
| Figure 4.23 Sucrose solubility in water/methanol and water/ethanol mixtures. Experimental data: $\blacklozenge \triangle \times$ (Peres, 1998); — A-UNIFAC model; --- P&M UNIFAC model..... | 84 |
| Figure 4.24 Sugar solubility in ethanol/methanol mixtures. Experimental data: $\blacklozenge \triangle \times$ (Peres, 1998); — A-UNIFAC model; --- P&M UNIFAC model. | 85 |
| Figure 4.25 D-fructose solubility in water/ethanol and water/methanol mixtures. Experimental data: $\blacklozenge \triangle \times$ (Peres, 1998); — A-UNIFAC model; --- P&M UNIFAC model..... | 85 |
| Figure 4.26 Sugar solubility in ethanol/water mixtures at 25°C. Experimental data: $\blacklozenge \triangle$ (Gabas <i>et al.</i> , 1988); — A-UNIFAC model prediction; ---P&M UNIFAC model..... | 86 |
| Figure 4.27 Solid-liquid equilibria of D-xylose/D-mannose/water at 25°C and 35°C: \blacklozenge experimental data (Gabas and Laguérie, 1990); — A-UNIFAC model; ---P&M UNIFAC model..... | 86 |
| Figure 4.28 Solid liquid equilibria of (a) D-glucose/sucrose/water and (b) D-fructose/sucrose/water at 70°C: \blacklozenge experimental (Abed <i>et al.</i> , 1992); — A-UNIFAC model; — P&M UNIFAC model. | 87 |
| Figure 4.29 Normal boiling point of quaternary aqueous solutions of D-glucose, D-fructose and sucrose: \blacklozenge Experimental data (Abderafi and Bounahmidi, 1994); — A-UNIFAC prediction — P&M UNIFAC prediction..... | 87 |
| Figure 4.30 Water activity of solutions containing D-fructose or sucrose and for an apple juice at 25°C. Experimental data: $\triangle +$ (Correa <i>et al.</i> , 1981); \bullet (Fontán <i>et al.</i> , 1981); — A-UNIFAC model prediction. | 88 |
| Figure 4.31 Water activity in synthetic honey at 25°C: Experimental data: \blacklozenge (Rüegg and Blanc, 1981); — A-UNIFAC model prediction; --- P&M UNIFAC model prediction. | 88 |
| Figure 5.1 Molecules model according to the SAFT equation: rigid spheres fluid \rightarrow chain formation \rightarrow associated complexes formation..... | 102 |
| Figure 6.1 Cyclic dimer representation..... | 114 |
| Figure 6.2 Fraction of non-bonded sites <i>versus</i> temperature: \bullet \circ GCA-EoS; — SAFT (Huang and Radosz, 1990). | 114 |
| Figure 6.3 Saturation compressibility factor <i>versus</i> temperature for acetic acid: \triangle Miyamoto <i>et al.</i> (1999); — GCA-EoS prediction; --- MHV2 prediction..... | 117 |
| Figure 6.4 VLE of heptane and pentanoic acid: exp. (Gmehling <i>et al.</i> , 1977); — GCA-EoS correlation; --- MHV2 prediction. | 118 |
| Figure 6.5 VLE of hexanoic acid and octanoic acid: exp. (Gmehling <i>et al.</i> , 1977); — GCA-EoS correlation; --- MHV2 prediction. | 118 |
| Figure 6.6 VLE of acetic acid and octane at 343 K: exp. (Gmehling <i>et al.</i> , 1977); — GCA-EoS correlation; --- MHV2 prediction. | 119 |
| Figure 6.7 VLE of hexane and acetic acid at 313 K: exp. (Miyamoto <i>et al.</i> , 2000); — GCA-EoS correlation; --- MHV2 prediction. | 119 |
| Figure 6.8 VLE of methane and a fatty acid: \bullet lauric acid; \triangle palmitic acid; exp. data (Shy <i>et al.</i> , 1993); — GCA-EoS prediction; ---MHV2 prediction..... | 119 |
| Figure 6.9 VLE of ethane and several solutes: exp. (Weng and Lee, 1992; Peter and Jakob, 1991; Rodrigues <i>et al.</i> , 1968); — GCA-EoS prediction. | 120 |
| Figure 6.10 VLE of binary mixtures of an alcohol and an acid at 1 bar: (a) 1-butanol and propanoic acid; (b) 1-butanol and acetic acid. Exp. data (Gmehling <i>et al.</i> , 1977); — GCA-EoS prediction; --- MHV2 prediction. | 120 |
| Figure 6.11 VLE of binary mixtures of an alcohol and an acid at 1 bar: (a) 2-butanol and acetic acid; (b) methanol and propanoic acid. Exp. data (Gmehling <i>et al.</i> , 1977); — GCA-EoS correlation; --- MHV2 prediction. | 121 |
| Figure 6.12 VLE of water and propionic acid: exp. (Gmehling <i>et al.</i> , 1977); — GCA-EoS correlation; ---MHV2 prediction. | 122 |
| Figure 6.13 VLE of water and acetic acid. Exp. data: \bullet (Ohtmer <i>et al.</i> , 1952a), \circ \times (Ermolaev <i>et al.</i> , 1971); — GCA-EoS prediction; ---MHV2 prediction..... | 122 |
| Figure 6.14 VLE of ethyl acetate and acetic acid: exp. (Gmehling <i>et al.</i> , 1977); — GCA-EoS correlation; --- MHV2 prediction. | 123 |

| | |
|--|-----|
| Figure 6.15 VLE of an ester and an acid at 1 bar (temperature <i>versus</i> composition): (a) propyl acetate and acetic acid; (b) acetic acid and butyl acetate. Exp. data (Gmehling <i>et al.</i> , 1977); — GCA-EoS correlation; - - -MHV2 prediction. | 124 |
| Figure 6.16 VLE of an alcohol and an ester: (a) 1-propanol and methyl propanoate; (b) 1-propanol and methyl butanoate. Exp. data (Gmehling <i>et al.</i> , 1977); — GCA-EoS correlation; - - -MHV2 prediction. .. | 125 |
| Figure 6.17 VLE of an ester and water (vapor phase mole fraction <i>versus</i> liquid phase mole fraction): (a) butyl acetate (1) and water (2) at 317 K; (b) water (1) and propyl acetate (2) at 353 K. Exp. data (Gmehling <i>et al.</i> , 1977); — GCA-EoS prediction; - - -MHV2 prediction. | 125 |
| Figure 6.18 VLE of water and acetone: exp. data (Griswold and Wong, 1952); — GCA-EoS correlation; - - -MHV2 prediction. | 126 |
| Figure 6.19 VLE of 2-butanone and water: exp. data (Othmer <i>et al.</i> , 1952b); — GCA-EoS prediction; - - -MHV2 prediction. | 126 |
| Figure 6.20 VLE of carbon dioxide and a carboxylic acid: (a) CO ₂ and acetic acid; (b) CO ₂ and butanoic acid. Exp. Data (Byun <i>et al.</i> , 2000); — GCA-EoS correlation. | 127 |
| Figure 6.21 Schematic representation of self- and cross-association in carboxylic acids. | 127 |
| Figure 7.1 Mono-, di- and triglyceride schematic representation. | 132 |
| Figure 7.2 The triglyceride (TG) group. | 132 |
| Figure 7.3 Pressure-temperature diagrams for the six types of phase behaviour obtained for binary systems (Van Konynenburg and Scott, 1980): g: vapour; l: liquid; U: upper critical end point; L: lower critical end point; dashed lines correspond to the critical locus, <i>i.e.</i> , curve that connects all the critical points where two phases converge to one phase; Full lines correspond to the pure components vapour pressure finishing at the pure component critical points C ₁ and C ₂ | 133 |
| Figure 7.4 Pressure <i>versus</i> composition projections at three temperatures obtained from Type V diagram. | 135 |
| Figure 7.5 UCEP and LCEP for binary mixtures of propane with n-carboxylic acids, n-alkanols and n-alkanes (Source: Peters, 1994). | 135 |
| Figure 7.6 VLE of CO ₂ and methylpalmitate: exp. (Inomata <i>et al.</i> , 1989); — GC-EoS predictions. | 137 |
| Figure 7.7 VLE and LLE predictions using the GC-EoS for propane + tripalmitin mixture. Exp. (Coorens <i>et al.</i> , 1988). | 137 |
| Figure 7.8 Binary VLE of CO ₂ and palmitic acid: Exp. data (Yau <i>et al.</i> , 1992); — GCA-EoS predictions. | 138 |
| Figure 7.9 Binary VLE of CO ₂ and fatty acids. Exp. data: Δ • (Bharath <i>et al.</i> , 1993); \times (Byun <i>et al.</i> , 2000). Model: — GCA-EoS prediction. | 138 |
| Figure 7.10 Binary VLE of CO ₂ and oleic acid: exp. (Bharath <i>et al.</i> , 1992); — GCA-EoS prediction. | 138 |
| Figure 7.11 Binary VLE of CO ₂ and unsaturated fatty acids at 313.15 K. Exp. data: • oleic acid (Bharath <i>et al.</i> , 1992); o linoleic acid (Chen <i>et al.</i> , 2000). Model: — GCA-EoS predictions. | 138 |
| Figure 7.12 Binary VLE and LLE for propane and oleic acid. Exp. data (see Hixson and Bockelmann, 1942); — GCA-EoS predictions. | 139 |
| Figure 7.13 LLE of C ₃ H ₈ -oleic acid-cottonseed oil at T = 371.65 K and P = 44 bar (compositions in weight fractions): —■— exp. (Hixson and Bockelmann, 1942); — GCA-EoS. | 141 |
| Figure 7.14 Vapour-liquid equilibria for the system CO ₂ + methyl oleate + oleic acid for several mixtures with overall fixed mole fractions (R=oleic acid mole fraction on a CO ₂ free basis). Exp. data: $\square \times \Delta$ (Yu <i>et al.</i> , 1993); — (Inomata <i>et al.</i> , 1989); • (Bharath <i>et al.</i> , 1992). Model: — GCA-EoS predictions. | 142 |
| Figure 7.15 Ternary VLE of CO ₂ , oleic acid and triolein at P = 250 bar :-■— exp. (Bharath <i>et al.</i> , 1992); — GCA-EoS prediction. | 142 |
| Figure 8.1 Representation of γ^{∞} of isooctane <i>versus</i> the molar fraction of palmitic acid at 353.15K: ■ ○ experimental data. | 148 |
| Figure 8.2 Temperature dependence of γ^{∞} for heptane, ethanol and trichloroethylene in a mixture containing 50 % palmitic acid / 50 % tripalmitin. | 148 |
| Figure 8.3 Representation of γ^{∞} of heptane <i>versus</i> the molar fraction of palmitic acid at 353.15K: ■ ○ experimental data (Ferreira and Foco, 2003); — GCA-EoS correlation. | 149 |

| | |
|---|-----|
| Figure 8.4 γ^{∞} of alcohols in triacetin versus temperature: \blacklozenge \circ experimental data (Foco et al., 2000); —GCA-EoS correlation. | 150 |
| Figure A.1 Selecting components from the database..... | 169 |
| Figure A.2 Set initial parameters values for the run. | 169 |
| Figure A.3 Selection of experimental binary VLE systems..... | 170 |
| Figure A.4 Set optimisation or simulation features..... | 171 |
| Figure A.5 View output results in a text file or excel file. | 172 |
| Figure A.6 View Output Results in a text file. | 172 |
| Figure A.7 No output results..... | 172 |
| Figure A.8 Select an existing input file. | 173 |
| Figure A.9 Selecting components from the database..... | 174 |
| Figure A.10 Adding a new component to the database..... | 174 |
| Figure A.11 Setting pure component properties..... | 175 |
| Figure A.12 Selecting file containing pure component properties. | 176 |
| Figure A.13 Set residual groups features in the database. | 177 |
| Figure A.14 Definition of a new group and corresponding subgroups..... | 178 |
| Figure A.15 Set association groups features in the database. | 178 |
| Figure A.16 Definition of a new association group. | 179 |
| Figure A.17 Set solvation parameters values in the database. | 180 |
| Figure A.18 View the references files..... | 180 |
| Figure A.19 Options window. | 181 |
| Figure B.1 The D-aldoses family tree (Fischer representation)..... | 182 |
| Figure B.2 The D-ketoses family tree (Fischer representation)..... | 183 |
| Figure B.3 Disaccharides chemical structure..... | 184 |

List of tables

| | |
|--|----|
| Table 2.1 Self-association types for pure components: simplifications in Δ and X^{A_i} and resulting expressions for X^{A_i} | 11 |
| Table 2.2 Cross-association models: approximations in Δ | 12 |
| Table 2.3 Parameters equivalence. | 15 |
| Table 2.4 Monomer fraction expressions obtained for mixtures of types I and II. | 16 |
| Table 3.1 Differences between the UNIFAC model and the modified UNIFAC models. | 23 |
| Table 3.2 Self-association models defined in the GCA-EoS model. | 32 |
| Table 3.3 Cross-association types defined in the A-UNIFAC model. | 33 |
| Table 3.4 VLE database used for A-UNIFAC parameters estimation | 35 |
| Table 3.5 Residual group interaction parameters $a_{m,n}$ (K) | 38 |
| Table 3.6 A-UNIFAC self-and cross-association parameters. | 38 |
| Table 3.7 Average errors in pressure ($\square P$) and composition ($\square y$) for the UNIFAC and A-UNIFAC models. | 39 |
| Table 3.8 Expressions obtained for X^{A_k} , X^{mon} and γ^{assoc} using the one and two sites models. | 47 |
| Table 3.9 Calculated number of associating groups | 50 |
| Table 3.10 Residual group interaction parameters $a_{m,n}$ (K) | 50 |
| Table 3.11 Average errors in pressure ($\square P$) and composition ($\square y$) for the UNIFAC and A-UNIFAC models. | 51 |
| Table 4.1 Annual production of simple sugars, sugar-derived alcohols, and acids compared to some petrochemically derived basic chemicals and solvents. | 55 |
| Table 4.2 Composition (%) of the different monosaccharides conformers in equilibrium in aqueous solution (Goldberg and Tewari,1989). | 59 |
| Table 4.3 Number of hydroxyl groups that are not in axial position for each conformer and calculated average number in aqueous solutions. | 60 |
| Table 4.4 Melting temperature and enthalpy of fusion values available in the literature. | 69 |
| Table 4.5 Melting temperature T_m , enthalpy of fusion ΔH_f and heat capacity difference ΔC_p used in this work to describe the solid-liquid equilibrium with the A-UNIFAC model. | 70 |
| Table 4.6 Structural volume (R_k) and area (Q_k) parameters for the new A-UNIFAC groups. | 72 |
| Table 4.7 Molecules decomposition in the groups defined for the A-UNIFAC model. | 72 |
| Table 4.8 Experimental database used in the optimization step: number of experimental points NP, range of temperature T and range of compositions X. | 75 |
| Table 4.9 Experimental database used in the optimization step (continuation): osmotic coefficients data of several mono and disaccharides. | 75 |
| Table 4.10 Experimental database used in the optimization step (conclusion): solubility data of sugars (D-glucose, D-fructose and sucrose) in several solvents (water and alcohols). | 75 |
| Table 4.11 Group interaction parameters (K). | 76 |
| Table 4.12 Calculated number of associating groups for each sugar. | 77 |
| Table 4.13 Correlation and prediction (*) results for D-glucose and sucrose binary aqueous mixtures: number of experimental points NP, range of temperature T; range of compositions X and average absolute deviations AAD for the A-UNIFAC models (in bold) and P&M UNIFAC. | 77 |
| Table 4.14 Correlation and prediction (*) results for D-fructose binary aqueous mixtures: number of experimental points NP, range of temperature T; range of compositions X and average absolute deviations AAD for the A-UNIFAC models (in bold) and P&M UNIFAC. | 81 |
| Table 4.15 Prediction results for lactose and maltose binary aqueous mixtures: number of experimental points NP, range of temperature T; range of compositions X and average absolute deviations AAD for the P&M UNIFAC and A-UNIFAC models (in bold characters). | 82 |

| | |
|---|-----|
| Table 4.16 Correlation (*) and prediction results for D-glucose, D-fructose and sucrose in mixed solvents (NP: number of experimental points; AAD: average absolute deviations for the P&M UNIFAC and A-UNIFAC models (in bold characters)). | 84 |
| Table 5.1 Integer constants (u and w) for cubic equations of state | 91 |
| Table 5.2 Comparison between the different G_{γ}^E /EoS mixing rules | 94 |
| Table 5.3 Association equations developed from the Heideman and Prausnitz approach. | 101 |
| Table 6.1 Association group models for water and alcohols used in the GCA-EoS. | 108 |
| Table 6.2 Self-association models defined in the GCA-EoS. | 109 |
| Table 6.3 Cross-association models defined in the GCA-EoS model. | 109 |
| Table 6.4 Experimental VLE database used for correlation (NS: number of data sets). | 112 |
| Table 6.5 Pure group parameters | 113 |
| Table 6.6 Binary interaction parameters | 113 |
| Table 6.7 GCA-EoS self and cross-association parameters. | 115 |
| Table 6.8 Pure component vapour pressure correlation. | 116 |
| Table 6.9 Z^{vap} prediction. | 117 |
| Table 6.10 Correlation results for VLE of acids and alkanes. | 118 |
| Table 6.11 Correlation results using the GCA-EoS and MHV2 models (alcohols + acids). | 121 |
| Table 6.12 Correlation results using the GCA-EoS and MHV2 models (water + acids). | 122 |
| Table 6.13 Correlation results using the GCA-EoS and MHV2 models (esters + acids). | 123 |
| Table 6.14 Correlation results using the GCA-EoS and MHV2 models (alcohols + esters). | 124 |
| Table 6.15 Correlation results using the GCA-EoS and MHV2 models (water or alcohols + ketones). | 126 |
| Table 6.16 Pure-group parameters | 128 |
| Table 6.17 Binary interaction parameters | 128 |
| Table 7.1 Infinite dilution activity coefficients of heptane and ethyl acetate in palmitic acid, mono-, di- and tripalmitin, a comparison between experimental data and model predictions. | 140 |
| Table 7.2 Glycerides composition (x_i) and correspondent aliphatic groups (n_{CH_2} and $n_{CH=CH}$) decomposition for cottonseed oil. | 140 |
| Table 8.1 Binary interaction parameters | 149 |
| Table C.1 Experimental γ^{∞} in mixtures of triacetin and palmitic acid | 186 |
| Table C.2 Experimental γ^{∞} in mixtures of tripalmitin and palmitic acid | 186 |
| Table C.3 Experimental γ^{∞} in mixtures of tripalmitin and palmitic acid. | 187 |
| Table C.4 Experimental γ^{∞} in mixtures of tripalmitin and palmitic acid. | 187 |

Nomenclature

| | |
|----------------|---|
| A | first coefficient of the Antoine equation |
| A | total energy of Helmholtz |
| A_α | association parameter from the modified UNIFAC model (Fu and Sandler, 1995) |
| a | molar energy of Helmholtz |
| a | energy parameter from the cubic EoS |
| a_i | activity of component i |
| a_{ij} | interaction parameter between component i and component j |
| a_{nm} | interaction parameters between groups n and m from the UNIFAC method |
| B | second coefficient of the Antoine equation |
| B_α | association parameter from the modified UNIFAC model (Fu and Sandler, 1995) |
| b | co-volume parameter from the cubic EoS |
| b_{ij} | interaction parameter between component i and component j |
| C | third coefficient of the Antoine equation |
| C_α | association parameter from the modified UNIFAC model (Fu and Sandler, 1995) |
| d | hard-sphere diameter |
| f_i° | fugacity evaluated at a reference state for component i |
| G | total Gibbs energy |
| g | attractive energy parameter per segment |
| g_{ii} | pure component i dispersive energy |
| g_{jk} | attractive energy parameter between the segment groups j and k |
| g_{jj}^\cdot | pure-group j energy parameter |
| g_{jj}^\cdot | pure-group j energy parameter |
| g_{jj}^* | pure-group j energy parameter |
| $g(d)$ | hard spheres radial distribution function |
| H | total enthalpy |
| h | molar enthalpy |
| K | equilibrium constant |
| k | Boltzmann constant |
| k_{ij} | binary interaction parameter between i and j |
| l_{ij} | binary interaction parameter between i and j |
| M | number of sites |
| M_w | molecular weight |
| m | molality |

| | |
|----------------|--|
| m | number of segments (SAFT equation) |
| N_{AV} | Avogadro's number |
| NC | number of components |
| NGA | number of associating groups |
| N_{OH} | number of equatorial hydroxyl groups of the constituent monosaccharides minus the ones used in the osidic bond |
| \bar{N}_{OH} | average number of equatorial OH groups |
| NP | number of experimental points |
| n | total number of moles |
| n_h | number of water molecules in the hydrated form |
| n_T | total real number of moles (after association) |
| n_o | number of moles before association |
| P | pressure |
| Q_k | group surface area |
| q | surface area |
| R | gas constant |
| R_k | group volume |
| r^{AB} | well width |
| r_i | volume for component i |
| S | total entropy |
| T | temperature |
| u | packaging factor |
| u | integer constant dependent of the equation of state |
| V | volume |
| w | integer constant dependent of the equation of state |
| y | vapour phase composition |
| X^{mon} | monomer fraction |
| X^{A_i} | fraction of non-bonded component i through site A |
| $X^{m,k}$ | fraction of non-bonded group k through site m |
| X^{A_k} | fraction of non-bonded group k , through site A , in the solution |
| $X_i^{A_k}$ | fraction of non-bonded group k , through site A , in component i |
| X_k | fraction of non-bonded group k in the solution |
| $X_{k,i}$ | fraction of non-bonded group k in component i |
| x | liquid phase composition |
| Z | compressibility factor |
| z | mole fraction |

\hat{z} number of nearest neighbors to any segment (set equal to 10)

Greek letters

| | |
|----------------------|---|
| $\alpha^{A_k B_j}$ | association parameter between site A of group k and site B of group j (Fu and Sandler, 1995) |
| α_{jk} | asymmetrical non-random parameter between the segment groups j and k |
| γ | activity coefficient |
| δ | average errors |
| Δ | property difference |
| Δ^{AB} | association strength between sites A and B |
| $\Delta^{A_i B_j}$ | association strength between site A of molecule (or group) i and site B of molecule (or group) j |
| ΔC_p | difference between the heat capacity of the pure liquid and solid |
| $\epsilon^{A_i B_j}$ | energy of association between site A of molecule (or group) i and site B of molecule (or group) j |
| η | reduced density |
| Θ_{jk} | group area fraction (Fu and Sandler, 1995) |
| θ | surface area fraction |
| κ^{AB} | volume of the well |
| $\kappa^{A_i B_j}$ | volume of association between site A of molecule (or group) i and site B of molecule (or group) j |
| λ | average length, surface or volume |
| ν^{OH} | number of OH groups |
| ν_k^i | number of groups k present in molecule i |
| ρ | molar density |
| ρ_k | density of group k density in the solution |
| $(\rho_k)_i$ | density of group k in pure component i |
| Γ_k | residual activity coefficient for group k in the solution |
| Γ_k^i | activity coefficient for group k in a reference solution containing type i molecules |
| τ_{nm} | Boltzmann factors between groups n and m |
| ϕ | osmotic coefficient |
| $\hat{\phi}_i$ | fugacity coefficient in the vapour phase |
| ϕ_i | volume fraction of component i |
| ϕ_i | fugacity coefficient of component i |

Superscripts

| | |
|-------|----------------------------|
| assoc | association |
| att | attractive |
| boil | boiling |
| comb | combinatorial |
| E | excess property |
| l | liquid |
| hs | hard-sphere |
| m | melting point |
| R | residual |
| rep | repulsive |
| res | residual |
| sat | saturation |
| seg | segment |
| t | triple point |
| v | vapour |
| vap | vapour |
| ° | standart state |
| ∞ | infinite dilution property |

Subscripts

| | |
|---|----------|
| c | critical |
| f | fusion |
| w | water |

Abbreviations

| | |
|------|--|
| AAD | average absolute deviations |
| EoS | equation of state |
| LCVM | linear combination Vidal-Michelsen mixing rule |
| LLE | liquid-liquid equilibria |
| MHV2 | modified Huron-Vidal second order mixing rule |
| PACT | perturberd anisotropic chain theory |
| SAFT | statistical associating fluid theory |
| SLE | solid-liquid equilibria |
| TAG | triacylglycerides |
| TG | triglyceride group |
| VLE | vapour-liquid equilibria |

Introduction

1.1 Introduction to the course

The course is the first of the computer science courses in the first year of the Bachelor's programme in Computer Science at the University of Twente. The course is designed to provide a solid foundation in the basic concepts and techniques of computer science. The course is divided into two parts: the first part covers the basic concepts and techniques of computer science, and the second part covers the application of these concepts and techniques to the design and implementation of computer systems.

The course is designed to be a self-contained introduction to the field of computer science. It is intended for students who are new to the field and who want to gain a solid foundation in the basic concepts and techniques of computer science. The course is also intended for students who want to refresh their knowledge of the basic concepts and techniques of computer science.

Chapter 1

Introduction

The course is designed to be a self-contained introduction to the field of computer science. It is intended for students who are new to the field and who want to gain a solid foundation in the basic concepts and techniques of computer science. The course is also intended for students who want to refresh their knowledge of the basic concepts and techniques of computer science.

The course is designed to be a self-contained introduction to the field of computer science. It is intended for students who are new to the field and who want to gain a solid foundation in the basic concepts and techniques of computer science. The course is also intended for students who want to refresh their knowledge of the basic concepts and techniques of computer science.

The course is designed to be a self-contained introduction to the field of computer science. It is intended for students who are new to the field and who want to gain a solid foundation in the basic concepts and techniques of computer science. The course is also intended for students who want to refresh their knowledge of the basic concepts and techniques of computer science.

1. Introduction

1.1 Importance and Motivation

This thesis is the result of the cooperation between the Laboratory of Separation and Reaction Engineering (LSRE), DEQ, *Faculdade de Engenharia da Universidade do Porto* and the *Planta Piloto de Ingeniería Química* (PLAPIQUI), *Universidad Nacional del Sur*, CONICET, Bahia Blanca, Argentina. Both institutions share a common interest in the application of process thermodynamics to the design and simulation of extraction, fractionation and purification processes of natural products.

The main purpose of this work is to develop practical engineering tools that can be used to predict the phase behaviour of highly complex mixtures. Three important characteristics of these highly complex mixtures will be taken into account:

- limited experimental information available. This characteristic suggests the use of a group-contribution approach because a large number of natural products can be described with a small number of groups.
- size differences between solvents and solutes.
- association effects.

This last point is very important because the thermodynamic modelling for mixtures where hydrogen bonding is present, in all range of compositions, is a difficult task for traditional activity coefficients models like the UNIFAC method or for equations of state models. This is particularly true for mixtures of associating components with inerts.

The equations developed and extended in this work should be readily applied to model the phase behaviour of two different natural products mixtures:

- The description of the low-pressure solid-liquid equilibria and vapor-liquid equilibria of carbohydrates (mono and disaccharides) in polar solvents (water and alcohols) has been studied at LSRE. These highly associated multi-component mixtures contain the sugar cyclic structures with many hydrophobic and hydrophilic substituents, mixed with polar solvents. This situation justifies the application of a group-contribution model with association.
- The study of fatty oils (triglycerides) and their derivatives (fatty acids, fatty acids esters, mono and diglycerides) in mixtures with near critical or supercritical fluids as solvents (propane or carbon dioxide), are being carried out at PLAPIQUI. These studies require a group-contribution thermodynamic model that can account for association effects and size differences. As a complement to the scarce experimental information for these systems, infinite dilution activity coefficients were measured by inverse gas chromatography.

In the next chapters, the development of two engineering tools for the description of mixtures with hydrogen bonding is presented: the A-UNIFAC model and the GCA equation of state. Moreover, the applications of these tools to low pressure carbohydrate mixtures with polar solvents (A-UNIFAC) and to high-pressure fatty oils and their derivatives with supercritical fluids (GCA-EoS) are shown.

1.2 Objectives

After presenting the main objectives and motivations for this work, a brief description of the remaining eight chapters that compose this thesis is presented.

Chapter 2 presents the main thermodynamic theories that have been proposed in the literature to describe association effects. A comparison between them is made, pointing out the main differences and similarities and the different approaches to self and cross-association models.

In this work, two models based on the perturbation theory are developed and presented: the A-UNIFAC model and the GCA equation of state. Each model development is followed by a case study.

The first model to be described is the A-UNIFAC method for the calculation of activity coefficients for liquid solutions (chapter 3). First, a brief description of the UNIFAC method and its modifications is given. Then, the analytical expressions for the association term from the A-UNIFAC model are presented, resulting in two different approaches for the extension of the model to cross-associating mixtures. The next steps are the parameterization and, finally, the presentation of the model correlation results and predictions obtained for mixtures containing esters, alcohols, water, acids, aromatics, alkyl chlorides and alkanes. The results are compared with those achieved for other equations based on the UNIFAC method.

Chapter 4 describes a low-pressure case study for the A-UNIFAC model: representation of the phase equilibria behaviour (vapour-liquid and solid-liquid equilibria) for mixtures of carbohydrates (mono and disaccharides) and solvents (water and/or alcohols).

The extension of the group-contribution association term to pressures up to the critical region demands the use of an equation of state.

Chapter 5 gives a general overview of the equations of state that are available for associating mixtures. Some of the modifications made for the description of these complex mixtures are presented, such as the introduction of new mixing rules or the development of specific association terms.

Then, the GCA-EoS model is presented in Chapter 6. The model is extended to several cross-associating mixtures containing esters, alcohols, water, acids, aromatics, carbon dioxide and alkanes. The parameterization strategy is described and followed by the presentation of correlation and prediction results obtained with the GCA-EoS. A comparison with the MHV2 equation of state is made.

Chapter 7 outlines a case study for the GCA-EoS model: the supercritical processing of vegetal oil derivatives. In this regard, the GCA-EoS is applied to mixtures of fatty oils and their derivatives (fatty acids, fatty acids esters, mono and diglycerides) with supercritical solvents like propane or carbon dioxide.

As a complement to the experimental information needed for the parameterization, experimental work was carried out, as described in Chapter 8. Infinite dilution activity coefficients of several components in mixtures of a triacylglyceride and a fatty acid were measured by inverse gas chromatography. The experimental technique, equipment and chemicals used and, the experimental data and corresponding parameterization are presented in this chapter.

Finally, the main conclusions are drawn on Chapter 9 together with some suggestions for future work.

Association Theories

2 Association Theories

2.1 Introduction

There are currently a large number of models available to describe the development of the human mind. This chapter will focus on the most widely used models, which are based on the idea of association. The main idea is that the mind is a collection of associations, and that the strength of these associations determines the behavior of the individual.

In the past, models of the mind have been based on the idea of a central processor, which takes in information from the environment and produces a response. This model is based on the idea of a central processor, which takes in information from the environment and produces a response. This model is based on the idea of a central processor, which takes in information from the environment and produces a response.

Chapter 2

Association Theories

2.2 Classical Theory

The theory of classical conditioning, developed by Ivan Pavlov, is one of the most widely used models of the mind. It is based on the idea of association, and it describes how the mind learns to associate a stimulus with a response. This model is based on the idea of association, and it describes how the mind learns to associate a stimulus with a response.

2. Association Theories

2.1 Introduction

There are essentially three different theories to describe association: the chemical theory, the quasi-chemical theory and the perturbation theory. These theories have been incorporated into activity coefficient models and into equations of state to model hydrogen bonding systems. The main differences are in the type of theoretical interpretation of the association.

In the next sections each of these theories is briefly described for some exemplifying mixtures containing self and cross-associating components with inerts. After this, a comparison between these theories is presented. As will be shown, despite the different origins of these theories, under some conditions, it is possible to find some similarities between them which can result in a numeric equivalence of the corresponding parameters.

In the last section of this chapter, various analytical and approximate solutions for mixtures containing cross-associating components are evaluated.

2.2 Chemical theory

This theory was initially developed by Dolezalek (1908). In this type of description, the hydrogen bonds result in the formation of new molecular species (oligomers) that interact with physical forces of the same type of the monomer. The oligomers distribution is defined by a chemical reactions equilibrium scheme, characterized in terms of temperature, composition and equilibrium constant.

2.2.1 Self-association

For example, consider a component M, with two association sites that can form linear chains. The equilibrium can be described by the infinite equilibrium model (e.g. alcohols):



$$\vdots$$


For a component N, with one association site, the following reaction is usually defined – the monomer-dimer model (e.g. acids).



To describe the equilibrium it is necessary to define some variables: the number of moles n_i , the mole fraction z_i and the correspondent activity \hat{a}_i for each oligomer of degree i in the mixture, the total true number of moles (after association) n_T and the total number of existent moles in the absence of association n_0 , as follows:

$$n_T = \sum_{i=1}^{\infty} n_i \quad (2.5)$$

$$n_0 = \sum_{i=1}^{\infty} i n_i \quad (2.6)$$

$$z_i = \frac{n_i}{n_T} \quad (2.7)$$

$$\frac{n_0}{n_T} = \sum_{i=1}^{\infty} i z_i \quad (2.8)$$

Each chemical reaction has an equilibrium constant K_{i+1} , defined as:

$$K_{i+1} = \frac{\hat{a}_{i+1}}{\hat{a}_i \hat{a}_1} = \exp\left(-\frac{\Delta H_{i+1}^0}{RT} + \frac{\Delta S_{i+1}^0}{R}\right) = \exp\left(-\frac{\Delta G_{i+1}^0}{RT}\right) \quad (2.9)$$

where ΔH^0 , ΔS^0 and ΔG^0 are the enthalpy, entropy and standard Gibbs energy of association, respectively, that correspond to the $i+1$ reaction and \hat{a}_i is the activity of species i in the solution.

For systems where the non ideality can be assigned exclusively to association, the solution properties can be obtained by solving the chemical equilibrium simultaneously with the material balances. Usually, it is assumed that, for the model of infinite equilibrium, the equilibrium constant does not depend on the chain size. In the case physical type interactions are not important, the oligomers mixture can be treated as an ideal solution. Then, Equation 2.9 is simplified since $\hat{a}_i = z_i$.

2.2.2 Cross-association

For mixtures containing more than one associating component, it is possible to define the following reaction schemes:

- (a) Monomers of different components (e.g. acetone and chloroform):



- (b) Oligomer of a component (e.g.: alcohol) + monomer of another component (e.g. acetone or chloroform);



- (c) Oligomers of different chemical species (e.g. alcohol and water).



In some cases, it is possible to estimate the cross equilibrium constants from the self-association equilibrium constants. Let us consider a mixture containing two components A and B that can self-associate to form dimers as described by equations 2.14 and 2.15, respectively. Additionally, they can cross-associate with each other forming the AB dimer (equation 2.13). In this case, the equilibrium constant K_{AB} can be calculated, by considering the cross dimerization reaction as a result of the sum of the following 3 reactions:



Assuming for reaction 2.13 that $\Delta H^\circ = 0$ (valid for components of similar chemical nature) and that $\Delta S^\circ = R \ln 2$ then,

$$\Delta G^{\circ}_{AB} = \Delta G^{\circ}_{2.13} + \Delta G^{\circ}_{2.14} + \Delta G^{\circ}_{2.15} = -RT \ln(2) + \frac{1}{2}(-RT \ln K_{A_2} - RT \ln K_{B_2}) \quad (2.17)$$

Finally, the cross dimerization equilibrium constant is given by:

$$K_{AB} = 2\sqrt{K_{A_2}K_{B_2}} \quad (2.18)$$

This result constitutes a reasonable approach for the situation where both components are chemically similar. It can be applied, for instance, to mixtures of two acids, using the monomer-dimer model.

2.3 Quasi-chemical theory

This approach is based on the theory of nets of liquids proposed by Guggenheim (1952). Molecules are considered to be positioned in a lattice structure and to interact with z neighbours.

Let us consider a binary mixture of A and B. The arrangement of the molecules will depend on the pair interaction energies between like (A - A and B - B) and unlike molecules (A - B), as in the following "reaction":



The correspondent equilibrium constant can be defined in function of the number of connections N as follows:

$$K = \frac{N_{AB}^2}{N_{AA}N_{BB}} \quad (2.20)$$

The association extension is calculated counting the number of connections between functional groups of adjacent cells. In this case, the hydrogen bonding interactions are not distinguished from the remaining interactions. They are represented by the same model with much stronger interaction energies. Contrary to the chemical theory there is no need to define previously which oligomers are being formed.

2.4 Physical theory

The fact that association interactions are short-ranged, strong and highly dependent on the orientation suggests their description through a potential model. In this context, Wertheim (Wertheim, 1984 a, b, 1986 a, b) developed a thermodynamic perturbation theory, based on statistical mechanics methods. An important practical result is the derivation of the expression for the residual energy of Helmholtz due to the association as a function of the fraction of molecules i not associated through the site A, X^A . Chapman *et al.* (1990) and, later, Huang and Radosz (1990) have simplified this theory, in order

to represent the specific interactions, applying the first order perturbation theory, TPT1 that is based on the following assumptions:

- the formation of net aggregates is allowed (for molecules with, at least, 2 sites), either linear or in chain, but not the formation of cyclical aggregates;
- the specification of sites angles is not allowed;
- the following hysterical effects can not be described for (Figure 2.1):

(a) Simultaneous bond between 1 site of a molecule *i* and 2 sites of a molecule *j*;

(b) Double bond between molecules (each one with 2 sites);

(c) Simultaneous bond of 2 molecules to the same site.

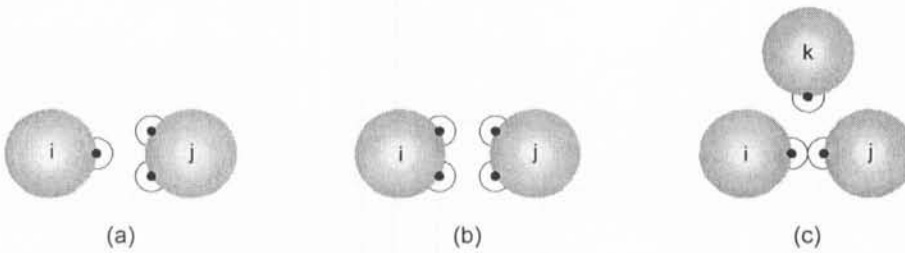


Figure 2.1 Schematic representation of the hysterical effects not allowed by TPT1.

- the activity of a given site is assumed to be independent of the other sites bonds in the same molecule (which means that the connection between two sites very close together in a given molecule with sites in two other different molecules is allowed).

This last argument allows the calculation of the oligomers distribution, using the Flory's distribution.

That is, the fraction of molecules *i* that exist as monomers (X_i^{mon}) is given by (Chapman *et al.*, 1990):

$$X_i^{\text{mon}} = \prod_{A_i} X^{A_i} \quad (2.21)$$

For instance, for a pure component with two association sites A and B, that can form linear chains, it is possible to evaluate the fraction of oligomers of degree *m*, *X* (*m*-mer), using the expression (Chapman *et al.*, 1990):

$$X(\text{m-mer}) = m(X^{A_i})^2(1 - X^{A_i})^{m-1} \quad (2.22)$$

In this case, $X^{A_i} = X^{B_i}$, so the monomer fraction is given by:

$$X^{\text{mon}} = X^{A_i} X^{B_i} = (X^{A_i})^2 \quad (2.23)$$

The fraction of molecules not associated through site A, X^{A_i} , is a function of the association strength between the sites A and B (Δ^{AB}). This association strength is quantified through a square well potential fluid model, as described in Figure 2.2. Each sphere has one different associating site (A or B). These two spheres can form an A-B dimer when their orientation and distance are adequate. The strength of that bond is a function of the association parameters ϵ^{AB} (depth of the well) and κ^{AB} (volume of the well, related with the distance r^{AB}).

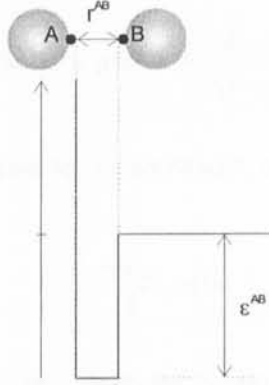


Figure 2.2 Schematic representation of the model of the square well potential.

The general expression for the residual Helmholtz energy for a pure component i , per mole of molecules, a^{assoc} , is (Chapman *et al.*, 1990):

$$\frac{a^{\text{assoc}}}{RT} = \sum_{A_i} \left(\ln X^{A_i} - \frac{X^{A_i}}{2} \right) + \frac{1}{2} M_i \quad (2.24)$$

where R is the universal gas constant, T is the absolute temperature of the system and M_i is the number of sites assigned to molecule i . The fraction of molecules not associated through the site A, X^{A_i} , is given by (Chapman *et al.*, 1990):

$$X^{A_i} = \left(1 + N_{AV} \sum_{B_i} \rho X^{B_i} \Delta^{AB} \right)^{-1} \quad (2.25)$$

where B_i represents all sites on molecule i , N_{AV} is the Avogadro number, ρ is the molar density of the mixture and Δ_{AB} is the association strength between sites A and B of the molecule and is expressed as (Chapman *et al.*, 1990):

$$\Delta^{AB} = d^3 g(d)^{seg} \kappa^{AB} \left[\exp\left(\frac{\epsilon^{AB}}{kT}\right) - 1 \right] \quad (2.26)$$

where k is the Boltzmann constant. The segment radial distribution function ($g(d)^{seg}$) is a function of the segment diameter d , and it quantifies the probability of a segment contacting another to establish a specific bond. The segments are represented as hard spheres which allows approximating $g(d)^{seg}$ as the hard sphere radial distribution function (Carnahan and Starling, 1969):

$$g(d)^{seg} \approx g(d)^{hs} = \frac{2 - \eta}{2(1 - \eta)^3} \quad (2.27)$$

where η is the reduced density, calculated for m segments, as follows:

$$\eta = \frac{\pi N_{AV}}{6} \rho d^3 m \quad (2.28)$$

The extension of TPT1 to mixtures with NC components, results in the following expressions, for the residual energy of Helmholtz,

$$\frac{a^{assoc}}{RT} = \sum_{i=1}^{NC} z_i \left[\sum_{A_i} \left(\ln X^{A_i} - \frac{X^{A_i}}{2} \right) + \frac{1}{2} M_i \right] \quad (2.29)$$

where z_i is the mole fraction of component i , and for the fraction not associated through site A:

$$X^{A_i} = \left(1 + N_{AV} \sum_{j=1}^{NC} \sum_{B_j} \rho_j X^{B_j} \Delta^{A B_j} \right)^{-1} \quad (2.30)$$

in which $\Delta^{A B_j}$ is the association strength between site A of molecule i and site B of molecule j and is given by:

$$\Delta^{A B_j} = d_{ij}^3 g_{ij}(d_{ij})^{seg} \kappa^{A B_j} \left[\exp\left(\frac{\epsilon^{A B_j}}{kT}\right) - 1 \right] \quad (2.31)$$

$$d_{ij} = \frac{d_{ii} + d_{jj}}{2} \quad (2.32)$$

The radial distribution function $g(d_{ij})$ for mixtures of hard spheres (Reed and Gubbins, 1973) quantifies the probability of a segment with diameter d_{ij} contacting a segment with diameter d_{jj} , forming an association bonding.

To model association, it is necessary to define the number of association groups, the number of active sites and, also, which interactions between association sites are different from zero. In the next sections, some of the self and cross-association models will be described. The analytical solution of equation 2.30 will be presented for the cases where it exists.

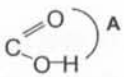
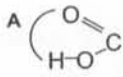
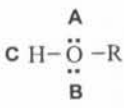
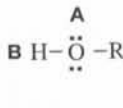
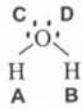
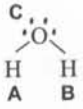
2.4.1 Self-association

The expressions obtained for X^{A_i} are presented for a pure component (Table 2.1) with the corresponding assumptions concerning Δ and X^{A_i} .

For each associating group it is necessary to specify the number of sites. Every site is labelled with a capital letter (A, B, C, etc). The interactions between each pair of sites is characterized by the correspondent association strength Δ .

On the second column the rigorous model that describes the association component is schematically presented. The approximated models, proposed by Huang and Radosz (1990), for the Statistical Associating Fluid Theory (SAFT), are also shown on the 3rd, 4th and 5th columns. For these cases, it is possible to find an analytical solution for X^{A_i} .

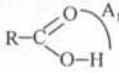
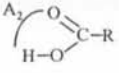
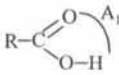
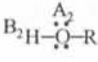
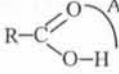

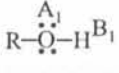
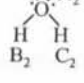
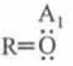
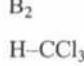
Table 2.1 Self-association types for pure components: simplifications in Δ and X^{A_i} and resulting expressions for X^{A_i} .

| Component | Rigorous Type | SAFT approximation | Simplifications in Δ and X^{A_i} | X^{A_i} |
|-----------|---|---|---|---|
| Acid | 1A  | 1A  | $\Delta_{AA} = \Delta \neq 0$ | $X^{A_i} = X^{\text{mon}} = \frac{-1 + \sqrt{1 + 4\rho\Delta}}{2\rho\Delta}$ |
| Alcohols | 3B  | 2B  | $\Delta_{AB} = \Delta_{BA} = \Delta \neq 0$ $\Delta_{AA} = \Delta_{BB} = 0$ $X^{A_i} = X^{B_i}$ | $X^{A_i} = \sqrt{X^{\text{mon}}} = \frac{-1 + \sqrt{1 + 4\rho\Delta}}{2\rho\Delta}$ |
| Water | 4C  | 3B  | $\Delta_{AA} = \Delta_{AB} = \Delta_{BB} = \Delta_{CC} = 0$ $\Delta_{AC} = \Delta_{BC} = \Delta \neq 0$ $X^{A_i} = X^{B_i}$ $X^{C_i} = 2X^{A_i} - 1$ | $X^{A_i} = \frac{-1 + \rho\Delta + \sqrt{(1 + \rho\Delta)^2 + 4\rho\Delta}}{4\rho\Delta}$ |

2.4.2 Cross-association

Table 2.2 shows some of the practical cases of binary mixtures with components that self-associate and/or suffer solvation. The models and the correspondent simplifications in Δ , were proposed by Huang and Radosz (1991) and Wolbach and Sandler (1998), for the extension of SAFT-EoS (Statistical Associating Fluid Theory Equation of State) to binary mixtures containing more than one associating component.

Table 2.2 Cross-association models: approximations in Δ .

| Mixture | Species 1 | Species 2 | Approximations in Δ |
|---------|---|---|---|
| 1A+1A |  |  | $\Delta_{A_1A_1} \neq \Delta_{A_2A_2} \neq \Delta_{A_1A_2} \neq 0$ |
| 1A+2B |  |  | $\Delta_{A_1A_1} \neq \Delta_{A_2A_2} \neq 0; \Delta_{A_1A_2} = \Delta_{A_1B_2} \neq 0$ others=0 |
| 1A+3B |  |  | $\Delta_{A_1A_1} \neq 0; \Delta_{A_2B_2} = \Delta_{A_2C_2} \neq 0$ $\Delta_{A_1A_2} = \Delta_{A_1B_2} = \Delta_{A_1C_2} \neq 0; \text{others}=0$ |
| 2B+3B |  |  | $\Delta_{A_1B_1} \neq 0; \Delta_{A_2B_2} = \Delta_{A_2C_2} \neq 0$ $\Delta_{A_1B_2} = \Delta_{A_1C_2} = \Delta_{A_2B_1} \neq 0; \text{others}=0$ |
| 1A+1B |  |  | $\Delta_{A_1A_1} = \Delta_{B_2B_2} = 0$ $\Delta_{A_1B_2} \neq 0$ |

From the cases described in the previous table, it is only possible to find an analytical solution for the not associated fractions of the last case (1A+1B). For a binary mixture (M+N) where each component has one association site and, association is only allowed between M and N, the following expressions are obtained:

$$X^{M_1} = \frac{2}{1 + \rho\Delta(x_2 - x_1) + \sqrt{(1 + \rho\Delta)^2 - 4(\rho\Delta)^2 x_1 x_2}} \quad (2.33)$$

$$X^{N_2} = \frac{1}{1 + \rho\Delta x_2 X^{M_1}} \quad (2.34)$$

For mixtures with more complex association models, in general, it is not possible to find an analytical solution. For these cases, approximate or numerical solutions are used to solve the non-linear systems of equations obtained from Equation 2.30.

2.4.2.1 Cross-association parameters

The extension of association models to mixtures with two or more associating species, requires not only a set of self-association parameters, but also specific cross-association parameters. These parameters are usually estimated by treating them as additional adjustable parameters, and/or by establishing appropriate combining rules between the self-association parameters:

- (a) A physically realistic hypothesis is to assume the geometric mean of the energies of association of the pure components and the arithmetic mean of the association volumes (Fu and Sandler, 1995);

$$\varepsilon^{A_i B_j} = \sqrt{\varepsilon^{A_i} \varepsilon^{B_j}}; \quad \kappa^{A_i B_j} = \frac{\kappa^{A_i} + \kappa^{B_j}}{2} \quad (2.35)$$

- (b) Suresh and Elliot (1992) have used the following geometric mean respect to the association strength:

$$\Delta^{A_i B_j} = \sqrt{\Delta^{A_i} \Delta^{B_j}} \quad (2.36)$$

- (c) When the self-association parameters differ much in size, an interaction parameter k_{ij} can be introduced:

$$\Delta^{A_1 A_2} = k_{ij} \sqrt{\Delta^{A_1} \Delta^{A_2}} \quad (2.37)$$

- (d) Voutsas *et al.* (1999) have also used other combining rules:

$$\varepsilon^{A_i B_j} = \frac{\varepsilon^{A_i} + \varepsilon^{B_j}}{2}; \quad \kappa^{A_i B_j} = \frac{\kappa^{A_i} + \kappa^{B_j}}{2} \quad (2.38)$$

$$\varepsilon^{A_i B_j} = \frac{\varepsilon^{A_i} + \varepsilon^{B_j}}{2}; \quad \kappa^{A_i B_j} = \sqrt{\kappa^{A_i} \kappa^{B_j}} \quad (2.39)$$

$$\varepsilon^{A_i B_j} = \sqrt{(\varepsilon^{A_i} \varepsilon^{B_j})}; \quad \kappa^{A_i B_j} = \sqrt{\kappa^{A_i} \kappa^{B_j}} \quad (2.40)$$

2.5 Equivalence between chemical and physical theories

Though the theories described in the previous section have different physical and mathematical basis, in some cases they result in analytical expressions with the same functional form. This can result in a numeric equivalence of the association parameters.

2.5.1 Ideal gas example

The monomer-dimer model will be applied to the vapour phase of an organic acid using the chemical and the TPT1 theories. From the chemical theory point of view, the following equilibrium constant can be defined:

$$K = \frac{z_2 \hat{\phi}_2}{z_1^2 \hat{\phi}_1^2} \frac{1 \text{ atm}}{P} \quad (2.41)$$

Where z_1 is the monomer fraction, z_2 is the dimer fraction and $\hat{\phi}_1$ and $\hat{\phi}_2$ are the monomer and dimer fugacity coefficients in the mixture, respectively. At low pressures, a reasonable assumption is to consider that the mixture of monomer and dimer molecules behave as an ideal gas. In that case the fugacity coefficients are unity. Then, replacing the material balance ($z_1 + z_2 = 1$) into Equation 2.41, simplifies it to:

$$K P z_1^2 + z_1 - 1 = 0 \quad (2.42)$$

$$z_1 = \frac{n_1}{n_1 + n_2} = \frac{n_1}{n_T} \quad (2.43)$$

The physical theory predicts a fraction of molecules not associated through the site A, X^{A_i} , as follows:

$$\rho \Delta (X^{A_i})^2 + X^{A_i} - 1 = 0 \quad (2.44)$$

$$X^{A_i} = \frac{n_1}{n_1 + 2n_2} = \frac{z_1}{2 - z_1} = \frac{n_1}{n_o} \quad (2.45)$$

Assuming again ideal gas behaviour, the density is given by:

$$\rho = \frac{n_o}{V} = \frac{P}{RT} \frac{n_o}{n_T} = \frac{P}{RT} \frac{n_o}{n_1} \frac{n_1}{n_T} = \frac{P}{RT} \frac{z_1}{X^{A_i}} \quad (2.46)$$

where V is the total volume. Replacing Equation 2.46 in Equation 2.44:

$$\begin{cases} \frac{1}{2} \frac{P}{RT} \Delta z_1^2 + z_1 - 1 = 0 \\ KPz_1^2 + z_1 - 1 = 0 \end{cases} \Rightarrow \Delta = 2RTK \quad (2.47)$$

On Table 2.3 are listed the expressions obtained for other cases, following the same procedure. In cases 3B and 4C, this equivalence is only valid in the limit case of infinite dilution of the associating component (Wolbach and Sandler, 1997).

Table 2.3 Parameters equivalence.

| Scheme | Equivalence |
|--------|--------------------------|
| 1A | $\Delta = 2RTK_{eq}$ |
| 2B | $\Delta = RTK_{eq}$ |
| 3B* | $\Delta = 0.5 RTK_{eq}$ |
| 4C* | $\Delta = 0.25 RTK_{eq}$ |

*in the limit of no association, that is, $X^A \rightarrow 1$

2.5.2 Real gas example

Economou and Donohue (1991) compared the three theories for the case where the non specific interactions are also important. These are taken into account by the following equations of state developed for associating fluids:

- APACT-EoS (Associated Perturbed Anisotropic Chain Theory) developed by Ikonomou and Donohue (1986) using the chemical theory;
- SLP-EoS (Sanchez-Lacombe-Panayiotou) proposed by Panayiotou and Sanchez (1991) based on the quasi-chemical theory;
- SAFT (Statistical Associating Fluids Theory) presented by Chapman *et al.*, 1990, that has an explicit association term derived from the first order perturbation theory.

As an example, Table 2.4 shows the results obtained for two types of mixtures:

- Mixture I: inert (N)+ self-associating component with one associating site (M);
- Mixture II: inert (N) + self-associating component with two sites (M).

For all the cases it is possible to find an analytical solution except for the SLP-EoS that cannot be applied to a binary mixture of type I.

Table 2.4 Monomer fraction expressions obtained for mixtures of types I and II.

| | Mixture I | Mixture II |
|-------|--|---|
| APACT | $\frac{2}{1 + \sqrt{1 + 4\rho K'' x_M}}$ | $\frac{2}{1 + 2\rho K' x_M + \sqrt{1 + 4\rho K'' x_M}}$ |
| SAFT | $\frac{2}{1 + \sqrt{1 + 4\rho \Delta' x_M}}$ | $\frac{2}{1 + 2\rho \Delta' x_M + \sqrt{1 + 4\rho \Delta x_M}}$ |
| SLP | ----- | $\frac{2}{1 + 2\rho K^* x_M + \sqrt{1 + 4\rho K^* x_M}}$ |

The association parameters K' , K'' and Δ are given by APACT : $K' = KRTe^g$; $K'' = 2KRTe^g$; SAFT : $\Delta = f(T, h)$; SLP : $K^ = K\nu^*/r$.

2.6 Chemical and physical cross-association solutions

The application of this model to mixtures containing more than one associating component requires solving a system of non-linear equations in X^{A_i} (obtained from Equation 2.30). In most cases, the system of equations has to be solved numerically. This situation increases the complexity of the calculations since the application of this theory to model liquid-liquid and vapour-liquid equilibria using excess Gibbs energy models or equations of state demands the calculation of first or second derivatives of the free energy with respect to composition.

Some alternatives to the numerical solution have been proposed. Sometimes it is possible to simplify the system of equations by setting some cross-association strengths equal to each other or adopting some combining rules to the cross-association parameters ε and κ (see section 2.4.2.1). Other authors have additionally developed approximate solutions to the fraction of non-bonded sites (Economou *et al.* 1990).

Some examples are considered. The expressions that can be obtained, in terms of variables of the physical theory, are presented for three examples of cross-association.

First, let us consider two different mixtures with the following composition:

- (a) Mixture I: inert component + component 1 with one site (A_1) + component 2 with one site (A_2). Both components can self-associate with association strengths $\Delta_{A_1A_1}$ and $\Delta_{A_2A_2}$, respectively, and cross-associate with strength $\Delta_{A_1A_2}$, that is:

$$\Delta_{A_1A_1} \neq \Delta_{A_2A_2} \neq \Delta_{A_1A_2} \neq 0 \quad (2.48)$$

- (b) Mixture II: inert component + component 1 with two sites (A_1 and B_1) + component 2 with two sites (A_2 and B_2). Again, both components can self-associate with association strengths $\Delta_{A_1B_1}$ and $\Delta_{A_2B_2}$, respectively. As a simplification, both cross-association strengths, $\Delta_{A_1B_2}$ and $\Delta_{A_2B_1}$, are assumed equal and different from zero.

$$\begin{cases} \Delta_{A_1B_1} \neq \Delta_{A_2B_2} \neq 0 \\ \Delta_{A_1B_2} = \Delta_{A_2B_1} = \Delta^* \neq 0 \end{cases} \quad (2.49)$$

Applying Equation 2.30, the following systems of non-linear equations are obtained:

| Mixture I | Mixture II |
|--|--|
| $\begin{cases} X^{A_1} = X_1 = \frac{1}{1 + \rho_1 X_1 \Delta_{A_1A_1} + \rho_2 X_2 \Delta_{A_1A_2}} \\ X^{A_2} = X_2 = \frac{1}{1 + \rho_1 X_1 \Delta_{A_1A_2} + \rho_2 X_2 \Delta_{A_2A_2}} \end{cases}$ | $\begin{cases} X^{A_1} = X^{B_1} = X_1 = \frac{1}{1 + \rho_1 X_1 \Delta_{A_1B_1} + \rho_2 X_2 \Delta^*} \\ X^{A_2} = X^{B_2} = X_2 = \frac{1}{1 + \rho_1 X_1 \Delta^* + \rho_2 X_2 \Delta_{A_2B_2}} \end{cases}$ |

Mathematically, these systems of equations are identical. For this reason, the several possible solutions will be presented in terms of the variables of example (b).

- Solution 1:

For these systems Equation 2.30 results in two independent quartic equations, for which there is an analytical solution (Kraska, 1998):

$$\begin{aligned} & (X_k)^4 \rho_k^2 \Delta_k (\Delta_1 \Delta_k - \Delta^*) + (X_k)^3 [2\rho_k \Delta_k \Delta_1 - \Delta^* \rho_k (\Delta_k + \Delta^*)] + \\ & + (X_k)^2 [\Delta_1 - 2\rho_k \Delta_k \Delta_1 + \Delta^* (\rho_k \Delta^* - 1) - \rho_1 \Delta^*] + (X_k) (-2\Delta_1 + \Delta^*) + \Delta_1 = 0 \end{aligned} \quad (2.50)$$

Here the self-association strength of a component k is referred to as Δ_k and $k \neq I$.

- Solution 2:

To assume that the cross-association strength is equal to the geometric mean of the self-association strengths ($\Delta_{A_1B_2} = \Delta_{A_2B_1} = \Delta^* = \sqrt{\Delta_{A_1B_1}\Delta_{A_2B_2}}$) reduces this quartic equation to a cubic (Suresh and Elliot, 1992):

$$(X_k)^3(\rho_k \Delta^* \Delta_k - \rho_k \Delta_k^2) + (X_k)^2[\Delta^* - \Delta_k - (\rho_k + \rho_l)\Delta_k \Delta^*] + (X_k)(-2\Delta^* + \Delta_k) + \Delta^* = 0 \quad (2.51)$$

- Solution 3

This approximate solution was derived by Economou *et al.* (1990), as a result of the application of the chemical theory to APACT-EoS, being expressed according to variables of the physical theory.

$$\begin{cases} X^{A_1} = X^{B_1} = X_1 = \frac{2}{1 + \sqrt{1 + 4\rho\Delta_{A_1B_1}}} \\ X^{A_2} = X^{B_2} = X_2 = \frac{2}{1 + \sqrt{1 + 4\rho\Delta_{A_2B_2}}} \end{cases} \quad (2.52)$$

In this case two self-associations are considered to exist in parallel. There is no cross interaction between the two associating groups.

- Solution 4

This approximation is also originated in a chemical theory model applied to a cubic equation of state by Anderko (1989), and is also expressed in terms of variables of the physical theory. The same association strength is assumed between sites A_1 and B_2 and sites A_2 and B_1 , *i.e.*, $\Delta_{A_1B_2} = \Delta_{A_2B_1} = \Delta^*$.

$$\begin{cases} X^{A_1} = X^{B_1} = X_1 = \frac{2}{1 + \sqrt{1 + 4(\rho_1\Delta_{A_1B_1} + \rho_2\Delta^*)}} \\ X^{A_2} = X^{B_2} = X_2 = \frac{2}{1 + \sqrt{1 + 4(\rho_2\Delta_{A_2B_2} + \rho_1\Delta^*)}} \end{cases} \quad (2.53)$$

- (c) Mixture III: inert component + component 1 with one site (A_1) + component 2 with two sites (A_2 and B_2).

In this last example, the following system of non linear equations is obtained:

$$\begin{cases} X^{A_1} = \frac{1}{1 + \rho_1 X^{A_1} \Delta_{A_1 A_1} + \rho_2 X^{A_2} \Delta_{A_1 A_2} + \rho_2 X^{B_2} \Delta_{A_1 B_2}} \\ X^{A_2} = \frac{1}{1 + \rho_1 X^{A_1} \Delta_{A_2 A_1} + \rho_2 X^{B_2} \Delta_{A_2 B_2}} \\ X^{B_2} = \frac{1}{1 + \rho_1 X^{A_1} \Delta_{B_2 A_1} + \rho_2 X^{A_2} \Delta_{A_2 B_2}} \end{cases} \quad (2.54)$$

Assuming that site A_1 associates with the same strength either with sites A_2 or B_2 , $\Delta_{A_1 A_2} = \Delta_{A_1 B_2} = \Delta^*$, the system 2.54 simplifies to:

$$\begin{cases} X^{A_1} = \frac{1}{1 + \rho_1 X^{A_1} \Delta_{A_1 A_1} + 2\rho_2 X^{A_2} \Delta^*} = X_1 \\ X^{A_2} = \frac{1}{1 + \rho_1 X^{A_1} \Delta^* + \rho_2 X^{B_2} \Delta_{A_2 B_2}} = X^{B_2} = X_2 \end{cases} \quad (2.55)$$

This system also results in the resolution of one quartic equation in X_2 :

$$\begin{cases} X_2^4 \rho_2^2 \Delta_2 (\Delta_2 \Delta_1 - 2\Delta^*) + X_2^3 [2\rho_2 \Delta_2 \Delta_1 - \Delta^* \rho_2 (\Delta_2 + 2\Delta^*)] + \\ + X_2^2 [\Delta_1 - 2\rho_2 \Delta_2 \Delta_1 + \Delta^* (2\rho_2 \Delta^* - 1) - \rho_1 \Delta^*] + X_2 (-2\Delta_1 + \Delta^*) + \Delta_1 = 0 \\ X_1 = \frac{1 - X_2 - \rho_2 \Delta_2 X_2^2}{1 + \rho_1 \Delta^* + X_2} \end{cases} \quad (2.56)$$

where $\Delta_{A_1 A_1} = \Delta_1$ and $\Delta_{A_2 B_2} = \Delta_2$. In this case, to consider the cross-association strength as the geometric mean of the self-association strengths does not result in a reduction of the grade of the polynomial.

2.7 Conclusions

In this chapter the chemical, quasi-chemical and perturbation theories have been briefly discussed and compared. The chemical theory describes hydrogen bonding by defining a chemical reaction scheme; the quasi-chemical theory counts the number of hydrogen bonds between proton donors and proton acceptors of adjacent cells and the TPT1 calculates the energy of hydrogen bonding by introducing a potential function. Ecomonou and Donohue (1991) showed that, in most cases, these theories result in expressions for the monomer fraction that have the same functional form. This allows a direct comparison between parameters of different theories and to express the approximate solutions used in the chemical theory in terms of physical theory variables, as shown by Kraska (1998). The expressions obtained for mixtures containing at most two cross-associating components have been derived. Whenever existent, the correspondent analytical solution has also been presented.

Phase equilibria described by G^E models

3.1 The binary G^E model

The phase diagram of a binary mixture of two liquids is shown in Fig. 3.1. The liquid phase is stable at high temperatures and low pressures. The solid phase is stable at low temperatures and high pressures. The critical point is the point at which the liquid and solid phases coexist at the highest temperature and pressure.

$$RT \ln \gamma_1 = G^E_1$$

3. Phase equilibria described by G^E models

3.1 Introduction

In general, local composition models do not describe appropriately the behaviour of liquid mixtures containing associating components. When present, the association and solvation effects have a major contribution to the properties of solutions. The modelling of activity coefficients in these solutions represents a difficult problem, particularly for the highly non-ideal mixtures between associating and non-polar species. Traditional thermodynamic models, such as UNIFAC (Fredenslund *et al.*, 1975) have difficulties in describing adequately the activity coefficients of these solutions in all range of compositions, from infinite dilution to high concentrations of the associating component.

Some modifications were developed to the original UNIFAC model (Fredenslund *et al.*, 1975) in order to improve its application range. The new models result from modifications in the combinatorial term and/or residual term (section 3.1.2), and/or by the explicit consideration of a separate association term based on a physical theory (section 3.1.3).

3.1.1 The original UNIFAC model

The original UNIFAC model (Fredenslund *et al.*, 1975; Fredenslund *et al.*, 1977) is a group-contribution method that calculates the logarithm of the activity coefficient γ as a sum of two contributions: a residual term (res) and a combinatorial term (comb).

$$\ln \gamma_i = \ln \gamma_i^{\text{comb}} + \ln \gamma_i^{\text{res}} \quad (3.1)$$

The combinatorial term takes into account the liquid phase non-idealities due to molecular size and molecular shape effects while the residual term quantifies the group energetic interactions.

The combinatorial term is a function of the volume fraction (ϕ_i) and surface area fraction (θ_i) for component i in the mixture (Fredenslund *et al.*, 1977):

$$\ln \gamma_i^{\text{comb}} = 1 - \frac{\phi_i}{x_i} + \ln \frac{\phi_i}{x_i} - 5q_i \left(1 - \frac{\phi_i}{\theta_i} + \ln \frac{\phi_i}{\theta_i} \right) \quad (3.2)$$

The first three terms are the Flory-Huggins expression and the last one is the Staverman-Guggenheim correction term. The molecular surface area and volume fractions are calculated, as follows:

$$\theta_i = \frac{q_i x_i}{\sum_j q_j x_j} \quad \text{and} \quad \phi_i = \frac{r_i x_i}{\sum_j r_j x_j} \quad (3.3)$$

The volume r_i and surface area q_i for component i are calculated from the group volume (R_k) and surface area (Q_k) values:

$$r_i = \sum_k v_k^i R_k \quad \text{and} \quad q_i = \sum_k v_k^i Q_k \quad (3.4)$$

where v_k^i is the number of groups k present in molecule i .

The residual contribution is calculated as the sum of the individual group-contributions in the solution minus the individual group-contributions in pure component i .

$$\ln \gamma_i^{\text{res}} = \sum_k v_k^i (\ln \Gamma_k - \ln \Gamma_k^i) \quad (3.5)$$

In this equation, Γ_k is the residual activity coefficient for group k in the solution and Γ_k^i is the activity coefficient for group k in a reference solution containing solely type i molecules:

$$\ln \Gamma_k = Q_k \left[1 - \ln \left(\sum_m \theta_m \tau_{mk} \right) - \sum_m \left(\frac{\theta_m \tau_{km}}{\sum_n \theta_n \tau_{nm}} \right) \right] \quad (3.6)$$

The surface area fraction (θ_m) for group m is calculated from the expression:

$$\theta_m = \frac{Q_m X_m}{\sum_n Q_n X_n} \quad (3.7)$$

where X_m is the mole fraction for group m . The Boltzmann factors (τ_{nm}) can be calculated from the interaction parameters a_{nm} between groups n and m :

$$\tau_{nm} = \exp\left(-\frac{a_{nm}}{T}\right) \quad (3.8)$$

The model was successfully applied to predict activity coefficients for non-polymeric, non-electrolyte mixtures in the temperature range from 275 to 425 K, at low to moderate pressures (Fredenslund *et al.*, 1977).

The original UNIFAC model, however, is not able to simultaneously represent vapour-liquid equilibria (VLE), liquid-liquid equilibria (LLE), excess enthalpy data (h^E) and infinite dilution activity coefficients (γ^∞) data with the same set of parameters. Magnussen *et al.* (1981) presented a specific parameter table for LLE and Bastos *et al.* (1988) proposed a parameter table based on infinite dilution activity coefficients data (γ^∞) using the modification suggested by Kikic *et al.* (1980) for the combinatorial term. The use of a single parameter table has been one of the motivations for the development of several modifications to the original UNIFAC model, namely: new expressions for the combinatorial term; the introduction of temperature dependent interaction parameters from the residual term and/or the adjustment of the R_k and Q_k parameters (Larsen *et al.*, 1987; Weidlich and Gmehling, 1987).

3.1.2 Modified UNIFAC models

The most divulged modified UNIFAC models are the modified UNIFAC of Dortmund (Weidlich and Gmehling, 1987) and the modified UNIFAC of Lyngby (Larsen *et al.*, 1987). Both models propose a different combinatorial part and different temperature dependence for the a_{nm} interaction parameter. The modifications introduced are resumed on Table 3.1. Additionally, Weidlich and Gmehling (1987) proposed different values for the R_k and Q_k parameters by treating them as adjustable parameters.

Small improvements have been obtained for VLE relative to the original UNIFAC model. On the other hand, the temperature dependent parameters have improved significantly the description of excess enthalpies data (h^E). The modified UNIFAC of Dortmund has also included infinite dilution activity coefficients data (γ^∞) in the correlation database which allows a better description of this type of data.

That was not the case of the modified UNIFAC of Lyngby that presents poorer results for γ^∞ .

Table 3.1 Differences between the UNIFAC model and the modified UNIFAC models.

| Model | $\gamma^{\text{combinatorial}}$ | γ^{residual} |
|----------------------------|---|--|
| Original UNIFAC | $1 - \frac{\phi_i}{x_i} + \ln \frac{\phi_i}{x_i} - 5q_i \left(1 - \frac{\phi_i}{\theta_i} + \ln \frac{\phi_i}{\theta_i} \right)$ | $\phi_i = \frac{r_i}{\sum_j r_j x_j}$ a_{nm} |
| Modified UNIFAC (Dortmund) | $1 - \frac{\phi'_i}{x_i} + \ln \frac{\phi'_i}{x_i} - 5q_i \left(1 - \frac{\phi'_i}{\theta_i} + \ln \frac{\phi'_i}{\theta_i} \right)$ | $\phi'_i = \frac{r_i^{3/4}}{\sum_j r_j^{3/4} x_j}$ $a_{nm} + b_{nm}T + c_{nm}T^2$ |
| Modified UNIFAC (Lyngby) | $1 - \frac{\phi''_i}{x_i} + \ln \frac{\phi''_i}{x_i}$ | $\phi''_i = \frac{r_i^{2/3}}{\sum_j r_j^{2/3} x_j}$ $a_{nm} + b_{nm}(T - T_o) + c_{nm} [T \ln(T/T_o) + T - T_o]$ |

3.1.3 G^E models that include the physical theory

Fu *et al.* (1996) have developed two association models using Wertheim's association theory. In both models an association term is added to the residual and combinatorial terms of the original UNIFAC model: in the case of the UNIFAC-AG model, association occurs between functional groups and in the case of the UNIFAC-AM model, association is assumed to occur between molecules. As an example, some of the key equations of the A-UNIFAC-AG model will be presented. The total residual energy of Helmholtz, based on a group-contribution approach, is calculated in the usual way:

$$\frac{a^{\text{assoc}}}{RT} = \sum_{k=1}^{\text{NGA}} z_k \left[\sum_{A_k} \left(\ln X^{A_k} - \frac{X^{A_k}}{2} \right) + \frac{1}{2} M_k \right] \quad (3.9)$$

where NGA is the number of associating groups. The fraction of non-bonded group k through site A (X^{A_k}) is approximately given as:

$$X^{A_k} = \frac{1}{1 + \sum_j \sum_{B_j} \Theta_{jk} \alpha^{A_k B_j} X^{B_j}} \quad (3.10)$$

where $\alpha^{A_k B_j}$ is the association parameter between site A of group k and site B of group j . The group area fraction Θ_{jk} is defined as:

$$\Theta_{jk} = \frac{\Theta_j \exp(-a_{jk}/T)}{\sum_n \Theta_n \exp(-a_{nk}/T)} \quad (3.11)$$

For the self-associating mixtures the residual interaction parameters are fitted simultaneously with the temperature dependent association parameter α ($\alpha = \exp(A_\alpha + B_\alpha/T)$). The cross-associating

parameters are estimated together with the residual interaction parameters. The procedure is similar for the UNIFAC-AM model with a slight difference: the molecular association parameter is a function of temperature and, also, of the molecular weight M_w , as follows: $\alpha = \exp(A_\alpha + B_\alpha/T + C_\alpha M_w)$.

The database used in the optimization step includes VLE of binary mixtures of alcohols, water, acids and inerts, VLE of chloroform and ketones binary mixtures and LLE of water-alkanes. Both models present slight improvements in the correlation of VLE data relatively to the original UNIFAC model. These models were applied for the prediction of the vapour-liquid equilibria of ternary mixtures containing at most two associating groups.

3.2 A-UNIFAC Model

Mengarelli *et al.* (1999) have recently presented a modified UNIFAC model that takes into account association effects. This model adds an association term to the original UNIFAC combinatorial and residual expressions (Fredenslund *et al.*, 1975). The association term is based on Wertheim's theory for fluids with highly directed attractive forces (Wertheim, 1984 a, b, 1986 a, b) and it follows the group-contribution approach proposed by Zabaloy *et al.* (1993) and Gros *et al.* (1996) for the GCA-EoS equation.

In the present work this UNIFAC association model (A-UNIFAC) is extended for the calculation of activity coefficients in mixtures containing alcohols, water, carboxylic acids, esters, alkanes, aromatic hydrocarbons and alkyl chlorides.

3.2.1 Description of the A-UNIFAC model

The non-ideal behaviour is described as the sum of three independent contributions to the excess Gibbs energy function G^E :

$$G^E = G^{\text{comb}} + G^{\text{res}} + G^{\text{assoc}} \quad (3.12)$$

which becomes in terms of activity coefficients:

$$\gamma = \gamma^{\text{comb}} \gamma^{\text{res}} \gamma^{\text{assoc}} \quad (3.13)$$

In these expressions the combinatorial (comb) and residual (res) contributions are the ones of the UNIFAC model (Fredenslund *et al.*, 1975) presented in section 3.1.1 (equations 3.2 to 3.8). The association contribution to the activity coefficient γ^{assoc} can be derived from the residual Helmholtz energy due to association, as it was done by Fu *et al.* (1995) for the UNIQUAC model (Abrams and Prausnitz, 1975).

Assuming an excess volume equal to zero, the activity coefficient expression can be related to the excess Helmholtz energy as follows:

$$\ln \gamma_i = \left(\frac{\partial G^E / RT}{\partial n_i} \right)_{T,P,n_{j \neq i}} = \left(\frac{\partial A^E / RT}{\partial n_i} \right)_{T,P,n_{j \neq i}} = \left(\frac{\partial (na^E / RT)}{\partial n_i} \right)_{T,P,n_{j \neq i}} \quad (3.14)$$

The excess molar Helmholtz energy a^E can be calculated as the difference between the solution residual property a^{res} and the energy corresponding to pure components a_i^{res} :

$$a^E = a - a^{id} = (a^{ig} + a^{res}) - \left[\sum_{i=1}^{NC} x_i (a_i^{ig} + a_i^{res}) + RT \sum_{i=1}^{NC} x_i \ln x_i \right] = a^{res} - \sum_{i=1}^{NC} x_i a_i^{res} \quad (3.15)$$

Replacing equation 3.15 in equation 3.14, one obtains the expression that relates γ_i^{assoc} with the association contribution to the total residual Helmholtz energy $A^{res,assoc}$ and to the molar residual Helmholtz energy of component i , $a_i^{res,assoc}$:

$$\ln \gamma_i^{assoc} = \left. \frac{\partial A^{res,assoc} / RT}{\partial n_i} \right|_{T,P,n_{j \neq i}} - \frac{a_i^{res,assoc}}{RT} \quad (3.16)$$

For multi-component mixtures the group version of $A^{res,assoc}$ is given by:

$$\frac{A^{res,assoc}}{RT} = \sum_{k=1}^{NGA} n_k \left[\sum_{A_k} \left(\ln X^{A_k} - \frac{X^{A_k}}{2} \right) + \frac{M_k}{2} \right] \quad (3.17)$$

where n_k and M_k are the number of moles and the number of sites of group k , respectively; NGA is the total number of associating groups and X^{A_k} is the fraction of non-bonded group k at site A . Applying equation 3.17 for a solution and a pure component and replacing in equation 3.16, the general expression for the association contribution to the activity coefficient is obtained:

$$\ln \gamma_i^{assoc} = \sum_{k=1}^{NGA} \left\{ v_k^i \sum_{A_k} \left[\ln \left(\frac{X^{A_k}}{X_i^{A_k}} \right) + \frac{X_i^{A_k} - X^{A_k}}{2} \right] + \sum_{A_k} \left(\frac{1}{X^{A_k}} - \frac{1}{2} \right) N_k \left(\frac{\partial X^{A_k}}{\partial n_i} \right)_{T,P,n_j} \right\} \quad (3.18)$$

where N_k is the number of moles of associating group k . The fraction X^{A_k} is a function of the association strength $\Delta^{A_k B_j}$ between site A of group k and site B of group j and of the density of group j , ρ_j , in the solution:

$$X^{A_k} = \frac{1}{1 + \sum_{j=1}^{NGA} \sum_{B_j} \rho_j \Delta^{A_k B_j} X^{B_j}} \quad (3.19)$$

Similarly, the fraction of non-bonded group k through site A in pure component i, $X_i^{A_k}$, is calculated as follows:

$$X_i^{A_k} = \frac{1}{1 + \sum_{j=1}^{NGA} \sum_{B_j} (\rho_j)_i \Delta^{A_k B_j} X_i^{B_j}} \quad (3.20)$$

In this equation, $(\rho_j)_i$ represents the density of group j, in pure component i.

The association strength is a function of the association parameters, energy $\varepsilon^{A_k B_j}$ and volume $\kappa^{A_k B_j}$ of association as follows:

$$\Delta^{A_k B_j} = \kappa^{A_k B_j} [\exp(\varepsilon^{A_k B_j} / kT) - 1] \quad (3.21)$$

The group densities in the solution ρ_k and in pure component i $(\rho_k)_i$ are adimensional and are given by:

$$\rho_k = \frac{\sum_{i=1}^{NC} v_k^i X_i}{\sum_{i=1}^{NC} r_i X_i} \quad (3.22)$$

$$(\rho_k)_i = \frac{v_k^i}{r_i} \quad (3.23)$$

where NC is the number of components, v_k^i is the number of associating groups k present in molecule i and r_i is the UNIQUAC volume parameter.

The final expression of γ^{assoc} will depend on the amount and type of associating sites and species present in the solution. For each case a system of non-linear equations will result from applying equation 3.19. Next, the final expressions for the association contribution to the activity coefficient for several possible systems with self-association and/or cross-association are presented.

3.2.2 Self-association

The simplest expression corresponds to mixtures in which only one associating group is present. A typical example is hydrogen bonding between an electropositive site H and an electronegative site O in alcohols represented by a two-sites model or an acid that usually is modelled with one associating site representing the complete group COOH. In these cases where only one associating group k is present in solution, equation 3.19 results in a quadratic equation.

$$X^{A_k} = \frac{-1 + \sqrt{1 + 4 \rho_k \Delta_k}}{2 \rho_k \Delta_k} \quad (3.24)$$

The following expression is a rearranged version of the expression presented by Mengarelli *et al.* (1999) and is valid for solutions having one associating group k with one ($M_k = 1$) or two ($M_k = 2$) bonding sites.

$$\ln \gamma_i^{\text{assoc}} = M_k \left\{ v_k^i \left[\ln \left(\frac{X^{A_k}}{X_i^{A_k}} \right) + \frac{X_i^{A_k} - X^{A_k}}{2} \right] - \left(\frac{1 - X^{A_k}}{2} \right) (v_k^i - r_i \rho_k) \right\} \quad (3.25)$$

3.2.2.1 Association at infinite dilution

The association contribution to the activity coefficient is very significant at infinite dilution. For a binary mixture of an inert compound with an associating compound having one associating functional group k , it is possible to derive from equation 3.25, the limiting $\gamma_i^{\infty, \text{assoc}}$ values for both, associating (1) and inert (2) components.

At very low concentrations of the associating component, the fraction of non-bonded group k in the solution (X^{A_k}) will be close to one ($X^{A_k} \rightarrow 1$). Equation 3.25 is then reduced to:

$$\ln \gamma_1^{\infty, \text{assoc}} = M_k v_k^1 \left[\ln \left(\frac{1}{X_1^{A_k}} \right) + \frac{X_1^{A_k} - 1}{2} \right] \quad (3.26)$$

On the other hand, the fraction of non-bonded groups in pure associating component ($X_1^{A_k}$) will always be a very small value at high liquid densities and the first term on equation 3.26 will be dominant. It is interesting to notice that the value of $\gamma_1^{\infty, \text{assoc}}$ is independent of the inert component. This is in accordance with experimental evidence for mixtures of an associating component in inert components (Figure 3.1).

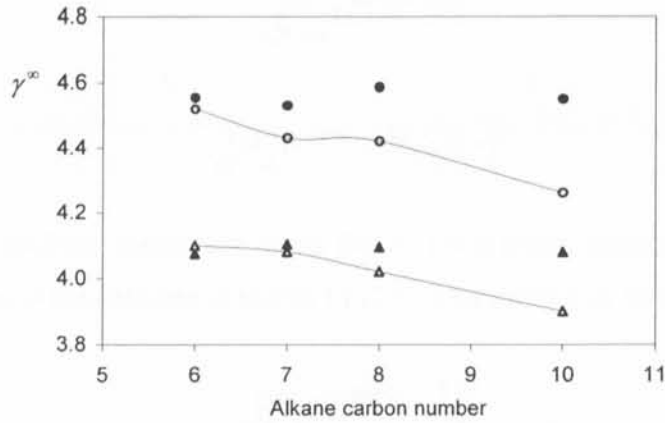


Figure 3.1 Infinite dilution activity coefficients of an alcohol (ethanol or methanol) in a series of n-alkane solvents at 298.15K. Experimental values (Dohnal and Vrbka, 1997): ○ - methanol, △ - ethanol; Residual and association contributions (calculated by subtracting the original UNIFAC combinatorial term): ● - methanol, ▲ - ethanol.

At infinite dilution of inert component (2), Equation 3.25 reduces to:

$$\ln \gamma_2^{\infty, \text{assoc}} = M_k \left(\frac{1 - X_1^{A_k}}{2} \right) r_2 \frac{v_k^1}{r_1} \quad (3.27)$$

According to Equation 3.27, $\gamma_2^{\infty, \text{assoc}}$ depends on the associating component and, particularly, on the number of bonding sites M_k of associating group k .

From the previous equations it can be concluded that:

- the infinite dilution activity coefficient of the associating component is highly dependent on the fraction of non-bonded sites ($X_1^{A_k}$), and hence on the values of the association parameters ε and κ ;
- the association parameters have hardly any effect on the value of the infinite dilution activity coefficient of the inert component; but the type of associating compound (identified by the number of bonding sites M_k) has an important influence in this limiting value.

Consequently, infinite dilution activity coefficients of binary mixtures with one associating and one inert component are a convenient source of experimental data to obtain the values of the association parameters and to choose the model of association (*i.e.* the number of bonding sites).

It is interesting to apply Equations 3.26 and 3.27 to the limiting case of complete association of pure component 1 ($X_1^{A_k} \rightarrow 0$). For this situation:

$$\lim_{x_1^{A_k} \rightarrow 0} \gamma_1^{\infty, \text{assoc}} = \infty \quad (3.28)$$

$$\lim_{x_1^{A_k} \rightarrow 0} \gamma_2^{\infty, \text{assoc}} = M_k \frac{1}{2} r_2 \frac{v_k^1}{r_1} \quad (3.29)$$

Applied to a monomer-dimer association model ($M_k = 1$) in a binary system in which the associating group k appears once in the associating specie 1 ($v_k^1 = 1$) Equation 3.29 reduces to:

$$\lim_{x_1^{A_k} \rightarrow 0} \gamma_2^{\infty, \text{assoc}} = \frac{1}{2} \frac{r_2}{r_1} \quad (3.30)$$

Equivalent expressions can be found for the traditional chemical theory of association applied to a binary system with one completely dimerized component 1 (dimerization equilibrium constant $K \rightarrow \infty$) and one non-polar inert component 2. In this case, the limiting values are (Prausnitz, 1999):

$$\lim_{K \rightarrow \infty} \gamma_1^{\infty} = \infty \quad (3.31)$$

$$\lim_{K \rightarrow \infty} \gamma_2^{\infty} = 2 \quad (3.32)$$

Contrary to Equation 3.32, which predicts a uniform limiting value of γ_2^{∞} for all inert compounds, Equation 3.30 agrees qualitatively with the experimental evidence; *i.e.* the value of γ_2^{∞} , in a given associating component, increases with the molecular chain of the non polar component (Figure 3.2).

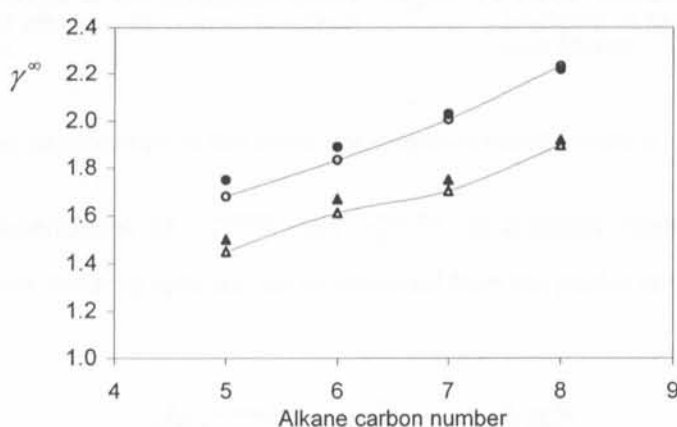


Figure 3.2 Infinite dilution activity coefficients of n-alkanes in methanol at 298.15K. Experimental values (Dohnal and Vrbka, 1997): ●- 1-propanol, ▲- 1-butanol; Residual and association contributions (calculated by subtracting the original UNIFAC combinatorial term): ○-1-propanol, △- 1-butanol.

3.2.2.2 Composition dependence of the association term

It is interesting to analyze the effect of composition on the values of the association contributions to the activity coefficients for both associating (Figure 3.3) and inert compounds (Figure 3.4). The curves shown in those figures correspond to the binary system ethanol + hexane and were calculated using the values of the association parameters determined in this work for the OH associating group ($\kappa = 0.0062$ and $\varepsilon/k = 3125$ K). For both species, γ^{assoc} goes to unity (the pure-component limiting value) with a zero slope, and the derivative increases towards the infinite dilution limit, which means that γ^{assoc} reaches its maximum value at infinite dilution. However, the effect of composition is dramatic for the associating component, whose γ^{assoc} derivative drops rapidly from its infinite dilution value, within a narrow range of compositions; then, it remains almost constant up to the pure-component limit. It can thus be concluded that γ^{assoc} represents a very important contribution to the infinite dilution activity coefficient of the associating component; however, this contribution remains at relatively low values at higher concentrations.

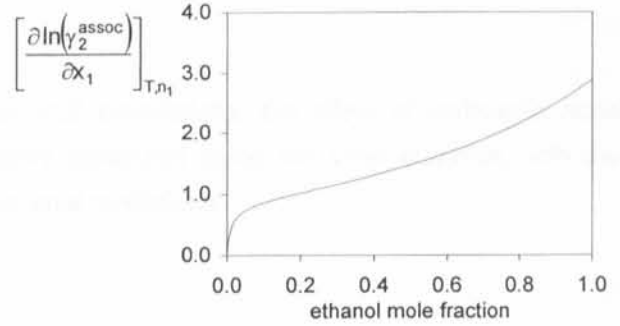
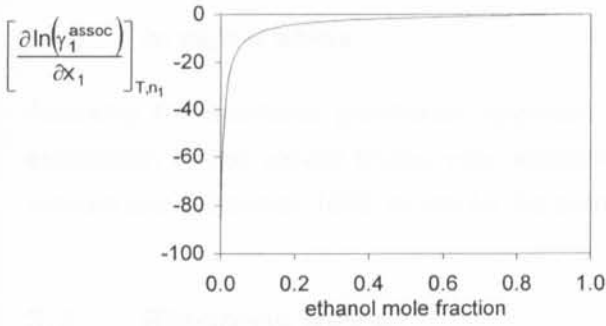


Figure 3.3 Partial derivative of the association activity coefficient of ethanol, with respect to ethanol mole fraction.

Figure 3.4 Partial derivative of the association activity coefficient of hexane, with respect to ethanol mole fraction.

3.2.2.3 Temperature dependence of the association term at infinite dilution

The temperature dependence of $\gamma_1^{\infty, \text{assoc}}$ and $\gamma_2^{\infty, \text{assoc}}$ in a binary mixture with one associating component (1) and one inert (2) species can be obtained from the partial derivatives of Equations 3.26 and 3.27:

$$\frac{\partial(\ln \gamma_1^{\infty, \text{assoc}})}{\partial T} = M_k v_k^1 \left[\left(\frac{1}{2} - \frac{1}{X_1^{A_k}} \right) \frac{\partial X_1^{A_k}}{\partial T} \right] \quad (3.33)$$

$$\frac{\partial(\ln \gamma_2^{\infty, \text{assoc}})}{\partial T} = M_k v_k^1 \left(-\frac{1}{2} \frac{r_2}{r_1} \frac{\partial X_1^{A_k}}{\partial T} \right) \quad (3.34)$$

where the partial derivative for the fraction of non-bonded groups ($X_1^{A_k}$) is given by:

$$\frac{\partial X_1^{A_k}}{\partial T} = \left[\frac{-(\rho_k)_1 (X_1^{A_k})^2}{1 + 2(\rho_k)_1 X_1^{A_k} \Delta_k} \right] \frac{\partial \Delta_k}{\partial T} \quad (3.35)$$

and the partial derivative of the association strength is:

$$\frac{\partial \Delta_k}{\partial T} = -\kappa_k \frac{\epsilon_k}{kT^2} \exp\left(\frac{\epsilon_k}{kT}\right) \quad (3.36)$$

For both limiting values ($\gamma_1^{\infty, \text{ASSOC}}$ and $\gamma_2^{\infty, \text{ASSOC}}$) it is observed that $\gamma^{\infty, \text{ASSOC}}$ decreases monotonically with temperature. This is the normal experimental behaviour found in mixtures with non-associating and self-associating compounds, which usually present positive excess enthalpies and excess Gibbs energies (Koenen and Gaube, 1982). Other temperature dependence on the activity coefficient values are taken into account by the residual term.

3.2.3 The vapour phase

Following the traditional gamma-phi approach for VLE calculations, the effect of carboxylic acids association in the vapour phase was independently computed using the virial equation, with the Hayden and O'Connell (1975) model for the second virial coefficients.

3.3 Rigorous model

As discussed before, the final expression for γ^{ASSOC} will depend on the amount and type of associating sites and species present in the solution. The simplest expression corresponds to mixtures in which only one associating group is present. When two associating groups are present in solution, it is possible to obtain quartic and cubic equations for the monomer fraction, by making some reasonable assumptions (Kraska, 1998). In the following sections, the extension of the model to mixtures containing alcohols, water, carboxylic acids, esters, aromatics and alkanes is described.

3.3.1 Model development

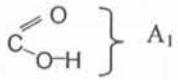
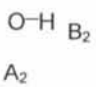


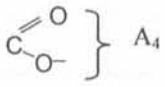
Each family of associating components is represented by a specific associating group. Therefore, four new associating groups are defined as follows:

- (a) The acid association group COOH with one site capable of both self- and cross-associating;

- (b) The hydroxyl association group OH with two sites capable of both self- and cross-associating to represent alcohols and water;
- (c) The ester association group COOR with one site that does not self-associate but can cross-associate with groups that have an electropositive site;
- (d) The aromatic ring association group A_{ring} with one site that does not self-associate but can cross-associate with groups that have an electropositive site (Wormald, 1997)

Table 3.2 shows schematically the four possible associating groups. For each new associating group it is necessary to specify the number of sites. Every site is labelled with a capital letter (A, B, etc) with a subscript number indicating the corresponding association group. Then, the interactions between a given site and the different sites in other associating groups must be defined by characterizing the correspondent association strength. The non-zero interactions between sites are used to calculate the fraction of non-bonded sites for each group. Ideally, the association strength for each pair of sites should be known quantitatively from spectroscopy data or from molecular simulation methods. That information, however, is scarce. The alternative is to use approximate models so that the number of parameters can be reduced. The number of sites assigned to each associating group is represented schematically on the first column of Table 3.2 and, on the second column, the different assumptions concerning the association strengths between each pair of sites. Finally, the association parameters that have to be fitted are on the third column.

Table 3.2 Self-association models defined in the GCA-EoS model.

| Self-association | | Assumptions | Association parameters |
|---|---|---|--|
| -COOH |  A_1 | $\Delta_{A_1A_1} \neq 0$ | $\varepsilon_{A_1A_1}$ $\kappa_{A_1A_1}$ |
| -OH |  A_2 B_2 | $\Delta_{A_2B_2} \neq 0$ $\Delta_{A_2A_2} = \Delta_{B_2B_2} = 0$ | $\varepsilon_{A_2B_2}$ $\kappa_{A_2B_2}$ |
|  |  A_3 | $\Delta_{A_3A_3} = 0$ | --- |
| -COOR |  A_4 | $\Delta_{A_4A_4} = 0$ | --- |

As can be seen from Table 3.2 the double hydrogen bond of the acids is represented by a strong single bond between sites A_1 . The formation of oligomers by water and alcohols is represented by the hydroxyl group with sites A_2 and B_2 . The aromatic and ester groups are represented by a single

electron-donor site, A_3 and A_4 , respectively, that is not able to self-associate, *i.e.*, their self-association strengths are zero. However, in some cases they can cross-associate, as shown on Table 3.3.

For mixtures containing more than one type of associating groups it is necessary to define the cross-association strengths between the different sites. Table 3.3 shows some of the assumptions made. For the cross-association strength between acids and alcohols it was assumed that the site A_1 of the acid interacts with same strength with sites A_2 or B_2 of the hydroxyl group. Moreover, that cross-association strength is estimated as the geometric mean of the self-association strengths (A_1 - A_1 and A_2 - B_2):

$$\Delta_{A_1B_2} = \Delta_{A_1A_2} = k_{12} \sqrt{\Delta_{A_1A_1} \Delta_{A_2B_2}} \quad (3.37)$$

As a first estimate in the optimization process, the k_{12} parameter will be considered to be equal to unity. Unfortunately, this rule can only be established for cross-interactions between groups that are also able to self-associate. For the cross-association between one associating group that can self-associate (hydroxyl or acid groups) and one group that can cross-associate but does not self-associate (the aromatic or ester groups) it is necessary to fit those cross-association parameters to cross-associated binary mixtures experimental information. For simplification, both aromatic and ester association groups are represented on Table 3.3 as group X with one electronegative site A_x ($x = 3, 4$ for the aromatic and ester group, respectively).

Table 3.3 Cross-association types defined in the A-UNIFAC model.

| Cross-association | | | Assumptions | Association parameters |
|--------------------------|--|--|---|---|
| OH-COOH | $\begin{matrix} \text{O-H} & B_2 \\ & \\ A_2 & \end{matrix}$ | $A_1 \left\{ \begin{array}{l} \text{O} \\ \parallel \\ \text{H-O-C} \end{array} \right.$ | $\Delta_{A_1A_2} = \Delta_{A_1B_2} \neq 0$ $\Delta_{A_1A_1} \neq 0 \quad \Delta_{A_2B_2} \neq 0$ | $\epsilon_{A_1A_2} = \epsilon_{A_1B_2} = \frac{\epsilon_{A_1A_1} + \epsilon_{A_2B_2}}{2}$ $K_{A_1A_2} = K_{A_1B_2} = \sqrt{K_{A_1A_1} K_{A_2B_2}}$ |
| OH- X_{group} | $\begin{matrix} \text{O-H} & B_2 \\ & \\ A_2 & \end{matrix}$ | $A_x \left\{ \begin{array}{l} X_{\text{group}} \end{array} \right.$ | $\Delta_{A_2B_2} \neq \Delta_{A_xB_2} \neq 0$ $\Delta_{A_xA_2} = 0$ | $\epsilon_{A_xB_2} \quad K_{A_xB_2}$ |
| COOH- X_{group} | $\left. \begin{array}{l} \text{O} \\ \parallel \\ \text{C} \\ \backslash \\ \text{O-H} \end{array} \right\} A_1$ | $A_x \left\{ \begin{array}{l} X_{\text{group}} \end{array} \right.$ | $\Delta_{A_1A_x} \neq 0$ | $\epsilon_{A_1A_x} \quad K_{A_1A_x}$ |

As an example of the type of expressions obtained for the activity coefficient let us consider a binary mixture containing two associating groups with one associating site each. In this case, equation 3.19 results in two independent quartic equations respect to the fraction of non-bonded sites:

$$\begin{aligned}
& X_k^4 \rho_k^2 \Delta_k (\Delta_l \Delta_k - \Delta^{*2}) + X_k^3 [2\rho_k \Delta_k \Delta_l - \Delta^* \rho_k (\Delta_k + \Delta^*)] + \\
& + X_k^2 [\Delta_l - 2\rho_k \Delta_k \Delta_l + \Delta^* (\rho_k \Delta^* - 1) - \rho_l \Delta^{*2}] + X_k (-2\Delta_l + \Delta^*) + \Delta_l = 0
\end{aligned} \tag{3.38}$$

The activity coefficient expression can be obtained by differentiating Equation 3.38 respect to the number of moles of component i:

$$\begin{aligned}
N_k \frac{\partial X_k}{\partial n_i} &= \frac{\text{num}}{\text{den}} \\
\text{num} &= \left\{ X_k^4 2\rho_k \Delta_k (\Delta_l \Delta_k - \Delta^{*2}) - X_k^3 [2\Delta_k \Delta_l - \Delta^* (\Delta_k + \Delta^*)] - X_k^2 (-2\Delta_k \Delta_l + \Delta^{*2}) \right\} N_k \left(\frac{\partial \rho_k}{\partial n_i} \right)_{T,P,j} + \\
&+ \left(X_k^2 \Delta^{*2} \right) N_k \left(\frac{\partial \rho_j}{\partial n_i} \right)_{T,P,j} \\
\text{den} &= 4X_k^3 \rho_k^2 \Delta_k (\Delta_l \Delta_k - \Delta^{*2}) + 3X_k^2 [2\rho_k \Delta_k \Delta_l - \Delta^* \rho_k (\Delta_k + \Delta^*)] + \\
&+ 2X_k [\Delta_l - 2\rho_k \Delta_k \Delta_l + \Delta^* (\rho_k \Delta^* - 1) - \rho_l \Delta^{*2}] - 2\Delta_l + \Delta^*
\end{aligned} \tag{3.39}$$

A particular case of the previous system is the case of two components that can cross-associate ($\Delta^* \neq 0$) but not to self-associate ($\Delta_l = \Delta_k = 0$), e.g., acetone (1 site O) and chloroform (1 site H). Equation 3.38 reduces to:

$$X_i = \frac{2}{1 + \Delta^* (\rho_j - \rho_i) + \sqrt{[1 + (\rho_i + \rho_j) \Delta^*]^2 - 4\Delta^{*2} \rho_i \rho_j}} \tag{3.40}$$

At infinite dilution of a given component i in component j, the previous expression takes the form:

$$X_i^\infty = \frac{1}{1 + \rho_j \Delta^*} \tag{3.41}$$

At low concentrations of one of the components, the fraction of non-bonded sites is a very a simple function of the cross-association strength. The other component will have a monomer fraction equal to unity since it cannot self-associate. In the case of components with similar size ($\rho_i = \rho_j$), the model foresees the same limit value for the infinite dilution of either component. Finally, the following expression is obtained for a component i infinitely diluted in j:

$$\ln \gamma_i^{\infty, \text{assoc}} = v_A^i \left(\ln X_A^\infty + \frac{1 - X_A^\infty}{2} \right) - 2\Delta^* \left[\frac{r_j + r_i + \Delta^* - 2\Delta^{*2}}{r_j + \Delta^* (r_i - \Delta^*)} \right] \tag{3.42}$$

3.3.2 Parameterization

The addition of an association term to the UNIFAC method makes it necessary not only to estimate the association parameters but also to re-parameterize the group interaction parameters of the residual term, since now these parameters will only take into account dispersive forces.

3.3.2.1 Database

The association and residual group parameters were estimated using experimental data on low-pressure VLE (Gmehling *et al.*, 1977), LLE (Sørensen and Arlt, 1979) for the water interactions with groups CH₂, ACH, COOH, OH and infinite dilution activity coefficients γ^{∞} of binary mixtures (Tiegs *et al.*, 1986; Dohnal and Vrbka, 1997). Table 3.4 shows the VLE database used in the correlation stage.

Table 3.4 VLE database used for A-UNIFAC parameters estimation

| System | C atoms in group 1 | C atoms in group 2 | NP | T range (K) |
|--------------------|--------------------|--------------------|-----|-------------|
| methanol + alkane | C1 | C4-C8 | 37 | 318-399 |
| methanol + alcohol | C1 | C2-C5 | 49 | 323-354 |
| methanol + water | C1 | --- | 125 | 285-373 |
| alcohol + alkane | C2-C5 | C5-C8 | 190 | 293-380 |
| water + alcohol | --- | C2-C4 | 231 | 303-412 |
| acid + alkane | C2-C5 | C6-C8 | 309 | 293-435 |
| water + acid | --- | C2-C4 | 232 | 293-432 |
| alcohol + acid | C2-C5 | C2-C3 | 195 | 298-415 |
| alcohol + ester | C2-C4 | C3-C6 | 202 | 298-396 |
| water + ester | --- | C3-C6 | 164 | 298-400 |
| acid + ester | C2-C3 | C3-C6 | 161 | 312-398 |
| alcohol + aromatic | C2-C4 | C6-C7 | 507 | 298-390 |
| acid + aromatic | C2-C3 | C6 | 91 | 293-392 |

The first mixtures studied contain only one self-associating group, that is, they are mixtures of alkanes and an associating component (*e.g.* water, alcohol or acid).

Mengarelli *et al.* (1999) studied the mixtures containing alcohols, water and alkanes. All association effects were represented by a single two sites OH associating group, the same for all alcohols and water. In this way a quadratic expression is obtained for the monomer fraction (Equation 3.24). These authors have calculated the association parameters in order to reproduce the monomer fraction curves predicted by the SAFT equation (Huang and Radosz, 1990) for ethanol and water at liquid conditions. The residual parameters were then estimated using infinite dilution activity coefficients data of binary systems containing water, ethanol or hexane.

Later, Ferreira *et al.* (1999) re-estimated those association parameters simultaneously with the residual parameters using a broader database that included γ^∞ of alcohols (from ethanol to 1-butanol) in alkanes (from n-hexane to n-decane) and VLE data for a larger number of alcohol-alkane binary mixtures (Table 3.4). The following values for the association parameters were obtained: $\epsilon_{OH} = 3125.0$ K and $\kappa_{OH} = 0.0062$.

As proposed by Mengarelli *et al.* (1999), alcohol and water molecules are represented by the same OH associating group. Figure 3.5 compares the monomer fraction calculated by the SAFT equation and by the A-UNIFAC model for liquid water (Figure 3.5a) and for liquid ethanol (Figure 3.5b). For each component the fraction of non-bonded sites was calculated at saturated liquid densities and at a constant liquid density. As can be seen, the same order of magnitude is predicted by both models using this simplified approach.

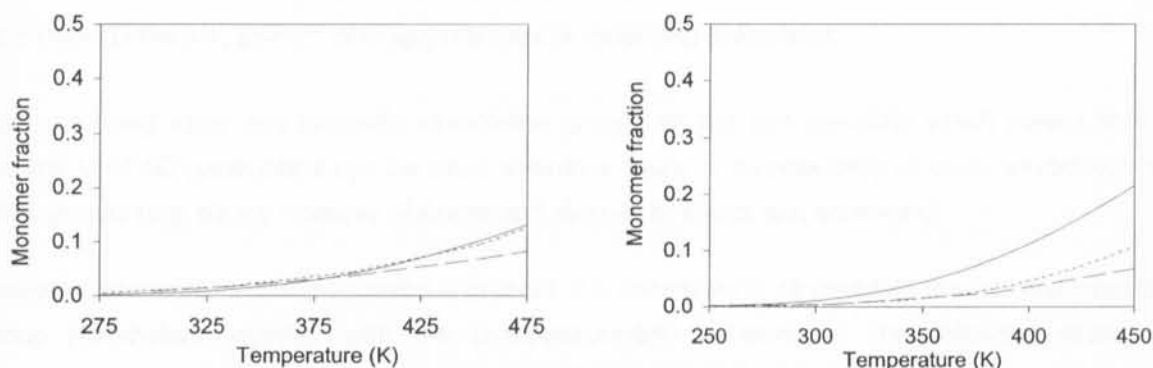


Figure 3.5 Monomer fractions: (a) liquid water; (b) liquid ethanol. Calculated: --- SAFT at saturated liquid densities; — SAFT at constant saturated liquid density at 298.15K; -·- A-UNIFAC model.

After calculating the hydroxyl associating parameters, the residual interactions between water and the alkane group were estimated using binary liquid-liquid equilibria data of water/n-alkanes and water/n-alkanols and VLE data of water/n-alkanols.

The first element of the alcohol series, methanol, is represented by a single group CH_3OH , from the residual term point of view. The residual group interaction parameters between the CH_2 and CH_3OH groups were estimated using binary VLE data of methanol-alkanes and γ^∞ of binary mixtures of methanol and heptane. The interaction residual parameters between the methanol group and the water or alcohol groups were calculated using binary VLE data of methanol-water and methanol-alcohol, respectively (Table 3.4).

The remaining self-association group is the acid associating group. This group is defined as an associating group with one site that can self-associate. Due to the lack of experimental information on infinite dilution activity coefficients of carboxylic acid + non-associating systems, new self-associating

parameters for the acid group were estimated simultaneously with the residual group interaction parameters, $a_{\text{CH}_2,\text{COOH}}$ and $a_{\text{COOH},\text{CH}_2}$, using binary VLE data for acids and alkanes (Table 3.4).

After calculating the self-association parameters, the focus is on the cross-associating mixtures:

For the interaction between acids and alcohols, good results were obtained using the mean geometric rule for the cross-association strength, *i.e.*, no further cross-association parameters had to be estimated. New interaction residual parameters between the acid and the alcohol groups were fitted to binary VLE systems of acids and alcohols (Table 3.4).

For the water-carboxylic acids mixtures, it was necessary to introduce an interaction parameter between the self-association strengths of water and acids. This interaction parameter is lower than unity ($k_{ij} = 0.63$), suggesting that the interaction between acids and water is closer to the water-water association strength than to the acid-acid interaction association strength. This interaction parameter was estimated together with the residual group interaction parameters $a_{\text{H}_2\text{O},\text{COOH}}$ and $a_{\text{COOH},\text{H}_2\text{O}}$ using VLE data (Table 3.4) and γ^∞ of binary mixtures of water and acetic acid.

The remaining ester and aromatic associating groups do not self-associate which means that the original UNIFAC parameters can be used whenever there is no possibility of cross-association with other groups (*e.g.* binary mixtures of esters and alkanes or esters and aromatics).

However, whenever cross-association is present, it is necessary to re-calculate the residual interaction group parameters together with the cross-association parameters. The following strategy of optimization was followed: first the cross-association parameters between the ester and hydroxyl associating groups were estimated simultaneously with the residual parameters using VLE data of esters and alcohols (Table 3.4) and γ^∞ of binary mixtures of ethyl acetate and ethanol.

As water is represented by the same hydroxyl association group, no further cross-association parameters were estimated to describe water and esters mixtures. For these systems, the missing residual interaction parameters were estimated using VLE data of water and esters (Table 3.4) and γ^∞ of binary mixtures of water and methyl acetate or ethyl acetate.

A similar procedure was followed for the estimation of the interaction parameters between the hydroxyl and the aromatic associating groups: First, the cross-association parameters between the aromatic and hydroxyl associating groups were estimated simultaneously with the residual parameters using VLE data (Table 3.4) and γ^∞ of binary mixtures of benzene and ethanol, 1-propanol or 1-butanol.

Then, the $a_{\text{H}_2\text{O},\text{ACH}}$ and $a_{\text{ACH},\text{H}_2\text{O}}$ residual parameters were estimated using LLE and γ^∞ data of binary mixtures of water and benzene.

Finally, the interactions between the acid and the ester or aromatic associating groups were estimated simultaneously with the correspondent residual interaction parameters. For the acid- ester interaction binary VLE data (Table 3.4) and γ^∞ of ethyl acetate and acetic acid were used and, for the acid-aromatic interaction, only binary VLE information was available.

The new group interaction parameters between paraffinic, aromatic, alcohol, water, ester and acid groups are presented on Table 3.5.

Table 3.5 Residual group interaction parameters $a_{m,n}$ (K)

| m \ n | CH ₂ | ACH | OH | CH ₃ OH | H ₂ O | CCOO | COOH |
|--------------------|---------------------|--------------------|--------|--------------------|------------------|--------------------|--------|
| CH ₂ | 0.0 | 61.13 ^b | 50.40 | 122.7 | 380.5 | 232.1 ^b | 260.7 |
| ACH | -11.12 ^b | 0.0 | 20.88 | n.a. | -31.17 | 5.994 ^b | 66.01 |
| OH | 387.4 | 359.6 | 0.0 | 110.9 | -127.3 | 325.5 | -143.9 |
| CH ₃ OH | -19.78 | n.a. | 60.18 | 0.0 | -167.6 | n.a. | n.a. |
| H ₂ O | 136.8 | 281.8 | 70.7 | 251.2 | 0.0 | 150.3 | 281.0 |
| CCOO | 114.8 ^b | 85.84 ^b | -8.433 | n.a. | -72.73 | 0.0 | 600.4 |
| COOH | 284.7 | 183.2 | 381.5 | n.a. | -350.6 | -215.1 | 0.0 |

a: n.a., not available; b: original UNIFAC parameters Gmehling *et al.* (1982).

Table 3.6 shows the self- and cross-association parameters estimated using this approach.

Table 3.6 A-UNIFAC self-and cross-association parameters.

| Self-association | | | |
|-------------------|-------------------|-----------------------|---------------|
| | | ϵ/k (K) | κ |
| COOH | | 4100.0 | 0.0020 |
| OH | | 3125.0 | 0.0062 |
| H ₂ O | | 3125.0 | 0.0062 |
| Cross-association | | | |
| i | j | ϵ_{ij}/k (K) | κ_{ij} |
| COOH | OH | 3612.5 | 0.0035 |
| | H ₂ O* | 3612.5 | 0.0035 |
| | COOR | 2912.0 | 0.0038 |
| | A _{ring} | 1810.0 | 0.0030 |
| OH | COOR | 1975.0 | 0.0710 |
| | A _{ring} | 1690.0 | 0.0635 |
| | H ₂ O | 3125.0 | 0.0062 |

*with $k_{\text{COOH,H}_2\text{O}} = 0.63$

3.3.3 Results

3.3.3.1 Vapour-liquid equilibria

Table 3.7 reports the average errors obtained in the correlation of VLE data with the A-UNIFAC model. For comparison the predictions from the original UNIFAC model are also shown. Slight improvements are obtained in the correlation of VLE data with the A-UNIFAC model, as compared to the original UNIFAC model.

Table 3.7 Average errors in pressure (δP) and composition (δy) for the UNIFAC and A-UNIFAC models.

| System | UNIFAC | | A-UNIFAC | |
|--------------------|------------|------------|------------|------------|
| | δy | δP | δy | δP |
| methanol + alkane | 3.3 | 4.6 | 2.4 | 3.3 |
| methanol + alcohol | 2.8 | 3.1 | 2.5 | 3.1 |
| methanol + water | 4.2 | 4.8 | 1.6 | 4.1 |
| alcohol + alkane | 3.8 | 6.8 | 3.1 | 6.6 |
| water + alcohol | 6.4 | 3.2 | 5.5 | 3.0 |
| acid + alkane | 4.2 | 2.4 | 3.3 | 2.2 |
| water + acid | 8.7 | 3.5 | 8.0 | 3.5 |
| alcohol + acid | 8.9 | 7.4 | 5.9 | 5.7 |
| alcohol + ester | 5.4 | 2.4 | 5.1 | 2.4 |
| water + ester | 7.4 | 7.0 | 6.7 | 6.4 |
| acid + ester | 7.5 | 2.3 | 7.6 | 2.2 |
| alcohol + aromatic | 5.6 | 3.2 | 4.5 | 2.9 |
| acid + aromatic | 4.2 | 4.3 | 3.0 | 4.1 |

$$\delta z = 100 \sqrt{\left(\sum_i \{ [z_i(\text{exp}) - z_i(\text{calc})] / z_i(\text{exp}) \}^2 / NP \right)}$$

where z represents y or P.

Figures 3.6 and 3.7 compare the A-UNIFAC model correlations with the original UNIFAC method predictions. Both models are able to describe satisfactorily the VLE for these mixtures.

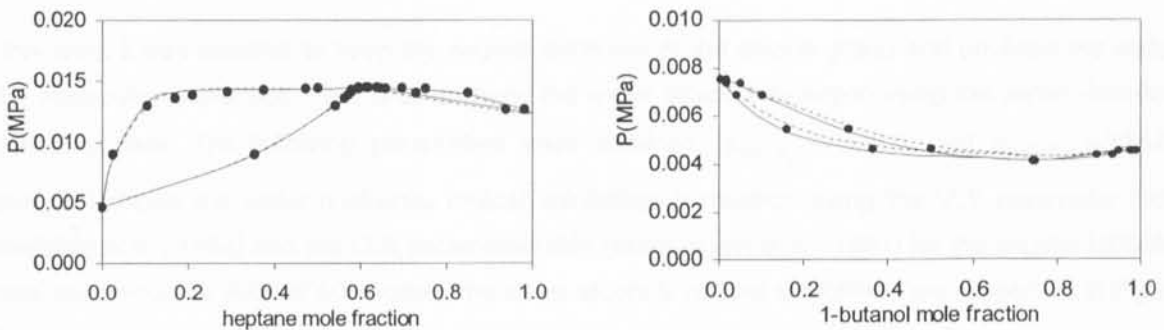


Figure 3.6 VLE of binary mixtures: (a) heptane + acetic acid at 313 K; (b) 1-butanol + acetic acid at 323 K. Exp. Data (Gmehling *et al.*, 1977); — A-UNIFAC; --- Original UNIFAC.

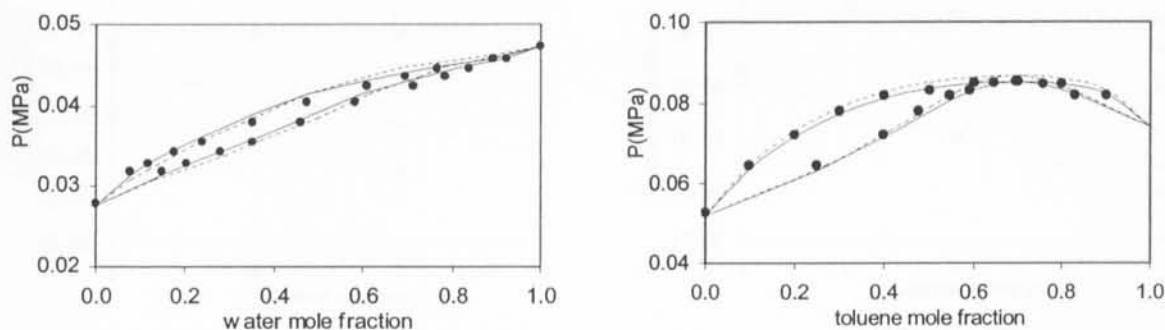


Figure 3.7 VLE of binary mixtures: (a) water + acetic acid at 353 K; (b) toluene + 1-butanol at 373 K. Exp. Data (Gmehling *et al.*, 1977); — A-UNIFAC; --- Original UNIFAC.

3.3.3.2 Mutual solubilities for aqueous systems

As a first approach, the H_2O-CH_2 interaction was estimated using the existing binary LLE data for water and alkanes. The parameters obtained were: $a_{CH_2,H_2O} = 381.5$ and $a_{H_2O,CH_2} = 274.5$. This set of parameters correlates very well the experimental data. After setting the water-alkanes interaction, the next step would be to estimate other water interaction parameters. Here some problems arose when trying to correlate simultaneously the solubilities and VLE of water and polar substances like alcohols or acids. This reflects the significant influence of the hydrophilic group on the alkane groups closely attached to it. A possible solution was proposed by Skjöld-Jørgensen (1988) for the GC-EoS equation of state, by introducing the so called “water-soluble alkane group”, WS- CH_2 . This group represents the alkane structural part in molecules having a water soluble group (like alcohols, acids, ketones, esters).

In the activity coefficients models this problem was already encountered by Magnussen (1980) when trying to correlate water-alkane and water-polar substances mutual solubilities. The objective was to build a UNIFAC parameter table to correlate and predict exclusively LLE data. The author ended up estimating the H_2O-CH_2 interaction using binary LLE data of water with polar substances containing also the alkane group. This allowed a much better prediction of the water-polar substances mutual solubilities in expense of the less important water-alkanes mutual solubilities.

In this work it was decided to keep the original definition of the alkane group and privilege the water-polar molecules interaction. That is to estimate the water alkane interaction using the water –alcohols equilibrium data. The following parameters were obtained: $a_{CH_2,H_2O} = 380.5$ and $a_{H_2O,CH_2} = 136.8$. Figure 3.8 shows the water *n*-alkanes mutual solubilities correlation using the VLE parameter table (Gmehling *et al.*, 1982) and the LLE parameter table (Magnussen *et al.*, 1981) for the original UNIFAC model and, also, the A-UNIFAC model. The water-alcohols mutual solubilities are presented in Figure 3.9.

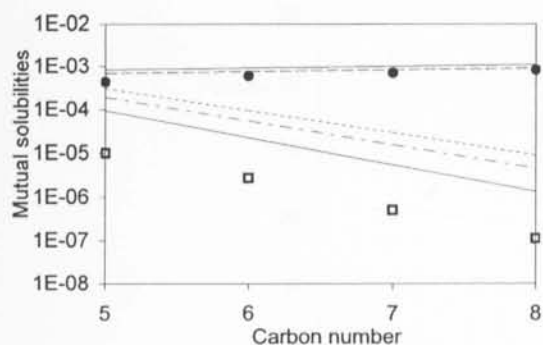


Figure 3.8 Water – hydrocarbon mutual solubilities at 298K. Experimental data (Sørensen and Arlt, 1979): ● water sol.; □ hydrocarbons sol.; — A-UNIFAC; --- VLE-UNIFAC (Gmehling *et al.*, 1982); - -LLE-UNIFAC (Magnussen *et al.*, 1981).

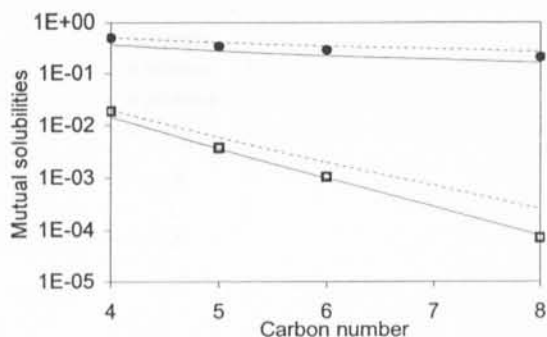


Figure 3.9 Water – alcohols mutual solubilities at 298K. Experimental data (Sørensen and Arlt, 1979): ● water sol.; □ alcohols sol.; — A-UNIFAC correlation; --- UNIFAC correlation.

Figures 3.10 and 3.11 present the water-acids and water-benzene mutual solubilities, respectively. As can be seen, the A-UNIFAC model slightly improves the results for the more diluted aqueous phase.

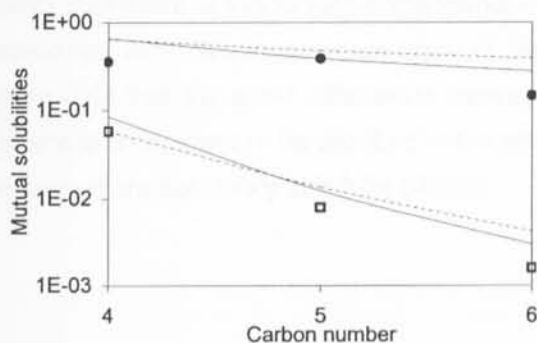


Figure 3.10 Water – acids mutual solubilities at 298K. Experimental data (Sørensen and Arlt, 1979): ● water sol.; □ acids sol.; — A-UNIFAC prediction; --- UNIFAC prediction.

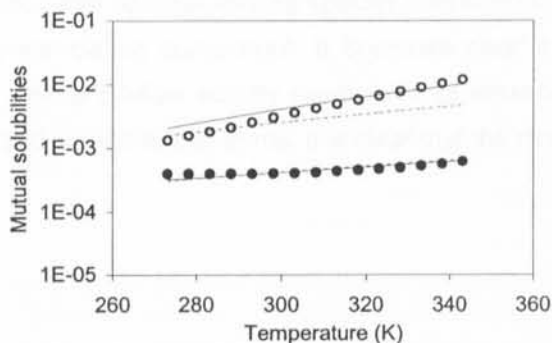


Figure 3.11 Water – benzene mutual solubilities *versus* temperature. Experimental data (Sørensen and Arlt, 1979): ○ water sol.; ● benzene sol.; — A-UNIFAC correlation; --- UNIFAC correlation.

3.3.3.3 Infinite dilution activity coefficients

The main improvements were obtained at the infinite dilution region of compositions where non-ideality due to association effects is more pronounced. This is particularly true for mixtures with one associating and one non-polar component. For this case, large improvements were achieved in the correlation and prediction of activity coefficients at diluted conditions. Figure depicts the $\gamma_{\text{alkanes}}^{\infty}$ of a series of alkanes in ethanol. For comparison, the results obtained with the UNIFAC model using the parameter table specially developed for the prediction of infinite dilution activity coefficients (Bastos *et al.*, 1988) are also shown.

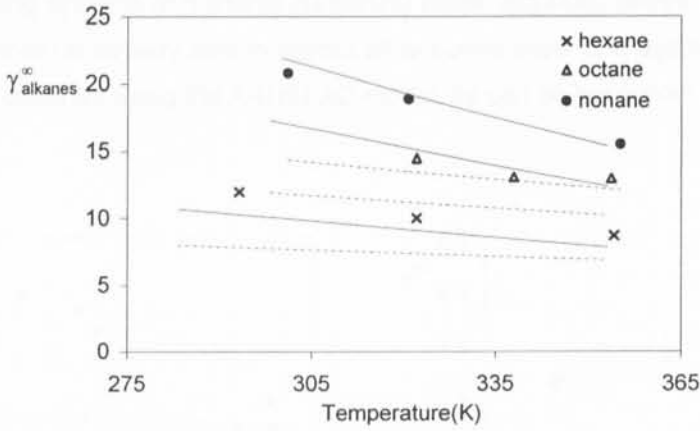


Figure 3.12 Infinite dilution activity coefficients of n-alkanes in ethanol *versus* temperature: \bullet Δ \times experimental data (Tiegs *et al.*, 1986); — A-UNIFAC; --- UNIFAC- γ^{∞} .

Figure 3.13, on the other hand, shows that the A-UNIFAC model is able to follow the temperature dependence of $\gamma_{\text{ethanol}}^{\infty}$ in alkanes. As previously discussed, the most important contribution to the activity coefficient of associating components in mixtures with non-associating species comes from the association term, which is independent of the non-associating component. It becomes clear from Figure 3.13 that the small differences between the infinite dilution activity coefficients of ethanol in heptane and decane can be ascribed to the residual and combinatorial terms. It is clear that the model performs more accurately at infinite dilution.

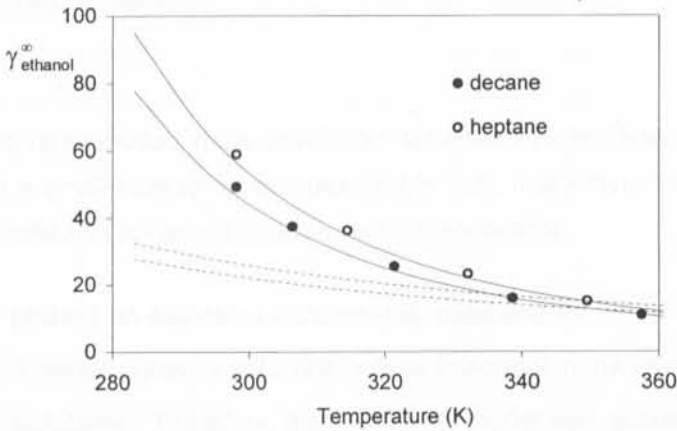


Figure 3.13 Infinite dilution activity coefficients of ethanol in n-alkanes, *versus* temperature: \bullet \circ experimental data (Tiegs *et al.*, 1986) — A-UNIFAC correlation; --- UNIFAC- γ^{∞} correlation.

For cross-associating systems of mixtures containing water, alcohols, esters, acids and aromatics, the original UNIFAC model is already able to predict an accurate order of magnitude. However, significant improvements are obtained using the A-UNIFAC model, as can be seen from Figure 3.14.

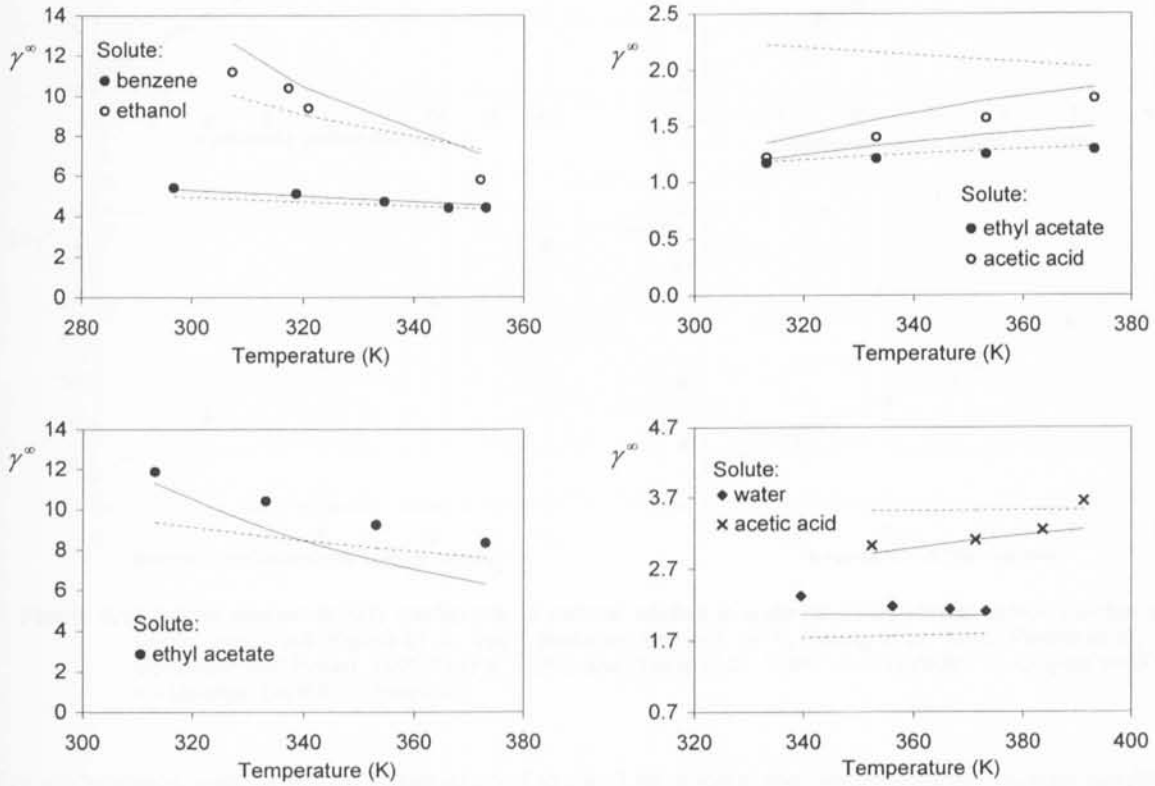


Figure 3.14 Infinite dilution activity coefficients of in binary mixtures of: (a) benzene and ethanol; (b) acetic acid and ethyl acetate; (c) ethyl acetate in water; (d) water and acetic acid. Exp. Data (Tiegs *et al.*, 1986); — A-UNIFAC; --- Original UNIFAC.

The A-UNIFAC model has included in the correlation database infinite dilution activity coefficients data for components with a small number of carbons (Table 3.4). It is interesting to see how the model behaves when it is applied for longer-chain associating components.

Kojima *et al.* (1997) present an extensive experimental database for γ^∞ of several solutes in water. This information about diluted aqueous solutions is quite important in the environmental area (*e.g.*, the removal of chemical pollutants). Therefore, the A-UNIFAC model was applied to the prediction of γ^∞ of several components (n-alkanes, n-alcohols, n-acetates, n-carboxylic acids, aromatics) in water.

The A-UNIFAC predictions are compared to two different UNIFAC based models predictions: the original UNIFAC-VLE and the Modified UNIFAC of Dortmund predictions. As can be seen from Figure 3.15, the A-UNIFAC model predicts more accurately the infinite dilution activity coefficients of the several solutes in water relatively to the other two models.

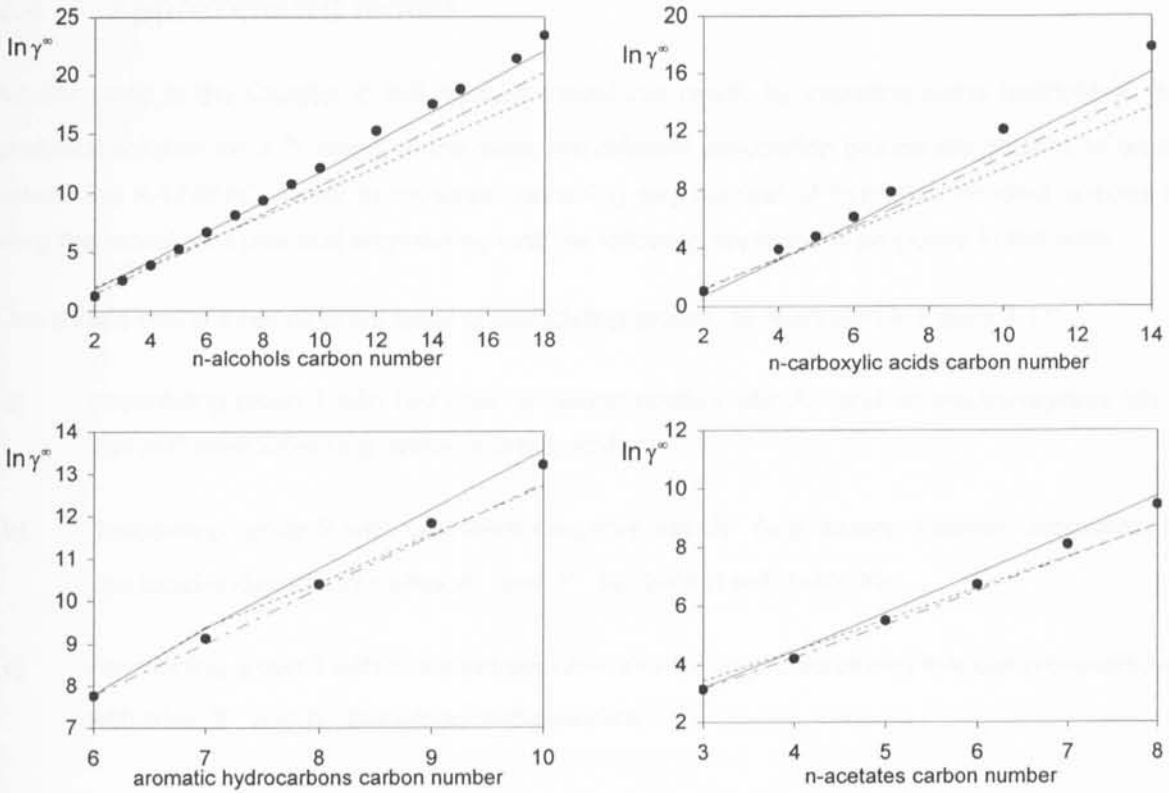


Figure 3.15 Infinite dilution activity coefficients of several solutes in water at 298K versus carbon number of the solute. Exp. Data (Kojima *et al.*, 1997; Sørensen and Arlt, 1979; Hwang *et al.*, 1992; Pierotti *et al.*, 1959; Bergmann and Eckert, 1991; Li *et al.*, 1993; see Zhang *et al.*, 1998); — A-UNIFAC; --- Original UNIFAC; - · - Modified UNIFAC (Dortmund).

For comparison with previous information, Figure 3.16 shows the water-alkanes mutual solubilities data written in terms of γ^∞ . As can be seen both the A-UNIFAC and the original UNIFAC models can describe accurately the solubility of water in n-alkanes, which is not the case for the Modified UNIFAC of Dortmund. However, the extremely low solubility of n-alkanes in water is not predicted by any of the models though the best approximation is given by the A-UNIFAC model.

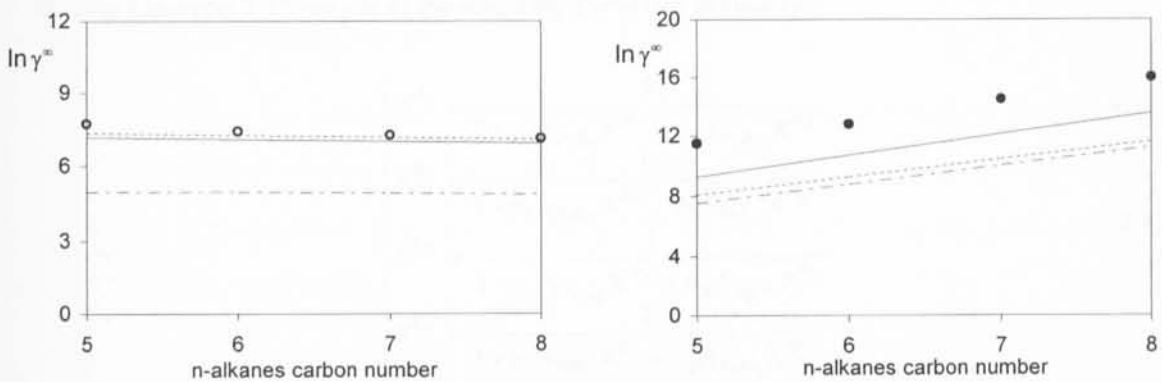


Figure 3.16 Infinite dilution activity coefficients at 298K versus carbon number of alkanes. Exp. Data (Sørensen and Arlt, 1979): ● n-alkanes in water; ○ water in n-alkanes. Models: — A-UNIFAC; --- Original UNIFAC; - · - Modified UNIFAC (Dortmund).

3.4 Approximated model

As discussed in the Chapter 2, the rigorous model can result, by imposing some restrictions, in an analytical solution for X^{A_k} when, at the most, two different association groups are present. In order to extend the A-UNIFAC model to mixtures containing any number of hydrogen bonding species and keep the model as a practical engineering tool, the following approach is proposed in this work.

One should define three different types of associating groups, as illustrated in Figure 3.17:

- Associating group 1 with two sites: an electropositive site A^+ and an electronegative site B^- that self-associates (e.g. water, alcohol, acid);
- Associating group 2 with one electronegative site N^- (e.g. esters, ketones, aromatics) that can cross-associate with sites A^+ and P^+ but cannot self-associate;
- Associating group 3 with one electropositive site P^+ (e.g. chloroform) that can cross-associate with sites B^- and N^- but cannot self-associate.

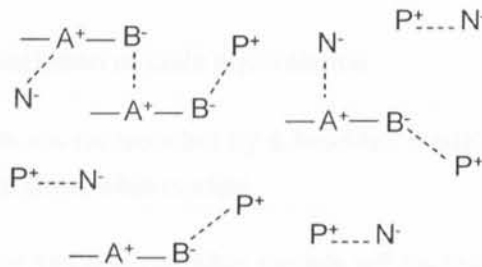


Figure 3.17 Schematic representation of the three types of associating groups.

Solving Equation 3.19 results in the following system of equations:

$$\begin{cases} X^{A_1} = \frac{1}{1 + \rho_1 \Delta_{A_1 B_1} X^{B_1} + \rho_2 \Delta_{A_1 N_2} X^{N_2}} \\ X^{B_1} = \frac{1}{1 + \rho_1 \Delta_{A_1 B_1} X^{A_1} + \rho_3 \Delta_{B_1 P_3} X^{P_3}} \\ X^{N_2} = \frac{1}{1 + \rho_2 \Delta_{A_1 N_2} X^{A_1} + \rho_3 \Delta_{N_2 P_3} X^{P_3}} \\ X^{P_3} = \frac{1}{1 + \rho_1 \Delta_{P_3 B_1} X^{B_1} + \rho_2 \Delta_{P_3 N_2} X^{N_2}} \end{cases} \quad (3.43)$$

In order to extend the model to mixtures containing any number of cross-associating species it will be assumed that the cross-association strengths will be equal to the self-association strength $\Delta_{A_i B_1}$. This simplification results in the following analytical solutions for the system of equations 3.43:

$$\Delta_{A_i B_1} = \Delta_{P_3 B_1} = \Delta_{A_i N_2} = \Delta_{N_2 P_3} = \Delta^* \quad (3.44)$$

$$X^{A_1} = X^{P_3} = \frac{2}{1 + (\rho_2 - \rho_3)\Delta^* + \sqrt{[1 + (\rho_2 - \rho_3)\Delta^*]^2 + 4(\rho_1 + \rho_3)\Delta^*}} \quad (3.45)$$

$$X^{B_1} = X^{N_2} = \frac{2}{1 + (\rho_3 - \rho_2)\Delta^* + \sqrt{[1 + (\rho_3 - \rho_2)\Delta^*]^2 + 4(\rho_1 + \rho_2)\Delta^*}} \quad (3.46)$$

Then, to distinguish between the different magnitudes of the association strength each family of compounds is considered to have a different concentration of the corresponding associating group. This "concentration" is represented by v_k^i , (*i.e.* the estimated number of times associating group k is present in molecule i) which then becomes a non-integer number that can be empirically adjusted. This means that mixtures containing several associating groups that self-and cross-associate can be modelled by equations 3.45 and 3.46.

3.4.1 One- and two-site association models equivalence

This approach requires that acids are represented by a two-sites model. This section discusses that possibility by comparing the one and two sites models.

The equivalence between the one site and two sites models will be made in order to reproduce the same association degree, *i.e.*, the same monomer fraction X^{mon} .

Let us consider again a mixture of one associating component (1) with one inert (2). Table 3.8 shows the equations obtained for $\gamma_1^{\infty, \text{assoc}}$ and $\gamma_2^{\infty, \text{assoc}}$ in terms of the fraction of monomers X^{mon} , for both, the one- and two-site association models.

As mentioned before, the most important contribution to the infinite dilution activity coefficient of the association component comes from the logarithmic term $\ln(1/X^{\text{mon}})$, which is the same for both models. However, for the inert component, the $\ln \gamma_2^{\infty, \text{assoc}}$ predicted by the one-site model is about half the value for the two-site model.

Table 3.8 Expressions obtained for X^{A_k} , X^{mon} and $\gamma^{\infty, \text{assoc}}$ using the one and two sites models.

| One site model | Two sites model |
|---|--|
| In both cases: | |
| $X^{A_k} = \frac{-1 + \sqrt{1 + 4 \rho_k \Delta_k}}{2 \rho_k \Delta_k}$ | |
| $X^{\text{mon}} = X^{A_k}$ | $X^{\text{mon}} = (X^{A_k})^2$ |
| $\ln \gamma_1^{\infty, \text{assoc}} = v_k^1 \left[\ln \left(\frac{1}{X^{\text{mon}}} \right) + \frac{X^{\text{mon}} - 1}{2} \right]$ | $\ln \gamma_1^{\infty, \text{assoc}} = v_k^1 \left[\ln \left(\frac{1}{X^{\text{mon}}} \right) + \sqrt{X^{\text{mon}}} - 1 \right]$ |
| $\ln \gamma_2^{\infty, \text{assoc}} = \frac{v_k^1}{2} (1 - X^{\text{mon}}) \frac{r_2}{r_1}$ | $\ln \gamma_2^{\infty, \text{assoc}} = v_k^1 (1 - \sqrt{X^{\text{mon}}}) \frac{r_2}{r_1}$ |

3.4.2 Association at infinite dilution

As already mentioned, the association contribution to the activity coefficient is very significant at infinite dilution. The expressions obtained for the limiting $\gamma^{\infty, \text{assoc}}$ values for a binary mixture containing one associating compound 1 having one self-associating group 1 with sites A^+ and B^- and one compound 2 with an electronegative site N^- that can cross-associate but not self-associate, will be presented. At very low concentrations of the self-associating component 1 ($\rho_1 \rightarrow 0$), the fractions X^{N_2} and X^{B_1} in solution will be close to one. And the fraction X^{A_1} will approach the limiting value $X^{A_1, \infty}$ given by:

$$X^{A_1, \infty} = \frac{1}{1 + \rho_2 \Delta^*} \quad (3.47)$$

this results in the following limiting value for the activity coefficient:

$$\ln \gamma_1^{\infty, \text{assoc}} = v_k^1 \left\{ \ln \left[\frac{X^{A_1, \infty}}{(X^{A_1})^2} \right] + X^{A_1} - \frac{1}{2} (X^{A_1, \infty} + 1) + \frac{\rho_2 \Delta^*}{1 + \rho_2 \Delta^*} \right\} \quad (3.48)$$

In this case the value of $\gamma_1^{\infty, \text{assoc}}$ depends on the other component.

When component 2 is an inert not capable of self-or cross-association ($\rho_2 \rightarrow 0$ and $X^{A_1, \infty} \rightarrow 1$)

Equation 3.26 will be obtained.

3.4.3 Parameterization

In general, association models require specific parameters to each associating species. This means that, when applied to a mixture with two or more associating species, these models need not only a set of self-association parameters, but also specific cross-association parameters (or the definition of appropriate combining rules between the self-association parameters). In this approximated approach all the cross-association strengths were assumed to be equal and the distinction between the different association strengths is done by calculating a different *density* for each associating group. This resulted in a significant simplification for the monomer fraction expressions. The improvements relatively to the original UNIFAC model are considerable, especially for the more diluted range of compositions. The same database used for this approach includes the one from the previous section (Table 3.4). Additionally, binary VLE of alkyl chlorides with alcohols, acids or esters were also used.

3.4.3.1 Association parameters

Similarly to the previous association approach, a single two-sites hydroxyl group is used to represent association effects for both water and alcohols. Therefore, for alcohols and water, the same method is followed and the parameters between those groups and alkanes have already been determined (Tables 3.5 and 3.6). And how can acids be represented?

It is known that carboxylic acids show a high degree of association even at low vapour densities and the formation of dimers in both, liquid and vapour phases, is generally accepted. The association of carboxylic acids in the vapour phase differs strongly from that of water and alcohols. In general, this association is calculated using the Hayden and O'Connell (1975) method, when the virial equation of state is applied together with activity coefficient models to correct for vapour-phase non-idealities. On the other side, carboxylic acids, water and alcohols present a similar degree of association at liquid like densities. Figure 3.18 shows the fraction of monomers calculated by the SAFT equation (Huang and Radosz, 1990) for ethanol and acetic acid at liquid conditions. The curves in Figure 3.18a correspond to saturated liquid conditions and they are shown to diverge at high temperatures, *i.e.* when the liquid density decreases towards the critical-point value. The curves in Figure 3.18b, on the other hand, were calculated at a constant liquid density, equal to that of the pure compound at 298K. Here the degree of association, as measured by the fraction of monomers, is similar for ethanol and acetic acid. This similarity supports the development of a single hydrogen-bonding model to account for the association of alcohols, water and carboxylic acids in the liquid phase, where activity coefficient models are applied.

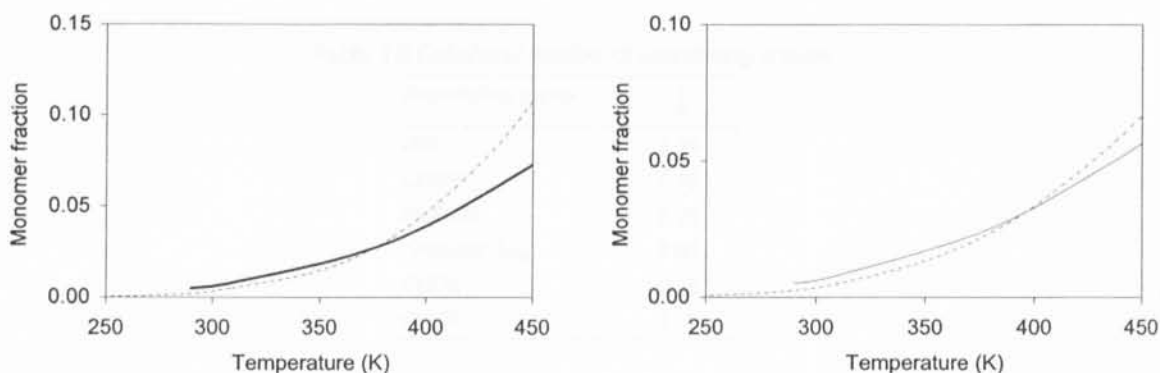


Figure 3.18 Monomer fractions predicted by SAFT equation for liquid ethanol (---) and acetic acid (—). (a) at saturated liquid densities; (b) liquid densities at 298.15K.

When a single association group is considered to represent association in mixtures of alcohols, water and/or inert compounds the computation of the association contribution to the activity coefficients reduces to a single self-association model. In this situation there is an explicit solution to compute the fraction of non-bonded associating groups. In our case, it should be necessary to assign the same number of bonding-sites to the associating groups of carboxylic acid, alcohol and water molecules. Therefore, in this work a two-site hydrogen-bonding model is used to calculate the association contribution to the activity coefficients of carboxylic acids in the liquid phase. Following this assumption, the COOH ($M_k = 1$) associating group in carboxylic acids is described by the same hydroxyl OH group ($M_k = 2$) that is used in alcohols and water. According to the previous discussions (section 3.4.1), this simplifying assumption will have hardly any effect on the association contribution to the activity coefficients of carboxylic acids as predicted by the A-UNIFAC model. However, this is not the case for inert compounds in mixtures with carboxylic acids. For the inert compound a two-site model ($M_k = 2$) will tend to over predict the association contribution to the activity coefficient, as compared with the one-site model ($M_k = 1$). An empirical approach to overcome this problem is to consider v_k^A (*i.e.* the number of OH groups in carboxylic acid molecules) as an adjustable parameter. VLE data for carboxylic acids + alkanes binaries were used to simultaneously adjust the values of v_k^A and the residual interaction parameters between the paraffinic (CH_2) and carboxylic (COOH) functional groups ($a_{\text{CH}_2, \text{COOH}}$ and $a_{\text{COOH}, \text{CH}_2}$). A value of $v_k^A = 0.9$ was obtained and this was used to represent the number of OH associating groups in all carboxylic acid molecules. Water, alcohols and acids are considered to be a type 1 associating group. On the other hand, the ester group is considered to be a type 2 associating group, *i.e.*, it has a specific electronegative site that can cross-associate with electropositive sites but that does not self-associate. That is also the case of the aromatic ring group. Finally, alkyl chlorides are represented by a type 3 associating group.

The density of each associating group is calculated by adjusting the corresponding number of associating groups (Table 3.9).

Table 3.9 Calculated number of associating groups

| Associating group | v_k^i |
|--------------------|---------|
| OH | 1.00 |
| COOH | 0.90 |
| RCOOR | 0.25 |
| Aromatic ring | 0.05 |
| CHCl ₃ | 0.10 |
| CH ₂ Cl | 0.06 |

3.4.3.2 Residual parameters

Again, it is necessary to re-parameterize the group interaction parameters for the residual term. Table 3.10 reports the new values for the interaction parameters between paraffinic, aromatic, alcohol, water, ester, acid and chloride groups.

Table 3.10 Residual group interaction parameters $a_{m,n}$ (K)

| m \ n | CH ₂ | ACH | OH | CH ₃ OH | H ₂ O | CCOO | COOH | CCl | CCl ₂ | CCl ₃ | CCl ₄ |
|--------------------|---------------------|--------------------|--------|--------------------|------------------|--------------------|--------|---------------------|--------------------|--------------------|---------------------|
| CH ₂ | 0.0 | 61.13 ^b | 50.40 | 122.7 | 380.5 | 232.1 ^b | 10.57 | 35.93 ^b | 53.76 ^b | 24.90 ^b | 104.3 ^b |
| ACH | -11.12 ^b | 0.0 | -94.42 | n.a. | 251.2 | 5.994 ^b | -150.2 | n.a. | n.a. | n.a. | n.a. |
| OH | 387.4 | 280.4 | 0.0 | 110.9 | -127.3 | 93.92 | 50.2 | 369.9 | -224.5 | -142 | 250.0 |
| CH ₃ OH | -19.78 | n.a. | 60.18 | 0.0 | -167.6 | n.a. | n.a. | n.a. | n.a. | n.a. | n.a. |
| H ₂ O | 136.8 | 93.3 | 70.7 | 251.2 | 0.0 | 221.6 | 89.0 | n.a. | n.a. | n.a. | n.a. |
| CCOO | 114.8 ^b | 85.84 ^b | -23.97 | n.a. | -220.5 | 0.0 | 787.7 | n.a. | -53.71 | -211.1 | 54.47 ^b |
| COOH | 756.0 | 577.4 | -125.6 | n.a. | -203.3 | -255.1 | 0.0 | -167.4 | 404.5 | n.a. | 1381 |
| CCl | 91.46 ^b | n.a. | -75.96 | n.a. | n.a. | n.a. | 380.4 | 0.0 | 108.3 ^b | 249.2 ^b | 62.42 ^b |
| CCl ₂ | 34.01 ^b | n.a. | 475.0 | n.a. | n.a. | -24.27 | -143.5 | -84.53 ^b | 0.0 | 0.0 ^b | 56.33 ^b |
| CCl ₃ | 36.70 ^b | n.a. | 366.4 | n.a. | n.a. | 184.8 | n.a. | -157.1 ^b | 0.0 ^b | 0.0 | -30.10 ^b |
| CCl ₄ | -78.45 ^b | n.a. | 72.50 | n.a. | n.a. | 129.5 ^b | -105.7 | 11.80 ^b | 17.97 ^b | 51.90 ^b | 0.0 |

^a n.a., not available; ^b original UNIFAC parameters Gmehling *et al.* (1982).

3.4.4 Results

The assumption of only one association strength results in a less flexible model. The improvements relatively to the UNIFAC model are not as significant. However, this alternative approach can be used to improve the results at the more diluted region of compositions without significantly increasing the mathematical complexity of the UNIFAC model.

3.4.4.1 Vapour-liquid equilibria

Table 3.11 reports the average errors calculated in the correlation of VLE data with the UNIFAC and A-UNIFAC models. In general, slight improvements are obtained in the correlation of VLE data with the A-UNIFAC model, as compared to the original UNIFAC model.

Table 3.11 Average errors in pressure (δP) and composition (δy) for the UNIFAC and A-UNIFAC models.

| System | UNIFAC | | A-UNIFAC | |
|-----------------------|------------|------------|------------|------------|
| | δy | δP | δy | δP |
| methanol + alkane | 3.3 | 4.6 | 2.4 | 3.3 |
| methanol + alcohol | 2.8 | 3.1 | 2.5 | 3.1 |
| methanol + water | 4.2 | 4.8 | 1.6 | 4.1 |
| alcohol + alkane | 3.8 | 6.8 | 3.1 | 6.6 |
| water + alcohol | 6.4 | 3.2 | 5.5 | 3.0 |
| acid + alkane | 4.2 | 2.4 | 3.3 | 2.5 |
| water + acid | 8.7 | 3.5 | 9.6 | 4.5 |
| alcohol + acid | 8.9 | 7.4 | 6.1 | 6.0 |
| alcohol + ester | 5.4 | 2.4 | 5.3 | 2.8 |
| water + ester | 7.4 | 7.0 | 7.1 | 5.9 |
| acid + ester | 7.5 | 2.3 | 7.5 | 2.0 |
| alcohol + aromatic | 5.6 | 3.2 | 4.8 | 3.4 |
| acid + aromatic | 4.2 | 4.3 | 3.3 | 4.2 |
| alcohol + chlorinated | 6.5 | 3.4 | 6.4 | 3.2 |
| acid + chlorinated | 7.0 | 8.0 | 6.7 | 5.8 |
| ester + chlorinated | 2.5 | 1.4 | 2.0 | 1.1 |

$$\delta z = 100 \sqrt{\frac{1}{N} \sum_i (|z_i(\text{exp}) - z_i(\text{calc})| / z_i(\text{exp}))^2 / NP}$$

where z represents y or P.

3.4.4.2 Ternary liquid-liquid equilibria prediction

Figures 3.19 and 3.20 show the liquid-liquid equilibrium predictions for the ternary systems water - ethanol - hexane and water - acetic acid - hexane, respectively. Finally, Figure 3.21 shows the results for a ternary system containing three associating species: water, butyric acid and n-hexanol. Very good predictions of the distribution coefficients are obtained and the improvements over the original UNIFAC are particularly remarkable at low concentrations of the associating component, where the association effect is more relevant.

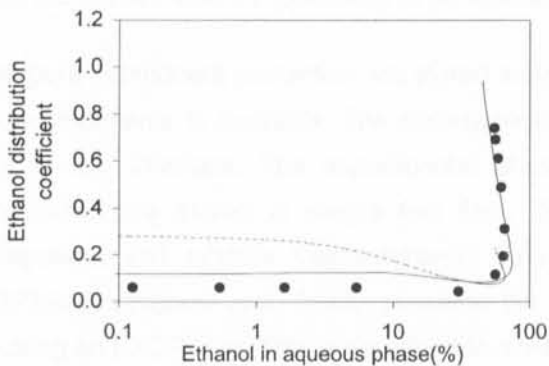


Figure 3.19 Ethanol distribution coefficients between hexane and water at 298K: \diamond experimental data (Roddy and Coleman, 1981); — A-UNIFAC; --- UNIFAC.

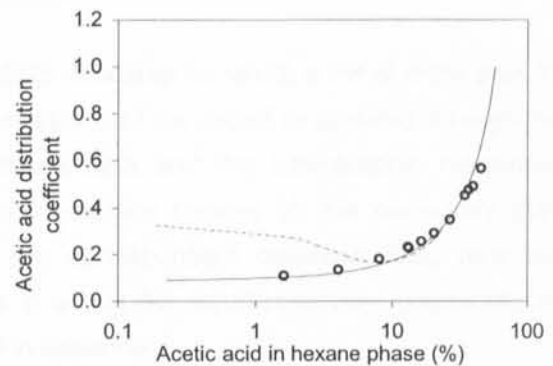


Figure 3.20 Distribution coefficients of acetic acid between hexane and water at 298K: \circ experimental data (Sørensen and Arlt, 1979); — A-UNIFAC; --- UNIFAC.

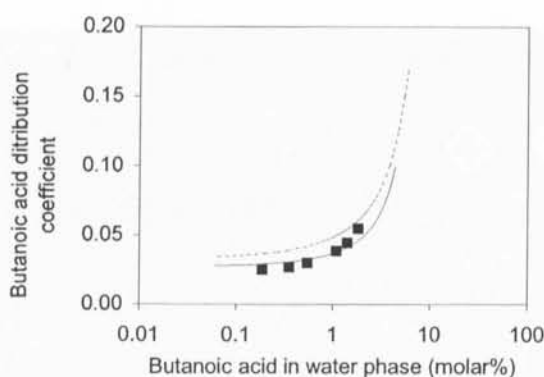


Figure 3.21 Distribution coefficients of butyric acid between 1-hexanol and water at 303K: ■ experimental data (Sørensen and Arlt, 1979); — A-UNIFAC; --- UNIFAC.

3.5 Software developed in FORTRAN and VISUAL BASIC languages

A program was developed in FORTRAN language to estimate the parameters using vapour-liquid equilibria, liquid-liquid equilibria, infinite dilution activity coefficients, solid-liquid equilibria, osmotic coefficients, vapour pressure, boiling point and freezing point of binary and ternary mixtures. The Levenberg-Marquardt algorithm (Marquardt, 1963) is used to optimize the residual and association parameters, using the ZXSSQ subroutine from IMSL (International and Mathematics and Statistical Libraries).

The extension of the A-UNIFAC parameter tables to a significant number of groups requires the use of several pure component properties as well as binary VLE, LLE or γ^∞ data. In order to access and store this information in a friendlier manner, a graphic interface was developed in VISUAL BASIC language.

The A-UNIFAC program is a visual interface for WINDOWS environment (Figure 3.22). The program allows the calculation of several thermodynamic properties using the original UNIFAC and the A-UNIFAC models with the possibility of parameters estimation.

The pure component properties are stored in an ACCESS database for which a list of more than 12 000 components is available. The correspondent information can be added or updated through the use of this interface. The experimental phase equilibria data and the bibliographic references information are stored in simple text files. The visual interface creates all the necessary pure component and mixture thermodynamic data from the correspondent database files, runs the FORTRAN program and, finally, presents the results in a text file or, alternatively, graphically by creating an EXCEL file. This is described in more detail in Appendix A.

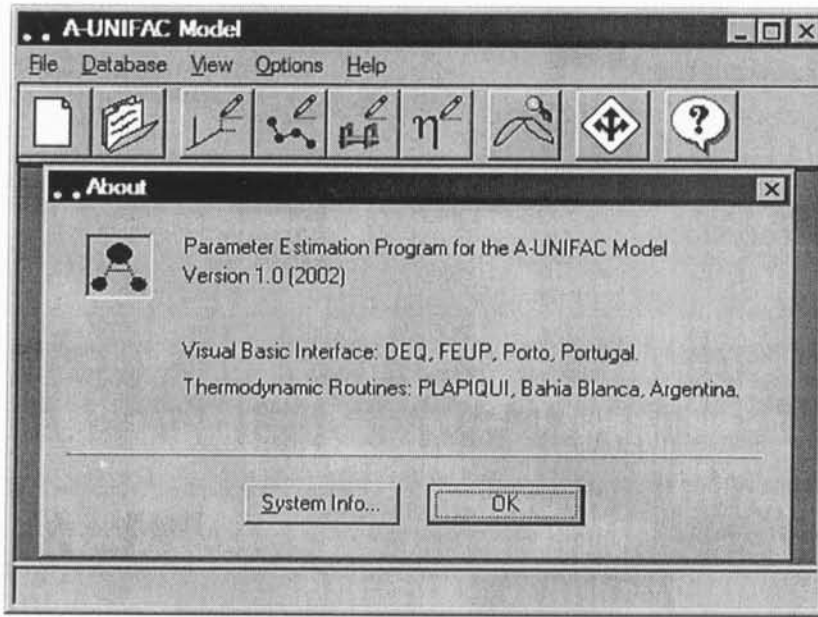


Figure 3.22 The A-UNIFAC program.

3.6 Conclusions

The A-UNIFAC model has been successfully applied to calculate activity coefficients in associating solutions containing water, alcohols, carboxylic acids, esters, alkanes, aromatic hydrocarbons and alkyl chlorides.

Two alternative approaches are proposed:

- The consideration of specific association strengths for each associating group resulted in a more flexible and rigorous model. Good results were obtained in the correlation and prediction of vapor-liquid equilibria and infinite dilution activity coefficients of binary mixtures containing alcohols, carboxylic acids, water, esters, aromatics and alkanes compared to the original UNIFAC model.
- In the approximated model all the cross-association strengths were assumed to be equal and the distinction between the different association strengths is done by calculating a different *density* for each associating group. Only two association parameters had to be determined and no combining rules are required to calculate cross-association from self-association parameters. This resulted in significant simplification for the monomer fraction expressions. The improvements relatively to the original UNIFAC model are considerable, especially in the more diluted range of compositions.

The approximated model can be used to account for associating effects, especially in the more diluted range of compositions, having the advantage of simplified expressions for the monomer fraction. The rigorous model is recommended for more accurate predictions.

4. Phase equilibria in sugar solutions with the A-UNIFAC model

1.1. Introduction

The present work is devoted to the study of phase equilibria in sugar solutions with the A-UNIFAC model. The first part of the paper is devoted to the description of the model and the calculation of the activity coefficients. The second part is devoted to the calculation of the phase equilibria. The third part is devoted to the comparison of the results with experimental data.

The A-UNIFAC model is a semi-empirical model for the calculation of the activity coefficients of components in liquid mixtures. It is based on the UNIFAC model, which is a group-contribution model for the calculation of the activity coefficients of components in liquid mixtures. The A-UNIFAC model is a modification of the UNIFAC model, which takes into account the specific interactions between the components of the mixture.

Chapter 4

Phase equilibria in sugar solutions with the A-UNIFAC model

4. Phase equilibria in sugar solutions with the A-UNIFAC model

4.1 Introduction

Carbohydrates are one of the most abundant classes of organic compounds that can be found in living organisms. This large natural resource has a broad range of applications in the chemical industry. They are present in a variety of industries (textile, paper, coatings, food) and are, also, used in several biological applications.

In this work, the focus is on the important fraction of carbohydrates made up of the smaller building units: the mono and the disaccharides. In order to have a better idea of the importance of these components in the world industry, Table 4.1 shows a list of the annual production of simple sugars and sugar derived components as compared to basic chemicals.

Table 4.1 Annual production of simple sugars, sugar-derived alcohols, and acids compared to some petrochemically derived basic chemicals and solvents.

| | Production * (t/year) | | Production (t/year) |
|----------------------------|--------------------------|------------------------|------------------------|
| Sugars | | Sugar alcohols | |
| Sucrose | 130 000 000 | D-Sorbitol | 900 000 |
| D-glucose | 5 000 000 | D-Xylitol | 30 000 |
| Lactose | 295 000 | D-mannitol | 50 000 |
| D-fructose | 60 000 | Amino acids | |
| Isomaltulose | 50 000 | L-Lysine | 40 000 |
| Maltose | 3000 | L-Glutamic acid | 500 000 |
| D-Xylose | 50 000 | Basic chemicals | |
| L-Sorbose | 60 000 | Aniline | 1 300 000 |
| Sugar-derived acids | | Acetaldehyde | 900 000 |
| D-gluconic acid | 60 000 | Adipic acid | 1 500 000 |
| L-Lactic acid | >100 000 | Solvents | |
| Citric acid | 500 000 | Methanol | 25 000 000 |
| L-Tartaric acid | 35 000 | Toluene | 6 500 000 |
| | | Acetone | 3 200 000 |

*Reliable data are only available for the world production of sucrose, the Figure given referring to the crop cycle 2000/2001 (International Sugar Organization, "World sugar production 2000/2001", Zuckerind, Berlin). All other data are average values based on estimates from producers and/or suppliers, as the production volume of many products is not publicly available (Lichtenthaler, 2002).

In a broader context, the large scale availability of sugars suggests their use, in the future, as biofeedstock for the production of organic chemicals, substituting the non renewable fossile resources (Lichtenthaler, 2002).

Nowadays, the larger part of sugars production is, mainly, used for the food industry. The most common process, in which sugars are involved, is crystallization, that demands a correct description of the solid-liquid equilibria (calculation of solubilities and freezing point) and vapour-liquid equilibria (boiling point and vapour pressure) of sugars in water. Another important property, particularly for the food industry, is the water activity of the solutions, since it is one of the factors that affects the microbiological activity and the development of chemical reactions in an aqueous medium.

Though most processes use water as solvent, in some cases, it is useful to add small amounts of alcohols. For example, in the case of the production of D-fructose as a sweetener, due to its high solubility in water, the addition of short-chain alcohols facilitates the crystallization processes, by decreasing its solubility and the viscosity of the solution (Flood *et al.*, 1996). Another possible application is the use of methanol or ethanol as co-solvents to selectively separate D-xylose from D-mannose in aqueous solutions (Gabas *et al.*, 1988).

Besides the traditional applications, many high value food and pharmaceutical products are being developed, using sugars as raw materials. For example, sucrose esters can have many applications, depending on the number and size of the substituents, in cosmetics, detergents, pharmaceuticals and food; sugar alcohols are used as sweeteners, amongst other applications.

Many of these products are obtained via enzymatic methods. Recent works in the biocatalysis area suggest the use of non-aqueous solvents as a medium for those reactions, *e.g.*, the monoacylation of D-fructose with long chain fatty acids in n-hexane or 2-methyl-2-butanol (Scheckerman *et al.*, 1995, Coulon *et al.*, 1997).

Which should be the model chosen to describe the thermodynamic properties of these mixtures? Usually, the number of components involved is large and the experimental information is scarce, so it is a good option to use a group-contribution method. Also, from the chemical interactions point of view, these solutions contain the sugar cyclic structures with many hydrophobic and hydrophilic substituents, and polar solvents like water and/or alcohols. These solutions exhibit a complex behaviour as they are highly associated. In this chapter, the application of the A-UNIFAC model to these complex mixtures is studied and discussed.

4.2 Chemical Structure

Originally, carbohydrates comprised only the carbon hydrates of formulae $C_n(H_2O)_n$ referring to the empirical formula of monosaccharides. Nowadays, the term includes not only, mono-, oligo- and polysaccharides but, also, other substances derived from them with different functionalities, besides hydroxyl groups, *e.g.*, alditols, uronic acids, deoxy-sugars, glycosylamines, amino sugars, etc.

In the next sections, the most important mono and disaccharides will be briefly described.

4.2.1 Monosaccharides

The simplest carbohydrates that cannot be hydrolyzed are called monosaccharides. Chemically, they are polyhydroxyaldehydes (aldoses) or polyhydroxyketones (ketoses). The smallest members are dihydroxyacetone and glyceraldehyde. The latter contains a stereocenter which results in the existence of two stereoisomers that are mirror images of each other (enantiomers), as shown on Figure 4.1.

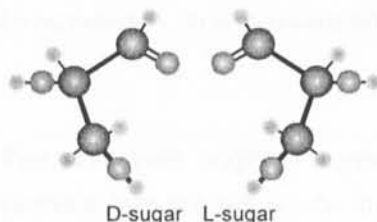


Figure 4.1 Enantiomeric forms of glyceraldehyde.

By convention, the (+)-glyceraldehyde is called D-(+)-glyceraldehyde and (-)-glyceraldehyde is designated L-(-)-glyceraldehyde. This nomenclature serves as a standard for the other monosaccharides. Almost all the monosaccharides synthesized in nature have the same configuration of the chiral carbon farthest away from the carbonyl group, *i.e.*, the same configuration of D- (+)-glyceraldehyde and they are referred to as D-sugars. The D-aldoses family tree is presented on Appendix B (Figure B.1).

D-glucose is the most abundant monosaccharide in nature, present in many fruits and plants and, also, in human blood. It constitutes the building block of starch, glycogen and cellulose. For the hexoses group, besides the D-glucose, it is worthwhile mentioning the D-galactose sugar which is part of lactose and raffinose and, also the D-mannose that occurs, naturally, in many polysaccharides. The pentoses group contains the building unit of the ribonucleic acids, D-ribose, and D-xylose found, mainly, in pentosans (xylans). For the D-ketoses family tree, shown on Appendix B (Figure B.2), the most common is the sweetest natural sugar, D-fructose, present in many fruits, in honey and as a building block in sucrose and, also, in the polysaccharide inulin.

As mentioned before, a monosaccharide molecule contains both functional groups C=O (aldehyde or ketone) and OH (hydroxyl). These groups can react to form more or less stable cyclic hemiketals (group ketone) or cyclic hemiacetals (group aldehyde) in equilibrium with the open-chain structure. For example, in the case of D-glucose, some cyclic forms (hemiacetals) can be formed by an intramolecular reaction of the aldehyde group either with the -OH group at carbon 4, forming a five-member ring (Figure 4.2a), or with the -OH group at carbon 5, forming a six-member ring (Figure 4.2b).

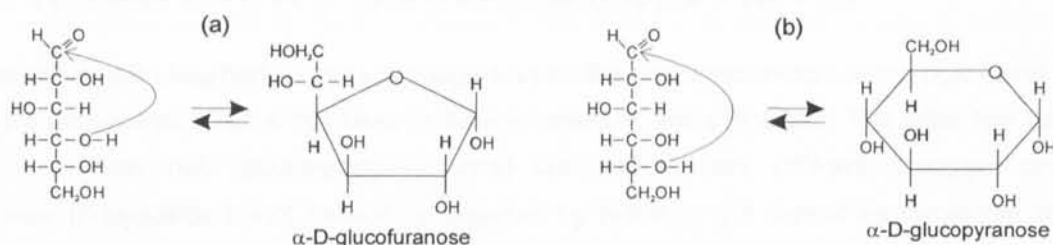


Figure 4.2 Ring formation: (a) furanose and (b) pyranose.

As can be seen from Figure 4.3, these reactions originate a new stereocenter at carbon one. This stereocenter results in two stereoisomers that are not mirror images of each other (*i.e.*, they are diastereomers). This particular type of diastereomers, that differ only in the configuration at carbon one, are designated by α (with the -OH down) and β (with the -OH up) anomers.

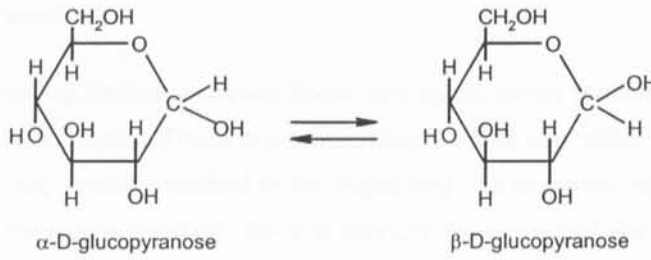


Figure 4.3 Diastereomers of D-glucopyranose.

Each pure anomer is characterized by a different optical rotation, melting and boiling points. However, in solution, for a given solvent, sugar concentration and temperature, a constant composition of the different conformers is achieved. Let us consider a solution of pure α -D-glucose which has an initial specific rotation of $+112^\circ$ and a solution of pure β -D-glucose with an initial specific rotation of $+18.7^\circ$. Ultimately, the rotation of both solutions will reach the same value of $+52.7^\circ$. The process of reaching this equilibrium between tautomers is called mutarotation.

4.2.2 Disaccharides

Another important group among the carbohydrates is the “disaccharides”. Their chemical structure is presented on Appendix B (Figure B.3). The most common that can be found in nature are: sucrose (“sugar table”), produced from sugar cane and sugar beet; lactose, one of the milk ingredients, and trehalose, present in fungi, mushrooms and algae. Other important disaccharides result from the hydrolysis of polysaccharides, e.g. maltose and isomaltose (products of the partial hydrolysis of starch) or cellobiose (one of the products of the partial hydrolysis of cellulose).

Disaccharides are classified as reducing sugars when the anomeric carbon on the right-hand sugar is part of a hemiacetal. That is the case of lactose, maltose and cellobiose. The latter two have very similar structures (two glucopyranoses units) but present very different biological properties: Cellobiose (β -glycoside bond) cannot be digested by humans and cannot be fermented by yeast. Maltose (α -glycoside bond), however, is digested without difficulty and is readily fermented. On the other hand, lactose contains two different units: D-glucose and D-galactose bonded from the anomeric carbon in the D-galactose ring to carbon four on the D-glucose ring. These reducing sugars have a free anomeric carbon on the glucopyranose ring (the right one), which allows them to mutarrotate.

Finally, both sucrose and trehalose are non reducing sugars. They result from the linkage at the two anomeric carbons of both monosaccharides units. Sucrose is composed of D-glucose and D-fructose joined by one α and one β glycoside bonds, whereas trehalose has two α glycoside bonds.

4.2.3 Mutarotation equilibria

As mentioned before, the equilibrium between linear and cyclic forms (furanose or pyranose rings) of sugars in solution is quite complex. There are several factors that can affect this equilibrium, namely, the type of substituents not directly attached to the sugar ring, the anomeric effect and the existence of inter or intramolecular hydrogen bonding. Several authors have studied the influence of the type of solvent and temperature of the solution on the mutarotation equilibrium of some common monosaccharides.

4.2.3.1 Influence of solvent

Goldberg and Tewari (1989) have studied the mutarotation of different monosaccharides in water. The composition of the different conformers is presented on Table 4.2.

Table 4.2 Composition (%) of the different monosaccharides conformers in equilibrium in aqueous solution (Goldberg and Tewari, 1989).

| | T (K) | α -pyranose | β -pyranose | α -furanose | β -furanose | Linear form |
|-------------|--------|--------------------|-------------------|--------------------|-------------------|-------------|
| D-fructose | 303.15 | 2 | 70 | 5 | 23 | 0.7 |
| D-glucose | 304.15 | 38 | 62 | 0 | 0.14 | 0.002 |
| D-galactose | 304.15 | 30 | 64 | 2.5 | 3.5 | 0.02 |
| D-mannose | 317.15 | 65.5 | 34.5 | 0.6 | 0.3 | 0.005 |
| D-xylose | 304.15 | 36.5 | 63 | <1 | <1 | 0.02 |

As can be seen, the pyranose forms prevail for monosaccharides in water. The higher proportion of the pyranose forms in water is usually attributed to the stabilization of these structures by the tridymite structure of water. Uedaira and Uedaira (2001) state that the equatorial alcoholic oxygen atoms may be placed in similar positions to the oxygen atoms of the water molecules. This should result in the formation of stronger hydrogen bonds between water and the equatorial hydroxyl groups on chair conformation of sugars. Catté *et al.* (1995) have used this stereochemical argument to set the hydration number of sugars equal to the number of OH groups that are not in axial position. Table 4.3 shows, for aqueous solutions, the number of hydroxyl groups that are not in axial position, for each conformer. For disaccharides, N_{OH} is given by the number of equatorial hydroxyl groups of the constituent monosaccharides minus the ones used in the osidic bond. In the last column, an average number of equatorial OH groups \bar{N}_{OH} for each mono and disaccharide is also presented. These values were calculated using the compositions of the different monosaccharide conformers in water (Table 4.2) as weight factors.

The \bar{N}_{OH} should be seen, only, as a first estimate of the number of groups available to cross-associate with water. The hydration extent will depend not only on the number of non-axial OH groups but also

on their relative position. The existence of intramolecular association and steric hindrance effects increases enormously the complexity of the sugars hydration.

The previous studies were performed for aqueous solutions. What happens, however, if one adds another solvent?

Flood *et al.* (1996) studied the D-fructose mutarotation equilibrium in several aqueous – ethanol solutions (3:1, 6:1 and 9:1 ethanol – water mass ratios), in the temperature range from 24°C to 50°C. They concluded that, for those conditions of temperature and composition, the furanose conformers are now in higher proportion in these solutions (about 60% against 28% in pure water). The addition of small amounts of ethanol destroys the ordered water structure that was considered to stabilize the β -pyranose tautomer. The increase in temperature has a similar effect as will be discussed next.

Table 4.3 Number of hydroxyl groups that are not in axial position for each conformer and calculated average number in aqueous solutions.

| Sugar | N_{OH} | | \bar{N}_{OH} | | |
|-------------|---------------------|--------------------|--------------------|-------------------|-----|
| Sucrose | 7 | | 7.0 | | |
| | α -conformer | β -conformer | | | |
| Maltose | 7 | 8 | 7.6 | | |
| Lactose | 6 | 7 | 6.6 | | |
| Cellobiose | 7 | 8 | 7.6 | | |
| | α -pyranose | β -pyranose | α -furanose | β -furanose | |
| D-fructose | 2 | 3 | 3 | 4 | 3.2 |
| D-glucose | 4 | 5 | - | - | 4.6 |
| D-galactose | 3 | 4 | 4 | 5 | 3.7 |
| D-mannose | 3 | 4 | - | - | 3.3 |
| D-xylose | 3 | 4 | - | - | 3.6 |

4.2.3.2 Influence of temperature

Maple and Allerhand (1987) and Lichtenthaler and Rönninger (1990) have studied the influence of temperature on the equilibrium composition of several furanoids and pyranoids in water. Figure 4.4 presents the results obtained for D-glucose and D-fructose.

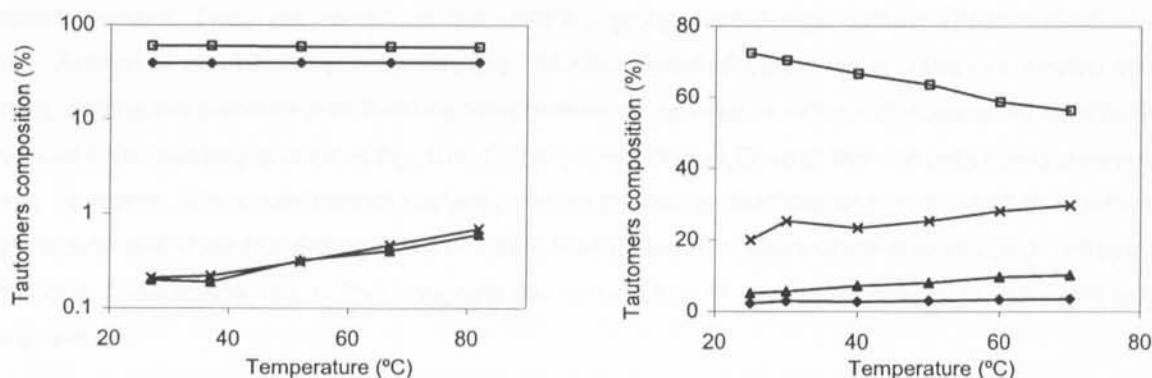


Figure 4.4 Tautomers equilibrium composition (mole %) of a sugar in water *versus* temperature: (a) D-glucose (Maple and Allerhand, 1987); (b) D-fructose (Lichtenthaler and Rönninger, 1990). Exp. data: —◆— α-pyranose; —□— β-pyranose; —▲— α-furanose; —×— β-furanose.

The proportion of the predominant tautomer (β-pyranose) decreases with rising temperature in favour of the three other forms. For the case of D-glucose, the same qualitative result is observed, though the change in the proportions of both pyranoses is small, in relative terms, compared to the increase of the furanose forms with temperature (Maple and Allerhand, 1987).

From this brief analysis, it is possible to conclude that the tautomers equilibria is quite complex and, yet, not fully understood. For the case of water, the most studied solvent until nowadays, both intra and intermolecular hydrogen bonding seem to play a very important role in the stabilization of some conformer over another.

4.3 Revision of available models

In the last decade a few number of models were specially developed or applied to the description of the phase equilibria of sugar mixtures. Some authors use a molecular approach: Abderafi and Bounahmidi (1994) use the Peng-Robinson equation (Peng and Robinson, 1976) to predict the vapour-liquid equilibria of the quaternary mixture D-glucose/D-fructose/sucrose/water. The binary interaction parameters water/sugar were estimated using binary aqueous sugar mixture data and the sugar/sugar interactions were, then, obtained by correlating ternary aqueous mixtures data. Catté *et al.* (1994) used a modified UNIQUAC (Larsen *et al.*, 1987) model with quadratic temperature dependent parameters to describe several thermodynamic properties of binary and multicomponent aqueous mixtures containing D-fructose, D-glucose and sucrose. This model uses the asymmetrical convention. Peres and Macedo (1996) also proposed a modified UNIQUAC model with some differences: the interaction parameters are taken as linearly temperature dependent and the symmetrical convention is used for all the components, which makes their extension to mixtures containing more than one solvent straightforward.

The majority of the models, however, follows a group-contribution approach, mainly, because of their predictive nature. They are based on the UNIFAC group-contribution method (Fredenslund *et al.*, 1977). Achard *et al.* (1992) have applied the UNIFAC model of Larsen *et al.* (1987) to predict water activity, boiling temperature and freezing temperature of aqueous solutions of sugars. To do this they have used the existing groups (CH₂, CH, C, OH, CHO and H₂O) and the corresponding parameter tables. However, this model cannot correctly predict properties that depend on the activity coefficient of the solute and does not distinguish the differences between carbohydrate isomers (*e.g.* D-fructose, D-glucose, D-galactose, etc.). This suggests the introduction of new main groups to represent sugar molecules.

Gabas and Laguérie (1990) and Abed *et al.* (1992) have used the UNIFAC model proposed by Fredenslund *et al.* (1977), with three new different groups to represent sugars molecules (Figure 4.5). This model was applied for the prediction of solid-liquid equilibrium of ternary aqueous systems.

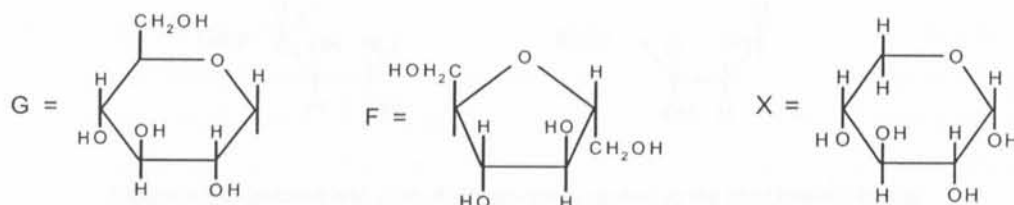


Figure 4.5 UNIFAC groups defined by Gabas and Laguérie (1990) and Abed *et al.* (1992) to represent sugar molecules.

Another model based on the UNIFAC method was proposed by Peres and Macedo (1997), here called P&M UNIFAC model. This model is based on the UNIFAC model of Larsen *et al.* (1987). Three new main groups were introduced to represent the pyranose ring (PYR), the furanose ring (FUR), the hydroxyl group directly attached to the ring (OH)_{ring} and the osidic bond (-O-) as shown on Figure 4.6:

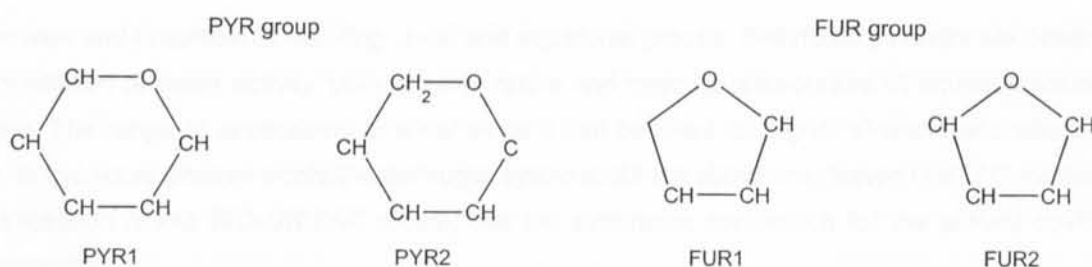


Figure 4.6 UNIFAC groups proposed by Catté *et al.* (1995) to represent sugar molecules.

All the interaction parameters were estimated using sugars thermodynamic experimental data. Additionally, it was necessary to adjust the heat capacity difference for each sugar, whenever there

was enough solubility experimental data available. Good predictions of thermodynamic properties dependent both on sugar and solvent activity coefficients, were obtained. However, a significant simplification was made: all the interaction parameters between alcohols, water and alkane groups were set equal to zero, based on the fact that the existing ones had been estimated using VLE data and, therefore, were not adequate to predict the SLE. This simplification does not allow the extension of the model to systems containing higher alcohols, alkanes and two liquid phases alcohol/water/sugar systems.

Kuramochi *et al.* (1997) presented the Bio-UNIFAC model, based on the UNIFAC method of Larsen *et al.* (1987). It was developed to represent the activity coefficients of biochemicals in water. This model is based on the asymmetrical convention for activity coefficients and it was also applied to sugar aqueous mixtures by defining four different main groups to represent, D-mannose, D-galactose, D-glucose and D-fructose. Figure 4.7 shows the two groups defined for the last two sugars:



Figure 4.7 D-glucose and D-fructose groups proposed in the Bio-UNIFAC model.

Spiliotis and Tassios (2000) proposed the S-UNIFAC model that uses the UNIFAC LLE model of Magnussen *et al.* (1981) to represent phase equilibria between existing groups. In this case, two new main UNIFAC groups were introduced to represent sugars: $(\text{CHOH})_{\text{sugar}}$ with the subgroups CH_2OH , CHOH_{ax} , CHOH_{eq} , COH_{ax} , COH_{eq} and the group CH-O-CH for the disaccharide osidic bond. Each sugar is represented by a unique species, more specifically the predominant anomer in the aqueous solution. Besides the residual interaction parameters, additional parameters were estimated: a different group area Q parameter was used in the combinatorial and residual terms. It is related to the group area Q parameter of the residual term as follows $Q'_i = c_i Q_i$, where c_i is an adjustable parameter and i represents non-ring, axial and equatorial groups. Satisfactory results are obtained for the prediction of water activity, boiling temperature and freezing temperature of aqueous solutions of sugars. The range of applicability is wider since it can be used for higher alcohols and alkanes and, also, to two liquid phases alcohol/water/sugar systems. All the above-mentioned UNIFAC models, with the exception of the BIO-UNIFAC model, use the symmetric convention for the activity coefficients normalization.

Besides the definition of new UNIFAC groups to represent sugars, some authors have introduced other modifications, to take into account the existence of specific hydrogen bonding interactions.

This is the case of a physical chemical UNIFAC model developed by Catté *et al.* (1995) for aqueous solutions of sugars. The physical part is given by Larsen *et al.* (1987) and the chemical part describes the conformational equilibria of sugars and the solvation equilibria between water and sugars. The physical part is described in terms of three new UNIFAC groups used to represent the sugar molecules: pyranose ring, furanose ring that are shown on Figure 4.6 and osidic bond.

The group interaction parameters are considered to be temperature dependent. Besides estimating the usual group interaction parameters for the physical part it is necessary to determine the numerous parameters for the chemical part: for one sugar with NC conformers there are NC hydration numbers, NC solvation equilibrium constants and NC conformational equilibrium constants. In order to reduce the number of adjustable parameters, some considerations had to be made, which resulted in the adjustment of only one extra parameter, besides the residual UNIFAC parameters: the temperature dependent g_B^∞ representing the partial molar Gibbs energy of the hydrogen bond. The optimization was carried out using binary thermodynamic data (water activity, osmotic coefficients, activity coefficients, boiling and freezing temperatures, excess Gibbs energy and excess enthalpy) for aqueous sugar mixtures (D-glucose, D-mannose, D-galactose, D-fructose, sucrose, lactose, maltose). Satisfactory results were obtained for the prediction of water activity of ternary systems water - sucrose - D-glucose and excess Gibbs energy at 298 K of binary water - sugar (D-xylose and raffinose). This model uses the asymmetric convention for activity coefficients and it is only applicable to aqueous sugar mixtures.

All the mentioned models need experimental thermodynamic data for sugars to estimate the interaction parameters. More recently, Jónsdóttir and Rasmussen (1999) and Jónsdóttir *et al.* (2002) have calculated UNIQUAC interaction parameters using molecular mechanics methods. By considering that water can only interact with a small fraction of the larger molecules, the interaction energies were determined between water and a functional subunit of the sugars molecules, the 1,2-propanediol molecule. This method was used for the prediction of VLE and SLE of aqueous sugar solutions. Jónsdóttir and Rasmussen (1999) have applied this method to binary mixtures of water and one sugar (D-glucose or sucrose). Satisfactory results were obtained in the calculation of water activities, freezing temperatures and solubilities of these two sugars. In the sugar solubilities calculation, the model is not totally predictive since the heat capacity difference between the pure liquid and solid (ΔC_p) is not known experimentally. These authors have approximated the heat capacity of the solution at infinite dilution as the pure liquid heat capacity. Jónsdóttir *et al.* (2002) have extended this method to the solubility calculation of a larger number of mono and disaccharides in aqueous systems. Satisfactory results are obtained for the monosaccharides. However, for the disaccharides only one acceptable agreement is achieved. As mentioned by the authors, the predictive ability of the above-mentioned methods is limited by good experimental values to describe the solid-liquid transition.

4.4 The A-UNIFAC model for sugar mixtures

The A-UNIFAC model presented in the previous chapter is used for the modelling of aqueous and non aqueous mixtures of sugars. This model is based on the symmetric activity coefficients convention normalization and should be readily extended to the highly associated sugar mixtures. The combinatorial, residual and association terms of the model are given by the equations 3.2 to 3.8 and equations 3.18 to 3.23.

4.4.1 Calculation of thermodynamic properties

The phase equilibrium of sugar mixtures involves the calculation of vapour-liquid equilibria (boiling point, vapour pressure, water activity and osmotic coefficient) and solid-liquid equilibria (freezing point and sugar solubilities). All the mentioned properties depend on the solvent activity coefficient, with the exception of the sugar solubility that involves the calculation of the sugar activity coefficient. The equations used for the calculation of the thermodynamic properties are presented here.

The equilibrium between two phases, α and β , in a closed system, is characterized by the equality of temperature and pressure:

$$T^\alpha = T^\beta \quad (4.1)$$

$$P^\alpha = P^\beta \quad (4.2)$$

And for every component i , in the mixture, by the isofugacity criterion:

$$f_i^\alpha = f_i^\beta \quad (4.3)$$

4.4.1.1 Vapour-Liquid equilibria

The fugacity equality between a liquid and a vapour phase can be expressed as:

$$y_i \hat{\phi}_i P = x_i \gamma_i f_i^\circ \quad (4.4)$$

where x_i and y_i are the liquid and vapour phase compositions, respectively; $\hat{\phi}_i$ is the fugacity coefficient in the vapour phase at temperature T and pressure P ; γ_i is the activity coefficient; f_i° is the fugacity evaluated at a reference state.

Equation 4.4 can be further simplified due to the low pressures involved (atmospheric or lower), namely: to set the Poynting factor and ϕ_i^{sat} equal to one and to assume ideal gas behaviour, for which

$$\hat{\phi}_i = 1.$$

Vapour pressure

In the case of an aqueous solution of sugars, it is reasonable to assume that the vapour pressure of the sugar $P_{\text{sugar}}^{\text{sat}}$ is negligible (for example, the vapour pressure of D-glucose at $T = 473.15\text{K}$ is $P_{\text{sugar}}^{\text{sat}} = 54.5\text{ Pa}$). Then, equation 4.5 can be written in terms of water properties (subscript w) (its vapour pressure P_w^{sat} varies from $P_w^{\text{sat}} = 611\text{ Pa}$ at $T = 273.16\text{ K}$ to $P_w^{\text{sat}} = 2.19 \times 10^7\text{ Pa}$ at $T = 647.13\text{ K}$) which allows the calculation of the vapour pressure of the aqueous sugar mixtures as follows:

$$P = x_w \gamma_w P_w^{\text{sat}} \quad (4.5)$$

Boiling Point

Using Antoine's equation to evaluate the vapour pressure of water it is possible to calculate the boiling temperature T^{boil} of a sugar aqueous mixture, at a given pressure and composition, through an iterative procedure, by solving equation 4.6 with respect to temperature:

$$T^{\text{boil}} = \frac{B}{A - \log \left[\frac{P}{\gamma_w(x_w, T^{\text{boil}}) x_w} \right]} - C \quad (4.6)$$

The A, B and C coefficients of the equation of Antoine can be obtained from the database compiled by Gmehling *et al.* (1977).

Water activity

For a given composition x_w and temperature, the water activity (a_w) can be calculated directly from the following equation:

$$a_w = x_w \gamma_w \quad (4.7)$$

Osmotic coefficient

The osmotic coefficient (ϕ) of an aqueous solution, at a given composition and temperature can be obtained by:

$$\phi = -\frac{1000}{M_w m} \ln a_w \quad (4.8)$$

where M_w is the molecular weight of water (g/mol) and m is the molality of the solution (mol of solute per kg of solvent).

4.4.1.2 Solid-Liquid equilibria

The fugacity equality between a solid and a liquid phase can be expressed as:

$$x_i^s \gamma_i^s f_i^{o,s} = x_i^l \gamma_i^l f_i^{o,l} \quad (4.9)$$

where superscripts s and l refer to the solid and liquid phases, respectively; x_i is the composition, γ_i is the activity coefficient and f_i^o is the fugacity evaluated at a reference state for component i. Assuming that the solvent is not present in the solid phase, equation 4.9 can be written for the solute (component 2), where superscript l was omitted for simplicity, as:

$$x_2 = \frac{f_2^s}{\gamma_2 f_2^{o,l}} \quad (4.10)$$

Therefore, the solubility is not only a function of the activity coefficient of the solute (intermolecular forces in the solution) but also depends on the pure solid-liquid fugacity ratio that can be calculated using the solute properties (it is independent of the solvent).

In general $f_2^{o,l}$ is set equal to fugacity of the pure, subcooled liquid at the temperature of the solution and at a specified pressure. The fugacity ratio can be determined by calculating the molar Gibbs energy change for component 2, going from pure solid state to the pure subcooled liquid state, at the temperature of the solution T , using a thermodynamic cycle passing through the triple point temperature T_t as represented on Figure 4.8.

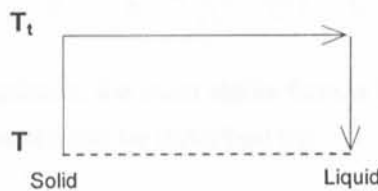


Figure 4.8 Thermodynamic cycle for the fugacity ratio calculation.

This results in the following expression for the fugacity ratio (Prausnitz *et al.*, 1999):

$$\ln\left(\frac{f_2^{o,l}}{f_2^s}\right) = \frac{\Delta H_{t,2}^f}{R} \left(\frac{1}{T} - \frac{1}{T_{t,2}}\right) + \frac{1}{R} \int_T^{T_t} \Delta C_{p,2} dT - \frac{1}{R} \int_{T_{t,2}}^T \left(\frac{\Delta C_{p,2}}{T}\right) dT \quad (4.11)$$

In this equation, $\Delta H_{i,2}^f$ is the melting enthalpy evaluated at T_i and ΔC_p is the difference between the heat capacity of the pure liquid and solid. Usually, the triple point temperature is replaced by the melting temperature since that, for most components, they do not differ significantly from each other (e.g. for water: $T_i = 273.16$ K and $T_m = 273.15$ K). Also, the melting enthalpy is evaluated at the normal melting temperature.

Freezing point

Equations 4.10 and 4.11 can also be used to calculate the freezing point depression of aqueous sugar mixtures. In this case it is usually assumed that this depression is small enough to consider constant heat capacities of pure liquid water and of pure ice. In this case, the freezing point of water T_w^m can be found iteratively from:

$$\ln(x_w, \gamma_w(x_w, T_w^m)) = \frac{\Delta H_w^f}{R} \left(\frac{1}{T_w^m} - \frac{1}{T^m} \right) - \frac{\Delta C_{p,w}}{R} \ln \left(\frac{T_w^m}{T^m} \right) - \frac{\Delta C_{p,w}}{R} \left(1 - \frac{T_w^m}{T^m} \right) \quad (4.12)$$

Sugar Solubility

Depending on the temperature of the system, some sugars have different stable forms on the solid state: hydrated or anhydrous forms. In the case where the solvent is not present in the solid phase, the anhydrous sugar solubility can be calculated using equation 4.13. Assuming no temperature dependence for ΔC_p , the final expression is:

$$\ln(x_2 \gamma_2) = \left[-\frac{\Delta H_2^m}{R} + \frac{\Delta C_{p_2}}{R} T_2^m \right] \left(\frac{1}{T} - \frac{1}{T_2^m} \right) + \frac{\Delta C_{p_2}}{R} \ln \left(\frac{T}{T_2^m} \right) \quad (4.13)$$

For some sugars, under certain conditions, the most stable form is the hydrated one. In that case, the equilibrium between the different species can be described by:



where n_h is the number of water molecules in the hydrated form. In this case, the solubility is calculated using the following equation, where subscript 1 refers to water, 2 to the anhydrous sugar and 3 to the hydrated form:

$$\begin{aligned} & \ln(x_2 \gamma_2) + n_h \ln(x_1 \gamma_1) = \\ & = \left[-\frac{\Delta H_3^m}{R} + \frac{\Delta C_{p_3}}{R} T_3^m \right] \left(\frac{1}{T} - \frac{1}{T_3^m} \right) + \frac{\Delta C_{p_3}}{R} \ln \left(\frac{T}{T_3^m} \right) + \ln \left(\frac{1}{1+n_h} \gamma_2(T_3^m) \right) + n_h \ln \left(\frac{n_h}{1+n_h} \gamma_1(T_3^m) \right) \end{aligned} \quad (4.15)$$

where $\Delta C_{p3} = C_{p2,l} + n_h C_{p1,l} - C_{p3,s}$.

When solvent and solute have a similar nature, $\gamma_i = 1$ and, therefore, the ideal solubility can be obtained from the pure solute properties.

4.4.2 Model parameters

4.4.2.1 Sugars Physical Properties

For the solid-liquid equilibrium calculations, some physical properties of the pure sugar are needed, namely, the melting temperature T_m , enthalpy of fusion ΔH_f and the difference between the heat capacities of the pure solid and the liquid sugar. Table 4.4 presents some of the physical properties reported by several authors. As can be seen, the discrepancies are quite large for some cases.

In general, in previous works (Peres, 1998; Spiliotis and Tassios, 2000), the values that best fitted the experimental data were chosen. This strategy is also adopted in this work.

Table 4.4 Melting temperature and enthalpy of fusion values available in the literature.

| Sugar | ΔH_f (J/mol) | T_m (K) | Sugar | ΔH_f (J/mol) | T_m (K) |
|-------------|----------------------|---------------------|------------------------|----------------------|---------------------|
| D-glucose | 32 428 ^a | 423.15 ^a | Sucrose | 41 076 ^a | 458.15 ^a |
| | 32 248 ^b | 431.15 ^b | | 40 391 ^b | 463.15 ^b |
| | | | | 56 946 ^c | 441.15 ^d |
| D-fructose | 32 428 ^a | 388.15 ^a | Maltose monohydrate | 45 400 ^b | 396.15 ^b |
| | 30 447 ^b | 400.15 ^b | | | 379.15 ^d |
| | 26 030 ^c | 378.15 ^a | | | |
| D-xylose | 42 028 ^a | 423.15 ^a | Lactose | 75 306 ^a | 468.15 ^a |
| | 31 650 ^b | 430.15 ^b | | | 487.15 ^b |
| | | | | | 474.15 ^d |
| D-galactose | 50 444 ^a | 438.15 ^a | Cellobiose | 54 768 ^a | 493.15 ^a |
| | 43 778 ^b | 443.15 ^b | | | 495.15 ^d |
| D-mannose | 24 687 ^b | 407.15 ^b | Trehalose dihydrate | 48 048 ^b | 370.15 ^b |
| | | | | | 368.15 ^d |

a: Raemy and Schweizer (1983); b: Roos (1993); c: Catté *et al.* (1994); d: Miller and Pablo (2000).

The values used in this work are shown on Table 4.5, together with the experimental or estimated values adopted for ΔC_p . For the monosaccharides, no experimental data is available for the liquid heat capacity. In order to keep the predictive nature of the model, it was decided to set a single ΔC_p , common to all monosaccharides. This value was estimated using binary solubility data of D-glucose in water measured in the temperature range between -12 to 90 °C. A value of 120 J/(mol K) was obtained. Fortunately, some experimental data for the heat capacity difference of disaccharides are

available. Pablo and Miller (2000) have measured the heat capacity difference at the glass transition temperature T_g .

Table 4.5 Melting temperature T_m , enthalpy of fusion ΔH_f and heat capacity difference ΔC_p used in this work to describe the solid-liquid equilibrium with the A-UNIFAC model.

| Sugars | ΔH_f (J/mol) | T_m (K) | ΔC_p (J mol ⁻¹ K ⁻¹) |
|---------------------|----------------------|---------------------|---|
| D-glucose | 32 248 ^b | 423.15 ^a | 120.0 ^e |
| D-fructose | 26 030 ^c | 378.15 ^a | 120.0 ^e |
| D-xylose | 31 650 ^b | 423.15 ^a | 120.0 ^e |
| D-galactose | 43 778 ^b | 438.15 ^b | 120.0 ^e |
| D-mannose | 24 687 ^b | 407.15 ^b | 120.0 ^e |
| Sucrose | 56 946 ^c | 458.15 ^a | 254 ^f (73.4°C) |
| Lactose | 75 306 ^a | 474.15 ^d | 239 ^f (112.3°C) |
| Cellobiose | 54 768 ^a | 495.15 ^d | 263 ^f (108.1°C) |
| Maltose monohydrate | 45 400 ^b | 379.15 ^d | 231 ^f (100.6°C) |
| Trehalose dihydrate | 48 048 ^b | 368.15 ^d | 241 ^f (116.9°C) |

a: Raemy and Schweizer (1983); b: Roos (1993); c: Catté *et al.* (1994); d: Miller and Pablo (2000); e: estimated in this work; f: Miller and Pablo (2000) the heat capacity difference is evaluated at the glass transition temperature T_g (in parenthesis).

The model predictions for the sugar solubilities depend not only on the activity coefficient of the sugar in the solution but, also, on the fugacity ratio $f_{\text{sugar}}^{\text{solid}} / f_{\text{sugar}}^{\text{liquid}}$ that can be calculated using the pure sugar properties. The fugacity ratio, *i.e.*, the ideal solubility of sugars can be calculated using equations 4.13 or 4.15, with $\gamma_2 = 1$. Figures 4.9 and 4.10 show the ideal solubilities predicted for the mono and disaccharides, respectively, using the experimental pure solute properties presented on Table 4.5. In these calculations, no temperature dependence was considered for the heat capacity difference for all mono and disaccharides. As can be seen for the monosaccharides, the ideal solubility already predicts the very different solubilities from the less soluble D-galactose to the more soluble D-fructose. The monosaccharides D-xylose and D-glucose have solubilities with a similar order of magnitude. As these solutions are very non-ideal, the sugars are actually more soluble than the ideal prediction, that is, the sugar activity coefficients are expected to be lower than 1. However, the solid fugacity ratio already orders and follows the relative positions observed for the experimental solubilities.

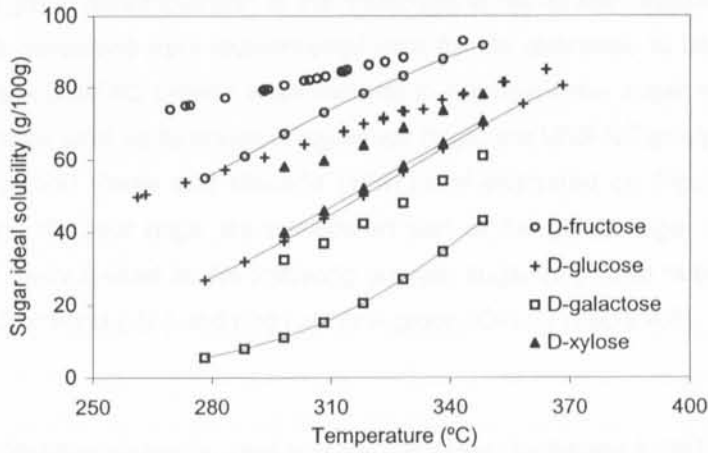


Figure 4.9 Monosaccharides solubility in binary aqueous mixtures versus temperature. Experimental data: \blacktriangle \square (Jónsdóttir *et al.*, 2002); \circ (Vasátko and Smelk, 1967; Abed *et al.*, 1992; Young *et al.*, 1952); $+$ (Stephen and Stephen, 1963; Young, 1957); Sugars Ideal solubility: $-\blacktriangle-$; $-\square-$; $-\circ-$; $-\text{+}-$.

For disaccharides, both sucrose and lactose present an ideal solubility lower than the experimental one, which, again, indicates that $\gamma_{\text{sugar}} < 1$. That is also observed for the hydrated forms of maltose and trehalose. However, for cellobiose the prediction is quite different: the experimental solubilities are lower than the predicted ideal solubility, which would mean that $\gamma_{\text{cellobiose}} > 1$.

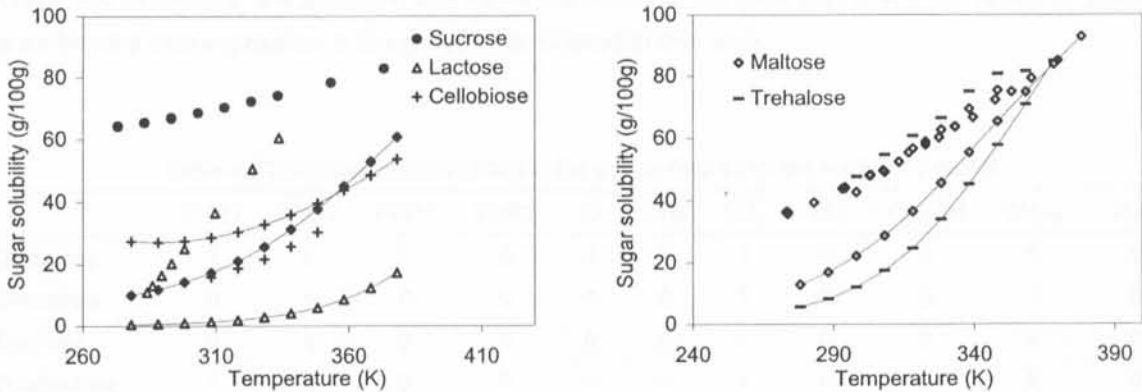


Figure 4.10 Disaccharides solubility in binary aqueous mixtures versus temperature. Experimental data: \blacksquare $+$ (Jónsdóttir *et al.*, 2002); \triangle (Mullin, 1972); \bullet (Mullin, 1972; Young and Jones, 1949); \diamond (Mullin, 1972; Jónsdóttir *et al.*, 2002; Stephen and Stephen, 1963); Sugars ideal solubility: $-\blacksquare-$; $-\text{+}-$; $-\triangle-$; $-\bullet-$; $-\diamond-$.

4.4.2.2 Residual Parameters

In chapter 3, the residual parameters between the groups H_2O , OH , CH_3OH and CH_2 were estimated using VLE, LLE and γ^∞ of water, alcohols and alkanes (Tables 3.5 and 3.6).

As an initial guess, a group decomposition of the molecules in the already existent groups was tested. This resulted in large deviations from experimental data for the quantities to be reproduced. For this reason three new main UNIFAC groups were defined to represent the sugar molecules. Due to the fact that sugar molecules exist as furanose or pyranose rings, the UNIFAC groups definition proposed by Catté *et al.* (1995) and Peres and Macedo (1997) and illustrated on Figure 4.6, was selected. However, in this work, the four rings are considered part of the same sugar ring main group. The sugar molecules are decomposed in the following groups: sugar ring (with subgroups PYR1, PYR2, FUR1 and FUR2), osidic bond (-O-) and ring hydroxyl group (OH_{ring}) (Table 4.6).

Table 4.6 Structural volume (R_k) and area (Q_k) parameters for the new A-UNIFAC groups

| Main Group | Sub-groups | R_k | Q_k |
|--------------------|--------------------|--------|-------|
| PYR/FUR | PYR1 | 2.4784 | 1.380 |
| | PYR2 | 2.7059 | 1.692 |
| | FUR1 | 1.8041 | 0.924 |
| | FUR2 | 2.0315 | 1.152 |
| -O- | -O- | 0.2439 | 0.240 |
| OH _{ring} | OH _{ring} | 1.0000 | 1.200 |

As discussed before, sugars exist as an equilibrium of conformers in solution. It was decided to represent them by the conformer in majority in water. The reducing sugars can also have different conformations which result in three different possible group decompositions. Accordingly, for maltose, lactose and cellobiose, the structure that better represented the data was selected. Table 4.7 presents the molecules decomposition in the groups considered in this work.

Table 4.7 Molecules decomposition in the groups defined for the A-UNIFAC model.

| | PYR1 | PYR2 | FUR1 | FUR2 | -O- | CH ₃ | CH ₂ | OH | CH ₃ OH | OH _{ring} | H ₂ O |
|-------------|------|------|------|------|-----|-----------------|-----------------|----|--------------------|--------------------|------------------|
| D-glucose | 1 | 0 | 0 | 0 | 0 | 0 | 1 | 0 | 0 | 5 | 0 |
| D-fructose | 0 | 1 | 0 | 0 | 0 | 0 | 1 | 0 | 0 | 5 | 0 |
| D-xylose | 0 | 1 | 0 | 0 | 0 | 0 | 0 | 0 | 0 | 4 | 0 |
| D-galactose | 1 | 0 | 0 | 0 | 0 | 0 | 1 | 0 | 0 | 5 | 0 |
| D-mannose | 1 | 0 | 0 | 0 | 0 | 0 | 1 | 0 | 0 | 5 | 0 |
| Lactose | 2 | 0 | 0 | 0 | 1 | 0 | 2 | 0 | 0 | 8 | 0 |
| Maltose | 2 | 0 | 0 | 0 | 1 | 0 | 2 | 0 | 0 | 8 | 0 |
| Sucrose | 1 | 0 | 1 | 0 | 1 | 0 | 3 | 0 | 0 | 8 | 0 |
| Trehalose | 2 | 0 | 0 | 0 | 1 | 0 | 2 | 0 | 0 | 8 | 0 |
| Water | 0 | 0 | 0 | 0 | 0 | 0 | 0 | 0 | 0 | 0 | 1 |
| Ethanol | 0 | 0 | 0 | 0 | 0 | 1 | 1 | 1 | 0 | 0 | 0 |
| Methanol | 0 | 0 | 0 | 0 | 0 | 0 | 0 | 0 | 1 | 0 | 0 |

As can be seen, from the residual point of view only, this model does not distinguish between isomers. For example, D-galactose, D-mannose and D-glucose are represented by the same groups. The distinction is made from the association point of view, *i.e.*, they will have a different capacity to hydrogen bond (a different v^{OH}), as will be discussed in the next section.

4.4.2.3 Association Parameters

In order to reduce the number of adjustable parameters, it was decided to use the same OH associating group defined, already, for alcohols and water to model hydrogen bonding between sugars, water and alcohols. As a result, no new volume and energy of association were estimated from thermodynamic data of sugar mixtures.

As a first optimization approach, it was decided to set the number of associating groups of each sugar equal to the number of OH groups that are not in axial position, *i.e.*, $v^{\text{OH}} = \bar{N}_{\text{OH}}$ (Table 4.3). First, the residual parameters between the groups $\text{PYR/FUR, H}_2\text{O}$ and $\text{OH}_{\text{ring}}, \text{H}_2\text{O}$ were estimated using solubility, freezing point, boiling point, water activity data of binary D-glucose and D-fructose aqueous mixtures. Satisfactory results were obtained in this optimization step with residual parameters: $a_{\text{PYR/FUR, H}_2\text{O}} = -157.8$; $a_{\text{H}_2\text{O, PYR/FUR}} = 163.6$; $a_{\text{H}_2\text{O/OH}_{\text{ring}}} = 161.0$; $a_{\text{OH}_{\text{ring}}/\text{H}_2\text{O}} = -183.9$. As an example, Figure 4.11 gives the results obtained for D-galactose, D-xylose and D-glucose solubilities.

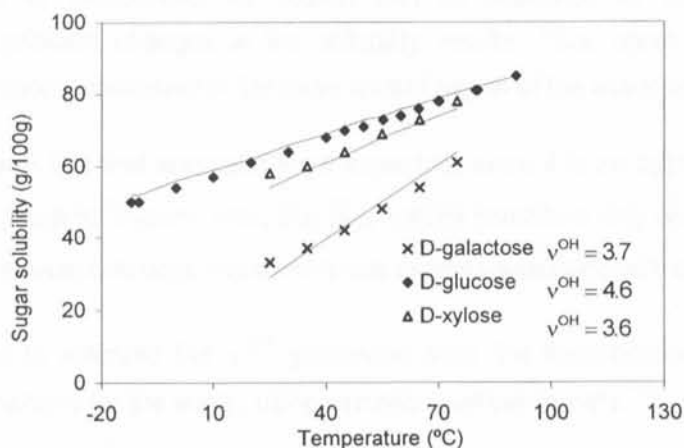


Figure 4.11 Sugar solubility in binary aqueous mixtures *versus* temperature. Experimental data: \circ \triangle (Jónsdóttir *et al.*, 2002); \blacklozenge (Stephen and Stephen, 1963; Young, 1957, Abed *et al.*, 1992); — A-UNIFAC model correlation (D-glucose) and prediction (D-galactose and D-xylose).

As previously mentioned (Chapter 3), it is advisable to use thermodynamic data in the infinite dilution region of compositions to estimate the association parameters. Also, preferentially, the same type of data should be available for a large number of monosaccharides. That is the case of osmotic coefficients experimental data that can be found for D-glucose, D-galactose, D-mannose and D-xylose in the range of compositions from 0.002 to 0.1 (mole fraction). The calculated A-UNIFAC parameters

were used to predict the osmotic coefficients for several monosaccharides. The prediction results are shown on Figure 4.12.

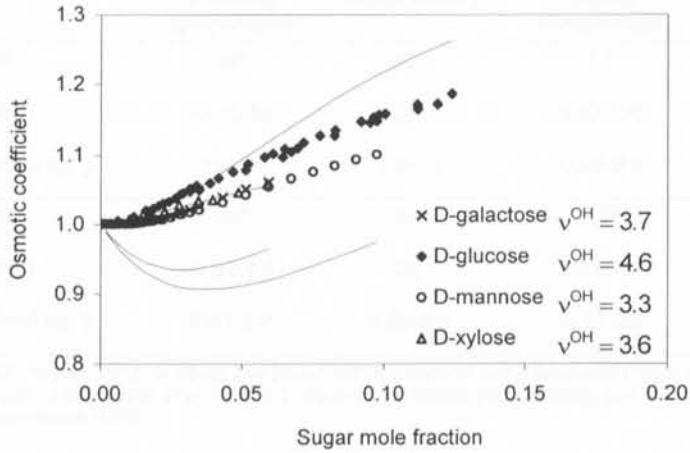


Figure 4.12 Osmotic coefficients prediction for binary aqueous sugar mixtures at 298 K. Experimental data: ◆ ○ × (Miyajima *et al.*, 1983a); △ (Uedaira and Uedaira, 1969); — A-UNIFAC model predictions.

The difference in the capacity to hydrogen bonding seems to be overestimated. If one changes \bar{N}_{OH} value for D-galactose or D-mannose the results can be improved for the osmotic coefficient predictions without significant changes in the solubility results. This, again, indicates the strong influence of the association parameters in the more diluted region of the associating component.

The results obtained with this first approach were expected, since it is an approximation to consider the same associating group for sugars. Also, the \bar{N}_{OH} values constitute only an approximation for the number of OH groups available in each sugar molecule to cross-associate with other molecules.

Finally, it was decided to estimate the v^{OH} parameter from the thermodynamic data in the more diluted range of compositions for the sugar, using osmotic coefficients data.

4.4.3 New parameters for sugar/solvents

4.4.3.1 Database and optimization strategy

Peres (1998) has presented a very extensive database of thermodynamic data of sugar mixtures in water, ethanol and methanol. In this work an updating is made since from 1998 up to now, new data for sugar mixtures have been published. Moreover, the new data also includes other solvents, that is, higher order alcohols like 1-propanol, 1-butanol (Moyé, 1972) and t-pentanol (Coulon *et al.*, 1997).

The experimental database used for the parameters optimization is presented on Tables 4.8, 4.9 and 4.10.

Table 4.8 Experimental database used in the optimization step: number of experimental points NP, range of temperature T and range of compositions X.

| | | Freezing temperature | Water activity | Boiling temperature | Vapour pressure |
|-----------|--------------------------|----------------------|-----------------|---------------------|-----------------|
| D-glucose | NP | 38 ^a | 22 ^b | 11 ^c | 33 ^d |
| | T(°C) | -0.15-30 | 25 | 100-106 | 25-65 |
| | X(mol kg ⁻¹) | 1.4-13 | 1.2-7.2 | 0.26-9.9 | 0.66-14 |
| Sucrose | NP | 24 ^e | 33 ^f | 19 ^g | |
| | T(°C) | -0.03-4.5 | 25 | 100-119 | n.a. |
| | X(mol kg ⁻¹) | 0.01-2.0 | 0.20-5.9 | 0.17-26 | |

n.a. not available; **a** Young (1957), Weast (1972); **b** Rügge and Blanc (1981); **c** Abderafi and Bounahmidi (1994); **d** Taylor and Rowlinson (1955); **e** Young and Jones (1949), Weast (1972), Lericci *et al.* (1983); **f** Chuang and Toledo (1976), Rügge and Blanc (1981), Lericci *et al.* (1983); **g** Leschke (1987), Abderafi and Bounahmidi (1994).

Table 4.9 Experimental database used in the optimization step (continuation): osmotic coefficients data of several mono and disaccharides.

| | | D-glucose | D-xylose | D-galactose | D-mannose | Sucrose | Maltose |
|----------------------|--------------------------|-----------------|----------------|-----------------|-----------------|------------------|-----------------|
| Osmotic coefficients | NP | 54 ^a | 9 ^b | 18 ^b | 23 ^b | 110 ^c | 32 ^d |
| | T(°C) | 25-60 | 25 | 25 | 25 | 25 | 25 |
| | X(mol kg ⁻¹) | 0.34-10 | 0.56-3.5 | 0.1-3.5 | 0.1-6.0 | 0.15-5.7 | 0.1-3.0 |

a Bonner and Breazeale (1965), Stokes and Robinson (1966), Miyajima *et al.* (1983a); **b** Miyajima *et al.* (1983a); **c** Robinson and Sinclair (1934) Scatchard *et al.* (1938), Robinson *et al.* (1942), Robinson and Stokes (1961); **d** Uedaira and Uedaira (1969), Miyajima *et al.* (1983b).

Table 4.10 Experimental database used in the optimization step (conclusion): solubility data of sugars (D-glucose, D-fructose and sucrose) in several solvents (water and alcohols).

| Solvent | | Water | Methanol and ethanol | 1-propanol and 1-butanol | t-pentanol | Mixed solvents (water/methanol) |
|------------|--------------------------|-----------------|----------------------|--------------------------|----------------|---------------------------------|
| D-glucose | NP | 19 ^a | 4 ^b | | | 21 ^b |
| | T(°C) | -12-91 | 40-60 | n.a. | n.a. | 40; 60 |
| | X(mol kg ⁻¹) | 50-85 | 0.44-6.6 | | | 0-100 |
| D-fructose | NP | | 6 ^b | | 7 ^c | |
| | T(°C) | n.i. | 25-60 | n.a. | 30-90 | n.i. |
| | X(mol kg ⁻¹) | | 1.7-63 | | 0.59-3.1 | |
| Sucrose | NP | 46 ^d | 6 ^b | 6 ^e | | |
| | T(°C) | -3-100 | 25-60 | 80-120 | n.a. | n.i. |
| | X(mol kg ⁻¹) | 64-83 | 0.05-1.83 | 0.12-0.74 | | |

n.a. not available; n.i. not included; **a** Young (1957), Stephen and Stephen (1963), Mullin (1972), Abed *et al.* (1992); **b** Peres (1998), **c** Coulon *et al.* (1997); **d** Chuang and Toledo (1976), Rügge and Blanc (1981), Lericci *et al.* (1983); **e** Moyé (1972).

The strategy to estimate the parameters presented on Tables 4.11 and 4.12 was the following:

First, the UNIFAC interaction parameters between the sugar groups (PYR/FUR and $(OH)_{ring}$) and H_2O were estimated using freezing point, boiling point, osmotic coefficient, vapour pressure and water activity data of binary D-glucose in aqueous mixtures, simultaneously with the $v_{D-glucose}^{OH}$ parameter. The number of hydroxyl groups determined is 2.60. Then, the heat capacity ΔC_p of D-glucose was adjusted to solubility data. This value ($\Delta C_p = 120 \text{ J}/(\text{mol K})$) was set common to all monosaccharides. The interaction between $H_2O/-O-$ was obtained simultaneously with $v_{sucrose}^{OH}$, using freezing point, boiling point, solubility, osmotic coefficient and water activity data of sucrose aqueous mixtures.

The extension of this model to other mono (D-xylose, D-galactose and D-mannose) and disaccharides (maltose) is made using the A-UNIFAC group parameters estimated above. The only additional parameter that is needed is the number of OH groups v^{OH} . This parameter was estimated using osmotic coefficients data in aqueous binary solutions for each monosaccharide (Table 4.9). In the case of the monosaccharides (D-fructose) and disaccharides (lactose, trehalose, cellobiose), for which there is no osmotic coefficients data available, it was decided to follow a simple rule: to set the v^{OH} value of D-fructose equal to $v_{D-glucose}^{OH} = 2.60$ and to set the v^{OH} value of the disaccharides equal to $v_{sucrose}^{OH} = 4.30$.

After this, the group interaction parameters between the sugar (PYR/FUR and OH_{ring}) and alcohols groups (CH_2 , OH, CH_3OH) were estimated (Table 4.10).

The group interaction parameters obtained are given on Table 4.11. Due to the scarce experimental data available, some interactions were set equal to zero. Table 4.12 shows the concentration of associating group obtained for each sugar.

Table 4.11 Group interaction parameters (K).

| | PYR/FUR | -O- | CH_2 | OH | CH_3OH | H_2O | OHring |
|----------|------------------|------------------|---------------------|-------------------|--------------------|---------------------|------------------|
| PYR/FUR | 0.0 | 0.0 ^a | 0.0 ^a | 50.4 | -33.8 | -154.3 | 0.0 ^a |
| -O- | 0.0 ^a | 0.0 | 0.0 ^a | 0.0 ^a | 0.0 | -508.034 | 0.0 ^a |
| CH_2 | 0.0 ^a | 0.0 ^a | 0.0 | 50.4 ^b | 122.7 ^b | 380.5 ^b | -60.2 |
| OH | 387.4 | 0.0 ^a | 387.4 ^b | 0.0 | 110.9 ^b | -127.3 ^b | 72.2 |
| CH_3OH | -139.7 | 205.8 | -19.78 ^b | 60.2 ^b | 0.0 | -167.6 ^b | 31.9 |
| H_2O | 108.4 | 155.3 | 136.8 ^b | 70.7 ^b | 251.2 ^b | 0.0 | 87.8 |
| OHring | 0.0 ^a | 0.0 ^a | 703.4 | 715.1 | 681.8 | -174.4 | 0.0 |

a: set equal zero; b: estimated, in chapter 3, using binary γ^∞ , VLE and LLE data of mixtures containing water, n-alcohols and n-alkanes.

Table 4.12 Calculated number of associating groups for each sugar.

| Sugar | ν^{OH} |
|-------------|-------------------|
| D-glucose | 2.60 |
| D-fructose | 2.60 |
| D-mannose | 2.35 |
| D-galactose | 2.40 |
| D-xylose | 2.10 |
| Sucrose | 4.30 |
| Lactose | 4.30 |
| Maltose | 3.80 |
| Trehalose | 4.30 |

4.4.4 Results and Discussion

In the next sections the correlation results and predictions obtained with the A-UNIFAC model are presented. For comparison, the results obtained with the P&M UNIFAC model are also shown.

4.4.4.1 Correlation Results

The correlation results obtained for binary aqueous solutions of D-glucose and sucrose are presented on Table 4.13. For comparison, the average absolute deviations obtained, using the P&M UNIFAC model, are also presented. For this model, some of the results for sucrose are predictions, as pointed out on Table 4.13.

Table 4.13 Correlation and prediction (*) results for D-glucose and sucrose binary aqueous mixtures: number of experimental points NP, range of temperature T; range of compositions X and average absolute deviations AAD for the A-UNIFAC models (in bold) and P&M UNIFAC.

| | | Water activity | Osmotic coefficients | Boiling temperature | Vapour pressure | Freezing temperature | Solubility |
|-----------|--------------------------|--------------------|----------------------|---------------------|--------------------|----------------------|-------------------|
| D-glucose | NP | 22 ^a | 54 ^b | 11 ^c | 33 ^d | 38 ^e | 19 ^f |
| | T(°C) | 25 | 25–60 | 100–106 | 25–65 | (-0.15)–(-30) | (-12)–(91) |
| | X(mol kg ⁻¹) | 1.2–7.2 | 0.34–10 | 0.26–9.9 | 0.66–14 | 1.4–13 | 49.81–84.90 |
| | AAD (%) | 0.34 ; 0.4 | 1.2 , 1.0 | 0.64 ; 0.5 | 0.41 ; 0.54 | 3.4 ; 1.3 | 2.0 ; 0.72 |
| Sucrose | NP | 33 ^l | 110 ^m | 19 ⁿ | | 24 ^o | 46 ⁱ |
| | T(°C) | 25 | 25 | 100–119 | n.a. | (-0.03)–(-4.5) | (-3)–(100) |
| | X(mol kg ⁻¹) | 0.20–5.9 | 0.15–5.7 | 0.17–26 | | 0.01–1.95 | 64.18–82.96 |
| | AAD (%) | 0.53 ; 0.7* | 2.7 ; 5.7* | 0.80 ; 0.56* | | 6.4 ; 3.8* | 6.3 ; 1.3 |

n.a. not available; **a** Rügge and Blanc (1981); **b** Bonner and Breazeale (1965), Stokes and Robinson (1966), Miyajima *et al.* (1983a); **c** Abderafi and Bounahmidi (1994); **d** Taylor and Rowlinson (1955); **e** Young (1957), Weast (1972); **f** Young (1957), Stephen and Stephen (1963), Mullin (1972), Abed *et al.* (1992); **g** Chuang and Toledo (1976), Rügge and Blanc (1981), Lerici *et al.* (1983); **m** Robinson and Sinclair (1934) Scatchard *et al.* (1938), Robinson *et al.* (1942), Robinson and Stokes (1961); **n** Leschke (1987), Abderafi and Bounahmidi (1994); **o** Young and Jones (1949), Weast (1972), Lerici *et al.* (1983); **p** Young and Jones (1949), Stephen and Stephen (1963), Mullin (1972).

As mentioned before, the extension of the model to other monosaccharides (e.g., D-galactose or D-mannose) is made by estimating one additional parameter: the number of OH groups v_{OH} , using osmotic coefficients data in aqueous binary solutions for each monosaccharide. The correlation results are presented on Figure 4.13.

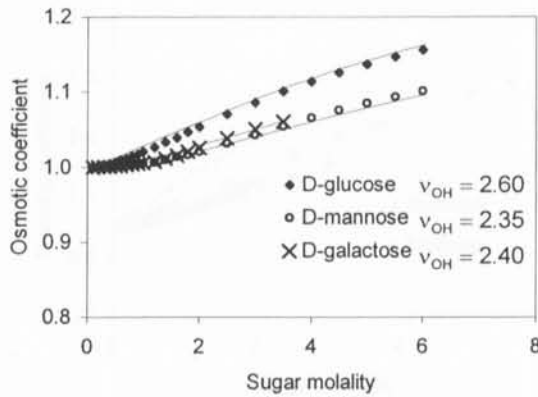


Figure 4.13 Osmotic coefficients data in binary aqueous sugar solutions at 298.15K. Experimental data: \blacklozenge \circ \times (Miyajima *et al.*, 1983a); — A-UNIFAC correlation.

The P&M UNIFAC model distinguishes between D-glucose and the two isomers, D-galactose and D-mannose, by assuming that the latter two are represented by a furanosidic structure (group FUR1). This was done although the three isomers are, predominantly, present in water as a pyranosidic ring (Table 4.2). The D-galactose and D-mannose are represented by the same groups, *i.e.*, are indistinguishable from this model point of view. Figure 4.14 shows the prediction results for the P&M UNIFAC model.

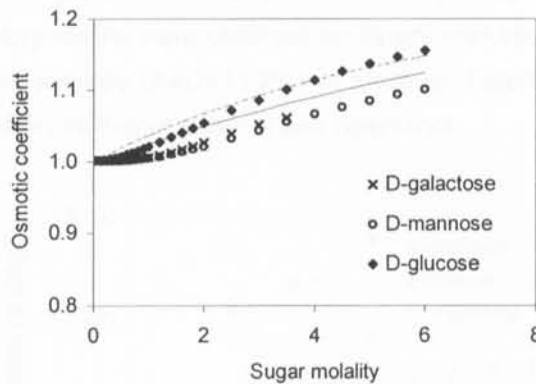


Figure 4.14 Osmotic coefficients data in binary aqueous sugar solutions at 298.15K. Experimental data: \blacklozenge \circ \times (Miyajima *et al.*, 1983a); P&M UNIFAC model: --- D-glucose(correlation); — D-galactose and D-mannose (prediction).

As can be seen the A-UNIFAC gives a more accurate representation of the osmotic coefficients data in binary aqueous sugar solution. The extension of the model to the disaccharides in aqueous

solutions is made by adjusting the corresponding v^{OH} value. All the remaining UNIFAC parameters were already determined. For maltose, it is possible to find a set of osmotic coefficients data. The results obtained for maltose are shown on Figure 4.15. For comparison, the results for sucrose are also presented.

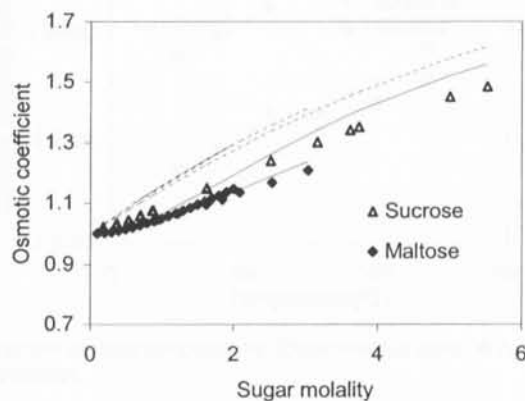


Figure 4.15 Osmotic coefficients data in binary aqueous sugar solutions at 298.15K. Experimental data: Δ (Scatchard *et al.* 1938); \blacklozenge Uedaira and Uedaira (1969), Miyajima *et al.* (1983b). Models: — A-UNIFAC correlation; ---P&M UNIFAC prediction.

The A-UNIFAC model is able to describe, qualitatively, the difference between maltose and sucrose (AAD=1.0% and AAD=2.7%, respectively), which is not the case of the P&M UNIFAC model (AAD=10% and AAD=5.7%). In the case of the remaining disaccharides, due to the scarce experimental data available, their v^{OH} value was set equal to the one obtained for sucrose, *i.e.*, $v_{\text{sucrose}}^{\text{OH}} = 4.30$.

After presenting the results for aqueous solutions, the model correlations for sugars in alcohol solvents will be shown. Very satisfactory results were obtained for binary mixtures of D-glucose (AAD=13.4%), D-fructose (AAD=28.8%) and sucrose (AAD=11.2%) in alcohols. Figure 4.16 shows the correlation results obtained for D-fructose in methanol, ethanol and t-pentanol.

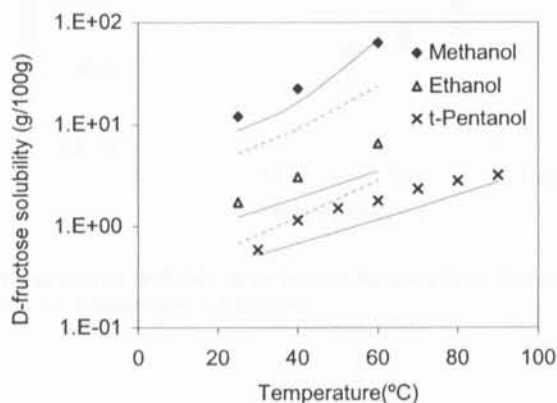


Figure 4.16 D-fructose solubility in alcohols *versus* temperature. Experimental data: \blacklozenge Δ (Peres, 1998); \times (Coulon *et al.*, 1997); — A-UNIFAC model correlation; --- P&M UNIFAC prediction.

And, Figure 4.17 presents the correlation results obtained for sucrose in alcohol binary mixtures.

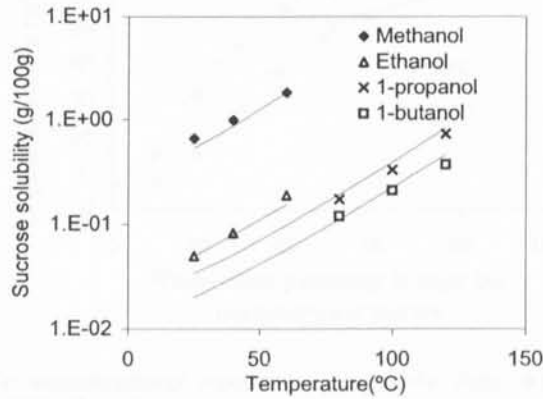


Figure 4.17 Sucrose solubility in alcohols *versus* temperature. Experimental data: \blacklozenge \triangle (Peres, 1998); \times \square (Moye, 1972); — A-UNIFAC model correlation.

The A-UNIFAC model correctly predicts the decrease in the solubility with the increase of the chain length of alcohols. This is not the case of the P&M UNIFAC model. This model did not include in the database alcohols higher than ethanol. And, to reduce the number of adjustable parameters, some interactions were set equal to zero, namely, the interactions between the CH_2 group and all the other groups. This explains the less accurate results obtained with this model that predicts that sucrose is more soluble in 1-butanol than in 1-propanol (Figure 4.18).

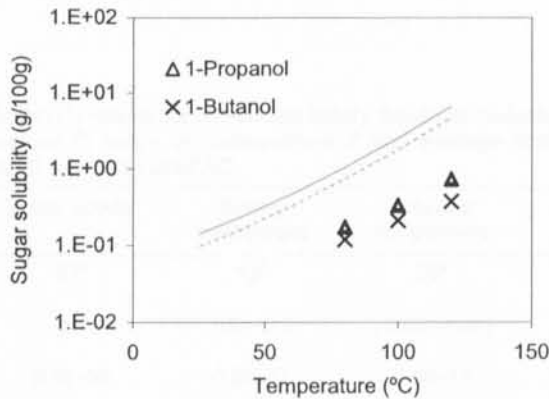


Figure 4.18 Sucrose solubility in 1-propanol and 1-butanol *versus* temperature. Experimental data: \times \triangle (Moye, 1972); P&M UNIFAC prediction: --- 1-propanol; — 1-butanol.

Finally, Figure 4.19 shows the A-UNIFAC correlation results for the solubilities of D-glucose in water/methanol mixtures (AAD=4.08%) and the P&M UNIFAC model predictions (AAD=10.6%). Good results are obtained with both models.

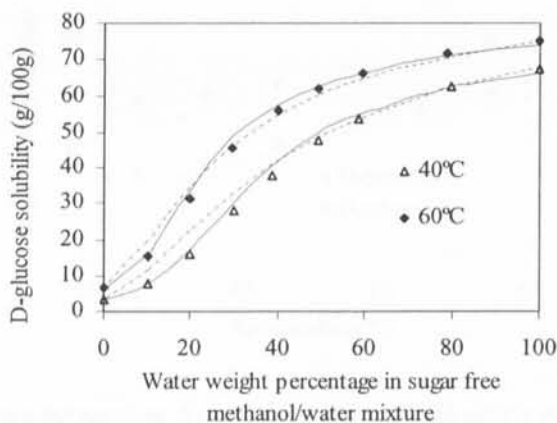


Figure 4.19 Sugar solubility in water/methanol mixtures. Experimental data: $\blacklozenge\triangle$ (Peres, 1998); — A-UNIFAC correlation; --- P&M UNIFAC prediction.

4.4.4.2 Predictions

In this section, the set of parameters estimated previously will be applied to the prediction of several thermodynamic properties of binary and multicomponent sugar mixtures.

Aqueous systems

The thermodynamic information for D-fructose was not used to optimize the parameters. In the absence of osmotic coefficients data, $v_{D\text{-fructose}}^{\text{OH}}$ value was set equal to $v_{D\text{-glucose}}^{\text{OH}}$. Good predictions are obtained for the solubility, freezing point, boiling point and water activity for D-fructose aqueous mixtures, as can be seen from Table 4.14.

Table 4.14 Correlation and prediction (*) results for D-fructose binary aqueous mixtures: number of experimental points NP, range of temperature T; range of compositions X and average absolute deviations AAD for the A-UNIFAC models (in bold) and P&M UNIFAC.

| | Water activity | Boiling temperature | Freezing temperature | Solubility |
|--------------------------|--------------------|---------------------|----------------------|--------------------|
| NP | 37 ^a | 12 ^b | 26 ^c | 20 ^d |
| T(°C) | 25 | 100–130 | (-0.05)–(-30) | (-3.9)–(70) |
| X(mol kg ⁻¹) | 0.62–22 | 0.26–37 | 0.03–13 | 74–93 |
| AAD (%) | 0.56* ; 0.6 | 1.5* ; 1.5 | 6.1* ; 1.2 | 2.8* ; 0.72 |

^a Rügge and Blanc (1981), Correa *et al.* (1993), Leric *et al.* (1983); ^b Abderafi and Bounahmidi (1994); ^c Young *et al.* (1952), Weast (1972), Leric *et al.* (1983); ^d Jackson *et al.* (1926), Young *et al.* (1952), Vasátko and Smelik (1967), Abed *et al.* (1992).

Satisfactory solubility predictions are, also, obtained for D-xylose and D-galactose, as shown on Figure 4.20, with both models: A-UNIFAC and P&M UNIFAC.

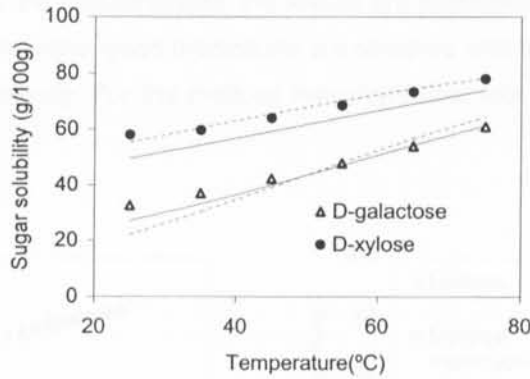


Figure 4.20 Solubility in water versus temperature. Experimental data: ● △ (Jónsdóttir *et al.*, 2002); Model predictions: - - P&M UNIFAC; — A-UNIFAC.

For the disaccharides, it was decided to set their v^{OH} value equal to the one obtained for sucrose, *i.e.*, $v_{\text{sucrose}}^{\text{OH}} = 4.30$, with the exception of D-maltose, for which there is enough available experimental information. Good results were obtained for the prediction of water activity and vapour pressure of aqueous solutions of lactose and, also, for the prediction of the freezing point of binary aqueous mixtures containing maltose or lactose, as can be seen from Table 4.15.

Table 4.15 Prediction results for lactose and maltose binary aqueous mixtures: number of experimental points NP, range of temperature T; range of compositions X and average absolute deviations AAD for the P&M UNIFAC and A-UNIFAC models (in bold characters).

| | | Lactose | Maltose |
|----------------------|--------------------------|----------------------------------|---------------------------------|
| Water activity | NP | 4 ^a | |
| | T(°C) | 25 °C | n.a. |
| | X(mol kg ⁻¹) | 0.03 – 0.25 mol kg ⁻¹ | |
| | AAD (%) | 0.19 ;0.18; | |
| Vapour pressure | NP | 6 ^c | |
| | T(°C) | 50 a 100 °C | n.a. |
| | X(mol kg ⁻¹) | 1.27 – 6.33 mol kg ⁻¹ | |
| | AAD (%) | 0.72 ; 0.89 | |
| Freezing temperature | NP | 19 ^d | 22 ^e |
| | T(°C) | -0.02 a -1.03 °C | -0.03 a -5.35 °C |
| | X(mol kg ⁻¹) | 0.01 - 1.56 mol kg ⁻¹ | 0.01 - 2.30mol kg ⁻¹ |
| | AAD (%) | 7.0 ; 3.7 | 6.5 ; 5.2 |

n.a. not available; a Lerici *et al.* (1983); b Uedaira and Uedaira (1969), Miyajima *et al.* (1983b); c Hudson (1908); d Hudson (1908), Weast (1972); e Weast (1972).

What about the solubilities of the disaccharides? As discussed before, the model predictions for the sugar solubilities are limited by a good estimation of the heat of fusion, melting point and heat capacity

difference of the sugars. For the disaccharides, the results are presented on Figure 4.21. For sucrose, lactose and trehalose monohydrate, good predictions are obtained with absolute average deviations of 6.3%, 5.8% and 8%, respectively. For the maltose monohydrate, fair predictions are achieved with AAD = 18%.

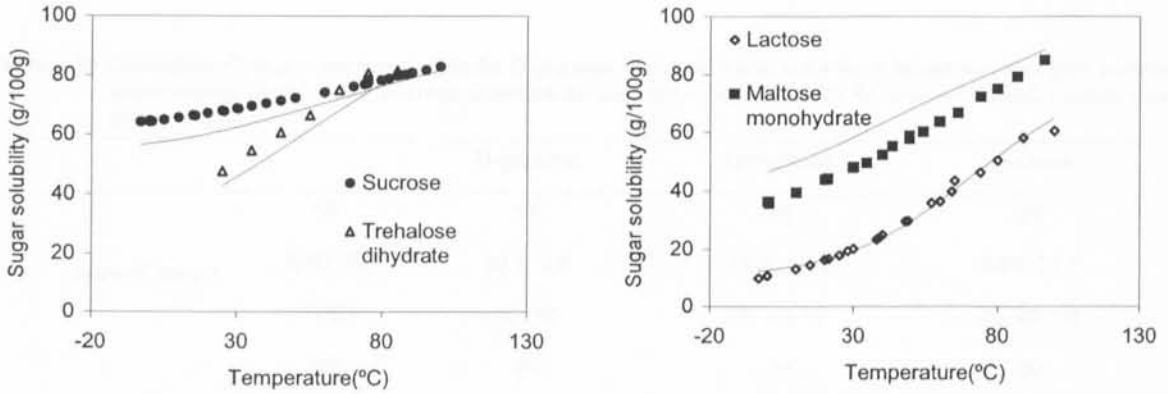


Figure 4.21 Disaccharides solubility in water versus temperature. Experimental data: \triangle (Jónsdóttir *et al.*, 2002); \diamond (Mullin, 1972); \bullet (Mullin, 1972; Young and Jones, 1949); \blacksquare (Mullin, 1972; Jónsdóttir *et al.*, 2002; Stephen and Stephen, 1963);—A-UNIFAC model.

However, for cellobiose, the model largely overpredicts its solubility in water with AAD = 266 %. As discussed previously, the calculated ideal solubility is already larger than the experimental data. The accurate determination of the melting enthalpy of disaccharides can be quite difficult since these compounds decompose easily before melting. For comparison purposes, Figure 4.22 presents the solubility prediction using experimental $\Delta H_{\text{cellobiose}}^m = 54768 \text{ J/mol}$ and, also, the curve obtained by adjusting the melting enthalpy ($\Delta H_{\text{cellobiose}}^m = 80500 \text{ J/mol}$).

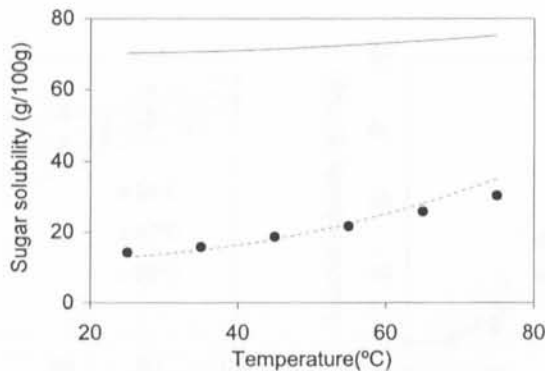


Figure 4.22 Cellobiose solubility in water versus temperature. Experimental data: \blacklozenge (Jónsdóttir *et al.*, 2002); — A-UNIFAC model prediction; --- A-UNIFAC model correlation.

Finally, Table 4.16 gives the results for the solubilities of D-glucose, D-fructose and sucrose in mixed solvents compared with the P&M UNIFAC predictions. In general, good results are obtained with both models. The A-UNIFAC model gives more accurate predictions, especially for the sucrose solubility in the various mixed solvents and, also, for the prediction of the solubility of D-fructose in the methanol richer region of compositions.

Table 4.16 Correlation (*) and prediction results for D-glucose, D-fructose and sucrose in mixed solvents (NP: number of experimental points; AAD: average absolute deviations for the P&M UNIFAC and A-UNIFAC models (in bold characters)).

| | | D-glucose | D-fructose | Sucrose |
|------------------|---------|--------------------|--------------------|--------------------|
| Water/Ethanol | NP | 18 | 29 | 29 |
| | AAD (%) | 10.1 ; 3.8 | 11.1 ; 17.3 | 8.81 ; 27.7 |
| | T(°C) | 40; 60 | 25; 40; 60 | 25; 40; 60 |
| Water/Methanol | NP | 20 | 29 | 29 |
| | AAD (%) | 4.08* ;10.6 | 4.58 ; 12.4 | 6.30 ;48.0 |
| | T(°C) | 40; 60 | 25; 40; 60 | 25; 40; 60 |
| Ethanol/Methanol | NP | 21 | 32 | 31 |
| | AAD (%) | 15.8 ;28.1 | 26.6 ; 50.3 | 11.3 ;55.3 |
| | T(°C) | 40; 60 | 25; 40; 60 | 25; 40; 60 |

*correlation results, the remaining are predictions.

Figure 4.23 shows the predictions obtained for sucrose in water/methanol water/ethanol mixtures using the A-UNIFAC model. For comparison, the P&M UNIFAC model predictions are also presented. Both models correctly predict the sugars solubility decrease with the addition of methanol or ethanol to aqueous mixtures.

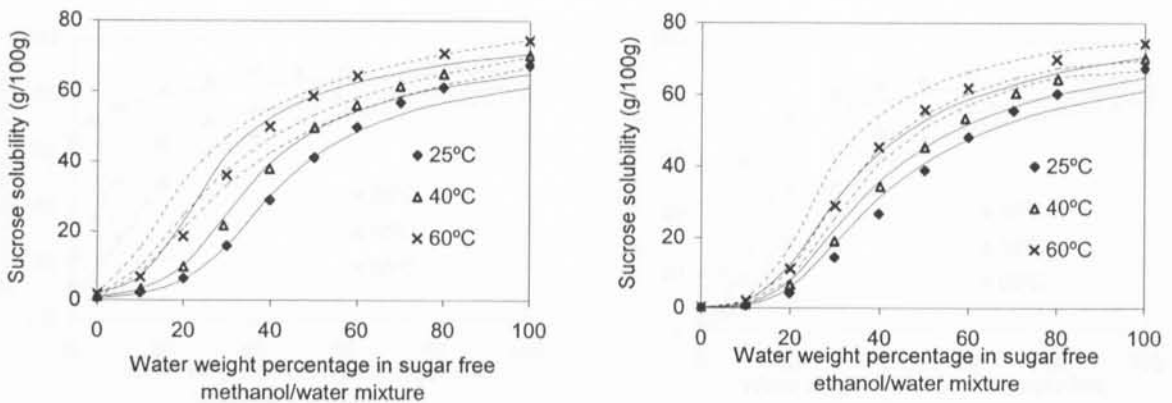


Figure 4.23 Sucrose solubility in water/methanol and water/ethanol mixtures. Experimental data: \blacklozenge \blacktriangle \times (Peres, 1998); — A-UNIFAC model; --- P&M UNIFAC model.

Figure 4.24 presents the predictions for D-fructose and sucrose solubility in mixed solvents of ethanol and methanol. For D-fructose, the A-UNIFAC model behaves better in the methanol richer range of compositions. For sucrose solubility, the A-UNIFAC model is able to correctly predict its solubility in the ethanol and methanol mixtures, which is not the case of the P&M UNIFAC model that predicts, wrongly, a solubility enhancement effect by adding methanol to ethanol.

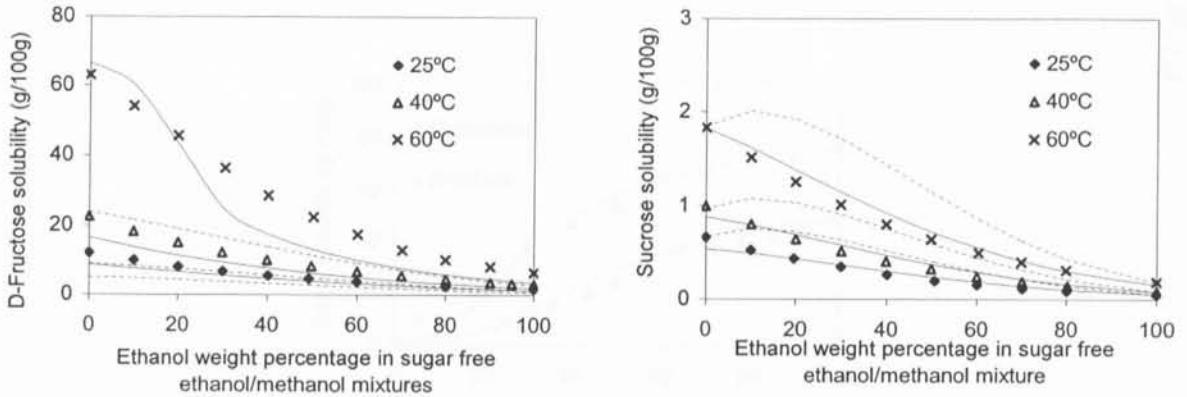


Figure 4.24 Sugar solubility in ethanol/methanol mixtures. Experimental data: $\blacklozenge \blacktriangle \times$ (Peres, 1998); — A-UNIFAC model; --- P&M UNIFAC model.

4.4.4.3 Predictions for sugar industrial systems

In this section some predictions are made for sugar industrial mixtures using the group-contribution approach A-UNIFAC model.

The addition of small alcohols to concentrated D-fructose syrups decreases its high solubility in water and the viscosity of those solutions, facilitating the crystallization of D-fructose (Flood *et al.*, 1996). Both models can predict decreasing solubility of the monosaccharide, by addition of the small alcohols, as shown on Figure 4.25. The A-UNIFAC model predicts more accurately the solubility of D-fructose in methanol, which improves the results in that region of compositions.

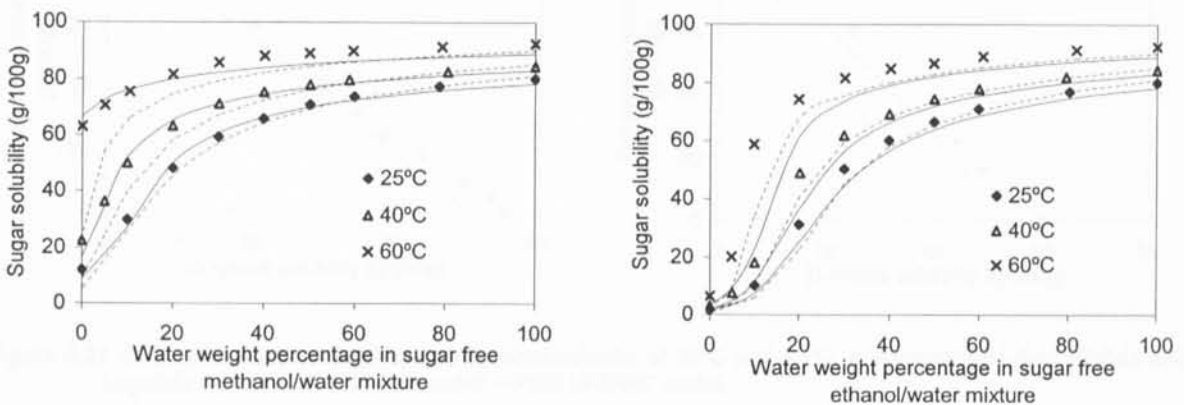


Figure 4.25 D-fructose solubility in water/ethanol and water/methanol mixtures. Experimental data: $\blacklozenge \blacktriangle \times$ (Peres, 1998); — A-UNIFAC model; --- P&M UNIFAC model.

Gabas *et al.* (1988) have measured the solubilities of D-xylose and D-mannose in water/ethanol mixtures at 25°C. The purpose of their work was to analyze the feasibility of selectively precipitate D-xylose from an aqueous plant extract containing also D-mannose, by adding ethanol. Figure 4.26 gives the A-UNIFAC and P&M UNIFAC model predictions for the solubilities of both monosaccharides in ethanol/water mixtures. As can be seen, both models are able to predict the decrease of solubility with the addition of the co-solvent ethanol.

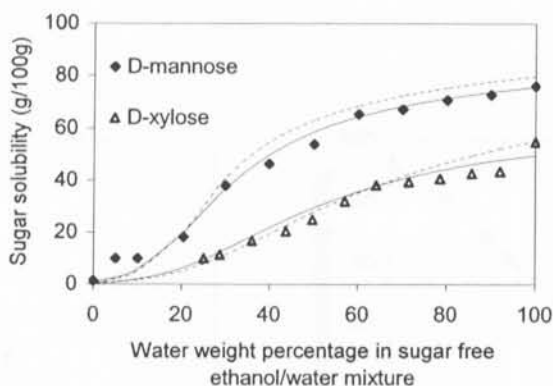


Figure 4.26 Sugar solubility in ethanol/water mixtures at 25°C. Experimental data: \blacklozenge \triangle (Gabas *et al.*, 1988); — A-UNIFAC model prediction; ---P&M UNIFAC model.

Later, Gabas and Laguérie (1990) have measured the solid-liquid equilibria of ternary systems containing D-mannose and D-xylose in aqueous solutions at 25 °C and 35 °C. Again, good predictions are obtained for these two monosaccharides, as shown on Figure 4.27.

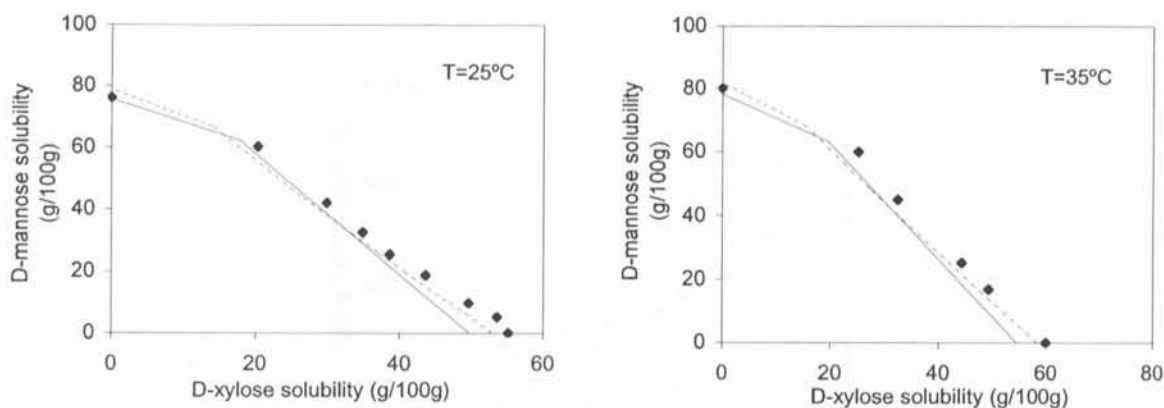


Figure 4.27 Solid-liquid equilibria of D-xylose/D-mannose/water at 25°C and 35°C: \blacklozenge experimental data (Gabas and Laguérie, 1990); — A-UNIFAC model; ---P&M UNIFAC model.

A good description of the SLE and VLE of aqueous mixtures containing high sugar content is very important to understand the behaviour of industrial multicomponent systems, e.g., fruit juices concentrates and honey. After this, some predictions will be made for systems with compositions similar to those food products. Fruit juices are composed, mainly, by D-fructose, D-glucose and sucrose in various proportions depending on the fruit. Abed *et al.* (1992) have studied the effects of D-glucose or D-fructose on the solubility of sucrose. Solid-liquid equilibria measurements were made for the ternary systems water-D-glucose-sucrose and water-D-fructose-sucrose, at 70°C. The prediction results of the A-UNIFAC model are compared to the experimental data on Figure 4.28.

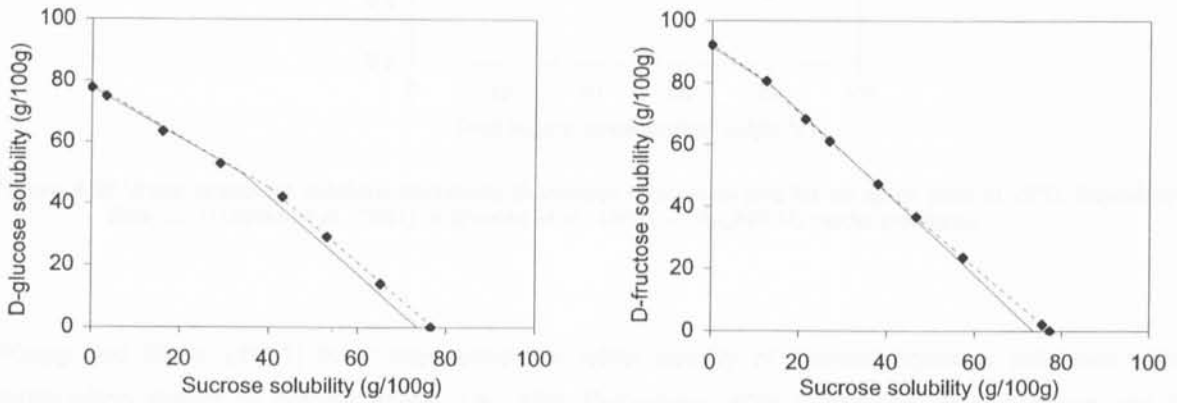


Figure 4.28 Solid liquid equilibria of (a) D-glucose/sucrose/water and (b) D-fructose/sucrose/water at 70°C: ◆ experimental (Abed *et al.*, 1992); — A-UNIFAC model; --- P&M UNIFAC model.

Abderafi and Bounahmidi (1994) measured the vapour-liquid equilibria of several ternary and quaternary aqueous mixtures of D-glucose, D-fructose and sucrose. Figure 4.29 shows the A-UNIFAC predictions for the normal boiling point of a quaternary mixture of those three sugars in water.

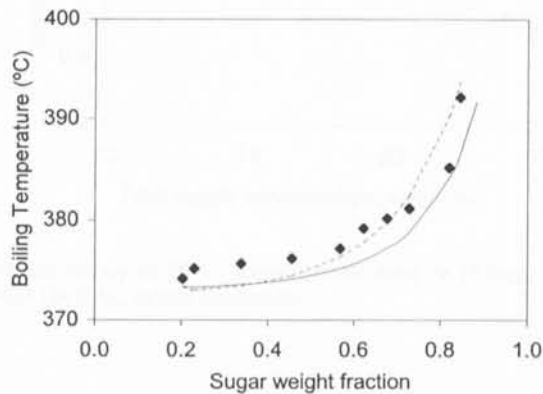


Figure 4.29 Normal boiling point of quaternary aqueous solutions of D-glucose, D-fructose and sucrose: ◆ Experimental data (Abderafi and Bounahmidi, 1994); — A-UNIFAC prediction --- P&M UNIFAC prediction.

Another important property is the water activity of food products. Figure 4.30 presents the predictions for the water activities in binary mixtures of D-fructose-water and sucrose-water. Additionally, the predicted water activity for an apple juice (containing 14.8 wt% of D-glucose, 62.4 wt% of D-fructose and 22.7wt% of sucrose) is also shown.

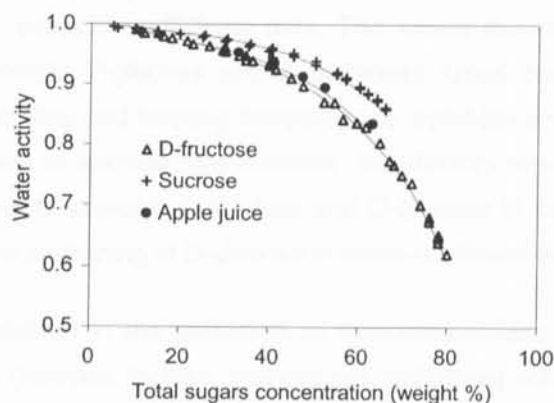


Figure 4.30 Water activity of solutions containing D-fructose or sucrose and for an apple juice at 25°C. Experimental data: Δ + (Correa *et al.*, 1981); \bullet (Fontán *et al.*, 1981); — A-UNIFAC model prediction.

Rüegg and Blanc (1981) have measured the water activity of several aqueous solutions with a composition similar to natural honey, i.e., 48% D-fructose, 40% D-glucose, 10% maltose and 2% sucrose. The water content changes from 16 to 28% (w/w). The A-UNIFAC model is able to correctly predict the water activity of synthetic honey, as shown on Figure 4.31.

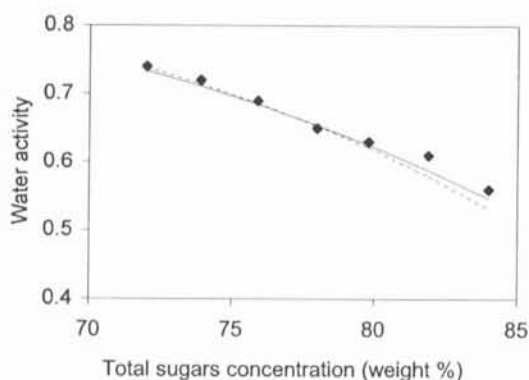


Figure 4.31 Water activity in synthetic honey at 25°C: Experimental data: \blacklozenge (Rüegg and Blanc, 1981); — A-UNIFAC model prediction; --- P&M UNIFAC model prediction.

4.5 Conclusions

A modified UNIFAC (A-UNIFAC) model that accounts explicitly for association effects was successfully applied to mixtures of sugars with water and alcohols (from methanol to t-pentanol).

Three new residual groups were defined: the sugar ring group representing the furanose and pyranose rings, the hydroxyl group representing the OH ring substituents and the group that represents the osidic bond between monosaccharide units. From the association point of view, the same hydroxyl group, already defined for water and alcohols, is used. Each sugar has a different concentration of that associating group that is adjusted to the available data in the sugar more diluted range of compositions, *i.e.*, osmotic coefficients data. This allows the model to distinguish between stereoisomers (*e.g.* D-galactose, D-glucose and D-mannose). Good correlation results for osmotic coefficients, water activity, boiling and freezing temperatures, solubility and binary data of mixtures of water and a sugar (D-glucose or sucrose) are obtained. Satisfactory results are also achieved in the correlation of binary systems of sucrose, D-fructose and D-glucose in alcohols (from methanol to t-butanol) and ternary systems containing of D-glucose in water-methanol ternary systems.

Successful results were obtained in the prediction of monosaccharides (D-galactose, D-xylose, D-fructose) and disaccharides (sucrose, lactose, maltose and trehalose) solubility in water, and, also, in the prediction of water activity, boiling and freezing point temperature of aqueous solutions containing lactose and maltose. For cellobiose, the solubility results are very poor. They were improved by adjusting the correspondent fusion enthalpy.

Finally, the model was successfully applied to multicomponent mixtures of industrial interest. Good results were obtained for the prediction of the solid-liquid equilibria of mixtures containing D-xylose and D-mannose in water and in mixed solvents of water/ethanol. The model was also able to correctly describe the solid-liquid equilibrium and vapour-liquid equilibrium of mixtures containing D-fructose, D-glucose and sucrose in water. The prediction of the water activity of a synthetic honey and of synthetic juices is very satisfactory.

Chapter 6

Equations of state for polar and associating mixtures – a general overview

Equations of state for polar and associating mixtures – a general overview

5. Equations of state for polar and associating mixtures – a general overview

5.1 Introduction

In this chapter, a review on phase equilibria for associating mixtures using equations of state is presented. This methodology allows the use of one thermodynamic model to evaluate the fugacities in all phases. For a binary mixture the isofugacity condition for component i between phases α and β can be written:

$$z_i^\alpha \hat{\phi}_i^\alpha = z_i^\beta \hat{\phi}_i^\beta \quad i = 1, 2 \quad (5.1)$$

where z_i and $\hat{\phi}_i$ are the mole fraction and the fugacity coefficient of component i in a given phase, respectively. This homogeneous approach allows the same model to be used at all ranges of densities up to the critical point, with no need of specifying a reference state.

The more traditional models are the cubic equations of state (EoS), like the van der Waals EoS, Peng-Robinson EoS (Peng and Robinson, 1976) or Soave-Redlich-Kwong EoS (Soave, 1972), among others. These equations can be described by the general expression:

$$P = \frac{nRT}{(V - nb)} - \frac{n^2 a(T)}{V^2 + unbV + wn^2 b^2} \quad (5.2)$$

where P is the total pressure of the system, n is the total number of moles, V is the volume and u and w are integer constants that depend on the EoS chosen (Table 5.1). The first term accounts for

repulsion due to the fact that molecules occupy a finite volume given by co-volume b . The second term quantifies the attractive interactions through the energy parameter a . These models differ not only on their functional form, but also on the way the a and b parameters are calculated for pure components.

Table 5.1 Integer constants (u and w) for cubic equations of state

| EoS | u | w |
|-------------------|-----|-----|
| van der Waals | 0 | 0 |
| SRK | 1 | 0 |
| Peng and Robinson | 2 | -1 |

The one fluid van der Waals concept allows the extension of these models to mixtures. It considers that the properties of a fluid mixture with composition z , at temperature T and pressure P , correspond to those of a hypothetical fluid at the same T and P . The a and b parameters of this hypothetical fluid are a function of the mixture composition given through the use of *mixing rules*. Their functional definition has a major influence on the phase equilibria description.

The van der Waals one fluid mixing rules usually behave well for simple mixtures of non-polar or slightly polar components with similar size and chemical nature (Han *et al.*, 1988). They can be written as follows:

$$a = \sum_i \sum_j z_i z_j a_{ij} \quad (5.3)$$

$$b = \sum_i \sum_j z_i z_j b_{ij} \quad (5.4)$$

The “interaction” parameters a_{ij} and b_{ij} are usually determined from pure component properties using the combining rules:

$$a_{ij} = (a_i a_j)^{1/2} (1 - k_{ij}) \quad (5.5)$$

$$b_{ij} = \left(\frac{b_{ii} + b_{jj}}{2} \right) (1 - l_{ij}) \quad (5.6)$$

In general l_{ij} is set equal to zero and the mixing rule given by Equation 5.4 becomes linear ($b = \sum_i z_i b_{ii}$) and the classical one parameter mixing rules are obtained.

The use of quadratic mixing rules implies a quasi-regular behaviour of the mixtures. The application of these models to more complex mixtures, *i.e.*, asymmetric mixtures with polar components or with

strong and well-oriented interactions, like hydrogen bonding, usually requires the use of more elaborated mixing and combining rules containing interaction parameters that are, in many cases, temperature or composition dependent (Adachi and Sugie, 1986; Kwak and Mansoori, 1986; Panagiotopoulos and Reid, 1986; Sandoval *et al.*, 1989).

From this starting point, many modifications have been proposed in the literature to improve the description of highly complex mixtures. The most common include the introduction of more flexible mixing rules (section 5.2) or the modification of the equation of state in order to explicitly account for association effects (section 5.3).

5.2 Mixing rules from activity coefficient models

Some strategies have been proposed to relate the local composition concept to equations of state. Section 5.2.1 presents some examples derived from the Huron and Vidal methodology (Huron and Vidal, 1979) and section 5.2.2 presents another strategy, proposed by Mollerup (1981) that results in density dependent mixing rules.

5.2.1 Huron and Vidal methodology

Huron and Vidal (1979) first proposed the possibility of incorporating excess Gibbs energy models, derived for highly non-ideal liquid mixtures (G_γ^E models), into the mixing rules for the attractive term of a cubic equation of state.

The excess Gibbs energy originated from the equation of state (G_{EoS}^E) can be matched to the G_γ^E models for liquid solutions at a given pressure P' :

$$G_{EoS}^E(T, P', z_i) = G_\gamma^E(T, z) \quad (5.7)$$

The G_γ^E function is related to the fugacity coefficient of the mixture ϕ and to fugacity coefficient of pure component i (ϕ_i) at T and P of the mixture, through the classical thermodynamics equation (Prausnitz, 1999):

$$\frac{G^E}{RT} = \ln \phi - \sum_i z_i \ln \phi_i \quad (5.8)$$

The large number of possible combinations between the various liquid activity coefficients models and cubic EoS, at a given pressure, resulted in several new models. Some will be described next.

The original proposal of Huron and Vidal (HV) was to match both Gibbs excess energies at infinite pressure, for which the free volume between molecules will tend to zero ($v \rightarrow b$; $v_i \rightarrow b_i$). This infinite pressure condition determines the use of the linear mixing rule for the co-volume, so that G_{EOS}^E reaches a finite value. These assumptions lead to the final expression of the HV mixing rules:

$$\alpha_{mix} = \sum_{i=1}^{NC} z_i \alpha_{ii} - \frac{1}{\Omega} \frac{G_Y^E}{RT} \quad (5.9)$$

where the summation is extended to NC components, $\alpha = a/bRT$ and Ω is a constant that depends on the cubic equation of state used.

The main disadvantage of this mixing rule is the fact that the match at infinite pressure does not recommend the use of the G_Y^E parameter tables published at low pressures (Gupté and Daubert, 1986).

To overcome this, and to be able to use the extensive parameter tables available for some G_Y^E models (e.g. UNIFAC, UNIQUAC), Mollerup (1986) suggested the zero-pressure match between G_{EOS}^E and G_Y^E functions. This approach was successfully used by Michelsen (1990a, b) and Heidemann and Kokal (1990), leading to density independent mixing rules.

Michelsen (1990b) proposed the modified Huron-Vidal first order (MHV1) for which good results are obtained, though some accuracy is lost in the low temperature range.

$$\alpha_{mix} = \sum_{i=1}^{NC} z_i \alpha_{ii} + \frac{1}{q_1} \left[\frac{G^E}{RT} + \sum_{i=1}^{NC} z_i \ln \left(\frac{b}{b_{ii}} \right) \right] \quad (5.10)$$

In order to improve the results in that temperature range and, at the same time, not lose accuracy relatively to the G_Y^E model, a second order approximation was suggested. The resulting modified Huron-Vidal second order (MHV2) mixing rule is an implicit expression in α (Michelsen, 1990b):

$$q_1 \left(\alpha_{mix} - \sum_{i=1}^{NC} z_i \alpha_{ii} \right) + q_2 \left(\alpha_{mix}^2 - \sum_{i=1}^{NC} z_i \alpha_{ii}^2 \right) = \frac{G^E}{RT} + \sum_{i=1}^{NC} z_i \ln \left(\frac{b}{b_{ii}} \right) \quad (5.11)$$

Holderbaum and Gmehling (1991) developed the PSRK mixing rule which is similar to the MHV1 mixing rule with a few minor differences: it assumes a pressure reference state equal to 1 atm and a different constant value for the packing factor ($u_{PSRK} = 1.1$) instead of $u_{MHV1} = 1$ used for the MHV1 mixing rule. The packing factor is defined as the ratio between the molar volume and the co-volume ($u = v/b = v_i/b_i$).

All the above mentioned mixing rules include the classical linear mixing rule for b , which is inconsistent with the low density boundary condition limit that predicts a quadratic dependence of the second virial coefficient with composition:

$$B = \sum_i \sum_j z_i z_j B_{ij} = \sum_i \sum_j z_i z_j \left(b - \frac{a}{RT} \right)_{ij} \quad (5.12)$$

Wong and Sandler (1992) proposed a new set of mixing rules that could satisfy this low boundary condition by using the excess Helmholtz energy of mixing (A^E) instead of the excess Gibbs energy of mixing. The fact that A^E is a weak function of pressure allowed the authors to consider the following equalities, for a mixture with composition \bar{x} at temperature T , assuming that P^* is a low pressure:

$$A^E(T, P = \infty, \bar{x}) \approx A^E(T, P^*, \bar{x}) = G^E(T, P^*, \bar{x}) - P^* V^E(T, P^*, \bar{x}) \approx G^E(T, P^*, \bar{x}) \quad (5.13)$$

This resulted in the following mixing rules:

$$\left\{ \begin{array}{l} \alpha_{\text{mix}} = \sum_{i=1}^{NC} z_i \alpha_{ii} + \frac{1}{\Omega} \frac{G^E}{RT} \\ b_{\text{mix}} = \frac{\sum_{i=1}^{NC} \sum_{j=1}^{NC} z_i z_j \left(b_i - \frac{a_i}{RT} + b_j - \frac{a_j}{RT} \right)_{ij}}{1 - \frac{1}{\Omega} \frac{G^E}{RT} \sum_{i=1}^{NC} z_i \alpha_{ii}} \end{array} \right. \quad (5.14)$$

Similarly to the MHV1 and MHV2 models, the W&S mixing rules can use interaction parameters previously estimated for a given activity coefficient model (e.g. UNIFAC model).

Fischer and Gmehling (1996) compared the different assumptions used to derive the mixing rules, namely, the pressure reference state, the packing factor u , the expression for the excess volume v^E and the expression obtained for A_{EOS}^E (Table 5.2).

Table 5.2 Comparison between the different G_{γ}^E / EoS mixing rules

| Mixing rules | Reference Pressure | Packaging factor u | v^E | A_{EOS}^E |
|--------------|--------------------|----------------------|----------|---|
| HV | ∞ | 1 | 0 | G_{γ}^E |
| MHV1 | 0 | 1.235 | 0 | $G_{\gamma}^E + RT \sum_i x_i \ln(b/b_i)$ |
| MHV2 | 0 | $f(a/b, a_i/b_i)$ | 0 | $G_{\gamma}^E + RT \sum_i x_i \ln(b/b_i)$ |
| PSRK | 1 atm | 1.1 | 0 | $G_{\gamma}^E + RT \sum_i x_i \ln(b/b_i)$ |
| W&S | ∞ | 1 | $\neq 0$ | G_{γ}^E |

All the above-mentioned models were successfully applied to multi-component polar mixtures up to 200 bar. For the systems containing gases (carbon dioxide, hydrogen, etc.), new interaction parameters between those light components and the groups defined in the corresponding G_γ^E model were determined. In most cases, temperature dependent interaction parameters were introduced. For example, the PSRK model uses the following temperature dependency (Fischer and Gmehling, 1996):

$$\tau_{nm} = \exp\left(-\frac{a_{nm} + b_{nm}T + c_{nm}T^2}{T}\right) \quad (5.15)$$

However, all these EoS present some failures when they are extended to mixtures containing asymmetric components. To overcome this, Boukovalas *et al.* (1994) proposed an empirical modification by formulating a linear combination of a zero-pressure reference pressure model (MHV1) and an infinite-pressure reference model, *i.e.*, the Linear Combination Vidal Michelsen mixing rule (LCVM). With this model satisfactory results were obtained for asymmetric systems.

Kontogeorgios and Vlamos (2000) proposed a different approach: instead of equating the total excess Gibbs energies, these authors suggested that there should be an equality between the separate contributions from the EoS (attractive and repulsive) and the correspondent activity coefficient model terms (residual and combinatorial) at zero pressure:

$$\begin{cases} (G_{EOS}^E)_{rep} = (G_\gamma^E)_{comb} \\ (G_{EOS}^E)_{att} = (G_\gamma^E)_{res} \end{cases} \quad (5.16)$$

By analyzing the general form for the G^E / EoS mixing rule, it is possible to conclude that the repulsive term generated from the EoS does not cancel out with the combinatorial term from the G_γ^E model. This difference will be erroneously incorporated into the energy parameter. This problem is especially relevant for highly asymmetric systems. The more empirical approach represented by the LCVM model results in a smaller difference between the repulsive and combinatorial terms, which explains the better predictions for these type of systems.

In order to improve the correlation for these mixtures, Chen *et al.* (2002) applied this new modified mixing rule for the α parameter of the PSRK model:

$$\alpha_{mix} = \sum_{i=1}^{NC} z_i \alpha_{ii} + \frac{1}{A} \frac{G_{res}^E}{RT} \quad (5.17)$$

The b parameter mixing rule was also modified. As an alternative to the linear mixing rule, a non-linear combination rule is used:

$$b_{ij}^{3/4} = \left(\frac{b_{ii}^{3/4} + b_{jj}^{3/4}}{2} \right) \quad (5.18)$$

Chen *et al.* (2002) concluded that a significant improvement is obtained for athermal mixtures using the new mixing rule for the α parameter. The improvement is better if the new combination rule for the b parameter is applied (e.g. for the VLE of the system ethane/n-eicosane in the temperature range from 270 to 450 K, the average relative deviation for pressure decreased from 30% to 7%).

5.2.2 Density dependent mixing rules - The group-contribution equation of state

Besides Huron and Vidal (1979), Mollerup (1981) also suggested that the non-randomness can be taken into account in the mixing rules for the attractive term. Mollerup developed a different strategy to combine a cubic EoS with an activity coefficient model through the use of density dependent mixing rules. The resulting models respect the low density boundary condition limit. The group-contribution equation of state (GC-EoS) results from the application of this methodology.

The GC-EoS was initially proposed by Skjold-Jorgensen (1984). The free volume molecular term $(A^R/RT)_{rep}$ includes the Carnahan-Starling expression for hard spheres and the attractive term $(A^R/RT)_{att}$ is an NRTL type equation:

$$\left(\frac{A^R}{RT} \right)_{T,V,n} = \left(\frac{A^R}{RT} \right)_{rep} + \left(\frac{A^R}{RT} \right)_{att} \quad (5.19)$$

The attractive term is similar to the van der Waals expression for the attractive term combined with a group version of an NRTL (Renon and Prausnitz, 1968) type equation. The interactions occur through the functional groups surfaces:

$$(A^R/RT)_{atr} = -\frac{\hat{z}}{2RTV} \sum_{j=1}^{NG} \bar{n}_j q_j \frac{\sum_{k=1}^{NG} \theta_k \tilde{q} g_{kj} \tau_{kj}}{\sum_{l=1}^{NG} \theta_l \tau_{lj}} \quad (5.20)$$

where

$$\bar{n}_j = \sum_i^{NC} n_i v_i^j \quad (5.21)$$

$$\tilde{q} = \sum_j^{NC} \bar{n}_j q_j \quad (5.22)$$

$$\theta_j = \frac{\bar{n}_j q_j}{\tilde{q}} \quad (5.23)$$

The surface area q_i and the dispersive energy g_{ii} are the pure group parameters. The attractive energy parameter g_{jk} quantifies the attractive interactions between the segment groups j and k with the correspondent asymmetrical random parameter α_{jk} . In the above expressions \bar{n}_j is the total number of moles of group j ; \tilde{q} is the total number of surface segments; θ_j is the surface fraction of group j , v_j^i is the number of groups of type j in molecule i ; \hat{z} is the number of nearest neighbours to any segment (set equal to 10). For a random mixture, $\alpha_{jk} = 0$, and the classical mixing rule for the attractive term is obtained. The density dependent local compositions term is calculated using the following expression:

$$\tau_{jk} = \exp \left[\frac{\alpha_{ij} (g_{jk} - g_{kk})_{ij} \tilde{q}}{RTV} \right] \quad (5.24)$$

The attractive energy g_{ij} is calculated from the energy between like-group segments through the following combination rule:

$$g_{ij} = k_{ij} (g_{ii} g_{jj})^{1/2} \quad (5.25)$$

where the binary interaction parameter k_{ij} is symmetrical ($k_{ij} = k_{ji}$). Both, the attractive energy between like segments and the binary interaction parameter are temperature dependent:

$$g_{jj} = g_{jj}^* \left[1 + g_{jj}^{\cdot} \left(\frac{T}{T_j^*} - 1 \right) + g_{jj}^{\ddot{}} \ln \left(\frac{T}{T_j^*} \right) \right] \quad (5.26)$$

$$k_{ij} = k_{ij}^* \{ 1 + k_{ij}^{\cdot} \ln [2T / (T_i^* + T_j^*)] \} \quad (5.27)$$

where T_j^* is an arbitrary, but fixed reference temperature for group j , g_{jj}^* , g_{jj}^{\cdot} and $g_{jj}^{\ddot{}}$ are pure-group energy parameters and k_{ij}^* and k_{ij}^{\cdot} are binary group interaction parameters.

The free volume contribution is represented by the extended Carnahan-Starling equation for mixtures of hard spheres developed by Mansoori and Leland (1972) and it is a function of the hard spheres diameter per mol of component i (d_i).

$$(A^R/RT)_{\text{rep}} = 3 \left(\frac{\lambda_1 \lambda_2}{\lambda_3} \right) (Y - 1) + \left(\frac{\lambda_2^3}{\lambda_3^2} \right) (Y^2 - Y - \ln Y) + n \ln Y \quad (5.28)$$

$$Y = \left(1 - \frac{\pi \lambda_3}{6V}\right)^{-1} \quad (5.29)$$

$$\lambda_k = \sum_{i=1}^{NC} n_i d_i^k \quad (5.30)$$

where n is the total number of moles, n_i is the number of moles of component i , V is the total volume and NC is the number of components. The temperature dependence of the diameter d_i is given by:

$$d_i = 1.066d_{ci} [1 - 0.12 \exp(-2T_{ci} / 3T)] \quad (5.31)$$

The critical diameter d_{ci} is the hard spheres diameter value at the critical temperature of pure component i , T_{ci} . This value is usually calculated using an arbitrary vapour pressure point for a given component.

5.3 Equations of state that include association

As mentioned before (Chapter 2) association is usually described by one of three theories: the chemical theory, the quasi-chemical theory and the physical theory. In the next sections, some examples concerning the introduction of these theories into equations of state will be given.

This methodology was applied not only to the empirical cubic equations of state but also to more sophisticated EoS with a theoretical basis, as for example:

- (a) the perturbed anisotropic chain theory – PACT (Vilmachand and Donohue, 1985) coupled with the chemical theory;
- (b) the statistical associating fluid theory – SAFT (Chapman *et al.*, 1990; Huang and Radosz, 1990), which is based on the first order perturbation theory developed by Wertheim;
- (c) the Sanchez Lacombe EoS (Sanchez and Lacombe, 1976), which uses the quasi-chemical approach.

5.3.1 Equations of state that include the chemical theory

In this approach the “physical” type interactions are quantified through an equation of state. The equilibrium constant of a chemical reaction can be written in terms of fugacity coefficients:

$$K_{i+1} = \frac{z_{i+1} \hat{\phi}_{i+1}}{z_i z_1 \hat{\phi}_i \hat{\phi}_1} \frac{1 \text{ atm}}{P} \quad (5.32)$$

Heidemann and Prausnitz (1976) developed a method to implement the chemical theory into an equation of state. The chemical equilibria equations are solved analytically, whenever possible, and the result is incorporated into a given equation of state. First, a reaction scheme is defined and, then, the combination rules that relate the oligomer parameters to the ones from the monomer are set. This method is exemplified for a general cubic equation of state (Equation 5.2). For the oligomers, the following combination rules are usually assumed:

$$b_i = i b_1 \quad (5.33)$$

$$a_i = i^2 a_1 \quad (5.34)$$

Considering the monomer-dimer reaction scheme:



The material balance results in the following equations:

$$\frac{n_o}{n_T} = \frac{n_1 + 2 n_2}{n_1 + n_2} = 2 - z_1 \quad (5.36)$$

$$z_1 + z_2 = 1 \quad (5.37)$$

where n_o is the number of moles before association and n_T is the true number of moles (after association). Assuming the classical quadratic mixing rules, it is possible to write the mixture a and b parameters, as a function of the association extent n_o/n_T :

$$a = \left(\frac{n_o}{n_T} \right)^2 a_1 \quad (5.38)$$

$$b = \left(\frac{n_o}{n_T} \right) b_1 \quad (5.39)$$

Replacing equations (5.38) and (5.39) into a cubic equation of state (equation 5.2), it is possible to write it in terms of the association extent and of the monomer parameters a_1 and b_1 (Twu *et al.*, 1993):

$$P = \frac{n_T}{n_o} \frac{RT}{(v - b_1)} - \frac{a_1}{v^2 + u b_1 v + w b_1^2} \quad (5.40)$$

where $v = V/n_o$. The association extent can be evaluated using the fugacity coefficients relation:

$$\frac{\hat{\phi}_2}{\hat{\phi}_1^2} = \frac{Kz_1^2}{z_2} P \quad (5.41)$$

The fugacity coefficients are calculated using the cubic EoS, through the classical thermodynamics relation (Prausnitz, 1999):

$$RT \ln \phi_i = \int_v^{\infty} \left[\left(\frac{\partial P}{\partial n_i} \right)_{T,V,n_{k \neq i}} - \frac{RT}{V} \right] dv - RT \ln \left(\frac{PV}{nRT} \right) \quad (5.42)$$

Solving the material balances, it is possible to obtain the following expressions:

$$\begin{cases} \frac{n_T}{n_o} = \frac{2(KRT\rho e^g - 1)}{4KRT\rho e^g - 1 - \sqrt{1 + 8KRT\rho e^g}} \\ g(\eta) = -\ln(1 - \eta) \end{cases} \quad (5.43)$$

where the molar density is $\rho = n_o/V$ and the reduced density is $\eta = n_o b_1/V$. The association contribution to the compressibility factor can be obtained by relating it to the association extent n_T/n_o :

$$Z = \frac{PV}{n_o RT} = 1 + Z^{\text{assoc}} + Z^{\text{phys}} \quad (5.44)$$

$$Z^{\text{assoc}} = \frac{n_T}{n_o} - 1 \quad (5.45)$$

If the same procedure is adopted for the infinite equilibria model, the extent of association is now given by:

$$\begin{cases} \frac{n_T}{n_o} = \frac{2}{1 + \sqrt{1 + 4KRT\rho e^g}} \\ g(\eta) = -\ln(1 - \eta) \end{cases} \quad (5.46)$$

Numerous association equations of state have been proposed from this methodology. They differ on the non-specific terms (repulsive and attractive) chosen and also on the type of mixing and combination rules assumed.

Table 5.3 shows some of the models in terms of their density functionality and the family of components studied.

Table 5.3 Association equations developed from the Heideman and Prausnitz approach.

| EoS | $g(\eta)$ | Systems studied |
|-----------------------|---|---|
| CS-VDW ^a | $\frac{4\eta - 3\eta^2}{(1-\eta)^2}$ | amphoteric+ inert |
| APACT ^b | 0 | amphoteric+ inert |
| ABPACT ^c | 0 | amphoteric+ Lewis acid or base amphoteric+ amphoteric Lewis acid + Lewis base |
| APACT-2 ^d | $0.2c_1 \frac{4\eta - 3\eta^2}{(1-\eta)^2}$ | amphoteric+ Lewis acid or base amphoteric+ amphoteric Lewis acid + Lewis base |
| AESD-EoS ^e | $-\ln(1-1.9\eta)$ | amphoteric+ inert |
| RK-EoS ^f | $-\ln(1-\eta)$ | pure amphoteric |

^aHeidemann and Prausnitz (1976); ^bIkonomou and Donohue (1986 and 1988); ^cEconomou *et al.* (1990); ^dEconomou and Donohue (1991); ^eElliott *et al.* (1990); Suresh and Elliott (1991); ^fTwu *et al.* (1993).

These models have been applied to mixtures containing at most two associating components. The extension of this type of approach to binary mixtures that cross-associate results in analytical expressions for the fraction of non-bonded sites in the following cases:

- monomers from different components (ex: acetone and chloroform, *i.e.*, bases and acids of Lewis);
- oligomer (ex: alcohol) + monomer (ex: acetone or chloroform).

For mixtures containing two amphoteric species, it is only possible to obtain a numerical solution, which results in high computational times. For this reason, some approximate results were presented as discussed in chapter 2. The resolution of this chemical problem is made by assuming that:

- only linear oligomers are formed;
- the equilibrium constants depend only on the monomers involved.



Ikonomou *et al.* (1988) used an approximate solution for the association perturbed anisotropic chain theory APACT to describe vapour-liquid equilibria for binary mixtures of alcohols and water by adjusting a binary interaction parameter. In this version, the cross-association between an amphoteric component like an alcohol and a Lewis base like acetone was not considered. This system could not be accurately modelled not even considering high interaction parameters. As a consequence,

Economou *et al.* (1990) have extended the model to systems containing amphoteric molecules and acid or bases of Lewis. This version is called “acid base associated perturbed anisotropic chain theory” - ABPACT. The APACT-2 model (Economou and Donohue, 1991) assumes different combination rules relatively to the APACT model, resulting in different g functions.

Elliot *et al.* (1990) presented a semi-empirical cubic equation for non-spherical molecules (AESD-EoS) that includes an association term based on the chemical theory. This model was applied to low pressure self-associating systems (alcohol + alkane or aromatic; acid + aromatic). Later, Suresh and Elliot (1991) have extended the model to a wider range of pressures and to mixtures containing at most two associating components using some of the approximations developed for the APACT model.

An empirical model was specially developed to represent the properties of pure carboxylic acids (Twu *et al.*, 1993), which incorporates the chemical theory into a cubic equation of state.

5.3.2 Equations of state that include a physical theory

The first order perturbation theory provides simple expressions for the residual Helmholtz energy of association A^{assoc} and for the association contribution to the compressibility factor Z^{assoc} . These partial terms can be added to the remaining non-specific terms, thus obtaining the global residual Helmholtz energy and the compressibility factor of the mixture. One of the most successful models presented in the literature is the Statistical Associating Fluid Theory, which has a strong theoretical basis. For comparison, a semi empirical model that combines the TPT1 theory with a cubic equation of state is also presented.

5.3.2.1 The Statistical Associating Fluid Theory – SAFT equation

Chapman *et al.* (1990) developed a theoretical equation of state for non-spherical molecules that includes on the reference fluid the shape and association effects. Other less important intermolecular effects are included through a mean field perturbation term. Figure 5.1 shows the construction model of a molecule according to the SAFT methodology.

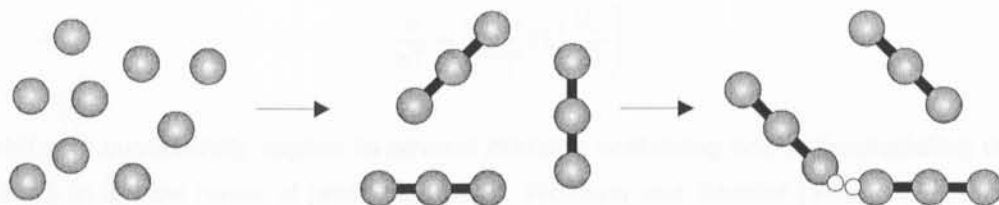


Figure 5.1 Molecules model according to the SAFT equation: rigid spheres fluid → chain formation → associated complexes formation.

The general expression, for pure components, for the residual Helmholtz energy per mol of molecules, is given by:

$$a^{\text{res}} = a^{\text{seg}} + a^{\text{chain}} + a^{\text{assoc}} \quad (5.47)$$

The residual energy of the m not associated segments, a^{seg} , can be expressed as:

$$a^{\text{seg}} = ma_0^{\text{seg}} = m(a_0^{\text{hs}} + a_0^{\text{disp}}) \quad (5.48)$$

where a_0^{disp} and a_0^{hs} are the dispersive and hard-spheres terms of the residual energy of Helmholtz, per mol of segments, for the non-associated spherical segments, respectively. The dispersive term a_0^{disp} is given by the square well potential depth u . The universal constants D_{ij} were fitted by Chen and Kreglewsky (1977) to thermodynamic data of argon.

$$\frac{a_0^{\text{disp}}}{RT} = \sum_i \sum_j D_{ij} \left(\frac{u}{kT} \right)^i \left(\frac{\eta}{0.74} \right)^j \quad (5.49)$$

a_0^{hs} is calculated using the expression from Carnahan and Starling (1969):

$$\frac{a_0^{\text{hs}}}{RT} = \frac{4\eta - 3\eta^2}{(1 - \eta)^2} \quad (5.50)$$

The chain formation energy (a^{chain}) is based on the association fluid theory by establishing that a covalent bond corresponds to an association bond with infinite energy:

$$\frac{a^{\text{chain}}}{RT} = (1 - m) \ln \left[\frac{1 - \frac{1}{2}\eta}{(1 - \eta)^3} \right] \quad (5.51)$$

The association term a^{assoc} is given by the first order perturbation theory as defined by equations 2.24 to 2.32.

For the extension of SAFT-EoS to mixtures, two types of mixing rules were used for the attractive term (Huang and Radosz, 1991): the classical van der Waals one fluid mixing rules and the volume fraction f_i mixing rules (equation 5.52).

$$\frac{u}{kT} = \sum_i \sum_j f_i f_j \left(\frac{u_{ij}}{kT} \right) \quad (5.52)$$

This model was successfully applied to several mixtures containing one self-associating component plus an inert, in a wide range of pressures. Later, Wolbach and Sandler (1998) have extended the model to binary cross-associating mixtures containing two associating components (acids, alcohols or water) and one self-associating component (water or methanol) and a cross-associating component (acetone or diethyl ether).

More recently, Chapman (2002) mentioned some of the future developments of the SAFT equation, namely, the modelling of the effects of intramolecular association and the effects of multiple polar groups.

5.3.2.2 Semi empirical cubic equations of state

Kontogeorgis *et al.* (1996) combined the SRK-EoS with the association term derived from the TPT1 to obtain the cubic plus association equation of state - CPA-EoS:

$$P = \frac{RT}{V-b} - \frac{\alpha}{V(V+b)} + \frac{RT}{V} \sum_i x_i \sum_j \rho_j \sum_{A_i} \left(\frac{1}{X_j^A} - \frac{1}{2} \right) \frac{\partial X_j^A}{\partial \rho_i} \quad (5.53)$$

$$\alpha = \alpha_o \left[1 + c_1 (1 - \sqrt{T_r}) \right]^2 \quad (5.54)$$

The association strength expression is slightly different from the SAFT equation:

$$\Delta^{A_i B_j} = g_{ij} \left[\exp \left(\frac{\varepsilon^{A_i B_j}}{RT} \right) - 1 \right] b_{ij} K_{A_i B_j} \quad (5.55)$$

where b_{ij} is the co-volume parameter. The radial distribution function g_{ij} for a hard spheres mixture is given by the expression:

$$g_{ij} = \left[\frac{2 - \eta}{2(1 - \eta)^3} \right] \quad (5.56)$$

$$\eta = \frac{b}{4V} \quad (5.57)$$

To facilitate the extension of the g_{ij} function to hard spheres mixtures, a linear mixing rule for the parameter b is used:

$$b = \sum_i x_i b_i \quad (5.58)$$

For parameter a , the classical van der Waals mixing rules were adopted. The combination rules are:

$$\begin{cases} a_{ij} = \sqrt{a_{ii} a_{jj}} (1 - k_{ij}) \\ b_{ij} = \frac{b_{ii} + b_{jj}}{2} \end{cases} \quad (5.59)$$

The CPA-EoS was used to model liquid-liquid equilibria (Voutsas *et al.*, 1997) and vapour-liquid equilibria (Yakoumis *et al.*, 1997) for binary mixtures of alcohols and alkanes. More recently, Voutsas *et al.* (1999) have extended the CPA-EoS to ternary mixtures containing water, alcohols and alkanes by using the approximation proposed by Suresh and Elliot (1992).

5.3.3 Equations of state that include a quasi-chemical theory

The quasi-chemical theory was first introduced by Guggenheim (1952) to model non-randomness in liquid mixtures. This theory does not take into account explicitly hydrogen bonding. However, it serves as the basis for the development of lattice equations of state.

More recently, Panayiotou and Sanchez (1991) developed a theoretical lattice equation of state that divides molecular interactions in two different types: physical interactions that are described by the SL-EoS (Sanchez and Lacombe, 1976) and an association term. This last term counts the number of possible hydrogen bonds arrangements. Similarly to the SAFT equation it is not necessary to *a priori* define the distribution of the oligomers.

Gupta *et al.* (1992) have used this theory for wide ranges of density to describe self-associating systems (pure water, methanol or ethanol and the binary mixture 1-hexanol-SF₆) and systems containing one acid and one base of Lewis (acetone and chloroform). As an example, the following expression is obtained for a binary mixture of a self-associating component with two sites (M) + inert (N):

$$X^{\text{mon}} = \frac{2}{1 + 2\rho K * x_M + \sqrt{1 + 4\rho K * x_M}} \quad (5.60)$$

5.4 Conclusions

Two main approaches have been adopted to model association effects:

One is the introduction of liquid activity coefficient models into the attractive parameter mixing rules of cubic equations of state. Several combinations of G^E and EoS models have been proposed. The greatest advantage is the possibility of using the extensive parameter tables available for several G^E models, like UNIQUAC, UNIFAC or modified UNIFAC methods. The extension of these models to mixtures containing gases demands the estimation of new interaction parameters that are, in many cases, temperature dependent. Satisfactory results are obtained with these models.

A more consistent approach is to modify the pure component equation of state in order to explicitly take into account association effects. Three different approaches have been proposed: the chemical, quasi-chemical and physical theories. All use a molecular approach for the association term, that is, for each associating component it is necessary to estimate the self- and cross-association parameters. The extension of these models to more than two associating components is quite cumbersome, since no analytical solution can be found.

6 Modelling of phase equilibria for associating mixtures using an equation of state

6.1 The group-contribution equation of state

The group-contribution equation of state (GC-EoS) was initially proposed by Gross et al. (1987). It consists of a cubic equation of state for the pure components, plus a mixing rule for the equation of state and a mixing rule for the group-contribution equation of state (GC-EoS) (Gross et al., 1987). The mixing rule for the GC-EoS is given by equations 6.15 to 6.21.

The mixing rule for the GC-EoS is given by equations 6.15 to 6.21. The mixing rule for the GC-EoS is given by equations 6.15 to 6.21. Chapter 6

Modelling of phase equilibria for associating mixtures using an equation of state

The equation of state for the pure components is given by equation 6.1. The equation of state for the pure components is given by equation 6.1. The equation of state for the pure components is given by equation 6.1.

6. Modelling of phase equilibria for associating mixtures using an equation of state

6.1 The group-contribution with association equation of state

The group-contribution with association equation of state -GCA-EoS- was initially proposed by Gros *et al.* (1996). It results from the addition of a third contribution, which quantifies the association forces, to the original repulsive and attractive terms of the group-contribution equation of state, GC-EoS (Skjold-Jorgensen, 1984, 1988). The repulsive and attractive terms are described by equations 5.19 to 5.31.

The association term results from the application of the group-contribution approach based on the first order perturbation theory presented by Chapman *et al.* (1990) and Huang and Radosz (1990).

The total energy of Helmholtz can be written as a sum of three terms:

$$\left(\frac{A^R}{RT}\right)_{T,V,n} = \left(\frac{A^R}{RT}\right)_{rep} + \left(\frac{A^R}{RT}\right)_{atr} + \left(\frac{A^R}{RT}\right)_{assoc} \quad (6.1)$$

The expression for the association term of the residual energy of Helmholtz is a function of the number of association groups NGA present in the mixture:

$$\left(\frac{A^R}{RT}\right)_{assoc} = \sum_{k=1}^{NGA} n_k^* \left[\sum_{A_k} \left(\ln X^{A_k} - \frac{X^{A_k}}{2} \right) + \frac{1}{2} M_k \right] \quad (6.2)$$

The number of moles of the association group k is calculated as follows:

$$n_k^* = \sum_{m=1}^{NC} v_k^m n_m \quad (6.3)$$

where v_k^m is the number of groups k in molecule m and n_m is the number of moles of component m . The mole fraction of group k not associated at site A, X^{A_k} is given by:

$$X^{A_k} = \left(1 + \sum_{j=1}^{NGA} \sum_{l=1}^{M_j} \rho_j^* X^{B_j} \Delta^{A_k B_j} \right)^{-1} \quad (6.4)$$

where ρ_j^* is the mole density of group j .

$$\rho_j^* = \frac{n_j}{V} \quad (6.5)$$

The association strength ($\Delta^{A_k B_j}$) is a simplified expression of the one proposed by Huang and Radosz (1991), since it does not include the radial distribution function g^* . In this way, the group-contribution character of the model is preserved (Gros *et al.*, 1996).

$$\Delta^{A_k B_j} = \kappa^{A_k B_j} \left[\exp\left(\frac{\varepsilon^{A_k B_j}}{kT}\right) - 1 \right] \quad (6.6)$$

The association parameters between site A of group k and site B of group j are the association energy ε and the corresponding bonding volume κ .

6.2 Extension of the model

6.2.1 Revision

Gros *et al.* (1996) have successfully applied the GCA-EoS to multi-component mixtures containing water, alcohols and any number of inert components by defining a single associating group, the hydroxyl group OH, to represent association effects in these mixtures. Each water molecule or alcohol molecule is considered to have one associating group with two sites (an electronegative site O and an electropositive site H). The rigorous and the approximate models are presented on Table 6.1. The rigorous model for the alcohol group with two electronegative sites (A_1 and B_1) and one electropositive site (C_1) is replaced by the approximate model with only one electronegative site and one electropositive site (A_1 and B_1 , respectively). The rigorous model for water (two electronegative sites + two electropositive sites) is also replaced by the hydroxyl associating group. This

approximation resulted in very good representation of the properties of solutions containing these associating components (Gros *et al.*, 1996).

Table 6.1 Association group models for water and alcohols used in the GCA-EoS.

| Component | Rigorous type | Approximation (GCA-EoS) |
|------------------|---|--|
| R-OH | $\begin{array}{c} A_1 \\ \vdots \\ R-\overset{\cdot\cdot}{O}-H C_1 \\ \vdots \\ B_1 \end{array}$ | $\begin{array}{c} A_1 \\ \vdots \\ \overset{\cdot\cdot}{O}-HB_1 \\ \vdots \end{array}$ |
| H ₂ O | $\begin{array}{c} A_1 \quad B_1 \\ \quad \vdots \\ \quad \quad O \\ \quad \quad \vdots \\ H \quad \quad H \\ C_1 \quad D_1 \end{array}$ | |

6.2.2 Model development

In this section the model is extended to mixtures containing, additionally, associating groups able to form dimers. Three new associating groups are defined as follows:

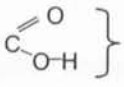
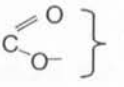
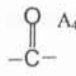
- The acid association group COOH with one site capable of both self- and cross-associating;
- The ester association group COOR with one site that does not self-associate but can cross-associate with groups that have an electropositive site;
- The ketone association group COR with one site that does not self-associate but can cross-associate with groups that have an electropositive site.

Therefore, the model is extended to mixtures containing four possible associating groups as described on Table 6.2. The same nomenclature already used in section 3.3.1 is adopted here.

On the first column of Table 6.2 are represented schematically the number of sites assigned to each associating group and, on the second column the different assumptions concerning the association strengths between each pair of sites. Finally, on the third column the association parameters that have to be fitted are shown.

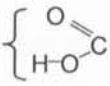
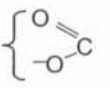
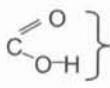
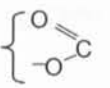

As can be seen from Table 6.2 the double hydrogen bond of the acids is represented by a strong single bond between sites A_1 . The ester group is represented by a unique electron-donor site A_3 and, that is also the case for the ketone group that has its own electron-donor site A_4 . These two latter associating groups (ester and ketone) do not self-associate, *i.e.*, their self-association strengths are zero.

Table 6.2 Self-association models defined in the GCA-EoS

| Self-association | | Assumptions | Association parameters |
|------------------|---|---|--------------------------------------|
| RCOOH |  } A_1 | $\Delta_{A_1A_1} \neq 0$ | $\epsilon_{A_1A_1} \quad K_{A_1A_1}$ |
| ROH | $O-H$ B_2 A_2 | $\Delta_{A_2B_2} \neq 0$ $\Delta_{A_2A_2} = \Delta_{B_2B_2} = 0$ | $\epsilon_{A_2B_2} \quad K_{A_2B_2}$ |
| RCOOR |  } A_3 | $\Delta_{A_3A_3} = 0$ | --- |
| RCOR |  A_4 | $\Delta_{A_4A_4} = 0$ | --- |

The groups defined on Table 6.2 are able to cross-associate in some situations. Table 6.3 describes the cross-association models developed in this work. The cross-association strength between the acid and the hydroxyl groups was estimated as the geometric average of the self-association strengths. For the cross-association between one associating group that can self-associate (hydroxyl or acid groups) and one group that can solely cross-associate (the ketone or ester groups) it is necessary to fit those cross-association parameters simultaneously with the attractive parameters.

Table 6.3 Cross-association models defined in the GCA-EoS model.

| Cross-association | | Assumptions | Association parameters |
|-------------------|---|--|---|
| ROH-RCOOH | $O-H$ B_2 A_1  | $\Delta_{A_1A_1} \neq 0, \Delta_{A_2B_2} \neq 0$ $\Delta_{A_1A_2} = \Delta_{A_1B_2} \neq 0$ | $\epsilon_{A_1A_2} = \epsilon_{A_1B_2} = \frac{\epsilon_{A_1A_1} + \epsilon_{A_2B_2}}{2}$ $K_{A_1A_2} = K_{A_1B_2} = \sqrt{K_{A_1A_1} K_{A_2B_2}}$ |
| ROH-RCOOR | $O-H$ B_2 A_3  | $\Delta_{A_2B_2} \neq 0, \Delta_{A_3A_3} = 0$ $\Delta_{B_2A_3} \neq 0, \Delta_{A_3A_2} = 0$ | $\epsilon_{A_3B_2} \quad K_{A_3B_2}$ |
| RCOOH-RCOOR |  } A_1 A_3  | $\Delta_{A_1A_1} \neq 0, \Delta_{A_3A_3} = 0$ $\Delta_{A_1A_3} \neq 0$ | $\epsilon_{A_1A_3} \quad K_{A_1A_3}$ |
| ROH-RCOR | $O-H$ B_2 A_4  | $\Delta_{A_2B_2} \neq 0, \Delta_{A_4A_4} = 0$ $\Delta_{B_2A_4} \neq 0, \Delta_{A_4A_2} = 0$ | $\epsilon_{B_2A_4} \quad K_{B_2A_4}$ |

The expressions calculated for the association term can be incorporated into the compressibility factor and fugacity coefficient calculations. The compressibility factor Z is calculated by differentiating the residual Helmholtz energy respect to volume:

$$Z = Z^{\text{rep}} + Z^{\text{atr}} + Z^{\text{assoc}} + 1 = -\frac{V}{n} \left. \frac{\partial (A^{\text{res}} / RT)}{\partial V} \right|_{T,n} + 1 \quad (6.7)$$

And the fugacity coefficient of component i is related to the residual Helmholtz energy as follows:

$$\ln \hat{\phi}_i = \ln \hat{\phi}_i^{\text{rep}} + \ln \hat{\phi}_i^{\text{atr}} + \ln \hat{\phi}_i^{\text{assoc}} - \ln Z = \left. \frac{\partial (A^{\text{res}} / RT)}{\partial n_i} \right|_{T,V,n_{j \neq i}} - \ln Z \quad (6.8)$$

The association contributions for Z and $\ln \hat{\phi}_i$ can be obtained from the energy of Helmholtz of association. The general expressions are:

$$Z^{\text{assoc}} = -\frac{V}{n} \sum_{k=1}^{\text{NGA}} \sum_{X^{A_k}} \left(\frac{1}{X^{A_k}} - \frac{1}{2} \right) n_k^* \left(\frac{\partial X^{A_k}}{\partial V} \right)_{T,n} \quad (6.9)$$

$$\ln \hat{\phi}_i^{\text{assoc}} = \sum_{k=1}^{\text{NGA}} \left\{ v_k^i \left[\sum_{X^{A_k}} \left(\ln X^{A_k} - \frac{X^{A_k}}{2} \right) + \frac{1}{2} M_k \right] + \sum_{X^{A_k}} \left(\frac{1}{X^{A_k}} - \frac{1}{2} \right) n_k^* \left(\frac{\partial X^{A_k}}{\partial n_i} \right)_{T,P,n_j} \right\} \quad (6.10)$$

It is interesting to analyze how these equations can be simplified for some particular cases:

Case I. One self-associating group with one site (acid group):

$$Z^{\text{assoc}} = -\frac{n_k^*}{n} \left[\frac{\rho \Delta}{2} (X^{\text{mon}})^2 \right] \quad (6.11)$$

$$\ln \hat{\phi}_i^{\text{assoc}} = v_k^i \ln X^{\text{mon}} \quad (6.12)$$

Case II. One self-associating group with two sites (alcohol):

$$Z^{\text{assoc}} = -\frac{n_k^*}{n} \rho \Delta X^{\text{mon}} \quad (6.13)$$

$$\ln \hat{\phi}_i^{\text{assoc}} = 2v_k^i \ln X^{\text{mon}} \quad (6.14)$$

These expressions can be simplified when applied to a binary mixture where one of the components is infinitely diluted in the other. At very low concentrations of the associating component, its monomer fraction will be close to one and the association contribution will tend to zero, *i.e.*, the component will behave as if it was not associated at all. On the other hand, at higher concentrations, association effects will have their major effect. Therefore, for the calculation of self-association parameters, pure component thermodynamic properties of the associating component are a convenient source of experimental data.

6.3 Parameterization

6.3.1 Computer programme

A program was written in FORTRAN language to estimate the parameters using vapour-liquid, liquid-liquid equilibria of binary mixtures, infinite dilution activity coefficients of binary and ternary mixtures and pure component vapour pressures. The optimization subroutine is the ZXSSQ subroutine from the IMSL (International Mathematics and Statistical Libraries) which uses an optimization algorithm based on the finite differences Levenberg-Marquardt method for non-linear problems. The objective function was defined to fit the different type of experimental data available, as a sum of three contributions:

$$F_{\text{obj}} = \sum_{i=1}^{\text{NVAP}} f_i^{\text{VAP}} + \sum_{i=1}^{\text{NTP}} f_i^{\text{TPE}} + \sum_{i=1}^{\text{NGAM}} f_i^{\text{GAM}} \quad (6.15)$$

The residual function f_i^{VAP} is used for pure components vapour pressure data:

$$f_i^{\text{VAP}} = W_1 \left(\frac{P^{\text{CALC}}}{P^{\text{EXP}}} - 1 \right)^2 \quad (6.16)$$

For two phases equilibria calculation the second residual function f_i^{TPE} can assume different forms according to the type of experimental information:

$$f_i^{\text{TPE}} = \begin{cases} W_2 \left(\frac{y_1^{\text{calc}}}{y_1^{\text{exp}}} - 1 \right)^2 + \left(\frac{P^{\text{calc}}}{P^{\text{exp}}} - 1 \right)^2 & \text{if T, x flash} \\ \left(\frac{X_1^{\text{calc}}}{X_1^{\text{exp}}} - 1 \right)^2 + W_3 \left(\frac{y_1^{\text{calc}}}{y_1^{\text{exp}}} - 1 \right)^2 & \text{if T, P flash} \\ \left(\frac{X_1^{\text{exp}} \hat{\phi}_{1,\text{exp}}^{\text{L}}}{y_1^{\text{exp}} \hat{\phi}_{1,\text{exp}}^{\text{V}}} - 1 \right)^2 + W_4 \left(\frac{X_2^{\text{exp}} \hat{\phi}_{2,\text{exp}}^{\text{L}}}{y_2^{\text{exp}} \hat{\phi}_{2,\text{exp}}^{\text{V}}} - 1 \right)^2 & \text{if isofugacity} \end{cases} \quad (6.17)$$

The first two options correspond to flash calculations at constant T and composition x or at constant T and P. They can be used when the composition of both phases are known accurately or when the isofugacity criterion is not sensitive to the composition. The isofugacity criterion, relative to the first component or to both components, can be used to get a first estimate of the parameters. Finally, f_i^{GAM} is the residual function for the activity coefficients data.

$$f_i^{\text{GAM}} = \sum_{i=1}^{\text{NC}} W_5 \left(\frac{\gamma_i^{\text{CALC}}}{\gamma_i^{\text{EXP}}} - 1 \right)^2 \quad (6.18)$$

The w_i weight factors ($i=1$ to 5) give the relative importance of the experimental data during the optimization. The phase equilibria were calculated using flash routines which perform the stability test proposed by Michelsen (1982).

6.3.2 Experimental Database

Table 6.4 shows the temperature and pressure ranges for the vapour-liquid equilibria used, together with the source of experimental data.

Table 6.4 Experimental VLE database used for correlation (NS: number of data sets).

| System | T range (K) | P range (bar) | NS | References |
|---|-------------|---------------|----|--|
| CH ₂ /CH ₃ (hexane, heptane; octane; cyclohexane) + COOH (acetic acid, propionic acid, butanoic acid, valeric acid, hexanoic acid, octanoic acid) | 313-443 | 0.010-1.0 | 15 | Gmehling <i>et al.</i> (1977) Miyamoto <i>et al.</i> (2000) |
| CH ₃ OH + COOH (acetic acid, propionic acid) | 333-411 | 0.20-1.8 | 5 | Gmehling <i>et al.</i> (1977) |
| CH ₂ OH (ethanol, 1-propanol, 1-butanol; 1-pentanol) + COOH (acetic acid, propionic acid) | 353-416 | 1.0 | 7 | Gmehling <i>et al.</i> (1977) |
| CHOH (2-propanol, 2-butanol)+COOH(acetic acid, propionic acid) | 357-412 | 1.0 | 3 | Gmehling <i>et al.</i> (1977) |
| H ₂ O + COOH (acetic acid, propionic acid, butyric acid) | 298-432 | 0.041-3.6 | 9 | Othmer <i>et al.</i> (1952a) Ermolaev <i>et al.</i> (1971) Gmehling <i>et al.</i> (1977) |
| CH ₃ COO (ethyl acetate; propyl acetate; butyl acetate) + COOH (acetic acid, propionic acid) | 315-398 | 0.030-2.0 | 11 | Gmehling <i>et al.</i> (1977) Miyamoto <i>et al.</i> (2001) |
| CH ₂ COO (ethyl propionate) + COOH (propionic acid) | 323 | 0.030-0.2 | 1 | Miyamoto <i>et al.</i> (2001) |
| CH ₂ OH (1-propanol, 1-butanol) + CH ₂ COO (methyl propionate, methyl butyrate) | 328-368 | 0.19-0.85 | 7 | Gmehling <i>et al.</i> (1977) |
| CH ₂ OH (ethanol, 1-propanol, 1-butanol) + CH ₃ COO (ethyl acetate, butyl acetate) | 323-328 | 0.22-0.53 | 3 | Gmehling <i>et al.</i> (1977) |
| H ₂ O + CH ₃ COO (methyl acetate, ethyl acetate, propyl acetate; butyl acetate) | 298-353 | 0.081-1.3 | 8 | Gmehling <i>et al.</i> (1977) |
| H ₂ O + CH ₃ CO (acetone and 2-butanone) | 308-523 | 0.18-68 | 9 | Griswold and Wong (1952) Lieberwirth and Schuberth (1979) Othmer <i>et al.</i> (1952b) |
| CH ₂ OH (ethanol, 1-propanol) + CH ₃ CO (acetone, 2-butanone) | 328-368 | 0.44-1.0 | 4 | Gmehling and Onken (1977); |
| CHOH (2-propanol) + CH ₂ CO (3-pentanone) | 355-373 | 1.0 | 1 | Wen <i>et al.</i> (1999) |
| CO ₂ +acids (acetic acid, butanoic acid) | 313-373 | 25-170 | 7 | Byun <i>et al.</i> (2000) |

The experimental database used in the optimization step includes vapour pressure (P^{vap}) of pure carboxylic acids (Daubert and Danner, 1989); binary low-pressure vapour-liquid equilibria (LPVLE) for mixtures of carboxylic acids with alkanes, alcohols, esters and water; high-pressure vapour-liquid

equilibria (HPVLE) for binary mixtures of carboxylic acids with carbon dioxide, HPVLE of water with ketones and infinite dilution activity coefficients (γ^∞) of alkanes in mixtures of triacetin with palmitic acid (Ferreira and Foco, 2003). The interactions between the ester group and the alcohol (or water) groups were estimated using LPVLE for binary mixtures of esters with alcohols (or water). In the same way, the interactions between the alcohol and ketone groups were estimated using LPVLE for binary mixtures of ketones with alcohols.

6.3.3 Attractive parameters

The group-contribution attractive term has five pure-group parameters (T_i^* , q , g^* , g' and g'') and four binary interaction parameters (the symmetrical k_{ij}^* and k_{ij}' and the asymmetrical non-randomness parameters α_{ij} and α_{ji}). The new acid group was added to the GCA-EoS parameter table. The attractive-energy parameters between this group and the paraffinic (CH_3 and CH_2), alcohol (CHOH , CH_2OH , CH_3OH), water (H_2O), triglyceride (TG), ester (CH_3COO and CH_2COO) and CO_2 functional groups were estimated using the experimental VLE database presented on Table 6.4 and the γ^∞ of alkanes in mixtures of triacetin with palmitic acid. Besides the association parameters, it was necessary to estimate binary interaction parameters in some cases (e.g. $\text{CH}_3\text{COO}/\text{CH}_2\text{OH}$; $\text{CH}_3\text{CO}/\text{CH}_2\text{OH}$). For the CO_2 -COOH interaction, it was necessary to calculate not only a $k_{\text{CO}_2,\text{COOH}}$, but also non-randomness parameters ($\alpha_{\text{CO}_2,\text{COOH}} = \alpha_{\text{COOH},\text{CO}_2}$). Tables 6.5 and 6.6 show the pure-group and the binary interaction parameters, respectively, together with the type of experimental data used in their estimation.

Table 6.5 Pure group parameters

| Group | T_i^* (K) | q | g^{**} | g' | g'' | Experimental information |
|-------|-------------|-------|----------|------|-------|--|
| COOH | 600 | 1.224 | 999600.5 | 0.0 | 0.0 | P^{vap} and LPVLE acids-alkanes |

Table 6.6 Binary interaction parameters

| i | j | k_{ij} | k'_{ij} | α_{ij} | α_{ji} | Experimental information |
|-------------------------|---|----------|-----------|---------------|---------------|----------------------------|
| COOH | CH_3/CH_2 | 0.8520 | 0 | 0 | 0 | LPVLE acids-alkanes |
| | CHOH | 1.1295 | 0 | 0 | 0 | LPVLE acids-alcohols |
| | CH_2OH | 1.0383 | 0 | 0 | 0 | LPVLE acids-alcohols |
| | CH_3OH | 1.0256 | 0 | 0 | 0 | LPVLE acids-methanol |
| | H_2O | 1.0479 | 0 | 0 | 0 | LPVLE acids-water |
| | $\text{CH}_3\text{COO}/$ CH_2COO | 1.0000 | 0 | 0 | 0 | LPVLE acids-esters |
| | TG | 1.1000 | 0 | 0 | 0 | γ^∞ |
| CH_2COO | CH_2OH | 1.0000 | 0 | 0 | 0 | LPVLE alcohols-esters |
| CH_3COO | H_2O | 1.0000 | 0 | 0 | 0 | LPVLE water-esters |
| | CH_2OH | 1.0174 | 0 | 0 | 0 | LPVLE alcohols-esters |
| CO_2 | COOH | 0.9592 | 0 | -3.0382 | -3.0382 | HPVLE acids- CO_2 |
| CH_3CO | H_2O | 1.0000 | 0 | 0 | 0 | HPVLE water-ketones |
| | CH_2OH | 0.979 | 0 | 0 | 0 | LPVLE alcohols-ketones |
| CH_2CO | CHOH | 1.0000 | 0 | 0 | 0 | LPVLE alcohols-ketones |

6.3.4 Association parameters

In order to model association using the GCA-EoS model, it is necessary to determine the number of associating groups, the number of active sites in each group and the values of the corresponding association strengths. Carboxylic acids present a high degree of non-ideality even at low pressures, which can be ascribed to the formation of oligomers in both, liquid and vapour phases. Generally, only the formation of dimers is considered, and it is possible to find in the literature (Gmehling *et al.*, 1977) the values of the vapour phase dimerization constants for a number of carboxylic acids. In this work, a new associating group (COOH) was defined as having one associating site that self-associates by double hydrogen bonding (Figure 6.1).

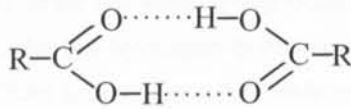


Figure 6.1 Cyclic dimer representation.

Following the procedure adopted by Gros *et al.* (1996) for the hydroxyl (OH) group, the COOH association parameters were determined by reproducing the fraction of non-bonded molecules predicted by the SAFT equation for linear acids from propanoic to decanoic at saturated liquid conditions (Huang and Radosz, 1990). The values obtained for the energy and volume of association are $\varepsilon/k^{\text{COOH}} = 6300 \text{ K}$ and $\kappa^{\text{COOH}} = 0.02 \text{ cm}^3/\text{mol}$, respectively. As expected, the COOH energy of association is much larger than that of the OH group ($\varepsilon/k^{\text{OH}} = 2700 \text{ K}$), which is in accordance with the higher degree of association of carboxylic acids. Figure 6.2 shows the results obtained. Huang and Radosz (1990) determined both association parameters from pure component properties (vapour pressure and liquid density data).

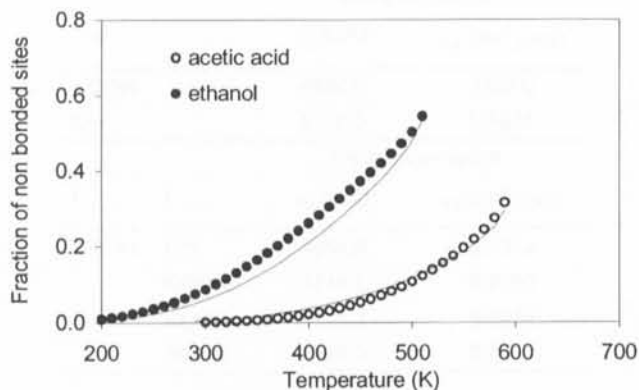


Figure 6.2 Fraction of non-bonded sites versus temperature: ● ○ GCA-EoS; — SAFT (Huang and Radosz, 1990).

The cross-association parameters between the hydroxyl group and the acid group were calculated using the following combination rules:

$$\begin{aligned}\varepsilon_{\text{COOH,OH}} &= \frac{\varepsilon_{\text{COOH}} + \varepsilon_{\text{OH}}}{2} \\ \kappa_{\text{COOH,OH}} &= \sqrt{\kappa_{\text{COOH}}\kappa_{\text{OH}}}\end{aligned}\quad (6.19)$$

In this way, the cross-association parameters were estimated using the already existent self-association parameters and no additional association parameters had to be calculated.

However, for the cross-association between the ester group and the OH or COOH groups, no combination rule can be established since the ester group does not self-associate. It was decided to set them as adjustable parameters. As the hydrogen bonding will be between a site O in the ester group and a site H in the OH or COOH groups, as a first estimate, the values of the self-association parameters values for the OH group were used. The cross-association parameters between the ester group and the OH group and between the ester and the acid group were estimated using low pressure vapour liquid equilibrium data (LPVLE) for esters and primary alcohols and for esters and acids, respectively.

The ketone group has the same type of association, *i.e.*, it can cross-associate with the OH group but does not self-associate. The cross-association parameters between the RCOR group and the OH group were estimated using low pressure vapour liquid equilibrium data (LPVLE) for ketones and primary alcohols and HPVLE of water and ketones.

The corresponding self-and cross-association parameters obtained in this work are presented on Table 6.7.

Table 6.7 GCA-EoS self and cross-association parameters.

| Self-association | | | |
|-------------------|------|-------------------------|--|
| | | $\varepsilon_{ij}/k(K)$ | $\kappa_{ij} (\text{cm}^3/\text{mol})$ |
| COOH | | 6300.0 | 0.0200 |
| OH | | 2700.0 | 0.8621 |
| Cross-association | | | |
| i | j | $\varepsilon_{ij}/k(K)$ | $\kappa_{ij} (\text{cm}^3/\text{mol})$ |
| COOH | OH | 4500.0 | 0.1313 |
| | COOR | 3248.8 | 0.7786 |
| OH | COOR | 2105.3 | 0.9916 |
| | RCOR | 2485.0 | 0.5000 |

6.3.5 Repulsive parameters

The critical diameter of components where the group described in the attractive term coincides with the molecule (H_2O , CH_3OH , CO_2) is given, rigorously, by the expression (Skjold-Jorgensen, 1988):

$$d_c = \left(0.08943 \frac{RT_c}{P_c} \right)^{\frac{1}{3}} \quad (6.20)$$

This expression is also valid for completely random mixtures, where $\alpha_{ij} = 0, \forall_{i,j}$. For the remaining cases, the critical diameter is fitted to a point of the vapour pressure curve, usually the normal boiling point.

6.3.6 Results and discussion

In this section some of the GCA-EoS correlations and predictions will be presented. For comparison, the results obtained with the group-contribution model MHV2 are also shown. This model was chosen as it also follows a group-contribution approach for which an extensive table of parameters is available (Dahl and Michelsen, 1990; Dahl *et al.*, 1991). Besides that, it does not take into account explicitly association effects.

6.3.6.1 Self-associating mixtures of acids and alkanes

The correlation of carboxylic acid vapour pressures gave an average relative error of 4% within a reduced temperature range between 0.55 and 0.90 (Table 6.8).

Table 6.8 Pure component vapour pressure correlation.

| Component | T(K) | Error $\Delta P/P(\%)*$ |
|----------------|---------|-------------------------|
| Acetic acid | 300-570 | 3.0 |
| Propanoic acid | 300-570 | 2.2 |
| Butanoic acid | 330-570 | 3.4 |
| Pentanoic acid | 325-575 | 5.0 |
| Hexanoic acid | 350-625 | 4.8 |
| Heptanoic acid | 390-570 | 5.3 |

$$\text{Error} = 100 \sqrt{\frac{\sum_i \{ [P_{\text{exp}} - P_{\text{calc}}] / P_{\text{exp}} \}^2 / \text{NP}}{2/\text{NP}}}, \text{NP: number of experimental data.}$$

Table 6.9 compares experimental vapour compressibility factors (Z) at saturation (Miyamoto *et al.*, 1999) with GCA-EoS *predictions*. The low values of Z reflect the strong association of carboxylic acids in the vapour phase, even at low pressures. It is interesting to notice that the GCA-EoS is able to follow the slight increase of Z with temperature evidenced by the experimental data.

Table 6.9 Z^{vap} prediction.

| Component | T(K) | $Z^{\text{vap}}_{\text{EXP}}$ | $Z^{\text{vap}}_{\text{CALC}}$ | Error(%)* |
|----------------|------|-------------------------------|--------------------------------|-----------|
| Acetic acid | 313 | 0.551 | 0.577 | 4.7 |
| | 323 | 0.569 | 0.583 | 2.5 |
| | 343 | 0.579 | 0.595 | 2.8 |
| | 363 | 0.595 | 0.606 | 1.8 |
| Propanoic acid | 323 | 0.611 | 0.646 | 5.7 |
| | 343 | 0.627 | 0.657 | 4.8 |
| | 363 | 0.638 | 0.668 | 4.7 |
| | 383 | 0.664 | 0.678 | 2.1 |
| Butanoic acid | 343 | 0.687 | 0.746 | 8.6 |
| | 363 | 0.706 | 0.752 | 6.5 |
| | 383 | 0.720 | 0.757 | 5.1 |
| | 403 | 0.741 | 0.761 | 2.7 |
| Pentanoic acid | 363 | 0.793 | 0.847 | 6.8 |
| | 383 | 0.805 | 0.845 | 5.0 |
| | 403 | 0.807 | 0.843 | 4.5 |
| | 423 | 0.801 | 0.840 | 4.9 |

$$*\text{Error} = \left\{ \frac{Z_{\text{calc}} - Z_{\text{exp}}}{Z_{\text{exp}}} \right\}$$

Figure 6.3 presents the saturation vapour and liquid compressibility factor for acetic acid. As can be seen, the GCA-EoS is able to correctly follow the shape of the curve: Z^{vap} presents a maximum and then decreases until it reaches the critical point value. However, the MHV2 model is not able to predict this behaviour.

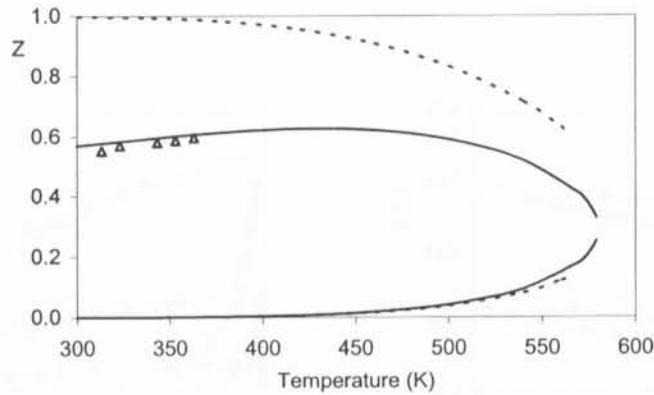


Figure 6.3 Saturation compressibility factor versus temperature for acetic acid: Δ Miyamoto *et al.* (1999); — GCA-EoS prediction; - - - MHV2 prediction.

The interaction parameters between the groups CH_3/CH_2 and COOH were calculated using not only pure carboxylic acids vapour pressures, but also low pressure binary VLE data of alkanes and acids.

Table 6.10 shows the average absolute deviation in composition δy and the average relative deviation in pressure $\delta P/P$ for both models. The GCA-EoS (average errors: $\delta P/P = 3.7\%$; $\delta y = 1.5\%$)

significantly improves the results obtained with the MHV2 model (average errors: $\delta P/P=6.2\%$; $\delta y=4.3\%$).

Table 6.10 Correlation results for VLE of acids and alkanes.

| System | NP | T (K) | P (bar) | GCA-EoS | | MHV2 | |
|-------------------------------|----|---------|-------------|------------------|----------------|------------------|----------------|
| | | | | $\delta P/P$ (%) | δy (%) | $\delta P/P$ (%) | δy (%) |
| heptane + propanoic acid | 7 | 323 | 0.087-0.18 | 7.4 | 0.6 | 13.6 | 4.7 |
| octane + butanoic acid | 13 | 398-434 | 1.0 | 3.5 | 2.7 | 10.0 | 2.8 |
| octane + acetic acid | 17 | 378-397 | 1.0 | 3.6 | 2.2 | 10.4 | 4.8 |
| octane + acetic acid | 18 | 343 | 0.19-0.29 | 2.6 | 1.6 | 2.4 | 10.3 |
| heptane + acetic acid | 15 | 303 | 0.071-0.091 | 3.0 | 0.8 | 2.0 | 10.5 |
| heptane + valeric acid | 5 | 323 | 0.11-0.17 | 1.6 | 0.30 | 5.7 | 0.51 |
| | 14 | 348 | 0.16-0.44 | 3.0 | 0.60 | 7.0 | 0.80 |
| | 11 | 373 | 0.23-0.91 | 6.1 | 1.8 | 6.4 | 0.96 |
| hexanoic acid + octanoic acid | 11 | 373-395 | 0.013 | 5.1 | 1.5 | 5.1 | 1.4 |
| | 15 | 423-443 | 0.13 | 5.2 | 1.6 | 3.7 | 3.8 |
| cyclohexane + acetic acid | 10 | 352-389 | 1.0 | 3.1 | 2.3 | 5.5 | 5.8 |
| | 9 | 313 | 0.086-0.25 | 6.1 | 3.7 | 16.0 | 4.1 |
| hexane + acetic acid | 9 | 313 | 0.10-0.37 | 3.4 | 1.0 | 7.6 | 5.1 |
| hexane + propionic acid | 9 | 313 | 0.041-0.37 | 4.3 | 0.38 | 2.2 | 2.4 |
| cyclohexane + propionic acid | 9 | 313 | 0.032-0.24 | 3.9 | 0.85 | 9.3 | 1.6 |

Good results are obtained as can be observed from figures 6.4 to 6.7. A more accurate description of the azeotropes is obtained by the GCA-EoS model compared to MHV2.

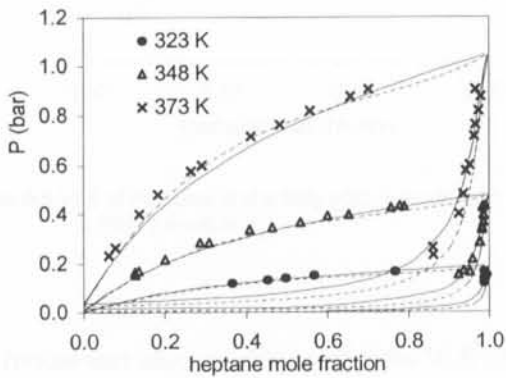


Figure 6.4 VLE of heptane and pentanoic acid: exp. (Gmehling *et al.*, 1977); — GCA-EoS correlation; - - -MHV2 prediction.

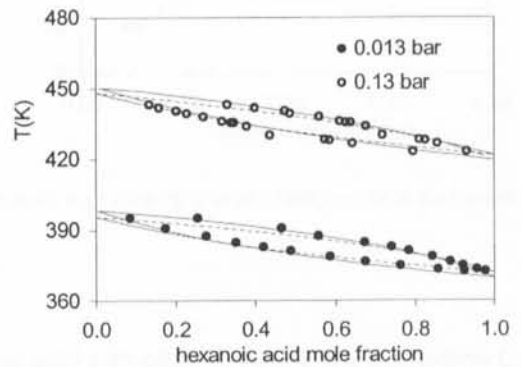


Figure 6.5 VLE of hexanoic acid and octanoic acid: exp. (Gmehling *et al.*, 1977); — GCA-EoS correlation; - - -MHV2 prediction.

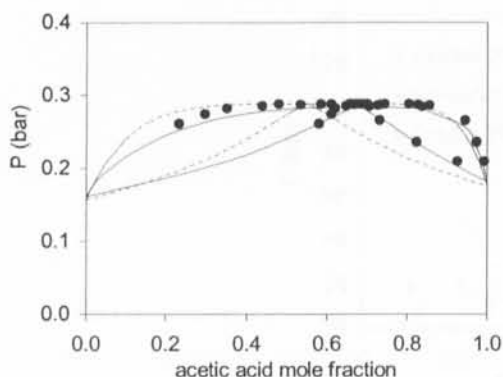


Figure 6.6 VLE of acetic acid and octane at 343 K: exp. (Gmehling *et al.*, 1977); — GCA-EoS correlation; - - -MHV2 prediction.

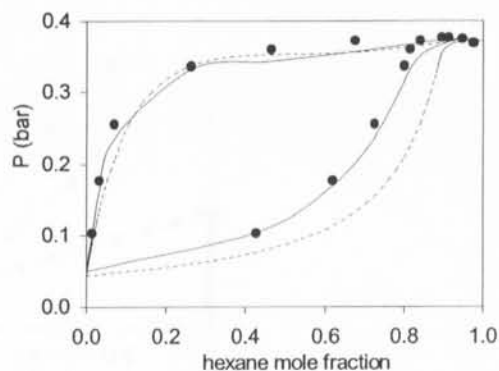


Figure 6.7 VLE of hexane and acetic acid at 313 K: exp. (Miyamoto *et al.*, 2000); — GCA-EoS correlation; - - -MHV2 prediction.

The same parameters obtained by correlating low-pressure VLE of acids and alkanes are now going to be applied to higher pressure mixtures. Figure 6.8 shows the solubility predictions of methane in either lauric or palmitic acids. Satisfactory results are obtained. The interaction $\text{CH}_4\text{-COOH}$ was set equal to the interaction $\text{CH}_3\text{-COOH}$ for both models, GCA-EoS and MHV2.

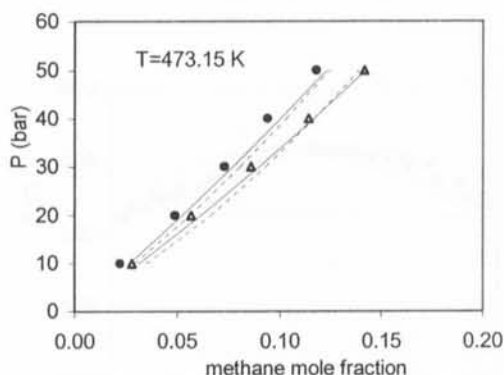
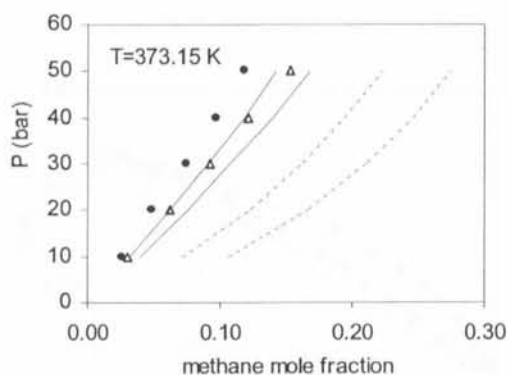


Figure 6.8 VLE of methane and a fatty acid: ● lauric acid; △ palmitic acid; exp. data (Shy *et al.*, 1993); — GCA-EoS prediction; - - -MHV2 prediction.

The model was also used to predict the VLE of nonanoic acid with ethane. Again, the interaction $\text{C}_2\text{H}_6\text{-COOH}$ was set equal to the interaction $\text{CH}_3\text{-COOH}$. Figure 6.9 shows that the predictions and experimental data are in good agreement.

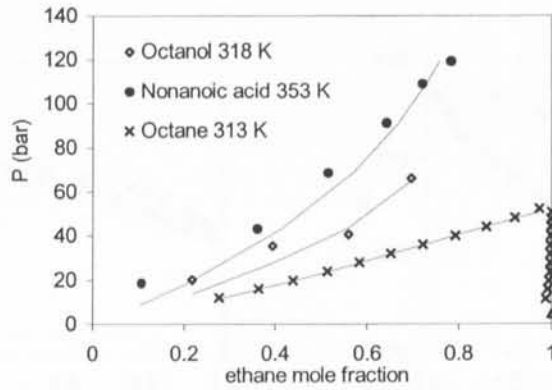


Figure 6.9 VLE of ethane and several solutes: exp. (Weng and Lee, 1992; Peter and Jakob, 1991; Rodrigues *et al.*, 1968); — GCA-EoS prediction.

6.3.6.2 Cross-associating mixtures with groups OH and COOH

As mentioned before the cross-association parameters between the OH associating group and the COOH group were obtained using the geometric mean of the self-association strengths. For these systems, good predictions were obtained without further estimating interaction parameters (Figure 6.10).

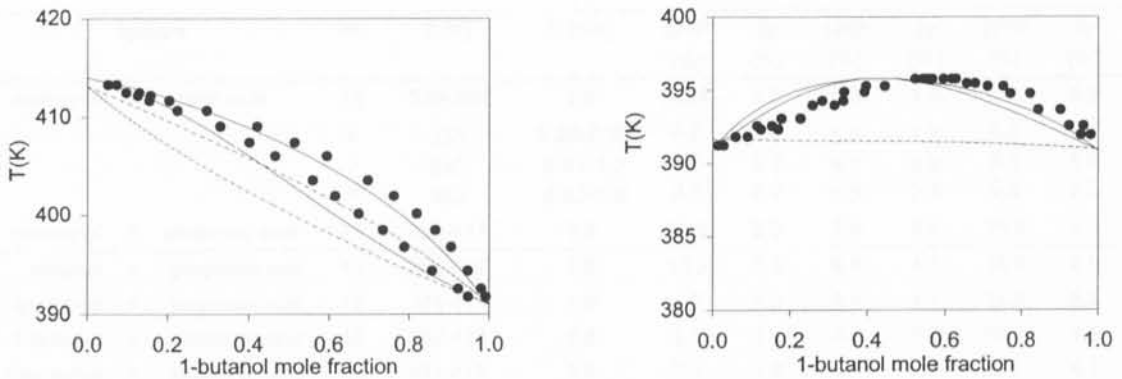


Figure 6.10 VLE of binary mixtures of an alcohol and an acid at 1 bar: (a) 1-butanol and propanoic acid; (b) 1-butanol and acetic acid. Exp. data (Gmehling *et al.*, 1977); — GCA-EoS prediction; - - - MHV2 prediction.

To improve the description of VLE for these systems a k_{ij} interaction parameter was estimated between the acid group and each of the alcohol attractive groups (CH_3OH , CH_2OH and CHOH).

Figure 6.11 shows the results obtained for binary VLE systems containing acids and alcohols (methanol, primary and secondary alcohol groups). Again the GCA-EoS model is able to describe more accurately the azeotropic data.

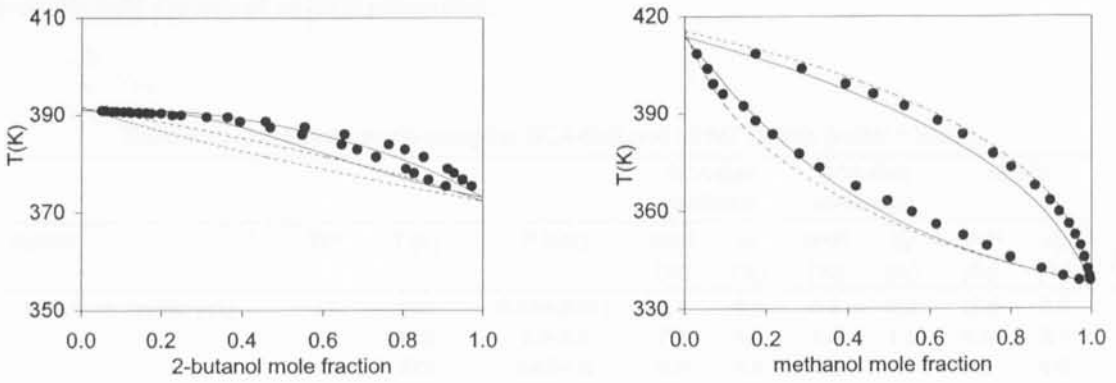


Figure 6.11 VLE of binary mixtures of an alcohol and an acid at 1 bar: (a) 2-butanol and acetic acid; (b) methanol and propanoic acid. Exp. data (Gmehling *et al.*, 1977); — GCA-EoS correlation; - - - MHV2 prediction.

Table 6.11 shows the average relative deviations in pressure ($\delta P/P$) and the absolute deviations in the vapour phase composition (δy) obtained using the GCA-EoS model (both correlation and prediction results) and with the MHV2 model for cross-associating mixtures containing alcohols and acids.

Table 6.11 Correlation results using the GCA-EoS and MHV2 models (alcohols + acids).

| System | NP | T (K) | P (bar) | GCA-EoS prediction | | GCA-EoS correlation | | MHV2 | |
|-----------------------------|----|---------|-----------|--------------------|----------------|---------------------|----------------|------------------|----------------|
| | | | | $\delta P/P$ (%) | δy (%) | $\delta P/P$ (%) | δy (%) | $\delta P/P$ (%) | δy (%) |
| methanol + acetic acid | 19 | 338-388 | 1.0 | 14.4 | 1.7 | 9.6 | 1.9 | 17.6 | 4.2 |
| | 6 | 333 | 0.20-0.93 | 4.0 | 2.5 | 5.7 | 1.8 | 6.3 | 3.7 |
| | 5 | 353 | 0.51-1.2 | 7.3 | 5.9 | 5.1 | 5.9 | 6.9 | 1.5 |
| | 6 | 363 | 0.63-1.8 | 8.6 | 2.9 | 5.5 | 2.4 | 9.2 | 5.2 |
| methanol + propionic acid | 21 | 338-411 | 1.0 | 10.2 | 2.9 | 7.9 | 3.5 | 16.8 | 2.3 |
| ethanol + propionic acid | 18 | 354-400 | 1.0 | 13.3 | 0.9 | 8.4 | 1.1 | 18.4 | 4.5 |
| 1-propanol + propionic acid | 18 | 373-411 | 1.0 | 7.5 | 1.0 | 4.6 | 1.1 | 13.6 | 4.2 |
| 1-butanol + propionic acid | 16 | 392-413 | 1.0 | 3.1 | 1.4 | 2.3 | 1.6 | 10.6 | 3.5 |
| 1-pentanol + propionic acid | 19 | 411-416 | 1.0 | 2.1 | 2.2 | 3.1 | 2.4 | 9.8 | 4.7 |
| ethanol + acetic acid | 16 | 353-388 | 1.0 | 13.1 | 1.4 | 7.7 | 1.2 | 16.2 | 5.5 |
| 1-propanol + acetic acid | 19 | 371-390 | 1.0 | 8.7 | 1.4 | 6.4 | 1.6 | 13.1 | 3.6 |
| 1-butanol + acetic acid | 19 | 392-396 | 1.0 | 2.9 | 2.2 | 4.0 | 2.5 | 9.3 | 3.6 |
| 2-propanol + propanoic acid | 18 | 358-412 | 1.0 | 15.0 | 0.9 | 6.1 | 1.2 | 17.6 | 4.5 |
| 2-propanol + acetic acid | 17 | 357-390 | 1.0 | 16.7 | 2.3 | 8.0 | 1.4 | 16.3 | 5.4 |
| 2-butanol + acetic acid | 18 | 375-391 | 1.0 | 10.5 | 2.2 | 4.8 | 1.9 | 12.9 | 4.5 |
| Average errors | | | | 9.5 | 1.9 | 6.1 | 1.9 | 14 | 4.1 |

The water/acid interaction was obtained by correlating binary VLE data shown on Table 6.12, using one interaction parameter k_{ij} . The MHV2 results in slightly lower average errors for these systems.

Figure 6.12 shows some correlation results obtained and Figure 6.13 shows the predictions for the water-acetic acid system at several pressures.

Table 6.12 Correlation results using the GCA-EoS and MHV2 models (water + acids).

| System | NP | T (K) | P (bar) | GCA-EoS prediction | | GCA-EoS correlation | | MHV2 | |
|------------------------|----|---------|-------------|--------------------|----------------|---------------------|----------------|------------------|----------------|
| | | | | $\delta P/P$ (%) | δy (%) | $\delta P/P$ (%) | δy (%) | $\delta P/P$ (%) | δy (%) |
| water + acetic acid | 11 | 298 | 0.024-0.031 | 9.4 | 6.9 | 5.2 | 2.2 | 13.5 | 6.6 |
| | 13 | 412 | 2.1-3.5 | 7.6 | 3.1 | 1.0 | 1.5 | 4.9 | 3.1 |
| | 13 | 372 | 0.62-1.0 | 8.6 | 4.4 | 2.5 | 1.5 | 8.5 | 4.8 |
| water + propionic acid | 8 | 313 | 0.041-0.071 | 9.6 | 4.4 | 4.4 | 3.2 | 3.9 | 2.0 |
| | 15 | 373 | 0.25-1.0 | 10.8 | 3.6 | 2.8 | 2.3 | 3.7 | 3.2 |
| | 18 | 353 | 0.19-0.46 | 10.3 | 3.3 | 6.5 | 4.0 | 2.7 | 3.3 |
| water + butyric acid | 26 | 373-432 | 1.0 | 12.0 | 4.7 | 5.5 | 4.1 | 4.2 | 0.81 |
| | 26 | 366-424 | 0.80 | 14.3 | 4.3 | 6.7 | 3.8 | 3.9 | 0.82 |
| | 25 | 356-405 | 0.54 | 14.7 | 4.2 | 7.0 | 3.7 | 4.2 | 1.0 |
| Average errors | | | | 11 | 4.3 | 5.1 | 3.2 | 5.0 | 2.4 |

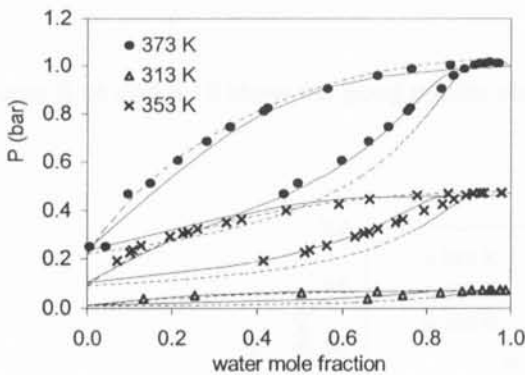


Figure 6.12 VLE of water and propionic acid: exp. (Gmehling *et al.*, 1977); — GCA-EoS correlation; - - -MHV2 prediction.

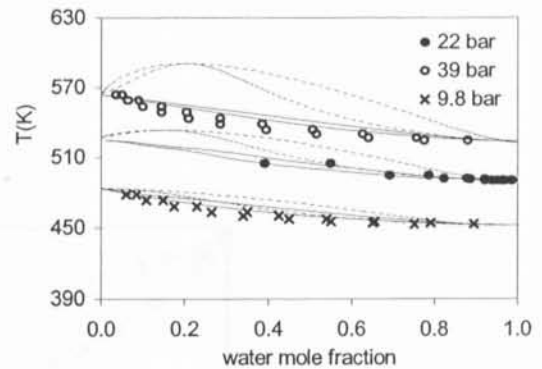


Figure 6.13 VLE of water and acetic acid. Exp. data: ● (Ohtmer *et al.*, 1952a), ○ × (Ermolaev *et al.*, 1971); — GCA-EoS prediction; - - -MHV2 prediction.

6.3.6.3 Cross-associating mixtures with groups COOH and COOR

As mentioned before, two cross-associating parameters have to be estimated as the ester group does not self-associate. The cross-association parameters were calculated using low pressure VLE data for acids and esters. As a first estimate for the optimization step, it was assumed that the association parameters between the COOR and COOH groups were equal to the ones from the alcohol group ($\epsilon_{OH}/k = 2700 \text{ K}$; $\kappa_{OH} = 0.8621 \text{ cm}^3/\text{mol}$). Furthermore, it was considered that $k_{\text{CH}_2\text{COO}/\text{CH}_3\text{COO},\text{COOH}} = 1.0$ and $\alpha_{\text{CH}_3\text{COO}/\text{CH}_3\text{COO},\text{COOH}} = \alpha_{\text{COOH},\text{CH}_3\text{COO}/\text{CH}_3\text{COO}} = 0.0$. The final values obtained for the cross-association parameters are: $\epsilon_{\text{COOH},\text{COOR}}/k = 3249 \text{ K}$; $\kappa_{\text{COOH},\text{COOR}} = 0.7786 \text{ cm}^3/\text{mol}$.

Table 6.13 compares the correlation results from the GCA-EoS to the MHV2 results for mixtures containing esters and acids. Again better results are obtained with the GCA-EoS.

Table 6.13 Correlation results using the GCA-EoS and MHV2 models (esters + acids).

| System | NP | T (K) | P (bar) | GCA-EoS | | MHV2 | |
|-----------------------------------|---------|---------|------------|------------------|----------------|------------------|----------------|
| | | | | $\delta P/P$ (%) | δy (%) | $\delta P/P$ (%) | δy (%) |
| methyl acetate + acetic acid | 14 | 333-378 | 1.0 | 3.7 | 3.3 | 3.9 | 8.4 |
| | 5 | 315-364 | 0.53 | 1.8 | 0.9 | 3.4 | 4.4 |
| ethyl acetate + acetic acid | 11 | 323 | 0.081-0.37 | 3.6 | 4.0 | 5.5 | 1.9 |
| | 11 | 338 | 0.19-0.55 | 2.9 | 2.8 | 2.9 | 5.2 |
| | 11 | 346 | 0.27-0.73 | 3.1 | 3.6 | 3.0 | 4.4 |
| | 11 | 373 | 0.58-2.0 | 2.8 | 3.6 | 4.1 | 1.4 |
| | 6 | 353-381 | 1.0 | 2.6 | 2.8 | 4.9 | 4.1 |
| 9 | 333-386 | 0.53 | 2.9 | 3.3 | 5.0 | 1.3 | |
| propyl acetate + acetic acid | 29 | 375-391 | 1.0 | 1.4 | 0.8 | 6.3 | 4.9 |
| butyl acetate + acetic acid | 15 | 390-398 | 1.0 | 1.3 | 1.3 | 10 | 20 |
| ethyl acetate + propionic acid | 9 | 323.2 | 0.030-0.39 | 4.9 | 0.8 | 2.2 | 3.1 |
| ethyl propionate + propionic acid | 9 | 323.2 | 0.027-0.17 | 3.2 | 0.9 | 4.0 | 3.4 |
| Average errors | | | | 2.7 | 2.2 | 5.0 | 5.9 |

Figures 6.14 and 6.15 show the good results obtained.

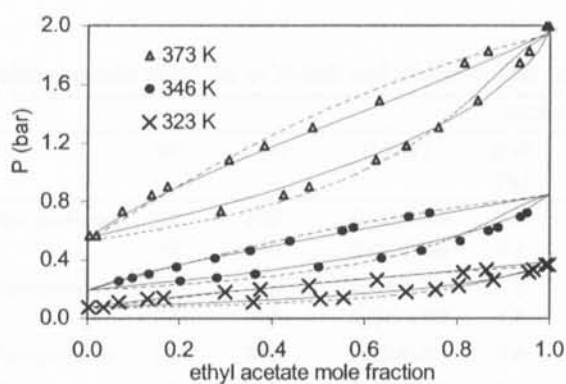


Figure 6.14 VLE of ethyl acetate and acetic acid: exp. (Gmehling *et al.*, 1977); — GCA-EoS correlation; - - -MHV2 prediction.

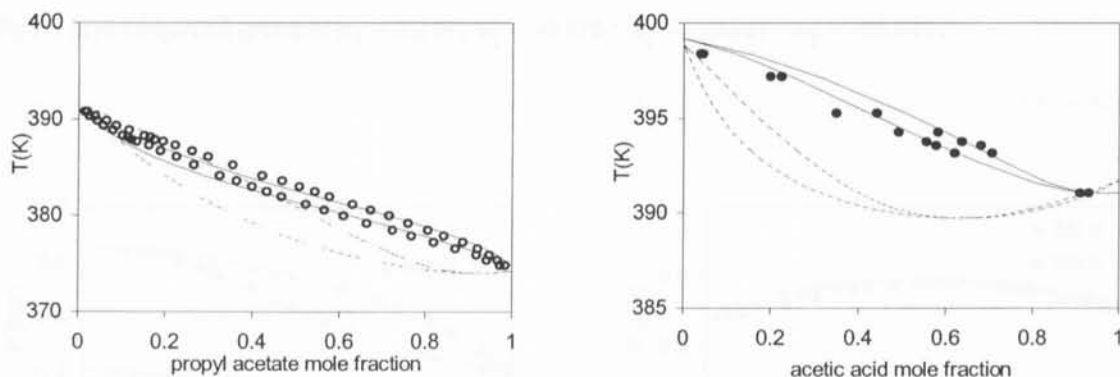


Figure 6.15 VLE of an ester and an acid at 1 bar (temperature versus composition): (a) propyl acetate and acetic acid; (b) acetic acid and butyl acetate. Exp. data (Gmehling *et al.*, 1977); — GCA-EoS correlation; - - MHV2 prediction.

6.3.6.4 Cross-associating mixtures with groups OH and COOR

For the cross-association between the hydroxyl and the ester associating groups, satisfactory results were obtained (Figure 6.16). In fact, for the binary mixtures containing the CH_2OH and CH_2COO groups, no additional attractive parameters had to be estimated. For the interaction $\text{CH}_2\text{OH}/\text{CH}_3\text{COO}$, it was necessary to estimate a $k_{\text{CH}_3\text{COO},\text{CH}_2\text{OH}}$. Table 6.14 compares the results obtained for mixtures containing esters and alcohols. The MHV2 gives slightly better results than the GCA-EoS.

Table 6.14 Correlation results using the GCA-EoS and MHV2 models (alcohols + esters).

| System | NP | T (K) | P (bar) | GCA-EoS | | MHV2 | |
|------------------------------|----|---------|-----------|------------------|----------------|------------------|----------------|
| | | | | $\delta P/P$ (%) | δy (%) | $\delta P/P$ (%) | δy (%) |
| 1-propanol + metilpropanoate | 18 | 328 | 0.18-0.42 | 3.2 | 2.6 | 1.29 | 0.91 |
| | 16 | 348 | 0.44-0.86 | 2.2 | 1.7 | 0.72 | 0.43 |
| 1-propanol + metilbutanoate | 17 | 333 | 0.21-0.26 | 1.9 | 1.8 | 2.34 | 0.99 |
| | 17 | 353 | 0.51-0.60 | 1.5 | 1.3 | 1.35 | 0.43 |
| 1-butanol + metilpropanoate | 20 | 348 | 0.22-0.83 | 2.4 | 1.3 | 0.7 | 1.4 |
| 1-butanol + metilbutanoate | 17 | 348 | 0.19-0.40 | 2.9 | 1.3 | 2.6 | 1.7 |
| | 17 | 368 | 0.46-0.79 | 2.6 | 1.0 | 0.9 | 0.7 |
| ethanol + ethyl acetate | 11 | 328 | 0.44-0.54 | 2.5 | 1.7 | 2.1 | 0.6 |
| 1-propanol + ethyl acetate | 12 | 328 | 0.23-0.46 | 5.9 | 1.5 | 3.4 | 0.5 |
| 1-butanol + butyl acetate | 7 | 323-328 | 0.22 | 0.96 | 1.5 | 0.7 | 0.6 |
| Average errors | | | | 2.6 | 1.6 | 1.6 | 0.8 |

It should be mentioned that as an alternative it was considered that no hydrogen bonding between esters and alcohols existed. That is, the alcohols-esters mixtures were considered to have only the OH self-associating group. It was verified that to have the same level of accuracy of the cross-

associating model it was necessary to use temperature dependent parameters between the attractive CH_2OH and CH_2COO groups: $k_{ij}^* = 0.910$; $k_{ij}^{\dagger} = -0.278$; $\alpha_{ij} = -10.307$; $\alpha_{ij} = -16.045$.

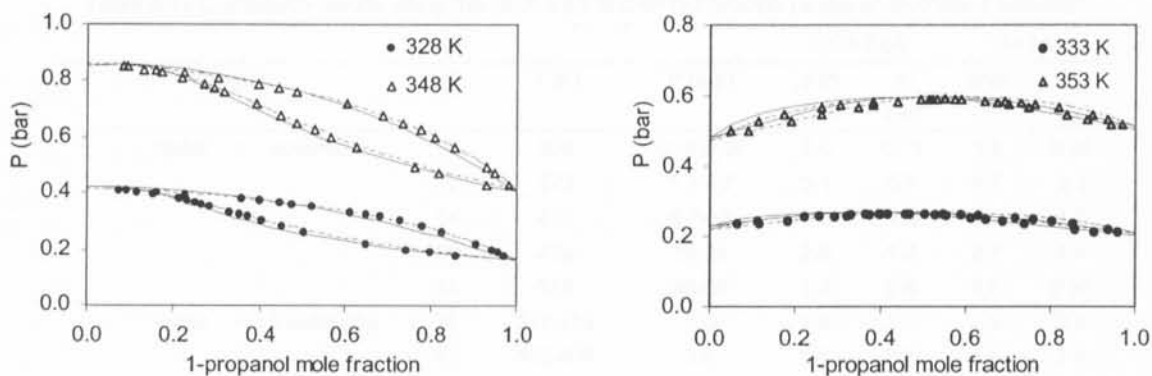


Figure 6.16 VLE of an alcohol and an ester: (a) 1-propanol and methyl propanoate; (b) 1-propanol and methyl butanoate. Exp. data (Gmehling *et al.*, 1977); — GCA-EoS correlation; - - -MHV2 prediction.

For the water/ester groups no additional parameters were estimated. Figure 6.17 shows two examples of the GCA-EoS predictions for these systems.

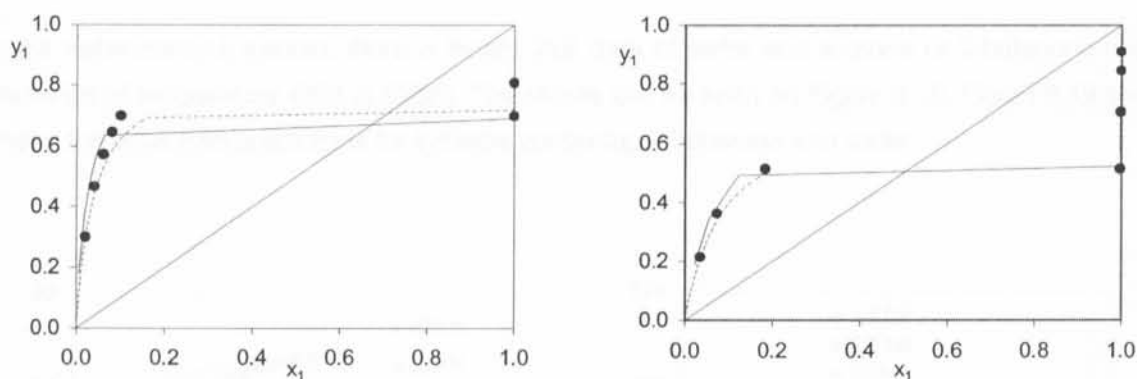


Figure 6.17 VLE of an ester and water (vapor phase mole fraction versus liquid phase mole fraction): (a) butyl acetate (1) and water (2) at 317 K; (b) water (1) and propyl acetate (2) at 353 K. Exp. data (Gmehling *et al.*, 1977); — GCA-EoS prediction; - - -MHV2 prediction.

6.3.6.5 Cross-associating mixtures with groups OH and RCOR

The cross-association parameters between the hydroxyl associating group (representing water and alcohols) and the ketone associating group were calculated using binary VLE for systems containing either water and ketones or alcohols and ketones. Again, as a first estimate for the cross-association parameters, the values for the energy and volume of association for the hydroxyl group were used.

An attractive interaction parameter between groups CH_3CO and CH_2OH was estimated, using binary VLE data of primary alcohols and ketones (acetone and 2-butanone).

Table 6.15 presents the correlation results obtained. Similar results are reached using both models.

Table 6.15 Correlation results using the GCA-EoS and MHV2 models (water or alcohols + ketones).

| System | NP | T (K) | P (bar) | GCA-EoS | | MHV2 | |
|--------------------------|----|---------|-----------|------------------|----------------|------------------|----------------|
| | | | | $\delta P/P$ (%) | δy (%) | $\delta P/P$ (%) | δy (%) |
| water + acetone | 19 | 308 | 0.18-0.46 | 1.0 | 0.71 | 1.5 | 0.86 |
| | 22 | 373 | 1.1-3.7 | 3.1 | 0.8 | 4.7 | 2.0 |
| | 14 | 423 | 6.7-12 | 3.5 | 1.9 | 3.1 | 1.8 |
| | 25 | 473 | 16-28 | 2.9 | 1.3 | 2.7 | 1.4 |
| | 14 | 523 | 40-68 | 1.3 | 0.6 | 0.8 | 0.90 |
| water + 2-butanone | 25 | 347-373 | 1.0 | 1.8 | 1.5 | 2.9 | 2.6 |
| | 19 | 385-406 | 3.4 | 5.0 | 3.5 | 3.6 | 2.5 |
| | 18 | 412-435 | 6.9 | 4.7 | 3.2 | 3.4 | 2.5 |
| | 18 | 453-474 | 17 | 3.9 | 1.8 | 3.0 | 1.2 |
| ethanol + acetone | 4 | 331-342 | 1.0 | 1.7 | 2.5 | 1.3 | 1.8 |
| ethanol + 2-butanone | 5 | 328 | 0.44-0.50 | 3.2 | 1.6 | 1.7 | 1.3 |
| | 5 | 348-350 | 1.0 | 1.1 | 1.6 | 2.1 | 1.3 |
| 1-propanol + 2-butanone | 15 | 353-368 | 1.0 | 1.7 | 0.8 | 1.3 | 0.7 |
| 3-pentanone + 2-propanol | 23 | 355-373 | 1.0 | 1.4 | 1.5 | 2.3 | 1.1 |
| Average errors | | | | 2.7 | 1.6 | 2.7 | 1.6 |

For the water-acetone system, there is binary VLE data of water and acetone or 2-butanone over a wide range of temperature (303 to 523K). The results can be seen on Figure 6.18. Figure 6.19 shows some of the GCA-EoS predictions for systems containing 2-butanone and water.

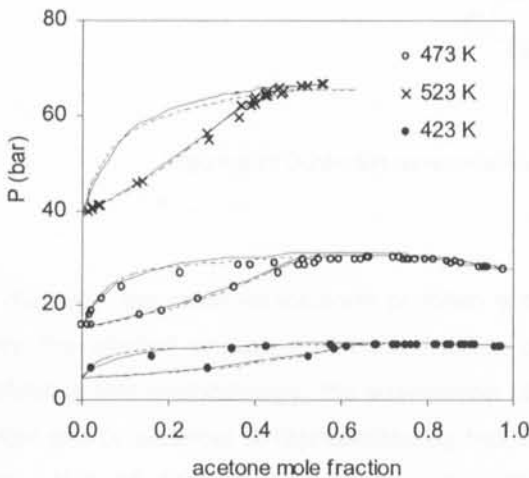


Figure 6.18 VLE of water and acetone: exp. data (Griswold and Wong, 1952); — GCA-EoS correlation; - - - MHV2 prediction.

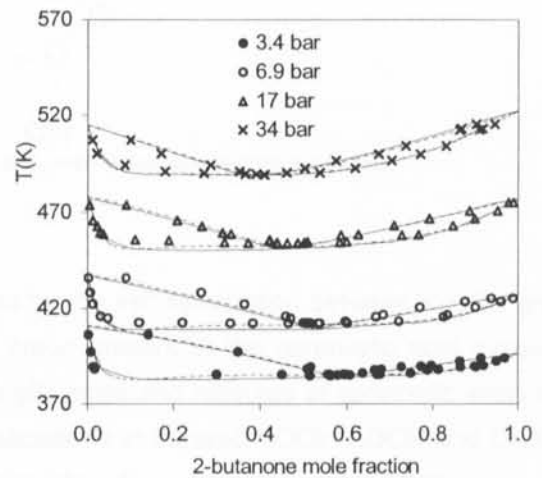


Figure 6.19 VLE of 2-butanone and water: exp. data (Othmer *et al.*, 1952b); — GCA-EoS prediction; - - - MHV2 prediction.

6.3.6.6 Interaction between groups COOH and CO₂

The interaction between the acid group and carbon dioxide was calculated using binary VLE data of CO₂ and acetic acid or butanoic acid. Figure 6.20 shows the satisfactory correlation results obtained. For the MHV2 model, no parameters are reported in the literature for these systems.

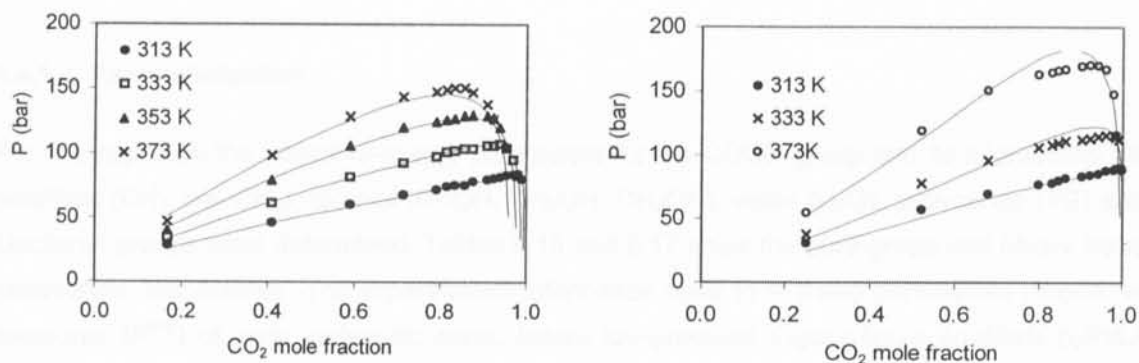


Figure 6.20 VLE of carbon dioxide and a carboxylic acid: (a) CO₂ and acetic acid; (b) CO₂ and butanoic acid. Exp. Data (Byun *et al.*, 2000); — GCA-EoS correlation.

6.4 Approximated approach

In this section, a different empirical approach is proposed to evaluate cross-association between the acid and the hydroxyl associating groups. From the point of view of association, each carboxylic acid molecule is considered to have two associating groups: one COOH group which self-associates through a double hydrogen bonding, and a certain fraction of OH group that has a remnant association capacity and can self-associate with another OH group (Figure 6.21).

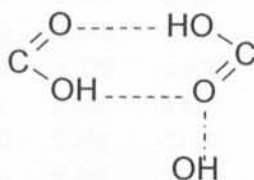


Figure 6.21 Schematic representation of self- and cross-association in carboxylic acids.

In this way, the cross-association problem is replaced by the self-association between the OH group from the alcohol or water, and the fraction of OH group present in the carboxylic acid molecule. Following this methodology, the association of carboxylic acids and mixtures of carboxylic acids with water and/or alcohols is represented by two self-associations in parallel: COOH/COOH and OH/OH. The value of each self-association strength is calculated from the respective COOH and OH association parameters $\epsilon/k^{\text{COOH}} = 6500 \text{ K}$ and $\kappa^{\text{COOH}} = 0.015 \text{ cm}^3/\text{mol}$, respectively. The fraction of associating OH group provided by the carboxylic acid molecules was empirically determined by fitting

vapour-liquid equilibrium (VLE) data for binary mixtures of acids with water or alcohols. A fraction of OH group equal to 0.25 gave the best correlation for these data. The methodology proposed here has the additional advantage of solving the association problem using two explicit mathematical expressions for the fraction of non-bonded COOH and OH associating groups. This makes straightforward the application of the GCA-EoS model to multicomponent mixtures of carboxylic acids, water, alcohols and inert components.

6.4.1 Parameterization

For this approach the attractive-energy parameters for the COOH group and its interactions with the paraffinic (CH₃ and CH₂), alcohol (CHOH, CH₂OH, CH₃OH), water (H₂O), triglyceride (TG) and CO₂ functional groups were determined. Tables 6.16 and 6.17 show the pure-group and binary interaction parameters, respectively. The experimental information used to fit these parameters include: vapour pressures (P^{vap}) of pure carboxylic acids; binary low-pressure vapour-liquid equilibria (LPVLE) for mixtures of carboxylic acids with alkanes, alcohols and water; high-pressure vapour-liquid equilibria (HPVLE) for binary mixtures of carboxylic acids with carbon dioxide; and infinite dilution activity coefficients (γ^∞) of alkanes in mixtures of triacetin with palmitic acid.

Table 6.16 Pure-group parameters

| Group | T* (K) | q | g* | g' | g'' | Experimental information |
|-------|--------|-------|-----------|---------|-----|------------------------------|
| COOH | 600 | 1.224 | 1211745.4 | -1.1105 | 0.0 | Pvap and LPVLE acids-alkanes |

Table 6.17 Binary interaction parameters

| i | j | k_{ij}^* | k_{ij}' | α_{ij} | α_{ji} | Experimental information |
|------|--------------------|------------|-----------|---------------|---------------|-----------------------------|
| COOH | CH ₃ | 0.932 | 0.0 | -2.946 | -2.424 | LPVLE acids-alkanes |
| | CH ₂ | 0.932 | 0.0 | -2.946 | -2.424 | LPVLE acids-alkanes |
| | CO ₂ | 0.892 | 0.0 | -2.370 | -2.370 | HPVLE acids-CO ₂ |
| | CHOH | 1.069 | 0.0 | 2.366 | -23.95 | LPVLE acids-alcohols |
| | CH ₂ OH | 1.096 | 0.0 | 2.366 | -23.95 | LPVLE acids-alcohols |
| | CH ₃ OH | 1.150 | 0.0 | 2.366 | -23.95 | LPVLE acids-alcohols |
| | H ₂ O | 1.140 | 0.0 | 18.66 | 4.000 | LPVLE acids-water |
| | TG | 1.062 | 0.0 | 0.0 | 0.0 | γ^∞ |

With this approach, and using a single set of parameters, satisfactory representation was obtained for pure component properties and phase equilibria in mixtures of carboxylic acids with inert compounds, alcohols and water at low and high pressures, with the same accuracy as with the rigorous approach.

6.5 Conclusions

Association effects were represented by a group-contribution approach. The GCA-EoS was extended to mixtures containing acids, esters and ketones, with water, alcohols and any number of inert components.

Two alternative approaches have been proposed to represent cross-association between the acid associating group and the hydroxyl associating group:

- In the first case, the cross-association parameters are calculated using the geometric mean of the self-association strengths as a combination rule.
- In the second case, an approximated solution was proposed where the cross-association problem was represented by two parallel self-association problems.

Both approaches result in good representation of pure component properties and phase equilibria for mixtures of carboxylic acids with inert compounds, alcohols and water at both low and high pressures.

Cross-association parameters between the ester (or ketone) associating group and either the acid or the hydroxyl associating groups were estimated using binary low-pressure vapour-liquid equilibria data. Again, very satisfactory results were obtained for these cross-associating mixtures.

The GCA-EoS model was compared to the group-contribution method MHV2, which does not take into account explicitly association effects. The results obtained with the GCA-EoS model are, in general, more accurate compared to the ones achieved by the MHV2 model with less number of parameters.

The group-contribution nature of the GCA-EoS allows its application to highly associated mixtures, for which experimental information is scarce or not available in all density range.

*Application of the GCA-EoS model to the
supercritical processing of fatty oil
derivatives*

7. Application of the GCA-EoS model to the supercritical processing of fatty oil derivatives

7.1 Introduction

The use of supercritical fluids as reaction media in the chemical processing industry has been well documented through the last few years (1997).

There being three sets of supercritical data available for the design process (i.e. critical temperature T_c) and their corresponding pressures (132, 311, and 311.3 bar), Chapter 7

Chapter 7

Application of the GCA-EoS model to the supercritical processing of fatty oil derivatives

In this work, the focus is on the modeling, respectively the design, of the supercritical processing. The use of the equation of state inside the design process of a supercritical process is considered and illustrated. The design of a supercritical process is illustrated by a case study. The design of a supercritical process is illustrated by a case study. The design of a supercritical process is illustrated by a case study.

7. Application of the GCA-EoS model to the supercritical processing of fatty oil derivatives

7.1 Introduction

The use of supercritical or quasi-critical fluids as solvents for numerous industrial processes has been well recognized (McHugh and Krukonis, 1994).

These fluids that are at a supercritical state (conditions over their critical pressure P_c and critical temperature T_c) or at near-critical conditions ($P > P_c$ and $0.9 T_c < T < T_c$) have special properties as solvents that lie between the ones from a liquid and a gas, namely, low viscosity, high density and high diffusion coefficient. At these states, the solvent strength can be readily adjustable by small changes in pressure or temperature.

Carbon dioxide is one of the most popular supercritical fluids as it has a low cost, it is non-toxic, not inflammable, has a low critical temperature and a moderate critical pressure. It is often used with co-solvents to enhance the solubility of high molecular components or polar solutes. Its low critical temperature allows its use with thermo-degradable substances.

In this work, the focus is on the possible applications for the fatty oils industrial processing. Some of the potential applications include the fractionation of a complex mixture of saturated and unsaturated triglycerides composed of fatty acids from butanoic acid to octadecanoic acids (butterfat) using carbon dioxide (Biernoth and Merk, 1985); recovery of monoglycerides and diglycerides from a mixture containing monoglycerides, diglycerides, and triglycerides using carbon dioxide as extractant and

propane or butane as co-solvents (Peter *et al.*, 1992); the purification of polyunsaturated fatty acids glycerides using carbon dioxide and a co-solvent like ethanol (Perrut *et al.*, 2001).

The design of extraction, fractionation and purification processes involving fatty oils and their derivatives, using near critical or supercritical fluids as solvents, requires the existence of thermodynamic models that are able to represent these highly complex mixtures that include high-molecular weight triglycerides and their derivatives with low-molecular weight solvents.

Usually, these natural products mixtures are described using cubic equations of state like the Peng-Robinson (Peng and Robinson, 1976) or Soave-Redlich-Kwong (Soave, 1972). Yu *et al.* (1993) used the Peng-Robinson EoS with the Panagiotopoulos and Reid mixing rules to correlate vapour-liquid equilibria (VLE) of ternary mixtures of CO₂ + methyl oleate + oleic acid. Two interaction parameters for each pair of components were estimated. De la Fuente *et al.* (1997) used the Soave-Redlich-Kwong EoS with quadratic mixing rules to correlate vapour-liquid and liquid-liquid equilibria (LLE) data for mixtures containing sunflower oil with ethane and propane. In order to predict the appearance of a liquid-liquid split, binary interaction parameters for both the attractive energy parameter and the co-volume were introduced. However, it was not possible to describe quantitatively both VLE and LLE using only one set of parameters for the co-volume, which indicated the limitations of the van der Waals repulsive term to describe these asymmetric mixtures. More recently, Araújo and Meireles (2000), used the Peng-Robinson EoS with the quadratic mixing rules coupled with several sets of combining rules (*e.g.* Kwak and Mansoori, 1986). As expected, two or three molecular interaction parameters had to be estimated for each pair of molecules, depending on the set of combining rules.

Due to the scarcity of experimental data available for this kind of systems, it is desirable to use a group-contribution method. Following this approach, Coniglio *et al.* (1996) applied several equation of state-excess Gibbs (or Helmholtz) function models (*e.g.* MHV1, LCVM) for the prediction of the fluid-liquid equilibria of CO₂ and fish oil esters and acids. New interactions between CO₂ and the corresponding UNIFAC groups were determined. Satisfactory results were obtained, except in the critical region.

Espinosa *et al.* (2000) extended the group-contribution equation of state to non-associating mixtures containing carbon dioxide with higher molecular components. The GC-EoS model was compared to the MHV2 and PSRK equations. All three models perform similarly for non-polar systems of low molecular weight and similar size. However, the MHV2 and PSRK models present some limitations when they are extended to very asymmetric mixtures. The Carnahan-Starling repulsive term of the GC-EoS allows a better description of these non-ideal mixtures. Later, Espinosa *et al.* (2002) apply the GC-EoS to describe the phase equilibria of the non-associating mixtures of triglycerides and fatty esters with near critical fluids.

Which should be the model used for the description of mixtures containing not only highly size-asymmetric mixtures but also, associating components?

The group-contribution with association equation of state (GCA-EoS) developed in Chapter 6 constitutes a good option. Relative to other group-contribution models, the GCA-EoS contains the Carnahan-Starling repulsive term to account for size differences and a specific association term to account for hydrogen bonding effects.

In the next sections, the chemical composition of these mixtures (section 7.1.1) and their phase behaviour (section 7.1.2) with the above-mentioned solvents is briefly described. Finally, on section 7.3, the GCA-EoS is applied to mixtures of fatty oils and their derivatives with supercritical solvents like propane or carbon dioxide.

7.1.1 Chemical composition

The main components of fatty oils are triglycerides and, in smaller quantities, free fatty acids and esters of glycerol (mono and di-glycerides). Their structure is shown on Figure 7.1.

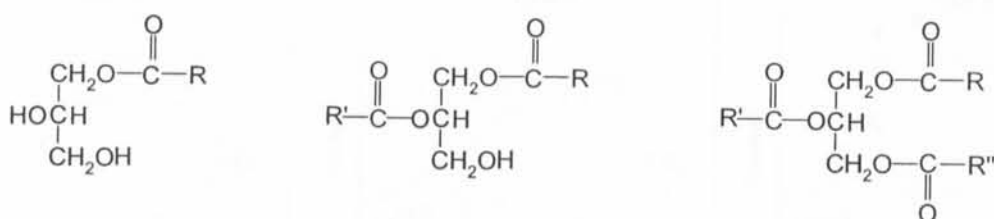


Figure 7.1 Mono-, di- and triglyceride schematic representation.

Usually, in nature, the fatty acids residues that compose these components have an even number of carbon atoms. The radicals R, R' and R'' are saturated or unsaturated aliphatic chains. The group-contribution approach makes possible to characterize, using a few number of functional groups, a large number of saturated and unsaturated oils and their derivatives.

Besides the aliphatic, ester, alcohol, acid groups, it was necessary to define a triglyceride (TG) group to characterize compounds derived from the triple esterification of glycerol. This is shown on Figure 7.2.

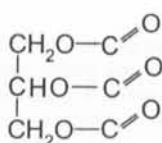


Figure 7.2 The triglyceride (TG) group.

From the association point of view, three groups can hydrogen bond: the ester, the alcohol and the acid group. Triglycerides are considered to have three esters associating groups.

7.1.2 Phase behaviour

At high pressures, these asymmetric systems present a complex multi-phase behaviour, difficult to model. Peters (1994) presented a review on the multiphase equilibria for systems containing near critical solvents (methane to butane and ethylene) and less volatile solutes, based on experimental results. Amongst the solutes studied are n-alkanes, triglycerides, n-carboxylic acids and n-alkanols.

The different possible types of phase behaviour are usually classified using six different diagrams, according to Van Konynenburg and Scott (1980). Figure 7.3 presents the pressure-temperature projections for these diagrams.

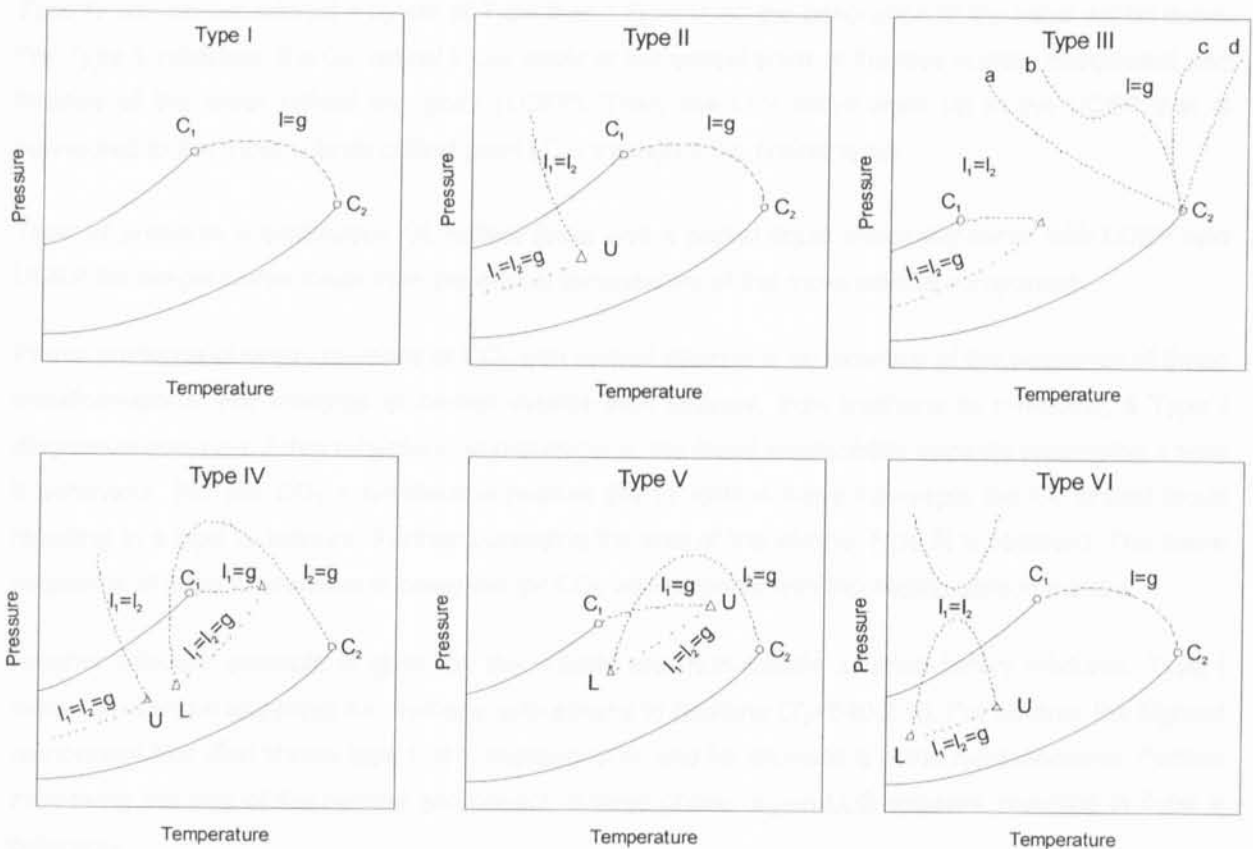


Figure 7.3 Pressure-temperature diagrams for the six types of phase behaviour obtained for binary systems (Van Konynenburg and Scott, 1980): g: vapour; l: liquid; U: upper critical end point; L: lower critical end point; dashed lines correspond to the critical locus, *i.e.*, curve that connects all the critical points where two phases converge to one phase; Full lines correspond to the pure components vapour pressure finishing at the pure component critical points C_1 and C_2 .

Type I diagram presents a continuous gas-liquid critical line representing all the critical points of the several mixtures where the liquid and vapour phases become identical. This is the behaviour expected for binary mixtures of components with a similar chemical nature and for which the critical properties are similar in magnitude.

If these components exhibit liquid-liquid immiscibility at a temperature lower than the critical temperature of the more volatile component a *Type II* diagram is obtained. The LL line extends to the upper critical end point (UCEP) where three phases are at equilibrium. The remaining LLG line represents the projections for all the liquid-liquid-gas curves.

If the immiscibility of these components is large enough to displace the LL critical locus to a higher temperature, greater than the critical temperature of the more volatile component, the liquid gas critical locus is intercepted and one obtains a *Type III* diagram. The a, b, c and d sequence of lines on this diagram corresponds to an increase in the differences components, *i.e.*, an increase of their immiscibility.

Type IV can be considered a hybrid of *Type II* and *Type V*, so the description of the latter will be done. For *Type V* mixtures, the GL critical locus starts at the critical point of the less volatile component and finishes at the lower critical end point (LCEP). Then, the LLV curve ends up at the UCEP that is connected to the more volatile critical point (C_1) through a GL critical locus.

Type VI presents a continuous GL critical locus and a partial liquid miscibility curve with LCEP and UCEP for temperatures lower than the critical temperature of the more volatile component.

Phase equilibria of binary mixtures of CO_2 with normal alkanes is an example of the sequence of these transformations. For mixtures of carbon dioxide with alkanes, from methane to n-hexane, a *Type I* diagram is obtained. From n-heptane to n-dodecane, the liquid immiscibility appears presenting a *type II* behaviour. For the CO_2 + n-tridecane mixture the LL critical locus intercepts the GL critical locus resulting in a *type IV* mixture. Further increasing the size of the alkane, *type III* is obtained. The same sequence of phase behaviour is observed for CO_2 with alcohols with increasing carbon number.

Another relevant example is given by the volatile and non-volatile alkanes binary mixtures. *Type I* behaviour can be expected for methane with ethane to heptane ($T_c=540.2$ K). For ethane, the highest component that also shows *type I*, is n-heptadecane, and for propane it is the n-nonacosane. Further increasing the size of the heavier component, a three phase region LLG appears, resulting in *Type V* behaviour.

As an example of the type of information that can be drawn from these diagrams, Figure 7.4 presents three projections (pressure *versus* composition) at three different temperatures T_1 , T_2 and T_3 derived from the *Type V* diagram. As can be seen near the critical point of the more volatile component, at temperature T_2 , a three phase liquid-liquid-vapour equilibrium exists.

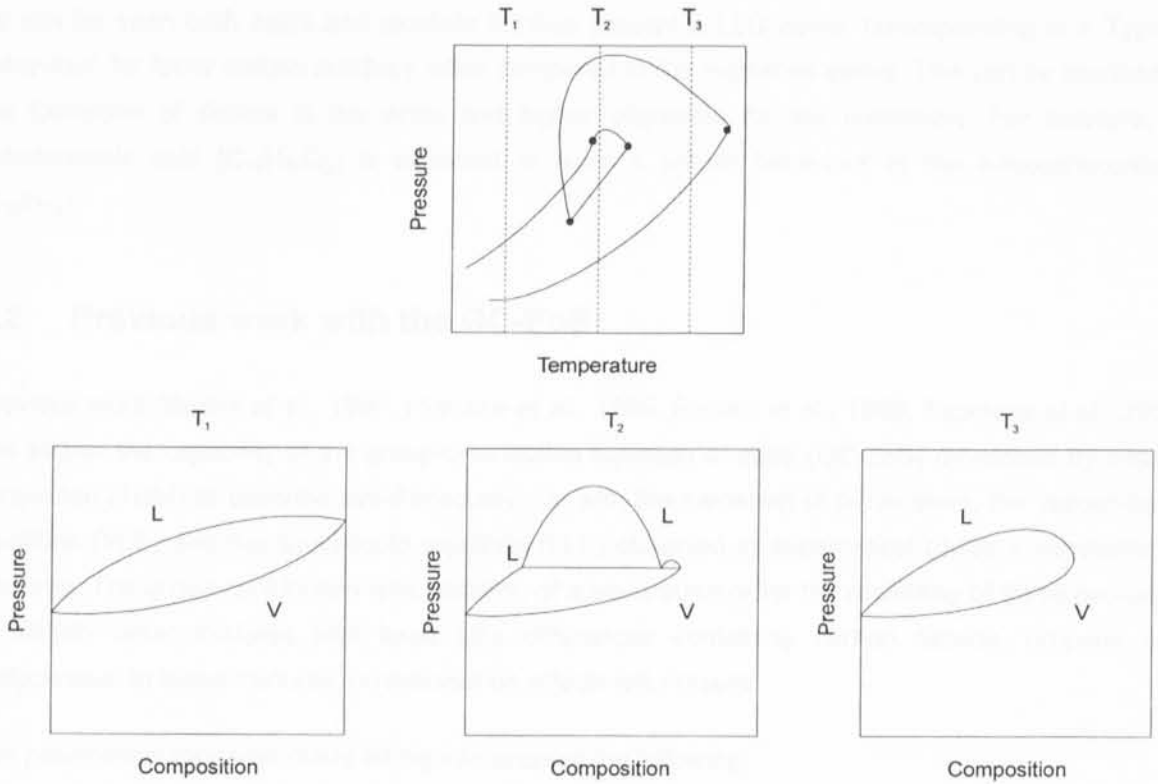


Figure 7.4 Pressure versus composition projections at three temperatures obtained from Type V diagram.

And what is the influence of the presence of functional groups like the alcohol or acid groups in the solute? Figure 7.5 compares the three phase behaviour LLG for n-alkanes, n-carboxylic acids and n-alkanols in propane, as a function of the carbon number.

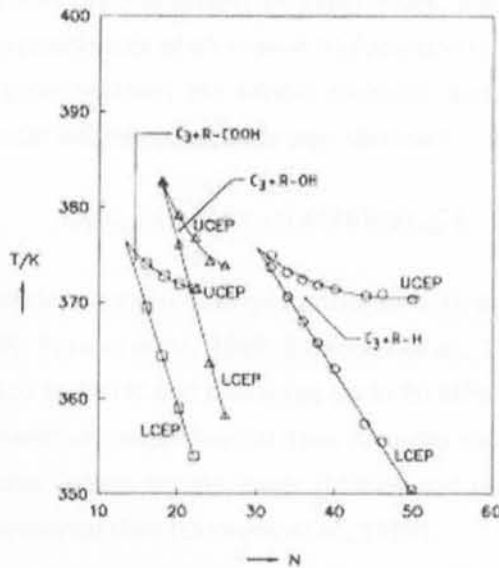


Figure 7.5 UCEP and LCEP for binary mixtures of propane with n-carboxylic acids, n-alkanols and n-alkanes (Source: Peters, 1994).

As can be seen both acids and alcohols families present a LLG curve, corresponding to a Type V behaviour, for lower carbon numbers when compared to the n-alkanes series. This can be ascribed to the formation of dimers in the acids and higher oligomers for the n-alkanols. For example, n-octadecanoic acid ($C_{18}H_{36}O_2$) is expected to have a similar behaviour to the n-hexatriacontane ($C_{36}H_{74}$).

7.2 Previous work with the GC-EoS

Previous work (Bottini *et al.*, 1999; Florusse *et al.*, 1999; Fornari *et al.*, 1999; Espinosa *et al.*, 2002) has shown the capability of the group-contribution equation of state (GC-EoS) developed by Skjold-Jorgensen (1984) to describe simultaneously, *i.e.* with the same set of parameters, the vapour-liquid equilibria (VLE) and the liquid-liquid equilibria (LLE) observed in supercritical gases + vegetable oil mixtures. The group-contribution with equation of state is suitable for the modelling of these non-polar or slightly polar mixtures with large size differences containing carbon dioxide, propane and triglycerides. In these mixtures, no association effects are present.

The parameterization was made taking into account the following:

- Pure group parameters for the TG group, and binary interaction parameters between this group and various non-associating groups functional groups.
- The repulsive molecular parameter (the critical hard sphere diameter, d_c) for the high molecular weight triglycerides was obtained from infinite dilution activity coefficient data of alkanes in these triglycerides, since critical properties or vapor pressure data cannot be used due the low volatility and thermal liability of triglycerides. Espinosa *et al.* (2002) have used infinite dilution activity coefficients of alkanes in triglycerides to estimate the critical diameter of the former. A correlation between the critical diameter and the van der Waals molecular volume of high molecular weight compounds was obtained:

$$\log(d_c) = 0.4152 + 0.4128 \log(r_{vdw}) \quad (7.1)$$

More than 10 different triglyceride + supercritical gas mixtures were satisfactorily predicted (Bottini *et al.*, 1999; Florusse *et al.*, 1999; Fornari *et al.*, 1999; Espinosa *et al.*, 2002) using the GC-EoS model, covering temperatures from 300 to 450 K and pressures up to 30 MPa. Figures 7.6 and 7.7 show that predictions are in good agreement with experimental data. Also, the model can predict the three phase LLV equilibrium with reasonable values for the lower (LCEP) and upper critical end point (UCEP), when compared with the experimental data (Coorens *et al.*, 1988).

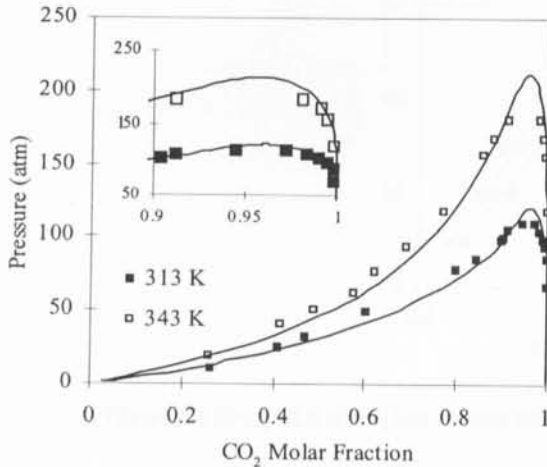


Figure 7.6 VLE of CO₂ and methylpalmitate: exp. (Inomata *et al.*, 1989); — GC-EoS predictions.

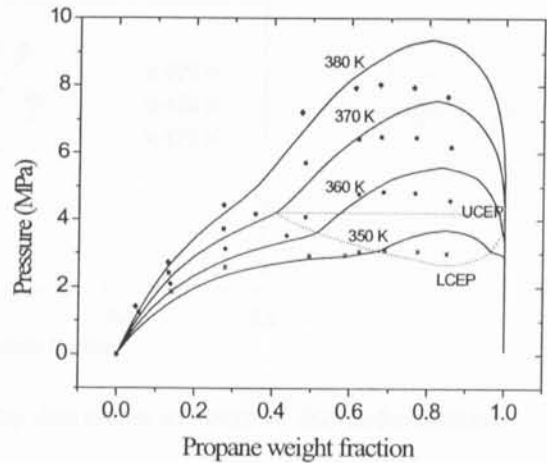


Figure 7.7 VLE and LLE predictions using the GC-EoS for propane + tripalmitin mixture. Exp. (Coorens *et al.*, 1988).

What happens if polar components that are capable to hydrogen bond are added to these mixtures?

The purpose of this chapter is to extend the GCA-EoS model, developed in chapter 6, to represent high pressure phase equilibria in mixtures of supercritical gases (carbon dioxide and propane) with fatty oil derivatives, such as mono- and diglycerides and fatty acids. Self- and cross-association between the associating groups present in these mixtures are considered through the association term.

7.3 Predictions using the GCA-EoS

The parameters obtained previously (Chapter 6) are now used to predict the behaviour of high pressure mixtures containing fatty oils and derivatives with solvents like propane and carbon dioxide. The parameters have been presented in Tables 6.5, 6.6 and 6.7. Additionally, it was necessary to estimate the interaction parameters between the acid and the triglyceride groups that are not available in the GCA-EoS parameters table. As the experimental information is scarce for these systems, infinite dilution activity coefficients were measured in order to fit those interaction parameters. The experimental data obtained and the correspondent parameterization are described in Chapter 8.

7.3.1 Binary systems of CO₂ and fatty acids

Figures 7.8 to 7.11 show some of the GCA-EoS predictions for the solubility of CO₂ in several fatty acids. Good results are obtained for the solubilities of carbon dioxide in the saturated fatty acids (Figures 7.8 and 7.9). Figure 7.10 shows the model predictions for the unsaturated oleic acid for which a qualitative agreement is obtained for the CO₂ solubility with temperature.

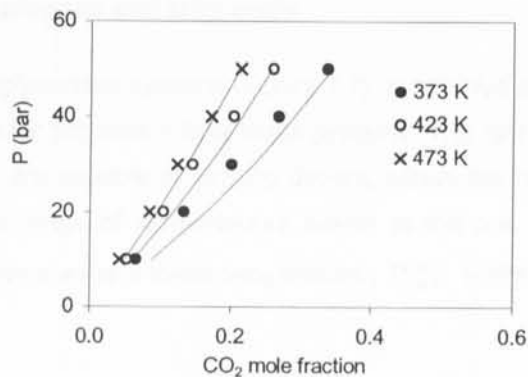


Figure 7.8 Binary VLE of CO₂ and palmitic acid: Exp. data (Yau *et al.*, 1992); — GCA-EoS predictions.

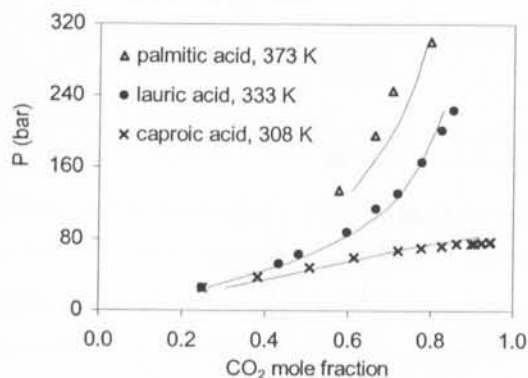


Figure 7.9 Binary VLE of CO₂ and fatty acids. Exp. data: Δ \bullet (Bharath *et al.*, 1993); \times (Byun *et al.*, 2000). Model: — GCA-EoS prediction.

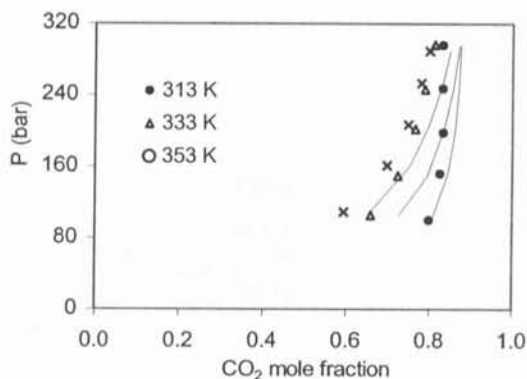


Figure 7.10 Binary VLE of CO₂ and oleic acid: exp. (Bharath *et al.*, 1992); — GCA-EoS prediction.

The model is also able to qualitatively distinguish between the oleic acid (9-octadecenoic acid) and linoleic acid (9,12-octadecadienoic acid), as can be seen from Figure 7.11.

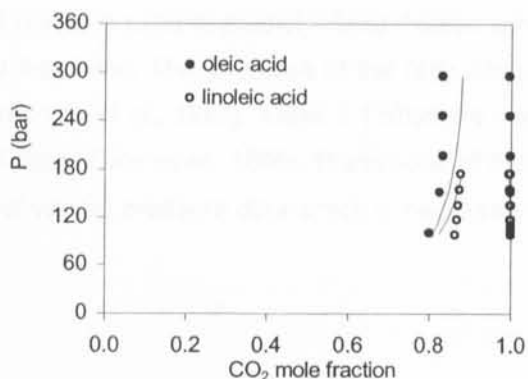


Figure 7.11 Binary VLE of CO₂ and unsaturated fatty acids at 313.15 K. Exp. data: \bullet oleic acid (Bharath *et al.*, 1992); \circ linoleic acid (Chen *et al.*, 2000). Model: — GCA-EoS predictions.

7.3.2 Binary systems of propane and fatty acids

Similarly to the propane + triglycerides systems (Figure 7.7), the GCA-EoS model is able to predict the three phase LLV equilibrium for propane + fatty acids systems. The fact that association is taken into account, *i.e.*, that fatty acids are capable of forming dimers, allows the model to predict the existence of liquid-liquid equilibria in a range of temperatures similar to the one predicted for an alkane with double size. The LCEP is estimated at a lower temperature ($T_{LCEP}^{CALC} = 358K$) than the experimental one ($T_{LCEP}^{EXP} = 363K$).

It should be mentioned that all the parameters were estimated using vapour pressure data of n-carboxylic acids (from acetic to decanoic acid) and binary low pressure VLE data for small acids with alkanes (heptane and octane). And, for this, it is reasonable that the predictions at these high pressures are less accurate.

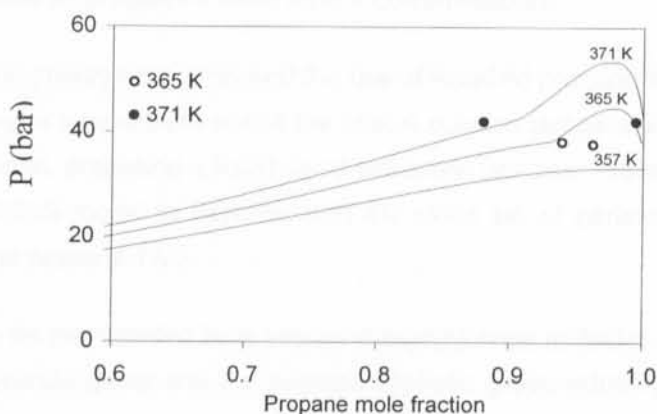


Figure 7.12 Binary VLE and LLE for propane and oleic acid. Exp. data (see Hixson and Bockelmann, 1942); — GCA-EoS predictions.

7.3.3 Infinite dilution activity coefficients

In this section, the GCA-EoS model is used to predict infinite dilution activity coefficients of alkanes in palmitic acid and mono- and dipalmitin. The d_c values of the fatty compounds were obtained from a vapour pressure data point (Formo *et al.*, 1982). Table 7.1 shows a comparison between the model predictions and experimental data (Foco *et al.*, 1996). Predictions of the model are quite satisfactory, taking into account the lack of vapour pressure data which is necessary to estimate the d_c value for the fatty oil derivatives.

Table 7.1 Infinite dilution activity coefficients of heptane and ethyl acetate in palmitic acid, mono-, di- and tripalmitin, a comparison between experimental data and model predictions.

| Solvents | T (K) | Solutes | | | | | |
|---------------|-------|---------|---------|-----------|---------------|---------|-----------|
| | | Heptane | | | Ethyl acetate | | |
| | | exp. | GCA-EoS | Error (%) | exp. | GCA-EoS | Error (%) |
| palmitic acid | 355 | 1.51 | 1.20 | 20 | 1.36 | 1.25 | 8 |
| | 366 | 1.54 | 1.21 | 21 | 1.32 | 1.23 | 7 |
| | 374 | 1.59 | 1.21 | 24 | 1.34 | 1.21 | 10 |
| monopalmitin | 355 | 2.07 | 1.72 | 17 | 1.33 | 1.17 | 12 |
| | 365 | 2.02 | 1.68 | 17 | 1.28 | 1.17 | 9 |
| | 375 | 2.02 | 1.64 | 19 | 1.15 | 1.18 | 3 |
| dipalmitin | 355 | 0.99 | 0.95 | 4 | 0.72 | 0.91 | 26 |
| | 365 | 0.96 | 0.91 | 5 | 0.69 | 0.87 | 27 |
| | 375 | 0.96 | 0.88 | 9 | 0.68 | 0.85 | 25 |
| tripalmitin | 351 | 0.61 | 0.63 | 3 | 1.23 | 1.37 | 11 |
| | 361 | 0.61 | 0.63 | 3 | 1.06 | 1.34 | 26 |
| | 368 | 0.61 | 0.63 | 3 | 1.11 | 1.31 | 18 |

7.3.4 Ternary systems of propane + oleic acid + cottonseed oil

Hixson and Bockelmann (1942) have proposed the use of liquefied propane to extract fatty acids from natural oils, by selecting a temperature above the critical solution temperature of the triglyceride and below that of the fatty acid, proposing a liquid-liquid extraction process. Previous work had shown the capabilities of the GC-EoS model to describe with the same set of parameters, the LLE and VLE observed in the systems propane-TAG.

The cottonseed oil can be represented by a pseudo-triacylglyceride molecule with the following group composition: one triglyceride group and the average aliphatic group values given on the last row of Table 7.2

Table 7.2 Glycerides composition (x_i) and correspondent aliphatic groups (n_{CH_2} and $n_{CH=CH}$) decomposition for cottonseed oil.

| Fatty acid | x_i | n_{CH_2} | $n_{CH=CH}$ |
|---------------|-------|------------|-------------|
| palmitic acid | 0.25 | 42 | 0 |
| oleic acid | 0.30 | 42 | 3 |
| linoleic acid | 0.45 | 36 | 6 |
| average value | | 39.3 | 3.60 |

After this, the correlation between the critical diameter and van der Waals molecular volume (given by equation 7.1) is used to estimate the critical diameter for this refined cottonseed oil. The following value is obtained: $d_c = 11.71$.

Figure 7.13 shows the satisfactory GCA-EoS predictions for this ternary system.

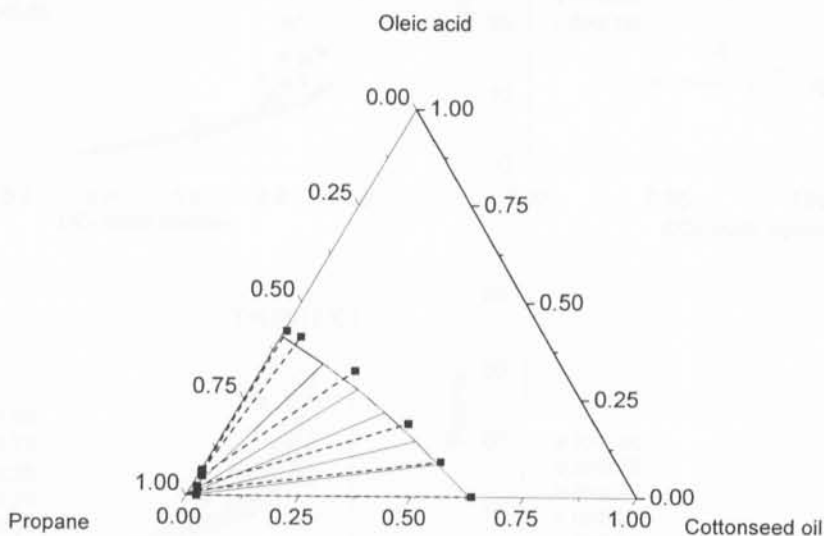


Figure 7.13 LLE of C_3H_8 -oleic acid-cottonseed oil at $T = 371.65$ K and $P = 44$ bar (compositions in weight fractions): —■— exp. (Hixson and Bockelmann, 1942); — GCA-EoS.

7.3.5 Ternary system of CO_2 + oleic acid + methyl oleate

Yu *et al.* (1993) have studied the fluid-liquid equilibria of the ternary system supercritical carbon dioxide with several mixtures of oleic acid and methyl oleate. Figure 7.14 shows the GCA-EoS predictions at the two temperatures for which data is available: 313 and 333 K.

As can be seen, the GCA-EoS predicts the sharp increase in the solubility for both components as carbon dioxide becomes supercritical: the solubilities for both components decrease with temperature (at constant pressure) and increase with pressure (at constant temperature). The model is also able to predict the higher solubility of the ester relatively to the acid at a given temperature and pressure. No additional parameters were estimated for this system. For pressures higher than 30 MPa, the GCA-EoS model predicts a curvature on the solubility of oleic acid which is not observed experimentally.

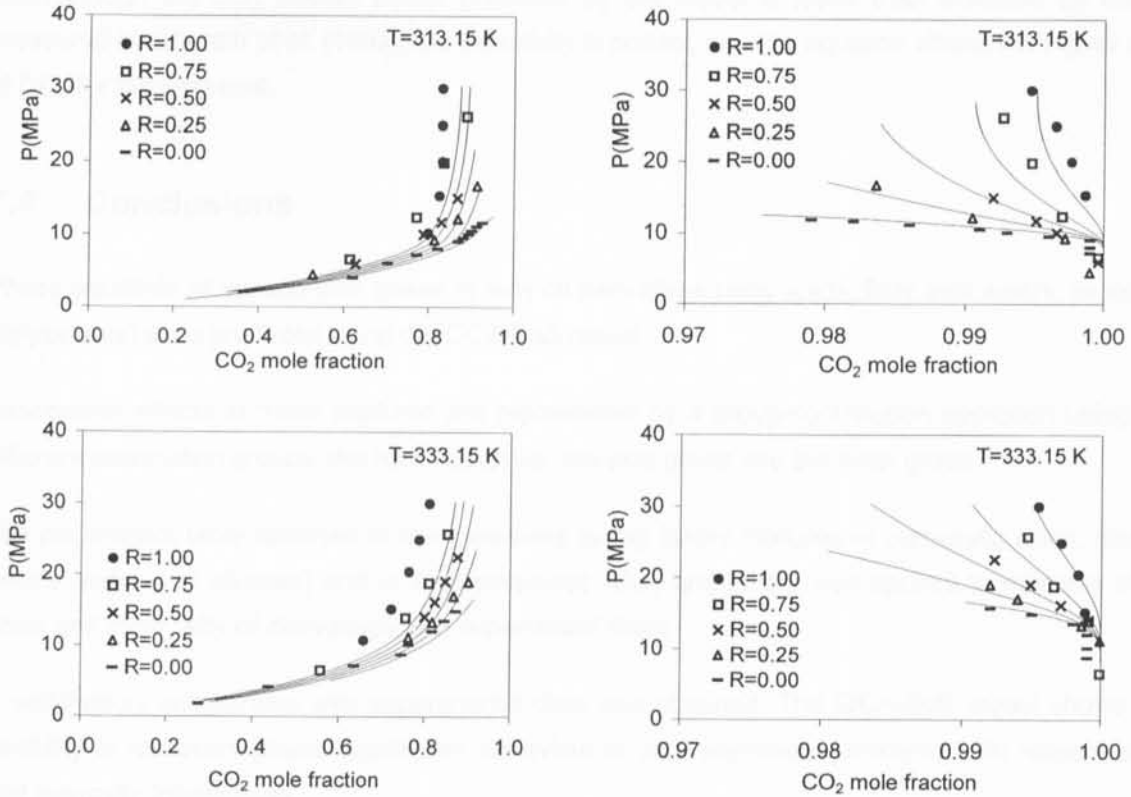


Figure 7.14 Vapour-liquid equilibria for the system CO_2 + methyl oleate + oleic acid for several mixtures with overall fixed mole fractions (R =oleic acid mole fraction on a CO_2 free basis). Exp. data: $\square \times \Delta$ (Yu *et al.*, 1993); $-$ (Inomata *et al.*, 1989); \bullet (Bharath *et al.*, 1992). Model: $-$ GCA-EoS predictions.

7.3.6 Ternary system of CO_2 +triolein+oleic acid

Carbon dioxide can be used as a solvent to remove fatty acids from oil mixtures. With this purpose, Bharath *et al.* (1992) measured data on the systems CO_2 , oleic acid and triolein (OOO), which are shown in Figure 7.15, together with the GCA-EoS predictions.

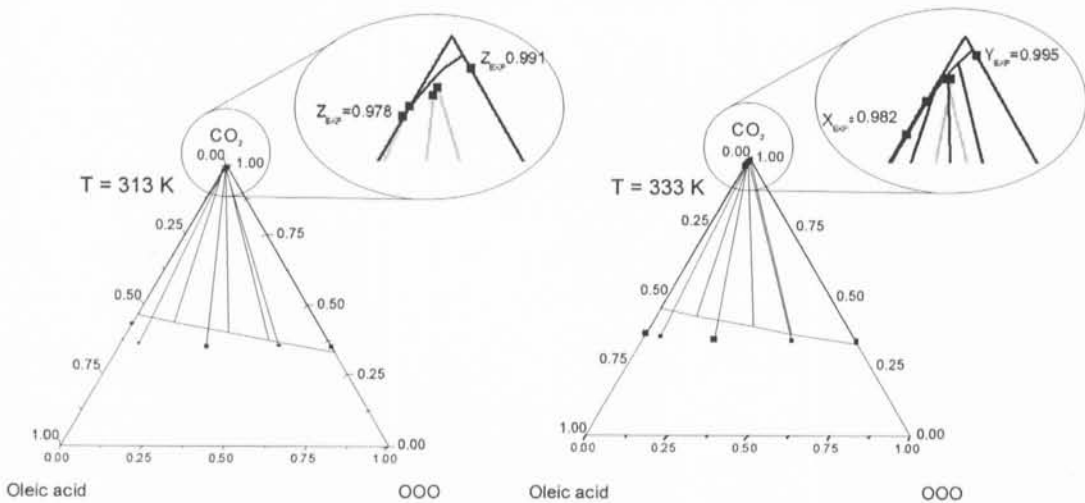


Figure 7.15 Ternary VLE of CO_2 , oleic acid and triolein at $P = 250$ bar: \blacksquare - exp. (Bharath *et al.*, 1992); $-$ GCA-EoS prediction.

Even though the CO₂ solvent power predicted by the model is lower than indicated by the data measured by Bharath *et al.* (1992), the selectivity is correct, *i.e.*, the equation shows the higher affinity of CO₂ for the fatty acid.

7.4 Conclusions

Phase equilibria of supercritical gases in fatty oil derivatives (fatty acids, fatty acid esters, mono- and diglycerides) were predicted using the GCA-EoS model.

Association effects in these mixtures are represented by a group-contribution approach using three different association groups: the hydroxyl group, the acid group and the ester group.

The parameters table obtained at low pressures (using binary mixtures of carboxylic acids, alcohols, esters, water and alkanes) and at high pressures (CO₂ and acids) was applied to mixtures of fatty acids and other fatty oil derivatives with supercritical fluids.

A satisfactory comparison with experimental data was obtained. The GCA-EoS model shows great flexibility to represent phase equilibrium behaviour in very asymmetric mixtures with respect to size and energetic interactions.

It is shown that the GCA-EoS is a powerful engineering tool for the optimization and design of extraction and fractionation processes of fatty oil derivatives with supercritical fluids.

Chapter 8
Infinite dilution activity coefficients of
solvents in fatty oil derivatives

8. Infinite dilution activity coefficients of solvents in fatty oil derivatives

8.1 Introduction

The design and synthesis of separation processes require the knowledge of the activity coefficients of solvents in various systems and several data require experimental information on thermodynamic properties of these systems and manufacturers (1-4).

This chapter presents information on activity coefficients, enthalpy and group contributions for the hydrocarbon-solvent and solvent-solvent systems of fatty oil derivatives.

Chapter 8

Infinite dilution activity coefficients of solvents in fatty oil derivatives

Keywords: activity coefficients; fatty oil derivatives; solvents

This chapter presents information on activity coefficients, enthalpy and group contributions for the hydrocarbon-solvent and solvent-solvent systems of fatty oil derivatives. The information is presented in the form of tables and graphs. The data are presented for the systems of fatty oil derivatives and solvents. The data are presented for the systems of fatty oil derivatives and solvents. The data are presented for the systems of fatty oil derivatives and solvents.

8. Infinite dilution activity coefficients of solvents in fatty oil derivatives

8.1 Introduction

The design and simulation of separation processes applied for the extraction and fractionation of fatty oil derivatives from vegetable and animal oils require experimental information on thermodynamic properties of fatty acids and triacylglycerides (TAGs).

That thermodynamic information is very useful to obtain molecular and group interaction parameters for the group-contribution with association equation of state GCA-EoS. In this model the functional groups characteristic of TAGs and fatty acids are, respectively, the triglyceride TG $((\text{CH}_2\text{COO})_2\text{-CHCOO})$ and acid (COOH) groups. The interaction parameters between the TG and COOH groups are not available in the GCA-EoS parameter table. Also, the interaction between TG and the primary (CH_2OH) and secondary (CHOH) alcohol groups are missing. The purpose of the experimental work carried out and presented in this chapter was to measure infinite dilution activity coefficients in order to fit those interaction parameters to the experimental data.

Foco *et al.* (1996) and Bermudez *et al.* (2000) measured infinite dilution activity coefficients (γ^∞) of a series of organic solutes in palmitic acid, tripalmitin and triacetin. These data were obtained by inverse gas chromatography, using the non volatile TAG or fatty acid as stationary phase and injecting the volatile solute at infinite dilution into the carrier gas stream.

The use of inverse gas chromatography to measure infinite dilution activity coefficients requires the solvent in the stationary phase to be a non-volatile compound, so that the amount of solvent in the stationary phase remains constant during the measurements. On the other hand, the solutes injected into the gas carrier should give sharp and neat chromatograms. Solutes of low volatility and/or highly retained in the stationary phase will give broad chromatographic peaks. In this case the values of the retention times, and consequently the calculated γ^∞ , would be uncertain.

All TAGs are low volatile compounds and can always be used as solvents in a chromatographic stationary phase. Even the first member of the family, triacetin, has negligible vapour pressures at temperatures up to 353 K ($P^{\text{vap}} = 42$ Pa). Unfortunately, carboxylic acids are highly retained in TAGs stationary phases; this makes inverse gas chromatography an unsuitable technique to measure γ^∞ of carboxylic acids in TAGs.

In order to obtain experimental information to fit the GCA-EoS interaction parameters between TG and COOH groups, an alternative procedure was followed in this work. Stationary phases were prepared using mixtures of TAGs with high molecular weight non volatile fatty acids. The γ^∞ of volatile solutes in these mixtures were measured. With these values and the corresponding γ^∞ of the same solutes in each pure solvent (TAG and fatty acid) it was possible to quantify the interaction between TG and COOH. Mixtures of palmitic acid with two different TAGs (triacetin and tripalmitin) were prepared, and the γ^∞ of a series of organic solutes in these mixtures have been measured.

8.2 Experimental technique

In this section a brief description of the experimental technique is presented.

8.2.1 Equipment

A Varian (Model Star 3400 C_x) gas chromatograph with a FID detector and a Hewlett-Packard integrator (model 3392) were used in the measurements. The column temperatures were measured by Platinum Resistance Thermometers (Systemtechnik S-1220) and the thermal stability was ± 0.1 K.

The pressure drop inside the column (with magnitude 200 - 300 mbar) was read with a cathetometer from a U-tube manometer with a resolution of ± 0.13 mbar. The column outlet pressure was measured with a quartz transducer (Paroscientific) with a resolution of ± 0.1 mbar. Hamilton gastight syringes, 1 μl capacity were used to inject the solutes into the carrier gas stream. The retention times were measured with resolution ± 0.12 s.

8.2.2 Stationary and Mobile Phases

The stationary phase of each column was prepared by dissolving in chloroform known masses of two solvents (triacetin/palmitic acid or tripalmitin/palmitic acid) and of an inert support (Chromosorb W 60/80 mesh), in a ratio of 3 parts of chromosorb per part of solvent. The chromosorb was slowly evaporated in a roto-evaporator (Heidolph) at 30 °C, in an inert atmosphere. The solvent mass in the column was measured with resolution ± 0.002 g. Stainless steel columns of 2 m length with 1/8 in outer diameter, filled with known masses of stationary phase (about 2/3 g), were used.

The carrier gas was hydrogen, with a flow rate of about 35 cm³/min, measured with a soap film meter with resolution ± 0.7 cm³/min. Methane was used as a tracer in order to obtain the reference retention volume and was injected together with each one of the solutes. To ascertain the stability of experimental conditions, during the experiments hexane was injected and the respective retention time was controlled.

8.2.3 Chemicals

Triacetin, tripalmitin, palmitic acid, hexane, hexene, 1,2-dichloroethane, trichloroethylene, anisole and ethylbenzene were purchased from Aldrich Chemical Co. Benzene, toluene, methanol, ethanol, 1-propanol, 2-propanol, 1-butanol, 2-butanol and chloroform were obtained from Dorwill, Heptane, ethyl acetate from Mallinkrodt and isooctane, cyclohexane from Sintorgan. All chemicals had a 99% purity. They were used without further purification.

8.3 Experimental data

The specific retention volume V_g^o , that is, the normalized carrier gas volume necessary to elute solute *i* from a column containing a known mass of solvent w_s at 273.15K, can be related to the retention time of solute t_i by the expression:

$$V_g^o = (t_i - t_a)F \frac{273.15}{T_f} \frac{P_f - P_w^s}{P_o} \frac{J_3^2}{w_s} \quad (8.1)$$

where t_a is the inert gas retention time; F is the saturated gas flow measured at temperature T_f and pressure P_f , P_w^s is the vapour pressure of water at T_f , P_o is the column outlet pressure and J_3^2 the James Martin correction factor for pressure gradient and gas compressibility inside the column (Conder and Young, 1979).

The infinite dilution activity coefficient of solute *i*, (γ_i^∞) is calculated from the solute retention volume using the following equation:

$$\ln(\gamma_i^\infty) = \ln\left(\frac{273.15 R}{M_w P_i^S V_g^0}\right) - \frac{B_{ii} - v_i P_i^S}{RT} \quad (8.2)$$

In this equation, the gas phase non idealities are taken into account using the virial equation; B_{ii} is the second virial coefficient, v_i the molar volume and P_i^S the saturation pressure of component i at temperature T ; M_w is the molecular weight of the solvent and R is the universal gas constant.

Infinite dilution activity coefficients γ^∞ were measured for a series of organic solutes infinitely diluted in the following mixtures:

- mixtures of palmitic acid (PA) with triacetin (AAA) with mole fractions: 0.70 PA + 0.30 AAA and 0.50 PA + 0.50 AAA, at 353 K;
- mixtures of palmitic acid (PA) with tripalmitin (PPP) with mole fractions: 0.77 PA + 0.23 PPP, 0.50 PA + 0.50 PPP, at three different temperatures (353 K, 363 K and 373 K).

An overall uncertainty of 3 to 5% is estimated for the measured γ^∞ values reported in Appendix C (Tables C.1 to C.4).

Figure 8.1 represents the experimental γ^∞ of isooctane in mixtures of PA + AAA and PA + PPP, as a function of the molar fraction of palmitic acid in the mixtures. The limiting values of γ^∞ in the pure solvents (palmitic acid, triacetin and tripalmitin) are also shown. It is interesting to notice the high γ^∞ value of isooctane in pure triacetin ($M_w = 218$ g/mol), the first member of the family of triglycerides. This indicates important energy interactions between the TG and paraffinic (CH_2/CH_3) functional groups, which are responsible for the partial liquid miscibility found in isooctane – triacetin mixtures. The effect of this strong interaction vanishes in the case of tripalmitin ($M_w = 806$ g/mol), due to the TAG long hydrocarbon chains. Here the combinatorial effects are predominant, and the γ^∞ values of isooctane in tripalmitin are lower than one. The addition of the long-chain palmitic acid to triacetin increases the combinatorial effects and dilutes the TG - CH_2 and $\text{COOH} - \text{CH}_2$ interactions; these combined effects lower drastically the γ^∞ values of isooctane. On the other hand, the addition of palmitic acid to PPP decreases the average molecular weight of the mixture and increases the energy interactions due to the presence of the COOH group in the mixture; this gives rise to higher γ^∞ values.

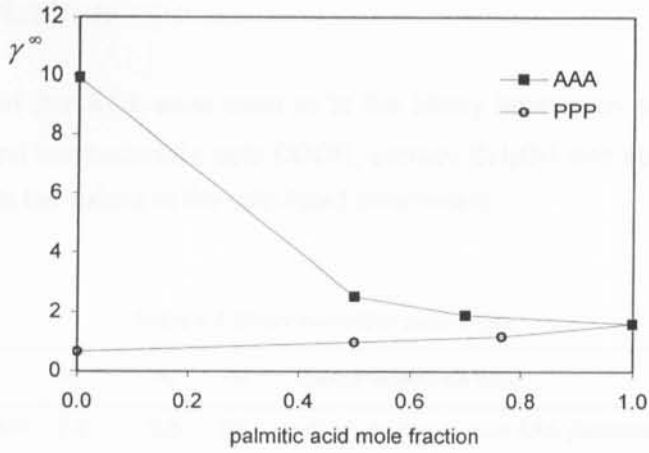


Figure 8.1 Representation of γ^∞ of isooctane versus the molar fraction of palmitic acid at 353.15K: ■ ○ experimental data.

In the narrow range of temperatures covered in this work, no temperature dependence of γ^∞ was observed, with the exception of the alcohol's series. The γ^∞ of these compounds decrease with temperature, which indicates positive partial excess enthalpies in fatty acids and TAGs solutions. Figure 8.2 shows the γ^∞ of heptane, ethanol and trichloroethylene in an equimolar solution of palmitic acid and tripalmitin, at the three temperatures measured in this work.

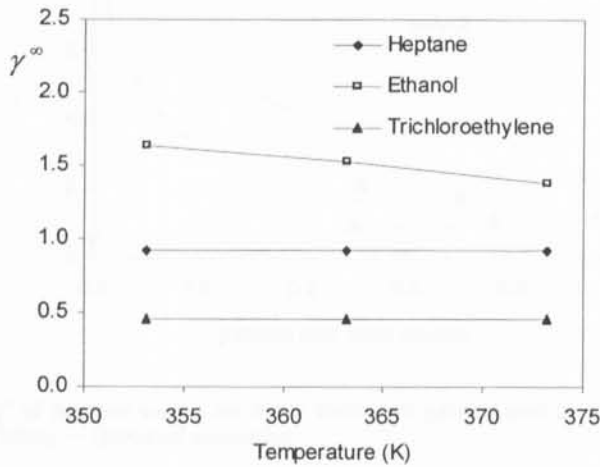


Figure 8.2 Temperature dependence of γ^∞ for heptane, ethanol and trichloroethylene in a mixture containing 50 % palmitic acid / 50 % tripalmitin.

8.4 Parameterization

The γ^∞ data obtained in this work were used to fit the binary interaction parameters between the triglyceride group TG and the carboxylic acid COOH, primary CH₂OH and secondary CHOH alcohol groups. Table 8.1 reports the values of the calculated parameters.

Table 8.1 Binary interaction parameters

| <i>i</i> | <i>j</i> | k_{ij}^* | k_{ij}' | α_{ij} | α_{ji} | Experimental data used |
|----------|--------------------|------------|-----------|---------------|---------------|---|
| TG | CHOH | 1.443 | 0.0 | 0.0 | 0.0 | γ^∞ of alcohols in pure AAA (Bermudez <i>et al.</i> , 2000) |
| | CH ₂ OH | 1.191 | 0.0 | 0.0 | 0.0 | |
| | COOH | 1.072 | 0.0 | 0.0 | 0.0 | γ^∞ of alkanes in mixtures of AAA with PA (this work). |

Figures 8.3 and 8.4 show the values of infinite dilution activity coefficients of heptane in mixtures of palmitic acid and a TAG and the γ^∞ of alcohols in triacetin, respectively, calculated by the GCA-EoS model.

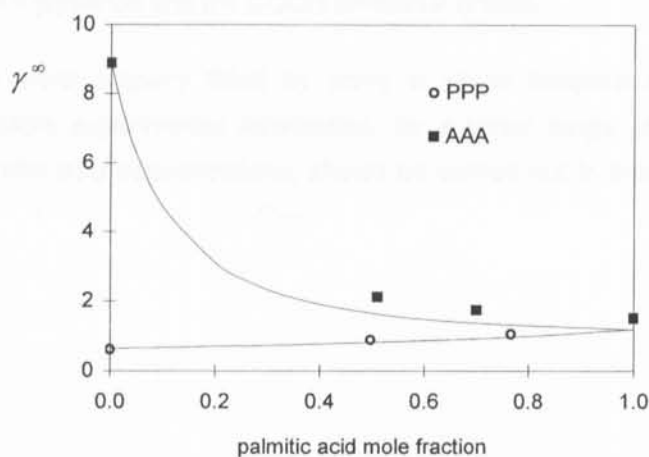


Figure 8.3 Representation of γ^∞ of heptane versus the molar fraction of palmitic acid at 353.15K: ■ ○ experimental data (Ferreira and Foco, 2003); — GCA-EoS correlation.

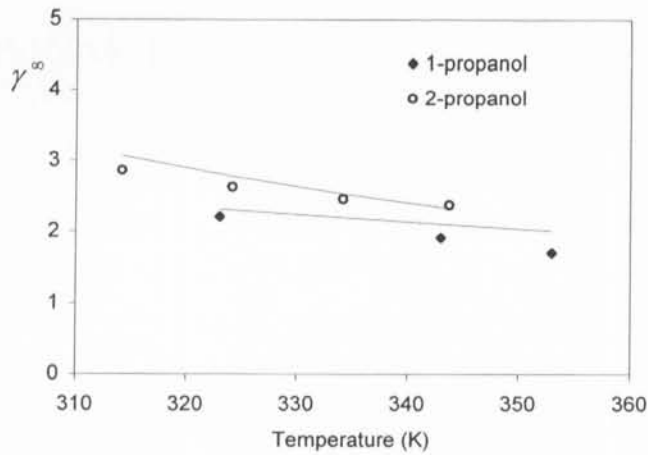


Figure 8.4 γ^∞ of alcohols in triacetin versus temperature: \blacklozenge \circ experimental data (Foco *et al.*, 2000); —GCA-EoS correlation.

8.5 Conclusions

In the experimental work proposed and presented in this chapter, γ^∞ of several components in mixtures of TAGs with palmitic acid were measured. The γ^∞ of alkanes were used to quantify the interactions between the triglyceride and the COOH functional groups.

The experimental data were properly fitted by using a single temperature independent binary interaction parameter. More experimental information, for a wider range of temperatures and for mixtures with lower palmitic acid concentrations, should be carried out in order to test the validity of these parameters.

Chapter 9

Conclusions and future work

Conclusions and future work

3.1 Conclusions

Several findings have been reported in the literature on model construction efforts for knowledge-based and expert systems shells and the performance issues. In some cases, it is possible to make a significant performance difference when different strategies are followed and those identified for the knowledge-based systems shells were found to be most effective. The importance of reducing complexity at this level was also indicated. It is suggested that both domain and user knowledge should be used to avoid the complexity associated with different groups and the quality of work.

Therefore, to make a more successful system, it is necessary to implement appropriate strategies to the reduction of the complexity of the knowledge-based systems. The use of the use of knowledge-based systems to support complex tasks is a well established practice. Chapter 9 describes a good model for knowledge-based systems, including a quality model, a task model,

Chapter 9

Conclusions and future work

The findings of this study have been discussed in the context of the knowledge-based systems shells. The findings indicate that the use of knowledge-based systems shells is a well established practice. The use of knowledge-based systems shells to support complex tasks is a well established practice. The use of knowledge-based systems shells to support complex tasks is a well established practice. The use of knowledge-based systems shells to support complex tasks is a well established practice.

Therefore, the findings of this study indicate that the use of knowledge-based systems shells to support complex tasks is a well established practice. The use of knowledge-based systems shells to support complex tasks is a well established practice.

9. Conclusions and future work

9.1 Conclusions

Several theories have been proposed in the literature to model association effects: the chemical theory, the quasi-chemical theory and the perturbation theory. In some cases, it is possible to make a numerical equivalence between them and to compare the different solutions obtained for the monomer fraction for some simple cases of self- and cross-association mixtures. The expressions for mixtures containing at most two cross-associating groups have been derived. It is possible to find one analytical solution, when there are at most two associating components with different groups plus any number of inerts.

Therefore, to follow a group-contribution approach presents a significant mathematical advantage in the extension of the model to mixtures containing several associating components, thanks to the use of associating groups to represent associating components. In this work association effects were described by a group-contribution approach, introducing a specific term in two models.

The A-UNIFAC model has been successfully applied to calculate activity coefficients in associating solutions containing water, alcohols, carboxylic acids, esters, alkanes, aromatic hydrocarbons and alkyl chlorides. Two alternative approaches have been proposed: an approximated one with simplified expressions for the monomer fraction and a lower number of parameters; and, the rigorous approach that consists in a more flexible model. Both methodologies result in great improvements in the more diluted range of compositions, where the non-ideality due to association is more pronounced.

However, the rigorous approach gives more accurate correlations and predictions for vapour-liquid equilibria and infinite dilution activity coefficients when compared to the original UNIFAC model.

The A-UNIFAC was successfully applied to mixtures of sugars with water and alcohols (from methanol to t-pentanol) by defining a single hydroxyl group to account for all association effects in these solutions. Water and alcohols have only one associating group and each sugar is considered to have a different concentration of that associating group. In this way, the model is able to distinguish between stereoisomers. Good correlation and prediction results are obtained in the description of solid-liquid equilibria (sugars solubility in water or alcohols and in mixed solvents, freezing point) and vapour-liquid equilibria (water activity, boiling point of aqueous solutions). Moreover, the model is able to accurately predict the phase behaviour for some multicomponent mixtures of industrial interest: SLE of D-xylose and D-mannose in water and in mixed solvents of water/ethanol; SLE and VLE of D-fructose, D-glucose and sucrose in water; water activity of a synthetic honey and of synthetic juices.

The need for a model that can be applied up to the critical region led to the extension of the group-contribution equation of state to mixtures containing several associating components.

The application of an equation of state to hydrogen-bonding mixtures motivated the appearance of new expressions to account specifically for association effects or the introduction of more flexible mixing rules. In general, a molecular approach is used which difficults the extension of these models to mixtures containing several associating components.

The group-contribution with association equation of state (GCA-EoS) was extended to mixtures containing acids, esters and ketones, with water, alcohols and any number of inert components. For the cross-association between acids and alcohols or water associating groups, two alternative approaches were proposed that resulted in satisfactory representation of pure component properties and phase equilibria for mixtures of carboxylic acids with inert compounds, alcohols and water at both low and high pressures. Very good results were also obtained in the correlation of cross-associating mixtures capable of forming dimers (esters, ketones). The GCA-EoS model is more accurate than the group-contribution method MHV2, which does not take into account explicitly association effects.

The flexibility of the GCA-EoS model was shown with the satisfactory prediction of phase equilibria of supercritical gases (propane and carbon dioxide) in fatty oil derivatives (fatty acids, fatty acid esters, mono- and diglycerides).

Infinite dilution activity coefficients measured by inverse gas chromatography are an important source of experimental data that can be used to quantify the interactions between heavy compounds (in this work, triglycerides or fatty acids) and different light solutes. The experimental data obtained in this work were used to determine binary interaction parameters for the GCA-EoS.

These results demonstrate that the GCA-EoS is a powerful engineering tool for the optimization and design of extraction and fractionation processes of fatty oil derivatives with supercritical fluids.

9.2 Future work

The models developed in this work have shown the possibility of using a group-contribution approach to represent association effects in mixtures containing water, alcohols, carboxylic acids, esters, ketones, aromatic compounds, alkyl chlorides and any number of inerts.

The first task that immediately arises is the extension of the parameter tables of the A-UNIFAC and GCA-EoS to a larger number of functional groups. In terms of associating molecules, amines, ethers, glycols, assume particular importance. When present, proximity and isomeric effects between molecules should also be taken into account.

In parallel to the modelling work, experimental data measurements should be carried out particularly for the natural products mixtures studied here. The data will be used to extend the applicability of the GCA-EoS and A-UNIFAC models.

These models can be applied in several other areas besides the case studies presented in this work. For example, an important application is the environmental area where very often the components to be removed are infinitely diluted and association effects are more pronounced.

In the growing field of green chemistry the use of supercritical reactors and separation processes is an area of work with great interest. The models developed in this thesis can be applied for the phase equilibrium engineering analysis of hydrogenation, hydrogenolysis, oxidation, hydroformylation and many other gas-liquid processes, as well as the application of non-contaminant solvents in the processing of natural products

In the area of product and molecular design the availability of more reliable predictions of infinite dilution activity coefficients is of great interest in the development of Computer Aided Molecular Design software for the identification of non-contaminant solvents.

As a major development of these models it is also possible to suggest the extension of this group-contribution association term to model phase behaviour of associating polymers and biomolecules.

References

References

- Abderafi, S., Bounahmidi, T., "Measurement and Modeling of Atmospheric Pressure Vapor-Liquid Equilibrium data for Binary, Ternary and Quaternary Mixtures of Sucrose, D-glucose, D-fructose and Water Components", *Fluid Phase Equilib.*, **93**, 337-351 (1994).
- Abed, Y., Gabas, N., Delia, M. L., Bounahmidi T., "Measurement of Liquid-Solid Phase Equilibrium in Ternary Systems of Water-Sucrose-Glucose and Water-Sucrose-Fructose, and Predictions with UNIFAC", *Fluid Phase Equilib.*, **73**, 175-184 (1992).
- Abrams, D.S., Prausnitz, J.M., "Statistical Thermodynamics of Liquid Mixtures: A New Expression for the Excess Gibbs Energy of Partly or Completely Miscible Systems", *AIChE J.* **21**, 116-128 (1975).
- Achard, C., Gros, J. B., Dussap, C.G., "Prédiction de l'activité de l'eau, des températures d'ébullition et de congélation de solutions aqueuses de sucres par un modèle UNIFAC", *Ind. Agric. Aliment.*, **109**, 93-101 (1992).
- Adachi, Y., Sugie, H. "A new mixing rule mixing rule-modified conventional mixing rule", *Fluid Phase Equilib.*, **28**, 103-118 (1986).
- Anderko, A., "Extension of the AEOs model to systems containing any number of associating and inert components", *Fluid Phase Equilib.*, **50**, 21-52 (1989).
- Araújo, M.E., Meireles, M.A., "Improving phase equilibrium calculations with the Peng Robinson EoS for fats and oils related compounds/supercritical CO₂ systems", *Fluid Phase Equilib.*, **169**, 49-64 (2000).
- Bastos, J.C, Soares, M.E., Medina, A.G., "Infinite dilution Activity Coefficients Predicted by UNIFAC Group-contribution", *Ind. Eng. Chem. Res.*, **27**, 1269-1277 (1988).
- Bergmann, D.L., Eckert, C.A., "Measurement of limiting activity coefficients for aqueous systems by differential ebulliometry", *Fluid Phase Equilib.*, **63**, 141-150 (1991).
- Bermudez, A., Foco, G., Bottini, S. B., "Infinite Dilution Activity Coefficients in Tributyl Phosphate and Triacetin", *J. Chem. Eng. Data*, **45**, 1105-1107 (2000).
- Bharath, R., Inomata, H., Adschiri, T., Arai, K., "Phase equilibrium study for the separation and fractionation of fatty oil components using supercritical carbon dioxide", *Fluid Phase Equilib.*, **81**, 307-320 (1992).
- Bharath, R., Yamane, S., Inomata, H, Adschiri, T., Arai, K., "Phase equilibria of supercritical CO₂-fatty oil component binary systems", *Fluid Phase Equilib.*, **83**, 183-192 (1993).

Biernoth, G., Merk, W., "Fractionation of butter fat using a liquified gas or a gas in the supercritical state", *United States Patent* 4,504,503 (1985).

Bonner, O.D., Breazeale, W.H., "Osmotic and Activity Coefficients of Some Nonelectrolytes", *J. Chem. Eng. Data*, **10**, 325-327 (1965).

Bottini, S.B., Fornari, T., Brignole, E.A., "Phase Equilibrium Modelling of Triglycerides with Near Critical Solvents", *Fluid Phase Equilib.*, **158-160**, 211-218 (1999).

Boukovalas, C., Spiliotis, N., Coutsikos, P., Tzouvaras, N., Tassios, D., "Prediction of vapor-liquid equilibrium with the LCVM model: a linear combination of the Vidal and Michelsen mixing rules coupled with the original UNIFAC and the t-mPR equation of state", *Fluid Phase Equilib.*, **92**, 75-106 (1994).

Byun, H.S., Kim, K., McHugh, M.A., "Phase behavior and modeling of supercritical carbon dioxide-organic acid mixtures", *Ind. Eng. Chem. Res.*, **39**, 4580-4587 (2000).

Carnahan, N.F., Starling, K.E., "Equation of state for Nonattracting Rigid Spheres", *J. Chem. Phys.*, **51**, 635-636 (1969).

Catté, M., Dussap, C.G., Achard, C., Gros, J.B., "Excess Properties and Solid-Liquid Equilibria for Aqueous solutions of Sugars using a UNIQUAC model", *Fluid Phase Equilib.*, **96**, 33-50 (1994).

Catté, M., Dussap, C.G., Gros, J.B., "A Physical Chemical UNIFAC model for Aqueous Solutions of Sugars", *Fluid Phase Equilib.*, **105**, 1-25 (1995).

Chapman, W., Gubbins, K., Jackson, J., Radosz, M., "New Reference Equation of State for Associating Liquids", *Ind. Eng. Chem. Res.*, **29**, 1709-1721 (1990).

Chapman, W.G., "Phase Behavior Applications of SAFT based Equations of State – from Associating Fluids to Polydisperse Polar Copolymers", EQUIFASE2002, Iguazu, Brazil, October 2002.

Chen, C. C., Chang, C.J., Yang, P.W., "Vapor-liquid equilibria of carbon dioxide with linoleic acid, α -tocopherol and triolein at elevated pressures", *Fluid Phase Equilib.*, **175**, 107-115 (2000).

Chen, J., Fischer, K., Gmehling, J., "Modification of PSRK mixing rules and results for vapor-liquid equilibria, enthalpy of mixing and activity coefficients at infinite dilution", *Fluid Phase Equilib.*, **200**, 411-429 (2002).

Chen, S.S., Kreglewsky, A., "Applications of the augmented van der Waals theory of fluids: I. Pure fluids", *Ber. Bunsen-Ges. Phys. Chem.*, **81**, 1048 (1977).

Chuang, L., Toledo, R.T., "Predicting the Water Activity of Multicomponent Systems from Water Sorption Isotherms of Individual Components", *J. Food Sci.*, **41**, 922-927 (1976).

- Conder, J., Young, C., *Physicochemical Measurements by Gas Chromatography*, Wiley Interscience, New York, 1979.
- Coniglio, L., Knudsen, K., Gani, R., "Prediction of supercritical fluid equilibria for carbon dioxide and fish oil related compounds through the equation of state – excess function (EoS-g^E) approach", *Fluid Phase Equilib.*, **116**, 510-517 (1996).
- Coorens, H.G.A, Peters, C.J., Swaan Arons, J., "Phase Equilibria in Binary Mixtures of Propane and Tripalmitin", *Fluid Phase Equilib.*, **40**, 135-151 (1988).
- Correa, A., Comesaña, J. F., Sereno, A. M., "Prediction of Water Activity in Non-Electrolyte Solutions by ASOG Group-contribution Method", CHEMPOR' 93, Porto, Portugal, April 1993.
- Coulon, D., Girardin, M., Engasser, J.M., Ghoul, M., "Investigation of key parameters of D-fructose oleate enzymatic synthesis catalysed by an immobilized lipase", *Ind. Crops and Products*, **6**, 375-381 (1997).
- Dahl, S., Fredenslund, A., Rasmussen, P., "The MHV2 model: A UNIFAC-based equation of state model for prediction of gas solubility and vapor liquid equilibria at low and high pressures", *Ind. Eng. Chem. Res.*, **30**, 1936-1945 (1991).
- Dahl, S., Michelsen, M.L., "High Pressure vapor-liquid equilibrium with a UNIFAC based equation of state", *Fluid Phase Equilib.*, **36**, 1829-1836 (1990).
- Daubert, T.E., Danner, R.P., *Physical and Thermodynamic Properties of Pure Chemicals: Data Compilation*, Hemisphere Publishing Corporation, 1989.
- De la Fuente, J.C., Fornari, T.B., Brignole, E.A., Bottini, S.B., "Phase equilibria in mixtures of triglycerides with low-molecular weight alkanes", *Fluid Phase Equilib.*, **128**, 221-227 (1997).
- Dohnal, V., Vrbka, P., "Limiting activity coefficients in the 1-alkanol- n-alkane systems: survey, critical evaluation and recommended values, interpretation in terms of association models", *Fluid Phase Equilib.*, **133**, 73-87 (1997).
- Dolezalek, F., "Zur Theorie der Binären Gemische und Konzentrierten Lösungen", *Z. Phys. Chem.*, **64**, 727 (1908).
- Economou, I.G., Donohue, M.D., "Chemical, Quasi-Chemical and Perturbation Theories for Associating Fluids", *AIChE. J.*, **37**, 1875-1894 (1991).
- Economou, I.G., Ikononou, G.D., Vimalchand, P., Donohue, M.D., "Thermodynamics of Lewis Acid-Base Mixtures", *AIChE. J.*, **36**, 1851-1864 (1990).

- Elliott, J.R., Suresh, J.S., Donohue, M.D., "Simple equation of state for nonspherical and associating molecules", *Ind. Eng. Chem. Res.*, **29**, 1476-1485 (1990).
- Ermolaev, M.I., Kapitanov, V.F., Nesterova, A.K., *Viniti*, **71**, 3716 (1971)
- Espinosa, S., Foco, G.M., Bermudez, A., Fornari, T., "Revision and extension of the group-contribution equation of state to new solvent groups and higher molecular weight alkanes", *Fluid Phase Equilib.*, **172**, 129-143 (2000).
- Espinosa, S., Fornari, T., Bottini, S.B., Brignole, E.A., "Phase equilibria in mixtures of fatty oils and derivatives with near critical solvents using the GC-EoS model", *J. Supercrit. Fluids*, **23**, 91-102 (2002).
- Ferreira, M.O., Brignole, E.A., Bottini, S.B., "A group-contribution model for activity coefficients in associating solutions", V Iberoamerican Conference on Phase Equilibria for Process Design, Vigo, Spain, June 1999.
- Ferreira, O., Foco, G.M., "Infinite Dilution Activity Coefficients of Solvents in Fatty Oil Derivatives", *Latin American Applied Research*, **33**, 257-260 (2003)
- Fischer, K., Gmehling, J., "Further development, status and results of the PSRK method for the prediction of vapor-liquid equilibria and gas solubilities", *Fluid Phase Equilib.*, **121**, 185-206 (1996).
- Flood, A.E., Johns, M.R., White, E.T., "Mutarotation of D-fructose in Aqueous-Ethanol Solutions and its Influence on Crystallisation", *Carbohydrate Res.*, **288**, 45-56 (1996).
- Florusse, L.J., Peters, C.J., Fornari, T., Bottini, S.B., Brignole, E.A., "Phase Behavior of the Binary System Near-Critical Dimethylether and Tripalmitin: Measurements and Thermodynamic Modeling. Fifth Conference on Supercritical Fluids and their Applications", Garda, Italy, June, 1999.
- Foco, G., Bermudez, A., Bottini, S.B., "Infinite Dilution Activity Coefficients in mono-, di-, tri-palmitin and palmitic acid", *J. Chem. Eng. Data*, **41**, 1071-1074 (1996).
- Fontán, C.F., Chirife, J., Boquet, R., "Water Activity in Multicomponent Non-Electrolyte Solutions", *J. Food Technol.*, **18**, 553-559 (1981).
- Formo, M.W., Jurgemann, E., Norris, F. A., Sonntag, N.O.V., *Bailey's Industrial Oils and Fats*, John Wiley & Sons, New York, 1982.
- Fornari, T., Bottini, S.B., Brignole, E.A., "Thermodynamic Modeling of Natural Fatty Oils and Derivatives with Supercritical Gases", Fifth Conference on Supercritical Fluids and their Applications, Garda, Italy, June, 1999.

- Fredenslund, A., Gmehling, A., Rasmussen, P., *Vapor-Liquid Equilibria using UNIFAC*, Elsevier, Amsterdam, 1977.
- Fredenslund, A., Jones, R.L., Prausnitz, J.M., "Group-contribution Estimation of Activity Coefficients in Non-Ideal Liquid Mixtures", *AIChE J.*, **21**, 1086-1099 (1975).
- Fu, Y.H., Sandler S.I., Orbey, H., "A Modified UNIQUAC Model That Includes Hydrogen Bonding", *Ind. Eng. Chem. Res.*, **34**, 4351-4363 (1995).
- Fu, Y.H., Orbey, H., Sandler S.I., "Prediction of vapor-Liquid Equilibria of Associating mixtures with UNIFAC Models That Include Association", *Ind. Eng. Chem. Res.*, **35**, 4656-4666 (1996).
- Fu, Y.H., Sandler, S.I., "A Simplified SAFT Equation of State for Associating Compounds and Mixtures", *Ind. Eng. Chem. Res.*, **34**, 1897-1909 (1995).
- Gabas, N., Carillon, T., Hiquily, N., "Solubilities of D-Xylose and D-Manose in Water-Ethanol Mixtures at 25 °C", *J. Chem. Eng. Data*, **33**, 128-130 (1988).
- Gabas, N., Laguérie, C., "Solubilité du Système Ternaire Eau-D-Xylose-D-Manose. Modélisation de l'Équilibre Liquide-Solide à l'Aide de la Méthode UNIFAC", *Bull. Soc. Chim. Fr.*, **127**, 391-395 (1990).
- Gmehling, J., Onken, U., Arlt, W., Grenheuser, P., *Vapor Liquid Equilibrium Data Collection*, DECHEMA Chemistry Data Series, DECHEMA, Frankfurt, 1977.
- Gmehling, J., Rasmussen, P., Fredenslund, A., "Vapor-Liquid Equilibria by UNIFAC Group-contribution. Revision and Extension. 2", *Ind. Eng. Chem. Process Des. Dev.*, **21**, 118-127 (1982).
- Goldberg, R.N., Tewari, Y.B., "Thermodynamic and transport properties of carbohydrates and their monophosphates: the pentoses and hexoses", *J. Phys. Chem. Ref. Data*, **18**, 809-880 (1989).
- Griswold J., Wong, S.Y., "Phase-equilibria of the acetone-methanol-water system from 100 °C into the critical region", *Chem. Eng. Progr. Symp. Ser.*, **48**, 18-34 (1952).
- Gros, H., Bottini, S.B., Brignole, E.A., "A group-contribution equation of state for associating mixtures", *Fluid Phase Equilib.*, **116**, 537-544 (1996).
- Guggenheim, E.A., *Mixtures*, Clarendon Press, Oxford, 1952.
- Gupta, R.B., Panayiotou, C.G., Sanchez, I.C., Johnston, K.P., "Theory of hydrogen bonding in supercritical fluids", *AIChE J.*, **38**, 1243-1253 (1992).
- Gupté, P.A., Daubert, T.E., "Extension of UNIFAC to high pressure VLE using Vidal mixing rules", *Fluid Phase Equilib.*, **28**, 155-170 (1986).

- Han, S.J., Lin, H.M., Chao, K.C., "Vapor-liquid Equilibrium data of molecular fluid mixtures by equation of state", *Chem. Eng. Sci.*, **43**, 2327-2367 (1988).
- Hayden, J.G., O'Connell, J.P., "A Generalized Method for Predicting Second Virial Coefficients", *Ind. Eng. Chem. Process Des. Dev.*, **14**, 209-216 (1975).
- Heidemann, R.A., Prausnitz, J.M., "A van der Waals type equation of state for fluids for associating molecules", *Proc. Natl. Acad. Sci.*, **73**, 1773-1776 (1976).
- Heidemann, R.A., Kokal, S.L., "Combined excess free energy models and equations of state", *Fluid Phase Equilib.*, **56**, 17-37 (1990).
- Hixson, A.W., Bockelmann, J.B., "Liquid-liquid extraction employing solvents in the region of their critical temperatures", *Trans. Am. Chem. Eng.*, **38**, 891-930 (1942).
- Holderbaum, T., Gmehling, J., "PSRK. A group contribution equation of state based on UNIFAC", *Fluid Phase Equilib.*, **70**, 251-265 (1991).
- Huang, S.H., Radosz, M., "Equation of State for Small, Large, Polydisperse and Associating Molecules", *Ind. Eng. Chem. Res.*, **29**, 2284-2294 (1990).
- Huang, S.H., Radosz, M., "Equation of State for Small, Large, Polydisperse and Associating Molecules: extension to fluid mixtures", *Ind. Eng. Chem. Res.*, **30**, 1994-2005 (1991).
- Hudson, C. S., "Further Studies on the Forms of Milk-Sugar", *J. Am. Chem. Soc.*, **30**, 1767-1783 (1908).
- Huron, M.J., Vidal, J., "New mixing rules in simple equation of state for representing vapour liquid equilibria of strongly nonideal mixtures", *Fluid Phase Equilib.*, **3**, 255-271 (1979).
- Hwang, Y.L., Olson, J.D., Keller II, G.E., "Steam stripping for removal of organic pollutants from water: 2. Vapor-liquid equilibrium data", *Ind. Eng. Chem. Res.*, **31**, 1759-1768 (1992).
- Ikonomou, G.D., Donohue, M.D., "Extension of the associated perturbed anisotropic chain theory to mixtures with more than one associating component", *Fluid Phase Equilib.*, **39**, 129-159 (1988).
- Ikonomou, G.D., Donohue, M.D., "Thermodynamics of hydrogen bonded molecules: The associated perturbed anisotropic chain theory", *AIChE J.*, **32**, 1716-1725 (1986).
- Inomata, H., Kondo, T., Hirohama, S., Arai, K., Suzuki, Y., Konno, M., "Vapor-Liquid Equilibria for Binary Mixtures of Carbon Dioxide and Fatty Acid Methyl Esters", *Fluid Phase Equilib.*, **46**, 41-52 (1989).
- Jackson, R.F., Silsbee, C.G., Profitt, M.J., *Sci. Papers Bur. Standards*, **20**, 588 (1926).

- Jónsdóttir, S.Ó., Cooke, S.A., Macedo, E.A., "Modeling and measurements of solid-liquid and vapour-liquid equilibria of polyols and carbohydrates in aqueous solutions", *Carbohydr. Res.*, **337**, 1563-1571 (2002).
- Jónsdóttir, S.Ó., Rasmussen, P., "Phase equilibria of carbohydrates in polar solvents", *Fluid Phase Equilib.*, **158-160**, 411-418 (1999).
- Kikic, I., Alessi, P., Rasmussen, P., Fredenslund, A., "On the combinatorial part of the UNIFAC and UNIQUAC models", *Can. J. Chem. Eng.*, **58**, 253-258 (1980).
- Koenen, H.E., Gaube, J., "Temperature Dependence of Excess Thermodynamic Properties of binary Mixtures of organic Compounds", *Phys. Chem.*, **86**, 31-36 (1982).
- Kojima, K., Zhang, S., Hiaki, T., "Measuring methods of infinite dilution activity coefficients and database for systems including water", *Fluid Phase Equilib.*, **131**, 145-179 (1997).
- Kontogeorgis, G.M., Vlamos, P.M., "An interpretation of the behaviour of EoS/GE models for asymmetric systems", *Chem. Eng. Sci.*, **55**, 2351-2358 (2000).
- Kontogeorgis, G.M., Voutsas, E.C., Yakoumis, I.V., Tassios, D.P., "Equation of state for associating fluids": *Ind. Eng. Chem. Res.*, **35**, 4310-4318 (1996).
- Kraska, T., "Analytic and fast Numerical Solutions and Approximations for Cross-association Models within Statistical Association Fluid Theory", *Ind. Eng. Chem. Res.*, **37**, 4889-4892 (1998).
- Kuramochi, H., Noritomi, H., Hoshino, D., Nagahama, K., "Representation of activity coefficients of fundamental biochemicals in water by the UNIFAC model", *Fluid Phase Equilib.*, **130**, 117-132 (1997).
- Kwak, T.Y., Mansoori, G.A., "Van der Waals mixing rules for cubic equations of state. Applications for supercritical fluid extraction modeling", *Chem. Eng. Sci.*, **41**, 1303-1309 (1986).
- Larsen, B. L., Rasmussen, P., Fredenslund, A., "A Modified UNIFAC Group-Contribution Model for Prediction of Phase Equilibria and Heat of Mixing", *Ind. Eng. Chem. Res.*, **26**, 2274-2286 (1987).
- Lerici, C.R., Piva, M., Rosa, M.D., "Water Activity and Freezing Point Depressiion of Aqueous Solutions and Liquid Foods", *J. Food Sci.*, **48**, 1667-1669 (1983).
- Leschke, R.J. "Techniques for Estimating the Vapor-Liquid Equilibrium of Sugar Solutions", *Biotechnology Progr.*, **3**, 205-211 (1987).
- Li, J., Dallas, A.J., Eikens, D.I., Carr, P.W., Bergmann, D.L., Hait, M.J., Eckert, C.A., "Measurement of large infinite dilution activity coefficients of nonelectrolytes in water by inert gas stripping and gas chromatography", *Anal. Chem.*, **65**, 3212-3218 (1993).

- Lichtenthaler, F.W., "The Carbohydrates" in *Ullmann's Encyclopedia Industrial Chemistry*, 6th Edn, 2002.
- Lichtenthaler, F.W., Rönninger, S., "Studies on Ketoses, 4. α -D-glucopyranosyl-D-fructoses: Distribution of Furanoid and Pyranoid Tautomers in Water, Dimethyl Sulphoxide, and Pyridine", *J. Chem. Soc., Perkin Trans.*, **2**, 1489-1497 (1990).
- Lieberwirth, I., Schuberth, H., "Isothermic vapor-liquid phase-equilibrium of the system acetone-water at 35°C". *Z. Phys. Chem-Leipzig*, **260**, 669-672 (1979).
- Magnussen, T., "Prediction of liquid-liquid Equilibria using UNIFAC", *PhD Thesis*, Lyngby, Denmark, 1980.
- Magnussen, T., Rasmussen, P., Fredenslund, A., "UNIFAC Parameter Table for Prediction of Liquid-Liquid Equilibria", *Ind. Eng. Chem. Process Des. Dev.* **20**, 331-339 (1981).
- Mansoori, G.A., Leland, T.W., "Statistical thermodynamics of mixtures", *J. Chem. Soc. Faraday Trans. II*, **68**, 320-344 (1972).
- Maple, S.R., Allerhand, A., "Detailed tautomeric equilibrium of aqueous D-glucose. Observation of six tautomers by ultrahigh resolution carbon-13 NMR", *J. Am. Chem. Soc.*, **109**, 3168-3169 (1987).
- Marquardt, D.W., "An algorithm for least squares estimation of non-linear parameters", *J. Appl. Math.*, **11**, 431-441 (1963).
- McHugh, M.A., Krukonis, V.J., *Supercritical fluid extraction. Principles and Practice*, Butterworth-Heinemann, USA, 1994.
- Mengarelli, A.C., Brignole, E.A., Bottini, S.B., "Activity coefficients of associating mixtures by group-contribution", *Fluid Phase Equilib.*, **163**, 195-207 (1999).
- Michelsen, M.L., "The isothermal flash problem. Part 1. Stability", *Fluid Phase Equilib.*, **9**, 1-19 (1982).
- Michelsen, M.L., "Modified Huron-Vidal mixing rule for cubic equations of state", *Fluid Phase Equilib.*, **60**, 213-219 (1990a).
- Michelsen, M.L., "A method for incorporating excess gibbs energy models in equations of state", *Fluid Phase Equilib.*, **60**, 47-58 (1990b).
- Miller, D.P., Pablo, J.J., "Calorimetric Solution Properties of Simple Saccharides and Their Significance for the Stabilization of Biological Structure and Function", *J. Phys. Chem. B*, **104**, 8876-8883 (2000).

- Miyajima, K., Sawada, M., Nakagaki M., Studies on Aqueous Solutions of Saccharides. II. Viscosity B-Coefficients, Apparent Molar Volumes, and Activity Coefficients of d-Glucose, Maltose and Maltotriose in Aqueous Solutions. *Bull. Chem. Soc. Jpn.*, **56**, 1954-1957 (1983b).
- Miyajima, K., Sawada, M., Nakagaki, M., "Studies on Aqueous Solutions of Saccharides. I. Activity Coefficients of Monosaccharides in Aqueous Solutions at 25 °C", *Bull. Chem. Soc. Jpn.*, **56**, 1620-1623 (1983a).
- Miyamoto, S., Nakamura, S., Iwai, F., Arai, Y., "Measurement of vapor phase compressibility factors of monocarboxylic acids using a flow type apparatus", *J. Chem. Eng. Data*, **44**, 48-51, (1999).
- Miyamoto, S., Nakamura, S., Iwai, Y., Arai, Y. "Measurement of Isothermal Vapor-Liquid Equilibria for Binary and Ternary Systems Containing Monocarboxylic Acid", *J. Chem. Eng. Data* **46**, 1225-1230 (2001).
- Miyamoto, S., Nakamura, S., Iwai, Y., Arai, Y., "Measurement of Isothermal Vapor-Liquid Equilibria for Hydrocarbon + Monocarboxylic Acid Binary Systems by a Flow-Type Apparatus", *J. Chem. Eng. Data*, **45**, 857-861 (2000).
- Mollerup, J., "A note on the derivation of mixing rules from excess Gibbs energy models", *Fluid Phase Equilib.*, **25**, 323-327 (1986).
- Mollerup, J., "Note on excess gibbs energy models, equations of state and the local composition concept", *Fluid Phase Equilib.*, **7**, 121-138 (1981).
- Moyé, C.J., "Non-aqueous Solvents for Carbohydrates", *Carboh. Chem.*, **27**, 85-125 (1972).
- Mullin, J. W., "*Crystallisation*", Butterworths, London, 1972.
- Othmer, D.F., Chudgar, M.M., Levy, S.L., "Binary and Ternary Systems of Acetone, Methyl Ethyl. Ketone, and Water", *Ind. Eng. Chem.*, **44**, 1872-1881 (1952b).
- Othmer, D.F., Silvis, S.J., Spiel, A., "Composition of Vapors from Boiling Binary Solutions: Pressure Equilibrium Still for Studying Water-Acetic Acid System", *Ind. Eng. Chem.*, **44**, 1864-1872 (1952a).
- Panagiotopoulos, A.Z., Reid, R.C., "New mixing rule for cubic equations of state for highly polar, asymmetric systems", *Amer. Chem. Symposium Ser.*, **300**, 571-582 (1986).
- Panayiotou, C., Sanchez, I.C., "Hydrogen bonding in fluids. An equation-of-state approach", *J. Phys. Chem*, **95**, 10090-10097 (1991).
- Peng, D.Y., Robinson, D.B., "A new two-constant equation of state", *Ind. Eng. Chem. Fundam.*, **15**, 59-64 (1976).

- Peres, A.M., "Equilíbrios Sólido-Líquido em Misturas Contendo Açúcares", *PhD Thesis*, Faculdade de Engenharia da Universidade do Porto, Portugal, 1998.
- Peres, A.M., Macedo, E.A., "A Modified UNIFAC Model for the Calculation of Thermodynamic Properties of Aqueous and Non-Aqueous Solutions Containing Sugars", *Fluid Phase Equilib.*, **139**, 47-74 (1997).
- Peres, A.M., Macedo, E.A., "Thermodynamic Properties of Sugars in Aqueous Solutions: Correlation and Prediction Using a Modified UNIQUAC Model", *Fluid Phase Equilib.*, **123**, 71-95 (1996).
- Perrut M., Majewski, W., Breivik, H., "Purifying polyunsaturated fatty acid glycerides", *United States Patent* 6,204,401 (2001).
- Peter, S., Jakob, H., "The rheological behavior of coexisting phases in systems containing fatty acids and dense gases", *J. Supercrit. Fluids*, **4**, 166-172 (1991).
- Peter, S.K., Weidner, E.O., Ender, U.M., Bernd A., "Process for the recovery of monoglycerides and diglycerides from a mixture containing monoglycerides, diglycerides, and triglycerides", *United States Patent* 5,110,509 (1992).
- Peters, C.J., "Multiphase equilibria in near-critical solvents", in *Supercritical Fluids*, E. Kiran and J.M.H. Levelt Sengers (eds.), Kluwer Academic Publishers, Dordrecht, 1994.
- Pierotti, G.J., Deal, C.H., Derr, E.L., "Activity coefficients and molecular structure", *Ind. Eng. Chem.*, **51**, 95-102 (1959).
- Prausnitz, J.M., Lichtenthaler, R.N., Azevedo, E.G., *Molecular Thermodynamics of Fluid-Phase Equilibria*, Prentice Hall, New Jersey, 1999.
- Raemy, A., Schweizer, T. F., "Thermal Behavior of Carbohydrates Studied by Flow Calorimetry", *J. Therm. Anal.*, **28**, 95-108 (1983).
- Reed, T.M., Gubbins, K.E., *Applied Statistical Mechanics*, McGraw-Hill, New York, 1973.
- Renon, H., Prausnitz, J.M., "Local composition in thermodynamics excess functions for liquid mixtures", *AIChE. J.*, **14**, 135-144 (1968).
- Robinson, R.A., Sinclair, D.A., "The Activity Coefficients of the Alkali Chlorides and lithium Iodide in Aqueous Solution from Vapor Pressure Measurements", *J. Am. Chem. Soc.*, **56**, 1830-1835 (1934).
- Robinson, R.A., Smith, P.K., Smith, E.R.B., "The Osmotic Coefficient of Some Organic Compounds in Relation to their Chemical Constitution", *Trans Faraday Trans.*, **38**, 63-70 (1942).

- Robinson, R.A., Stokes, R.H., "Activity Coefficients in Aqueous Solutions of Sucrose, Mannitol and their Mixtures at 25 °C", *J. Phys. Chem.*, **65**, 1954-1958 (1961).
- Roddy, J., Coleman, C., "Distribution of Ethanol-Water Mixtures to Normal Alkanes from C₆ to C₁₆", *Ind. Eng. Chem. Fundam.*, **20**, 250-254 (1981).
- Rodrigues, A.B.J., McCraffey, D.S., Kohn, J.P., "Heterogeneous phase and volumetric equilibrium in the ethane-n-octane system", *J. Chem. Eng. Data*, **13**, 165-168 (1968).
- Roos, Y., "Melting and Glass Transitions of Low Molecular Weight Carbohydrates", *Carbohydr. Res.*, **238**, 39-48 (1993).
- Rüegg, M., Blanc, B., "The Water Activity of Honey and Related Sugar Solutions", *Lebensm.-Wiss. u.-Technol.*, **14**, 1-6 (1981).
- Sanchez, I.C., Lacombe, R.H., "An Elementary Molecular Theory of Classical Fluids. Pure Fluids", *J. Phys. Chem.*, **80**, 2352-2362 (1976).
- Sandoval, R., Wilczek-Vera, G., Vera, J.H., "Prediction of ternary vapour-liquid equilibria with the PSRV equation of state", *Fluid Phase Equilib.*, **52**, 119-126 (1989).
- Scatchard, G., Hamer, W.J., Wood, S.E., "Isotonic Solutions. I. The Chemical Potential of Water in Aqueous Solutions of Sodium Chloride, Potassium Chloride, Sulfuric Acid, Sucrose, Urea and Glycerol at 25 °C", *J. Am. Chem. Soc.*, **60**, 3061-3070 (1938).
- Scheckermann, C., Schlotterbeck, A., Schmidt, M., Wray, V., Lang, S., "Enzymatic monoacylation of D-fructose by two procedures", *Enzyme and Microbial Technology*, **17**, 15-162 (1995).
- Shy, D.S., Yau, J.S., Tsai, F.N., "Phase behavior of methane with carboxylic acids", *J. Chem. Eng. Data*, **38**, 112-115 (1993).
- Skjold-Jørgensen, S., "Gas solubility calculations II. Application of a new group-contribution equation of state", *Fluid Phase Equilib.*, **16**, 317-351 (1984).
- Skjold-Jørgensen, S., "Group-contribution equation of state (GC-EoS): A predictive method for phase equilibrium computations over wide ranges of temperature and pressures up to 30 Mpa", *Ind. Eng. Chem. Res.*, **27**, 110-118 (1988).
- Soave, G., "Equilibrium constants from a modified Redlich-Kwong equation of state", *Chem. Eng. Sci.*, **27**, 1197-1203 (1972).
- Sørensen, J.M., Arlt, W., *Liquid-Liquid Equilibrium Data Collection*, DECHEMA Chemistry Data Series, Vol. V, Parts 1, 2, 3, Frankfurt, 1979.

- Spiliotis, N., Tassios, D., "A UNIFAC model for phase equilibrium calculations in aqueous and nonaqueous sugar solutions", *Fluid Phase Equilib.*, **173**, 39-55 (2000).
- Stephen, H., Stephen, T., *Solubilities of Inorganic and Organic Compounds. Binary Systems*, Vol. I, Parts 1 and 2, Pergamon Press, Oxford, 1963.
- Stokes, R.H., Robinson, R.A., "Interactions in Aqueous Nonelectrolyte Solutions. I. Solute-Solvent Equilibria", *J. Phys. Chem.*, **70**, 2126-2130 (1966).
- Suresh, S., Elliot, J., "Applications of a generalized equation of state for associating mixtures", *Ind. Eng. Chem. Res.*, **30**, 524-532 (1991).
- Suresh, S., Elliot, J., "Multiphase equilibrium analysis via a generalized equation of state for associating mixtures", *Ind. Eng. Chem. Res.*, **31**, 2783-2794 (1992).
- Taylor, J.B., Rowlinson, J.S., "The Thermodynamics Properties of Aqueous Solutions of D-glucose", *Trans. Faraday Soc.*, **51**, 1183-1192 (1955).
- Tiegs, D., Gmehling, J., Medina, A., Soares, M., Bastos, J., Alessi, P., Kikic, I. *Activity coefficients at Infinite Dilution*, DECHEMA Chemistry Data Series, Vol IX, Parts 1, 2 Frankfurt, 1986.
- Twu, C.H., Coon, J.E., Cunningham, J.R., "An equation of state for carboxylic acids", *Fluid Phase Equilib.*, **82**, 379-388 (1993).
- Uedaira, H., Uedaira, H., "Activity Coefficients of Aqueous D-xylose and Maltose Solutions", *Bull. Chem. Soc. Jpn.*, **42**, 2137-2140 (1969).
- Uedaira, H., Uedaira, H., "Role of hydration of polyhydroxy compounds in biological systems", *Cell. Mol. Biol.*, **47**, 823-829 (2001).
- Van Konynenburg, P.H., Scott, R.L., "Critical lines and phase equilibria in binary van der Waals mixtures", *Phil. Trans.*, **298**, 495-540 (1980).
- Vasátko, J., Smelík, "ARozpustnost' Bezvoděj β -D-fruktózy vo vode. *Chemické Zvesti*, **21**, 736-738 (1967).
- Vimalchand, P., Donohue, M.D., "Thermodynamics of quadrupolar molecules: the perturbed-anisotropic-chain theory", *Ind. Eng. Chem. Fundam.*, **24**, 246-257 (1985).
- Voutsas, E.C., Kontogeorgis, G.M., Yakoumis, I.V., Tassios, D.P., "Correlation of liquid-liquid equilibria for alcohol-hydrocarbon mixtures using the CPA equation of state", *Fluid Phase Equilib.*, **132**, 61-75 (1997).

- Voutsas, E.C., Yakoumis, I.V., Tassios, D.P., "Prediction of phase equilibria in water/alcohol/alkane systems", *Fluid Phase Equilib.*, **158-160**, 151-163 (1999).
- Weast R.C. Ed., *CRC Handbook of Chemistry and Physics*, The Chemical Rubber Co., Cleveland, 1972-73.
- Weidlich, U., Gmehling, J., "A modified UNIFAC model. 1. Prediction of VLE, h^E and γ^∞ ", *Ind. Eng. Chem. Res.*, **26**, 1372-1381 (1987).
- Wen, T.Y., Tang, M., Chen, Y.P., "Vapor-liquid equilibria of the binary mixtures 2-butanone + t-pentanol, t-pentanol + butyl acetate and 2-propanol + diethyl ketone at 101.3 kPa", *Fluid Phase Equilib.*, **163**, 99-108 (1999).
- Weng, W.I., Lee, M.J., "Phase equilibrium measurements for the binary mixtures of 1-octanol plus CO₂, C₂H₆ and C₂H₄", *Fluid Phase Equilib.*, **73**, 117-127 (1992).
- Wertheim, M., "Fluids with Highly Directional Attractive Forces. I. Statistical Thermodynamics", *Journal of Statistical Physics*, **35**, 19-34 (1984a).
- Wertheim, M., "Fluids with Highly Directional Attractive Forces. II. Thermodynamics Perturbation Theory and Integral Equations", *Journal of Statistical Physics*, **35**, 35-47 (1984b).
- Wertheim, M., "Fluids with Highly Directional Attractive Forces. III. Multiple Attraction Sites", *Journal of Statistical Physics*, **42**, 459-476 (1986a).
- Wertheim, M., "Fluids with Highly Directional Attractive Forces. IV. Equilibrium Polymerization", *Journal of Statistical Physics*, **42**, 477-492 (1986b).
- Wolbach, J.P., Sandler, S.I., "Using Molecular Orbital Calculations To Describe Phase Behavior of Hydrogen-Bonding Fluids", *Ind. Eng. Chem. Res.*, **36**, 4041-4051 (1997).
- Wolbach, J.P., Sandler, S.I., "Using molecular orbital calculations to describe the phase behavior of cross-associating mixtures", *Ind. Eng. Chem. Res.*, **37**, 2917-2928 (1998).
- Wong, D.S.H., Sandler, S.I., "Theoretically correct mixing rule for cubic equations of state", *AIChE J.*, **38**, 671-680 (1992).
- Wormald, C.J., "Intermolecular forces between hydrocarbons and ethers, ketones or alcohols", *Fluid Phase Equilib.*, **133**, 1-10 (1997).
- Yakoumis, I.V., Kontogeorgis, G.M., Voutsas E., Tassios, D.P., "Vapor-Liquid Equilibria for Alcohol/Hydrocarbon Systems Using the CPA Equation of State", *Fluid Phase Equilib.*, **130**, 31-47 (1997).

- Yau, J.S., Chiang, Y., Shy, D.S., Tsai, F.N., "Solubilities of carbon dioxide in carboxylic acids under high pressures", *J. Chem. Eng. Jpn.*, **25**, 544-548 (1992).
- Young, F.E., "D-Glucose-Water Phase Diagram", *J. Phys. Chem.*, **61**, 616-619 (1957).
- Young, F.E., Jones, F.T., "Sucrose Hydrates. The Sucrose-Water Phase Diagram.", *J. Phys. Chem.*, **53**, 1334-1350 (1949).
- Young, F.E., Jones, F.T., Lewis, H.J., "D-Fructose-Water Phase Diagram", *J. Phys. Chem.*, **56**, 1093-1096 (1952).
- Yu, Z.R., Zou, M., Bhaskar, A.R., Rizvi, S.S.H., Zollweg, J.A., "Fluid liquid Equilibria of Supercritical Carbon Dioxide + Methyl Oleate + Oleic acid", *J. Supercrit. Fluids*, **6**, 63-68 (1993).
- Zabaloy, M., Mabe G.D.B., Bottini S.B. and Brignole E.A., "Vapor liquid equilibria in ternary mixtures of water-alcohol-non polar gases", *Fluid Phase Equilib.*, **83**, 159-166 (1993).
- Zhang, S., Hiaki, T., Hongo, M., Kojima, K., "Prediction of infinite dilution activity coefficients in aqueous solutions by group-contribution models. A critical evaluation", *Fluid Phase Equilib.*, **144**, 97-112 (1998).

Appendix A

A-UNIFAC software developed in this work

A. A-UNIFAC software developed in this work

A.1 Introduction

This appendix explains the development of the A-UNIFAC software, its structure, and the management of the different data and files that provide the software files.

A.2 Input data files

A.2.1 Cross section input file

Input file for the cross section data. It is a text file with the following structure:

A.2.2 Parameter input file

Input file for the parameters. It is a text file with the following structure:

Appendix A

A-UNIFAC software developed in this work

A. A-UNIFAC software developed in this work

A.1 Introduction

This appendix reproduces the Help file created for the A-UNIFAC program. It describes the management of the different input and output data files and the database files.


A.2 Input data files

A.2.1 Create a new input file

Select **File-New-Input Data File** on the main menu to create a new input file.

A.2.1.1 Selection of components

Select at least two different components from the database (Figure A.1). This is done by filling the textbox and pressing the Find button. The search for the desired component can be made by one of the criteria: Name or Formula. The search results will appear on the first table. Each table includes the component identification number (ID), Name, Formula and Database condition. The 4th column indicates whether the component has its pure component properties stored in the database.

Only components whose properties are in the database (4th column=YES) can be selected. In case the user wants to add or update pure component properties, please see topic A.3.1.3. Then, transfer the chosen components to the second table, by pressing .

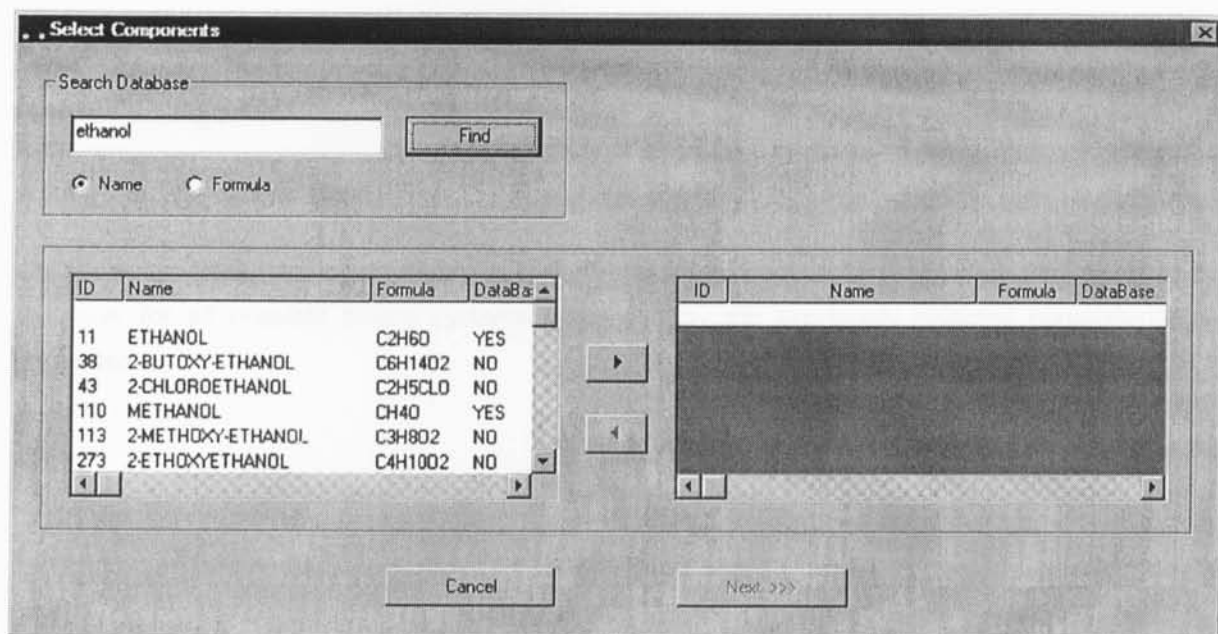


Figure A.1 Selecting components from the database.

After the transfer of a minimum of two different components to table 2, press the **Next** button.

A.2.1.2 Parameters initial values

On the upper table from Figure A.2, the user can view and edit the residual parameters values associated with the residual groups, which define the selected components. If any of the selected components have hydrogen bonding, then a second table appears with the corresponding association group parameters.

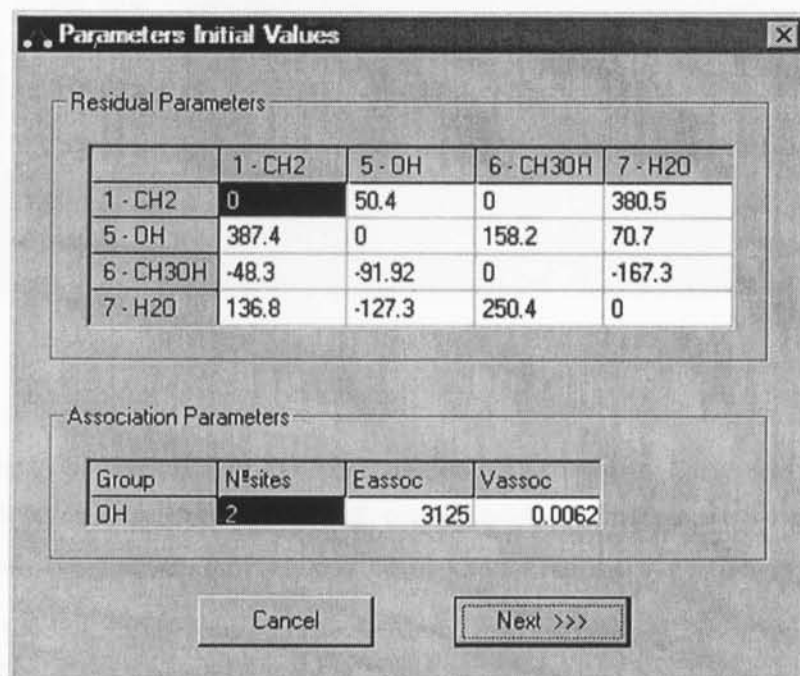


Figure A.2 Set initial parameters values for the run.

When the window is loaded, the tables contain the residual and association parameter values stored in the database. The parameters can be changed for a specific run by moving the cursor on the table cells and editing them.

A.2.1.3 Thermodynamic data

On the upper table, shown on Figure A.3, the vapour-liquid equilibria (VLE) data that exists in the database for all possible binary systems composed by the previously selected components are presented.

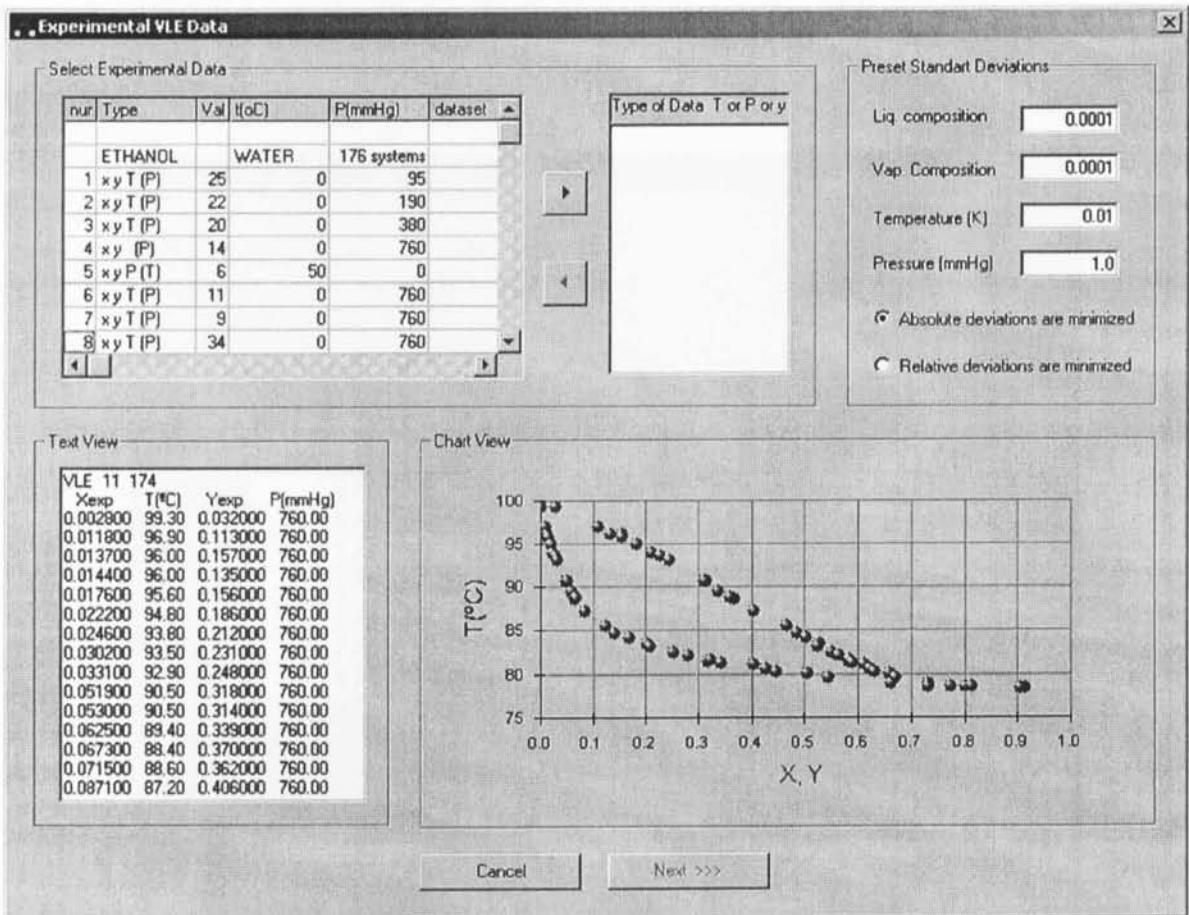


Figure A.3 Selection of experimental binary VLE systems.

If they exist in the database the user can view them in the textbox, by clicking on the corresponding row. Only the sets of data that contain full experimental information (liquid and vapour phase compositions, pressure and temperature) can be selected. This is done by pressing . It is also possible to change the preset standard deviations for the liquid phase composition, vapour phase composition, temperature and pressure. After selecting at least one VLE system the user can press the **Next** button.

A.2.1.4 Run

On the window (Figure A.4), the user chooses the type of calculation:

- Ⓐ **Simulation** of the model using the parameters defined in the second step, or:
- Ⓑ **Optimization** using the parameters defined in the second step as initial estimates.

In this case, the user must also define which variables are to be optimized:

- Ⓐ all variables;
- Ⓑ only the dependent variables (that is, the liquid phase composition and temperature are kept fixed).

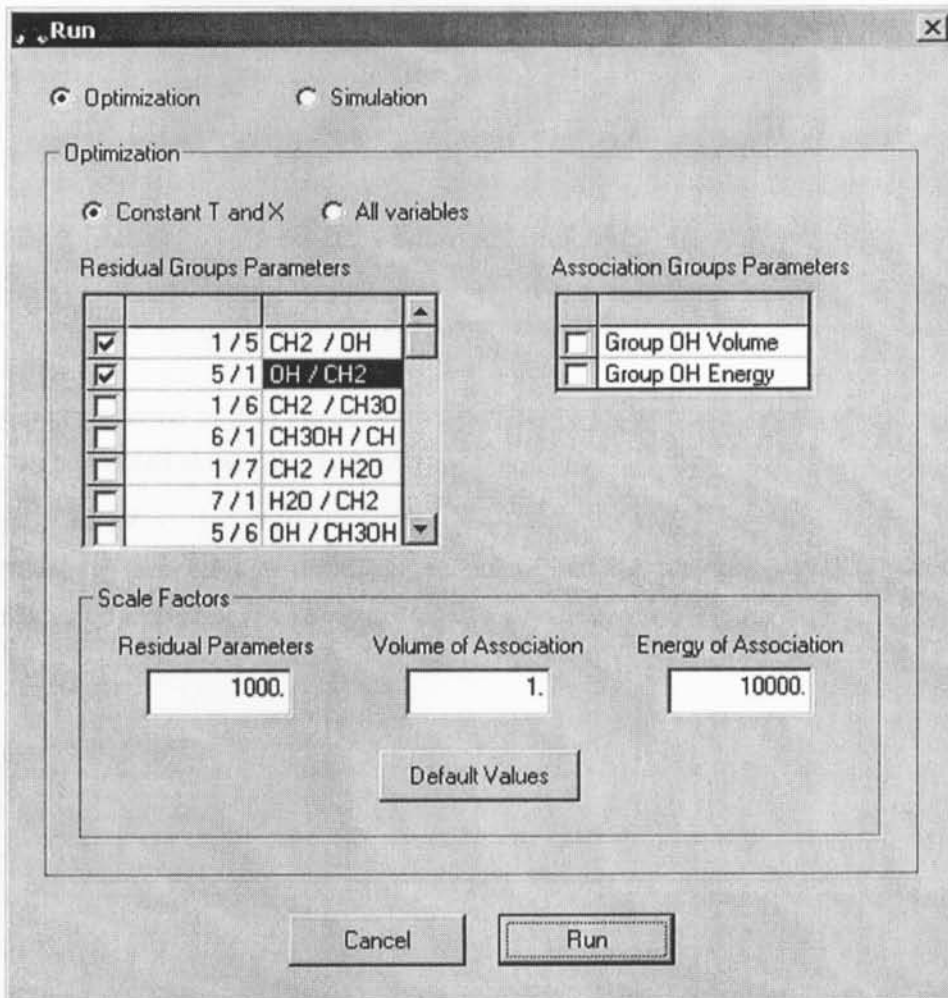


Figure A.4 Set optimisation or simulation features.

The user can select, in the tables, which parameters shall be optimized (residual parameters in the left table and association parameters in the right one).

Finally, it is possible to set the scale factors for the different type of parameters. Now, the user can press the **Run** button to start the calculations.

A.2.1.5 Output results

As the result of the calculations, two situations may occur:

1. The calculations finished without error. The following figure appears:

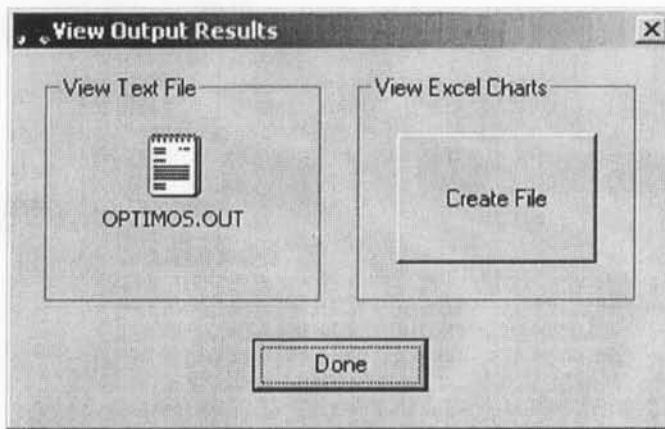


Figure A.5 View output results in a text file or excel file.

Now, the user can choose to view the generated output text file and/or to create an Excel File in which the results are presented in the graphical form.

2. The calculations finished with error, but an output text file was generated (Figure A.6) or the calculations finished with error and no output text file was generated (Figure A.7).

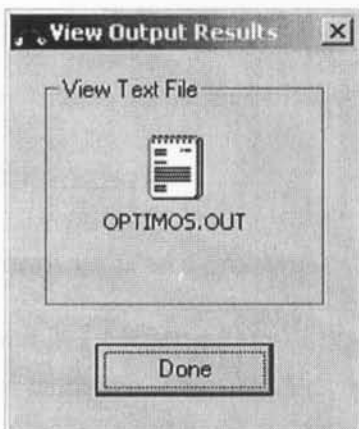


Figure A.6 View Output Results in a text file.

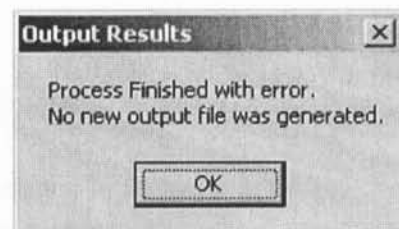


Figure A.7 No output results.

A.2.2 Open an input file

The user should use this option to make slight changes in the input file in a faster way. Select **File-Open-Input Data File** on the main menu to open an existing input file. After selecting the file, the user can view and edit it in the textbox. Then, press the **Run** button to start the calculations. The program will create an input file containing the text displayed in the textbox of Figure A.8.

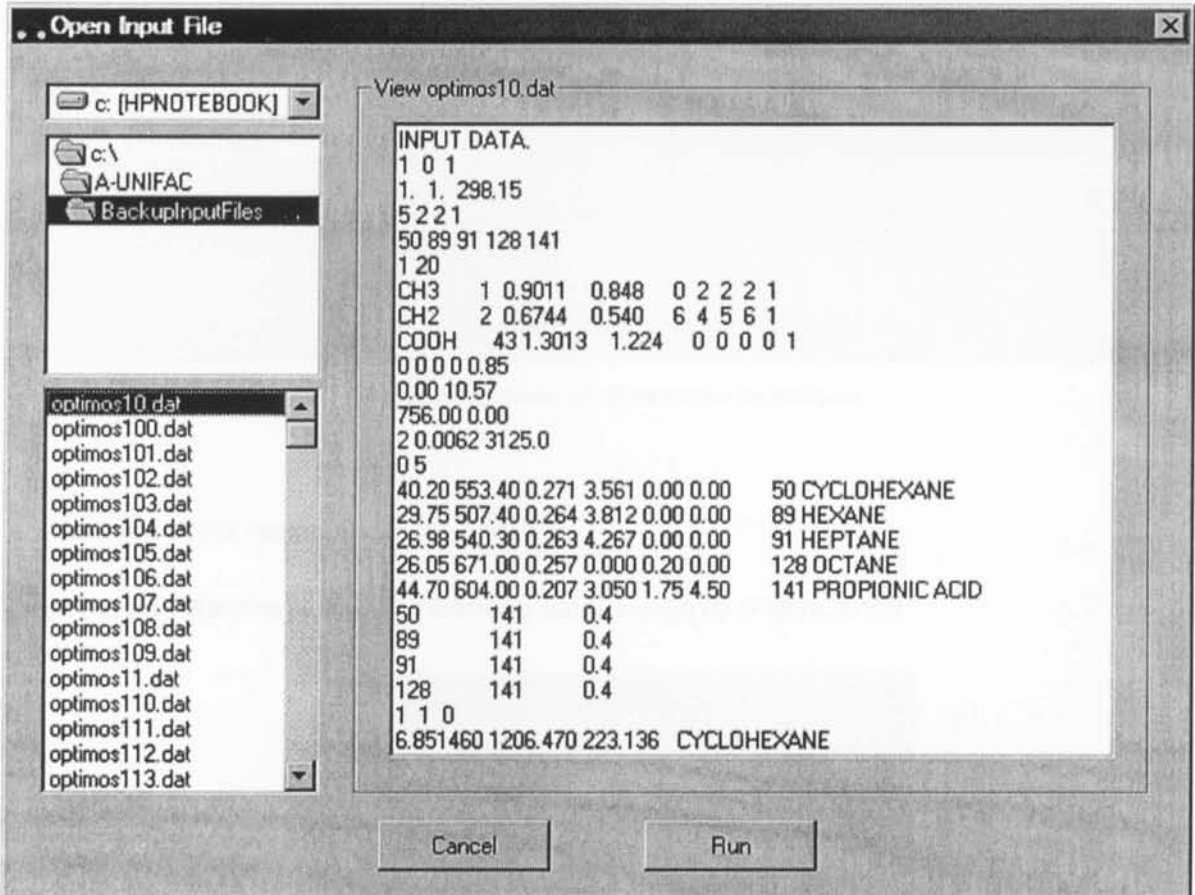


Figure A.8 Select an existing input file.

A.2.2.1 Output results

The same situation occurs as described before on section A.2.1.5.

A.3 Databases

A.3.1 Pure component properties

Select **Database - Add/Update Data - Pure Component** on the main menu to add or update pure component properties. The following window appears (Figure A.9):

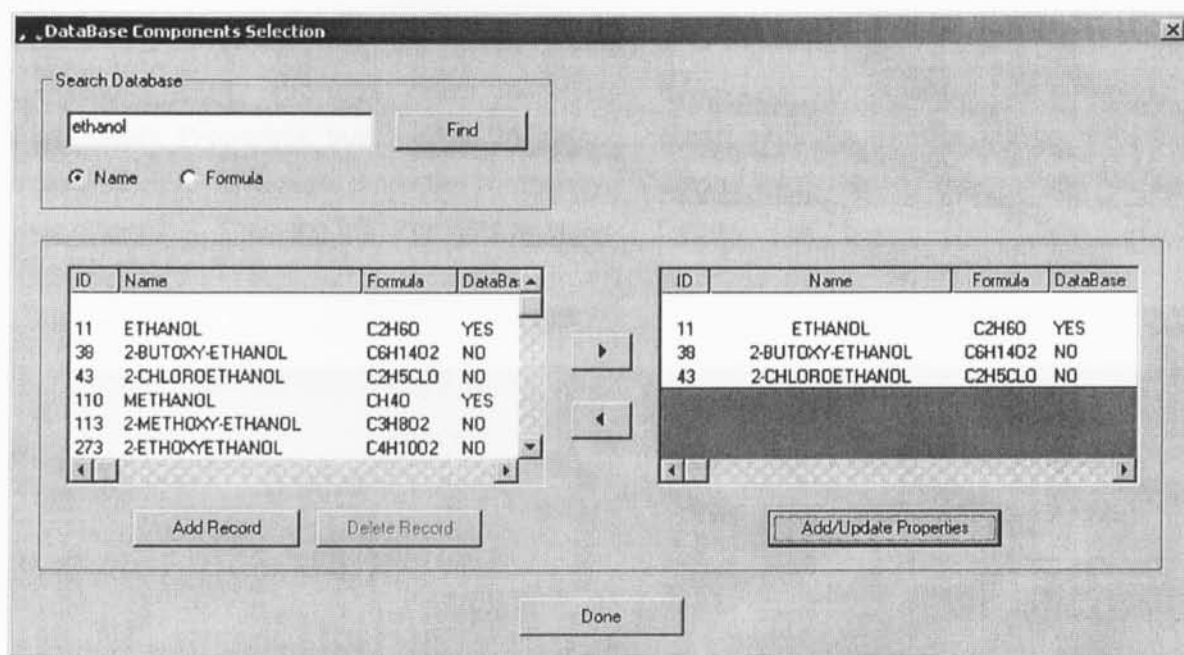


Figure A.9 Selecting components from the database.

A.3.1.1 Add a new component to the database

Press the **Add Record** button. The following window pops up (Figure A.10):

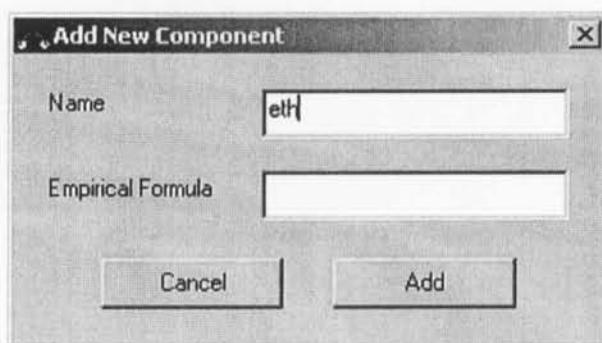


Figure A.10 Adding a new component to the database.


Fill in the empty boxes and press the **Add** button.

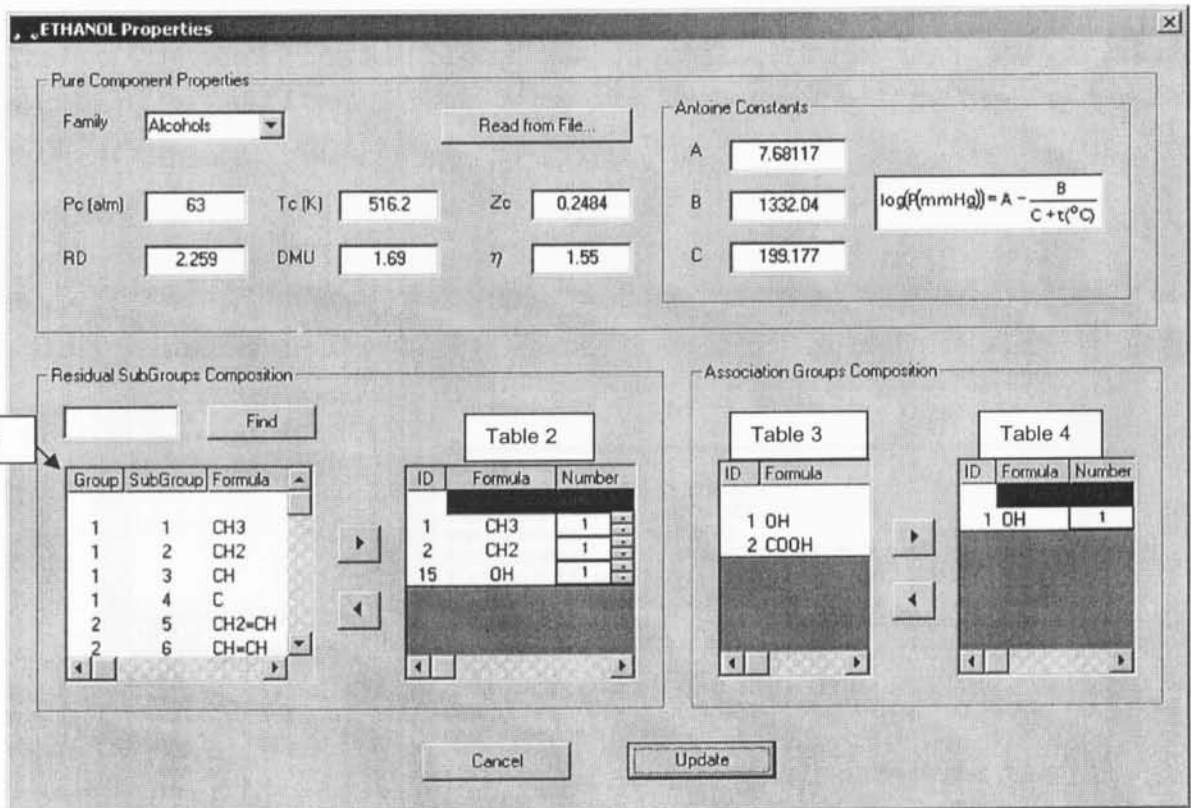
A.3.1.2 Delete record

Select the corresponding component row in the table and press the **Delete** button.

A.3.1.3 Add or update properties

The user can select a component from the database by searching it in the database (filling the textbox and pressing the **Find** button) or adding a new component to the database (see topic A.3.1.1). The

selected components are transferred to the right table by pressing . After moving the desired components to the right table, select one of them by clicking the respective row and press the **Add/Update Properties** button. The DATABASE column indicates whether the component has already its pure component properties completely included in the database (update properties) or not (add properties). Then, the following window appears (Figure A.11):



ETHANOL Properties

Pure Component Properties

Family: Alcohols

Pc (atm): 63 Tc (K): 516.2 Zc: 0.2484

RD: 2.259 DMU: 1.69 η: 1.55

Antoine Constants

A: 7.68117 B: 1332.04 C: 199.177

$$\log(P(\text{mmHg})) = A - \frac{B}{C + t(^{\circ}\text{C})}$$

Residual SubGroups Composition

Find

| Group | SubGroup | Formula |
|-------|----------|---------|
| 1 | 1 | CH3 |
| 1 | 2 | CH2 |
| 1 | 3 | CH |
| 1 | 4 | C |
| 2 | 5 | CH2=CH |
| 2 | 6 | CH=CH |

Table 2

| ID | Formula | Number |
|----|---------|--------|
| 1 | CH3 | 1 |
| 2 | CH2 | 1 |
| 15 | OH | 1 |

Association Groups Composition

Table 3

| ID | Formula |
|----|---------|
| 1 | OH |
| 2 | COOH |

Table 4

| ID | Formula | Number |
|----|---------|--------|
| 1 | OH | 1 |

Figure A.11 Setting pure component properties.

Following the traditional $\gamma - \phi$ approach, the vapour phase fugacity coefficient is calculated using the virial equation, with second virial coefficients estimated from the method of Hayden and O'Connell (1975). To apply this method some pure component parameters must be known:

Pc and **Tc**: Critical pressure and critical temperature;

RD: Mean radius of gyration in Å;

DMU: Dipole moments in Debye;

η : Association (for pure substances) and Solvation (for interaction between components in a mixture) parameters.

The vapour pressure of the components is calculated using the Antoine equation for which the **A**, **B** and **C** constants must be given (Ghmeling *et al.*, 1977).

After this, define the residual subgroups composition of the component by transferring them from table 1 to table 2 (Figure A.11). In the former table set the quantity of each subgroup. If the component has self-association then define also the association groups composition, setting also the quantity of each group. In case the user wants to add or update the residual subgroups or association groups please consult the topics A.3.2 and A.3.3, respectively.

The Pure Component Properties (the data contained in the upper frame) may be entered manually or by pressing the **Read from File** button. In this case, the file should be of the type shown on Figure A.12.

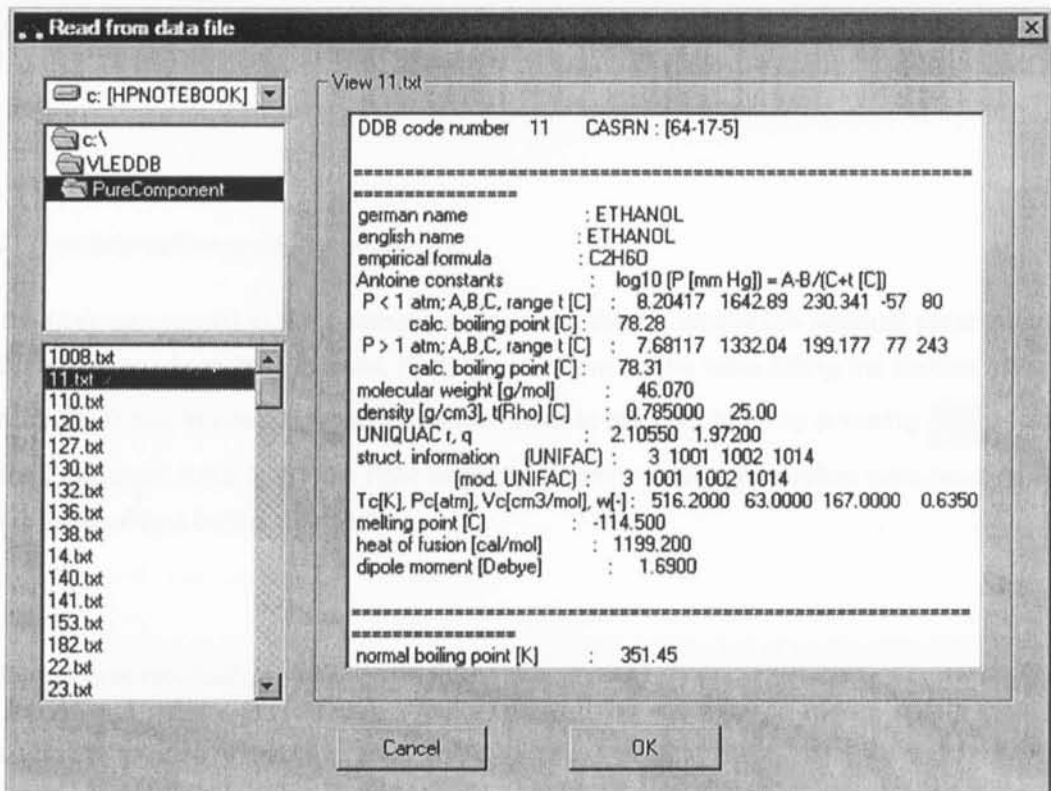


Figure A.12 Selecting file containing pure component properties.

A.3.2 Residual groups parameters

Select **Database - Add/Update Data - Residual Groups Parameters** on the main menu to add/update residual groups and subgroups data (Figure A.13).

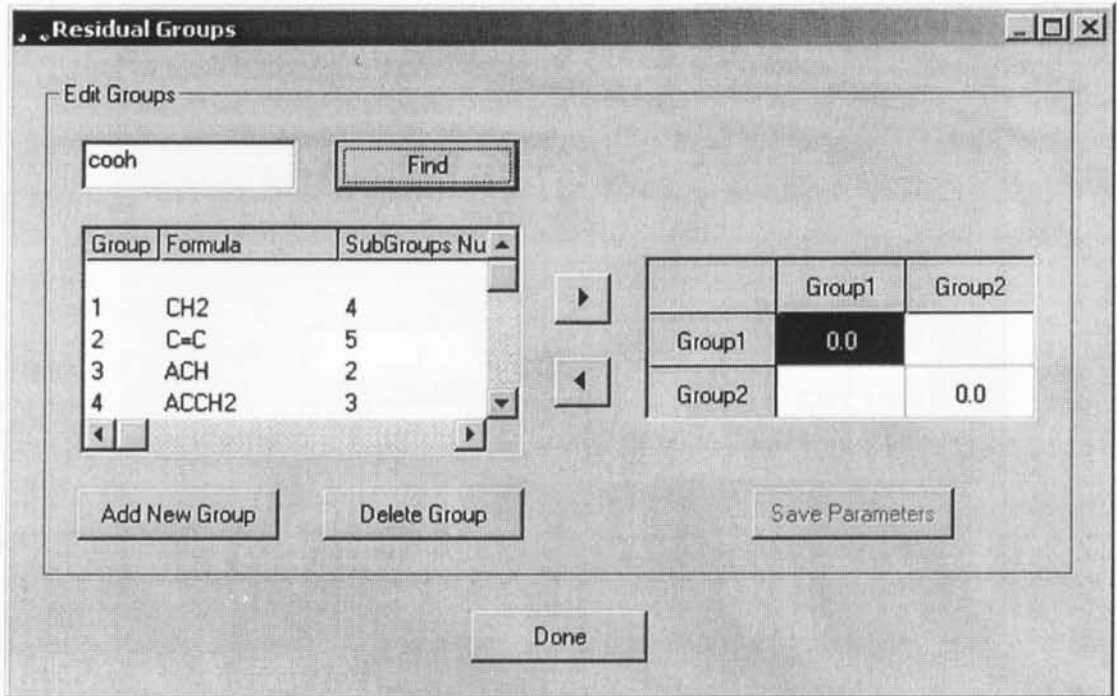




Figure A.13 Set residual groups features in the database.

A.3.2.1 New interaction residual parameters

Here, the user can record in the database new values for the interaction residual parameters. Select two different groups from the left table. First, search them on the table (filling the textbox and pressing the **Find** button) and in case they exist, transfer them to the right table by pressing . To create a new group see topic A.3.2.2. On the right table, the corresponding parameters cells must be filled and the **Save Parameters** button pressed.

A.3.2.2 Add new residual groups

First, define the formula of the new group and the number of subgroups. Then, for each subgroup k , fill the data (Formula, Surface Area R_k and Volume Q_k) inside the frame and transfer it to the table, by pressing . Finally, press the **Save** button, once all the subgroups data are registered on the table (Figure A.14).

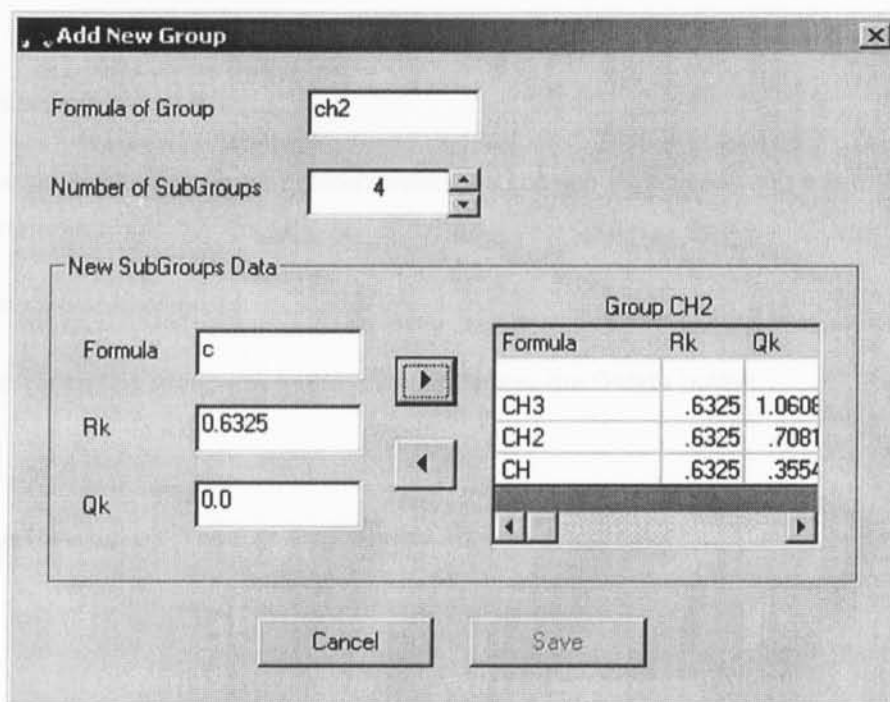


Figure A.14 Definition of a new group and corresponding subgroups.

A.3.2.3 Delete residual groups

Select the corresponding group row on the table and press the **Delete** button.

A.3.3 Association group parameters

Select **Database - Add/Update Data - Association Group Parameters** on the main menu to add/update association groups. The number of sites, the energy and volume of association can then be defined for each associating group (Figure A.15).

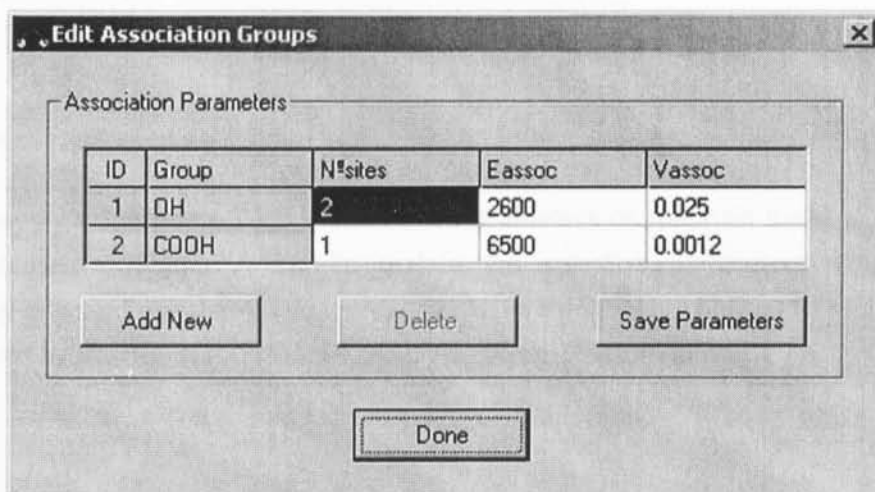


Figure A.15 Set association groups features in the database.

A.3.3.1 Update data

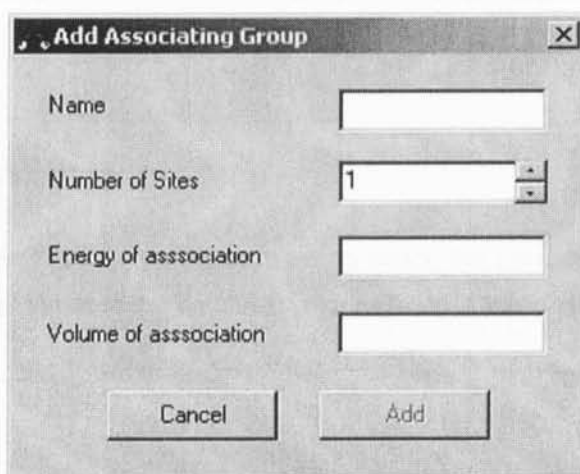
To update the association group parameters select the corresponding cells and edit them. Then press the **Save Parameters** button.

A.3.3.2 Delete association group

Select the corresponding group row in the table, and press the **Delete** button.

A.3.3.3 Add new associating group

Press the **Add New** button. The following window appears (Figure A.16):



The image shows a dialog box titled "Add Associating Group" with a close button (X) in the top right corner. The dialog contains four input fields: "Name" (a text box), "Number of Sites" (a spin box with the value "1" and up/down arrows), "Energy of association" (a text box), and "Volume of association" (a text box). At the bottom of the dialog are two buttons: "Cancel" and "Add".

Figure A.16 Definition of a new association group.

Fill all the empty boxes and then press the **Add** button.

A.3.4 Solvation parameters

Select **Database - Add/Update Data - Solvation Parameters** on the main menu to add/update the solvation parameters (Figure A.17). To update the solvation parameters simply select the corresponding cells and edit them. Then, press the **Save Parameters** button. To restore the original values, as given by Hayden and O'Connell, simply press the **Restore** button.

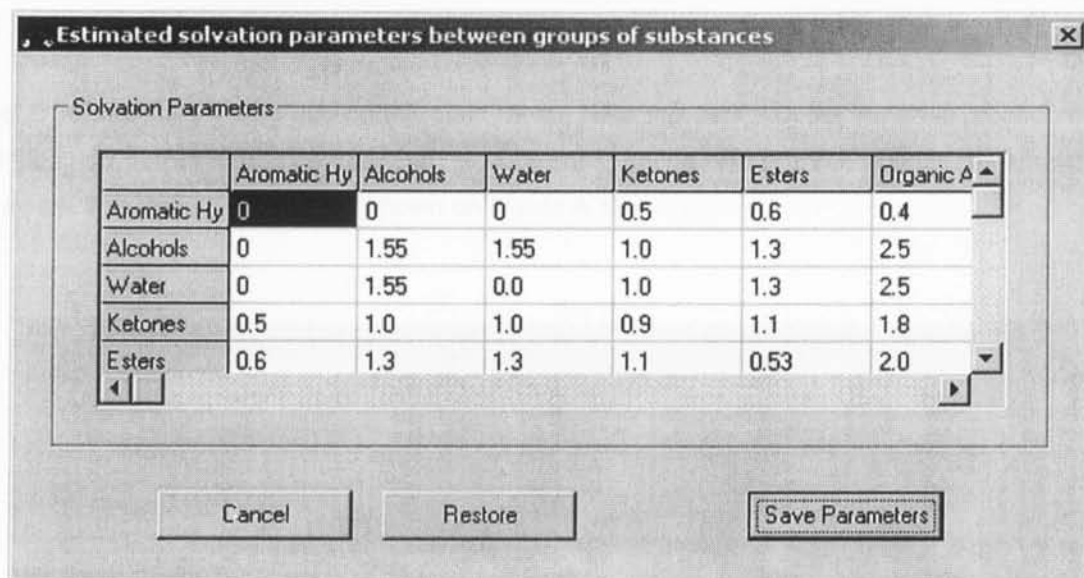


Figure A.17 Set solvation parameters values in the database.

A.4 View equilibria data

Select **View - Equilibrium Data** on the main menu to check the complete references of the binary VLE experimental data that exists in the database (Figure A.18). Click on the file name to view it in the textbox.

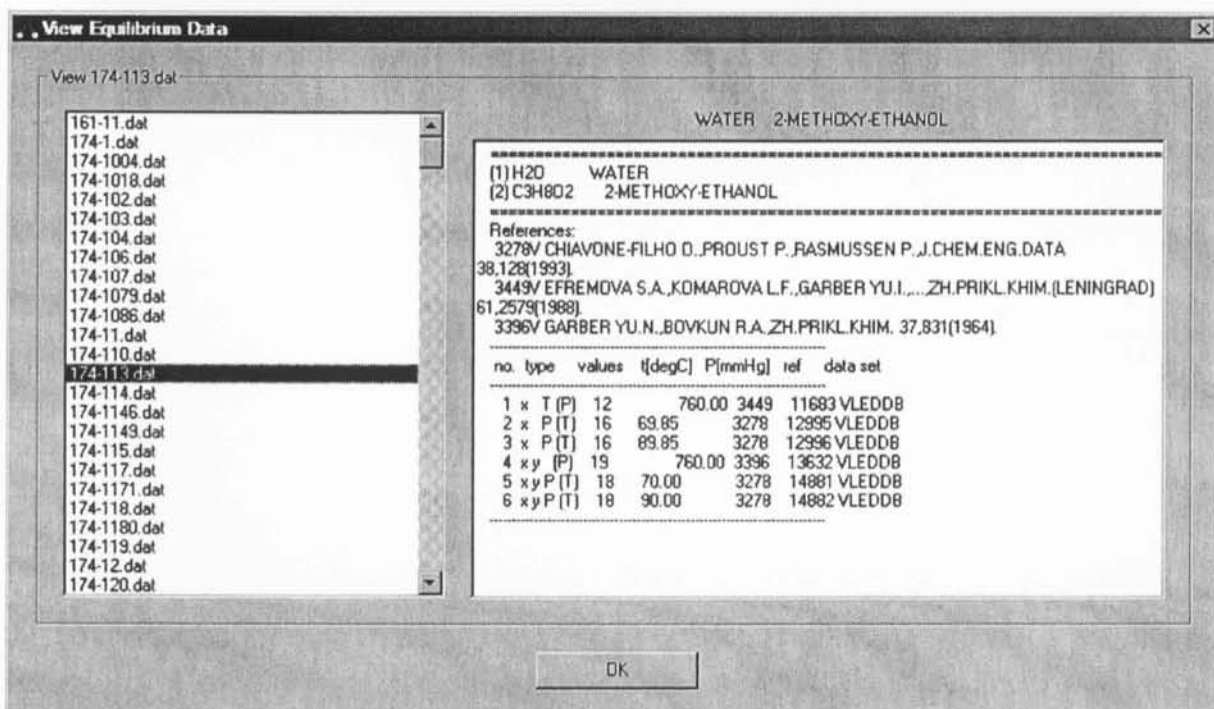


Figure A.18 View the references files.

A.5 Options

Select **Options-Save Text Files** on the main menu. Here the user can set the save procedure of the input files and output files. The user can, in each case, define one of three options, as shown in the next figure. The default options are shown on Figure A.19.

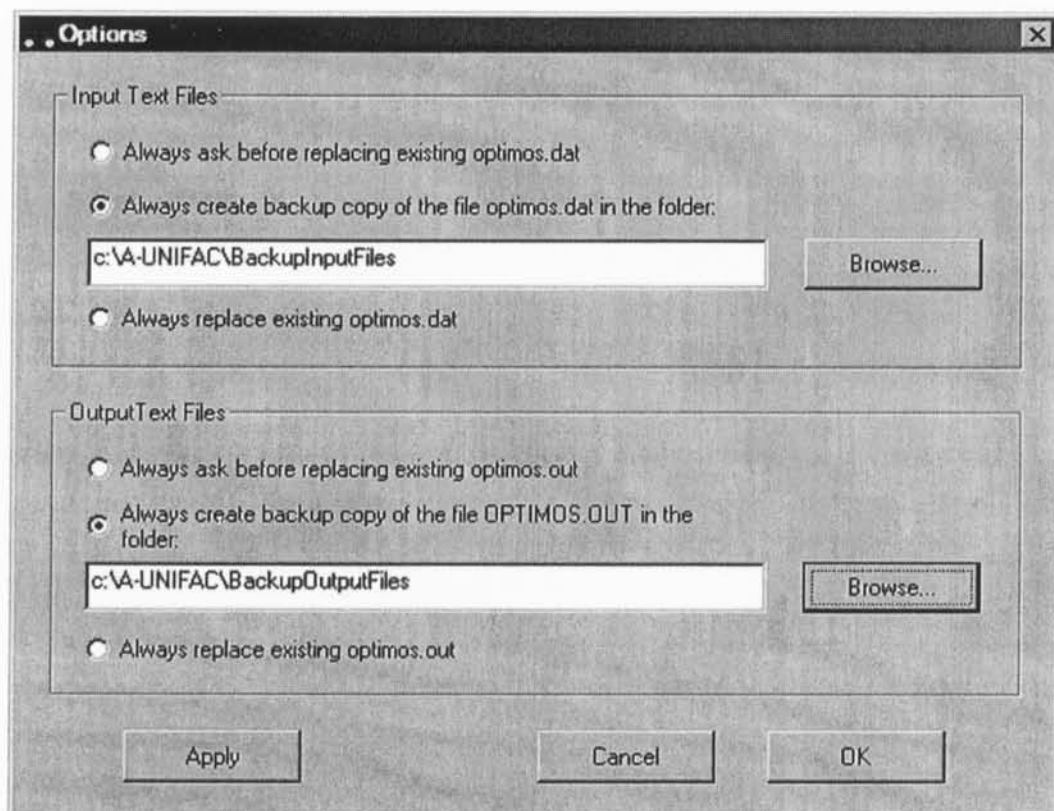


Figure A.19 Options window.

B. Structures of some sugars

B.1. D-aldoses



Appendix B

Structures of some sugars



Figure B.1 The structures of some monosaccharides.

B. Structures of some sugars

B.1 D-aldoses

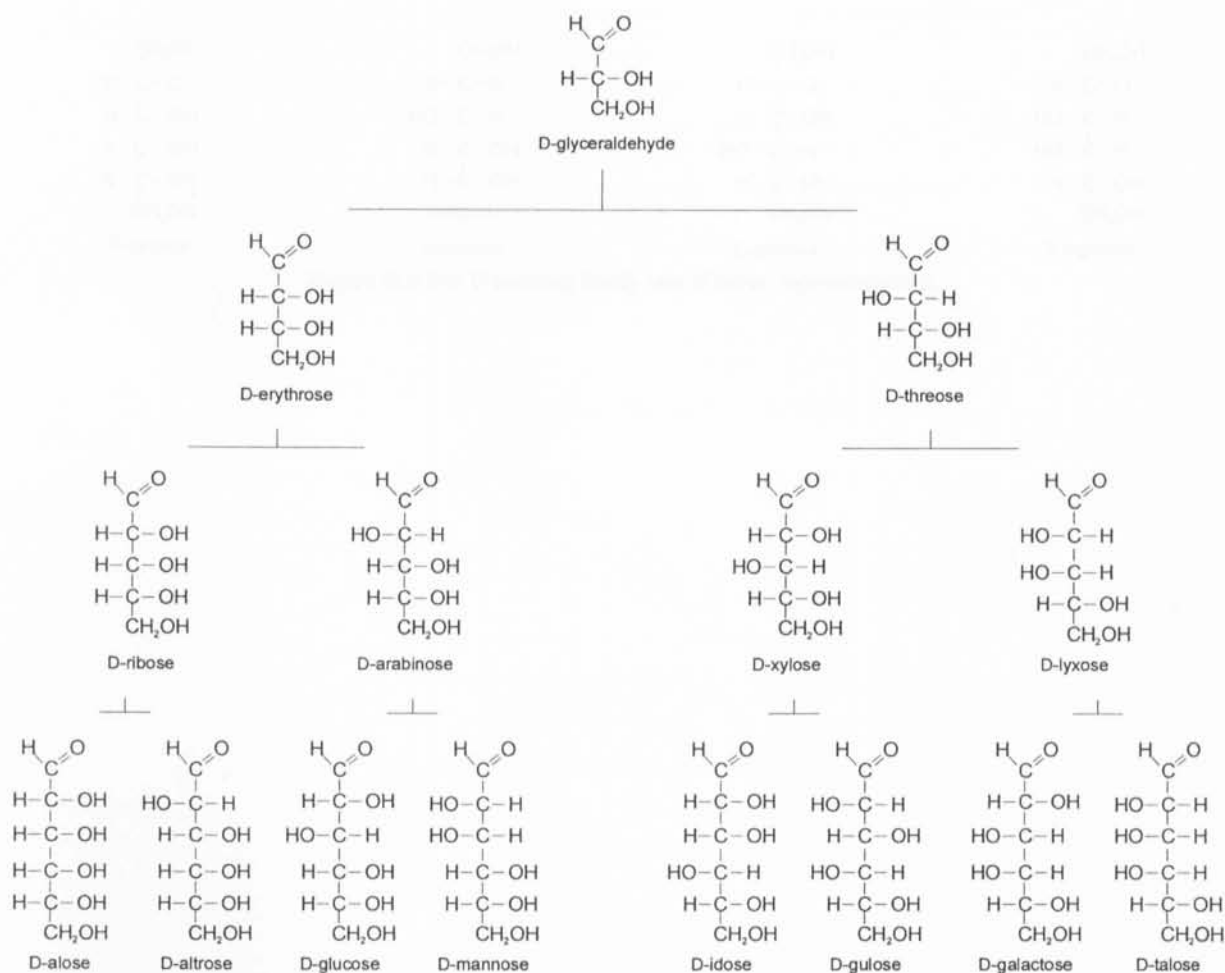


Figure B.1 The D-aldoses family tree (Fischer representation).

B.2 D-ketoses

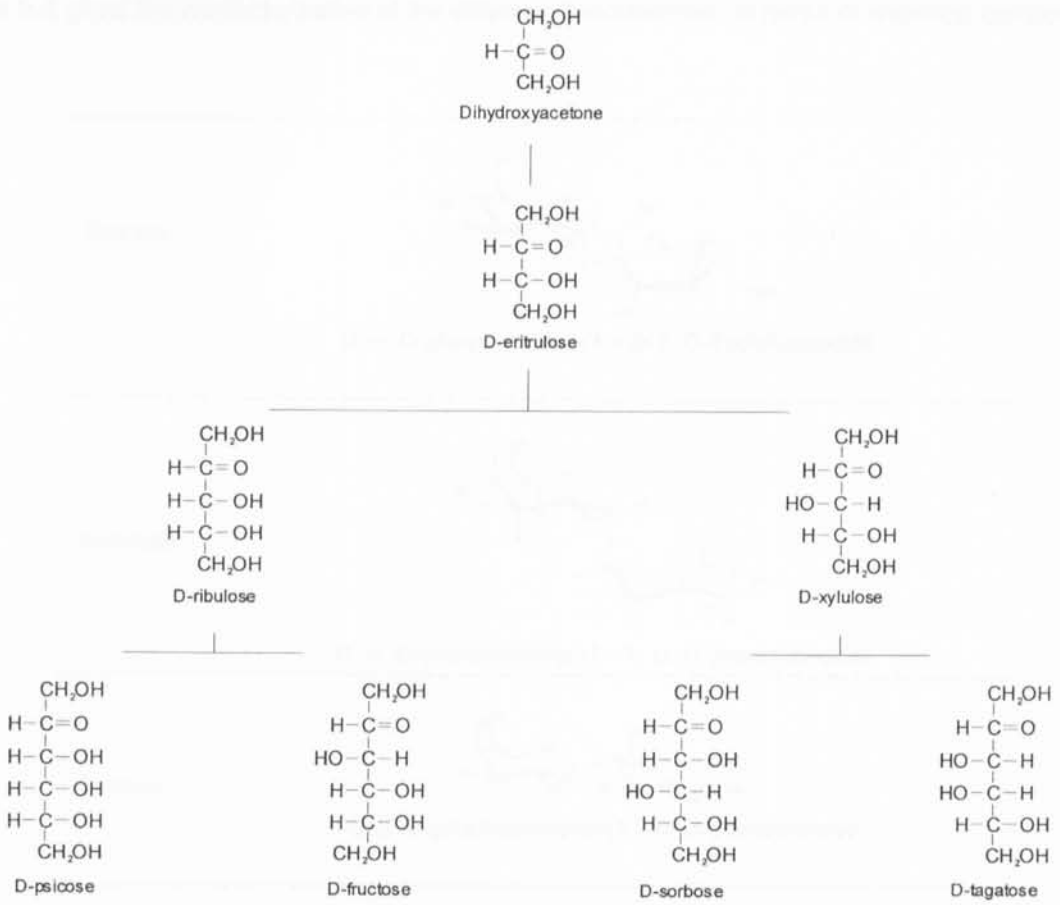


Figure B.2 The D-ketoses family tree (Fischer representation).

B.3 Disaccharides

Figure B.3 gives the characterization of the different disaccharides, in terms of chemical composition.

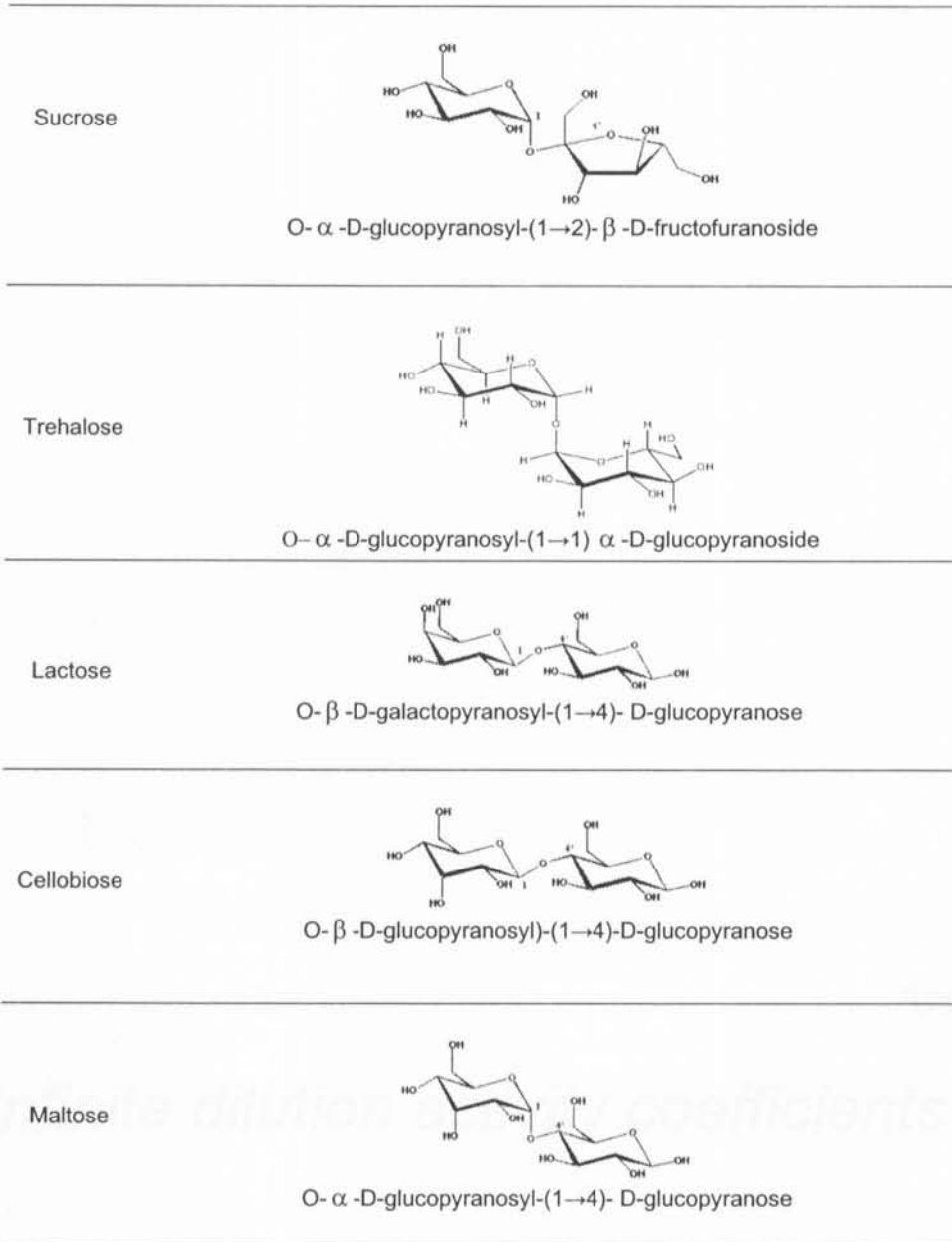


Figure B.3 Disaccharides chemical structure.

C. Infinite dilution activity coefficients data

C.1 Experimental data

Table C.1 presents, for a series of organic solutes, the infinite dilution activity coefficients γ^∞ measured at 353 K, in mixtures of palmitic acid (PA) with triacetin (AAA) for the following mole fractions: 0.50 PA + 0.50 AAA and 0.70 PA + 0.30 AAA. Tables C.2, C.3 and C.4 present the γ^∞ values obtained at 353 K, 363 K and 373 K, in two mixtures of palmitic acid (PA) with tripalmitin (PPP) 0.50 PA + 0.50 PPP, 0.77 PA + 0.23 PPP. The tables also show the γ^∞ of the solutes in the pure solvents (palmitic acid, triacetin and tripalmitin).

From a propagation of errors analysis, an overall uncertainty of 3 to 5% is estimated for the γ^∞ values reported in Tables C.1 to C.4.

Table C.1 Experimental γ^∞ in mixtures of triacetin and palmitic acid

| Solute | Palmitic acid (354.75K) | 30.0% AAA (353.15K) | 49.9% AAA (353.15K) | 100% AAA (353.15K) |
|-------------------|----------------------------|------------------------|------------------------|-----------------------|
| Heptane | 1.51 | 1.81 | 2.24 | 8.90 |
| Hexane | 1.43 | 1.75 | 2.13 | 7.03 |
| Cyclohexane | 1.12 | 1.28 | 1.63 | 4.81 |
| Isoctane | 1.60 | 1.89 | 2.54 | 9.93 |
| Benzene | 0.96 | 0.86 | 0.90 | 1.21 |
| Toluene | 0.99 | 0.93 | 1.02 | 1.59 |
| 1-Hexene | 1.32 | 1.43 | 1.74 | 4.60 |
| Ethanol | 1.85 | 1.38 | 1.37 | 1.59 |
| 1-Propanol | 1.65 | 1.47 | 1.29 | 1.69 |
| 2-Propanol | 1.41 | 1.34 | 1.20 | 1.69 |
| 1-Butanol | 1.58 | 1.47 | 1.30 | 2.06 |
| 2-Butanol | 1.60 | 1.91 | 1.60 | 1.78 |
| Chloroform | 1.01 | 0.72 | 0.60 | 0.62 |
| 1-2 DCE | 1.27 | 1.09 | 0.87 | 0.75 |
| Trichloroethylene | 0.89 | 0.93 | 0.90 | 1.30 |
| Ethyl-ether | | 1.03 | 1.07 | 1.96 |
| MTBE | | 1.23 | 1.30 | 2.69 |
| Ethyl acetate | 1.36 | 1.28 | 1.08 | 1.10 |
| Acetone | 1.60 | 1.42 | 1.07 | 0.98 |

Table C.2 Experimental γ^∞ in mixtures of tripalmitin and palmitic acid

| Solute | Palmitic acid (354.15K) | 23.4% PPP (353.25K) | 50.3% PPP (353.07K) | 100% PPP (350.55K) |
|--------------------|----------------------------|------------------------|------------------------|-----------------------|
| Hexane | 1.43 | 1.05 | 0.89 | 0.58 |
| Heptane | 1.51 | 1.10 | 0.92 | 0.61 |
| Isooctane | 1.60 | 1.19 | 1.00 | 0.67 |
| Cyclohexane | 1.12 | 0.79 | 0.66 | 0.44 |
| Benzene | 0.96 | 0.64 | 0.52 | 0.33 |
| Toluene | 0.99 | 0.67 | 0.55 | 0.35 |
| Hexene | 1.32 | 0.94 | 0.79 | 0.52 |
| Ethanol | 1.85 | 1.59 | 1.64 | 1.23 |
| 1-Propanol | 1.65 | 1.39 | 1.41 | 1.18 |
| 2-Propanol | 1.41 | 1.26 | 1.33 | 1.19 |
| 1-Butanol | 1.58 | 1.34 | 1.34 | 1.21 |
| 2-Butanol | 1.60 | 1.10 | 1.09 | 1.04 |
| Acetone | 1.60 | 1.21 | 1.08 | 0.77 |
| 1,2 Dichloroethane | 1.27 | 0.80 | 0.62 | 0.40 |
| Trichloroethylene | 0.89 | 0.59 | 0.46 | 0.31 |
| Chloroform | 1.01 | 0.51 | 0.38 | 0.25 |
| Anisole | 1.31 | --- | --- | 0.46 |
| Ethyl acetate | 1.36 | 1.03 | 0.90 | 0.64 |
| Ethyl-benzene | 1.11 | 0.77 | 0.62 | 0.40 |

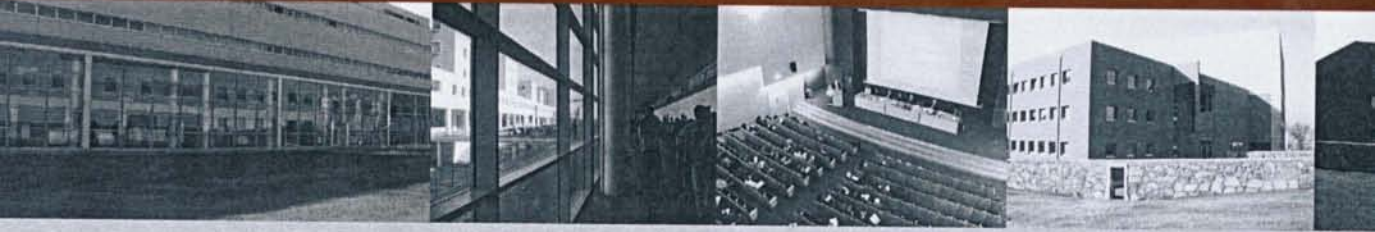
Table C.3 Experimental γ^∞ in mixtures of tripalmitin and palmitic acid.

| Solute | Palmitic acid (365.25K) | 23.4% PPP (363.25K) | 50.3% PPP (363.15K) | 100% PPP (360.75K) |
|--------------------|----------------------------|------------------------|------------------------|-----------------------|
| Hexane | 1.47 | 1.06 | 0.88 | 0.57 |
| Heptane | 1.54 | 1.11 | 0.92 | 0.61 |
| Isooctane | 1.64 | 1.20 | 1.00 | 0.67 |
| Cyclohexane | 1.12 | 0.80 | 0.65 | 0.43 |
| Benzene | 0.97 | 0.65 | 0.52 | 0.33 |
| Toluene | 1.00 | 0.68 | 0.55 | 0.35 |
| Hexene | 1.35 | 0.96 | 0.79 | 0.52 |
| Ethanol | 1.76 | 1.49 | 1.53 | 1.06 |
| 1-Propanol | 1.56 | 1.33 | 1.31 | 1.07 |
| 2-Propanol | 1.38 | 1.21 | 1.23 | 1.07 |
| 1-Butanol | 1.48 | 1.26 | 1.25 | 1.12 |
| 2-Butanol | 1.18 | 1.04 | 1.03 | 0.90 |
| Acetone | 1.56 | 1.13 | 1.03 | 0.73 |
| 1,2 Dichloroethane | 1.24 | 0.78 | 0.61 | 0.38 |
| Trichloroethylene | 0.90 | 0.59 | 0.46 | 0.30 |
| Chloroform | 0.84 | 0.50 | 0.39 | 0.24 |
| Anisole | 1.37 | 0.86 | 0.67 | 0.44 |
| Ethyl acetate | 1.32 | 1.01 | 0.87 | 0.63 |
| Ethyl-benzene | 1.18 | 0.77 | 0.60 | |

Table C.4 Experimental γ^∞ in mixtures of tripalmitin and palmitic acid.

| Solute | Palmitic acid (374.15K) | 23.4% PPP (373.15K) | 50.3% PPP (373.15K) | 100% PPP (368.05K) |
|--------------------|----------------------------|------------------------|------------------------|-----------------------|
| Hexane | 1.50 | 1.05 | 0.88 | 0.57 |
| Heptane | 1.59 | 1.10 | 0.92 | 0.61 |
| Isooctane | 1.68 | 1.21 | 1.00 | 0.67 |
| Cyclohexane | 1.15 | 0.79 | 0.65 | 0.43 |
| Benzene | 0.99 | 0.63 | 0.51 | 0.33 |
| Toluene | 1.05 | 0.68 | 0.54 | 0.35 |
| Hexene | 1.39 | 0.96 | 0.79 | 0.52 |
| Ethanol | 1.73 | 1.40 | 1.38 | 1.11 |
| 1-Propanol | 1.53 | 1.24 | 1.19 | 1.04 |
| 2-Propanol | 1.35 | 1.14 | 1.13 | 0.98 |
| 1-Butanol | 1.45 | 1.19 | 1.13 | 1.01 |
| 2-Butanol | 1.16 | 0.98 | 0.95 | 0.86 |
| Acetone | 1.53 | 1.14 | 1.00 | 0.71 |
| 1,2 Dichloroethane | 1.25 | 0.78 | 0.59 | 0.37 |
| Trichloroethylene | 0.93 | 0.61 | 0.46 | 0.30 |
| Chloroform | 0.87 | 0.51 | 0.39 | 0.25 |
| Anisole | 1.30 | 0.86 | 0.67 | 0.43 |
| Ethyl acetate | 1.34 | 1.00 | 0.84 | 0.61 |
| Ethyl benzene | 1.15 | 0.78 | 0.60 | 0.39 |





FACULDADE DE ENGENHARIA
UNIVERSIDADE DO PORTO BIBLIOTECA



0000079600